THE UNIVERSITY *of* EDINBURGH

High oxidation state carbene complexes for C-H bond activation catalysis

Stephen M. Pearson

Doctor of Philosophy
University of Edinburgh
2010

Declaration

Except where specific reference has been made to other sources, the work presented in this thesis is the original work of the author. It has not been submitted, in whole or in part, for any other degree.

Stephen M. Pearson

September 2010

Abstract

Chapter one is an introduction to the less common coordination and oxidation chemistry of palladium; complexes containing Pd-OR, Pd-NR_2 and those in the oxidation states of +IV. An outline of $Pd^{II/IV}$ catalysed ligand-directed oxidative functionalisation is also included.

Chapter two covers the design and synthesis of a range of tethered N-heterocyclic carbene (NHC) complexes of Pd. In addition, the syntheses of a number of new tethered NHC ligands are described. The use of Density Functional Theory (DFT) to model the complexes in this thesis was explored.

Chapter three describes the synthesis and characterisation of Pd^{IV} halide complexes. The relevance of these compounds to $Pd^{II/IV}$ catalysed ligand-directed oxidative functionalisation is explored. DFT was used to probe the reaction pathway for N-bromosuccinimide and iodobenzene dichloride.

Chapter four examines reactions with oxidants used to form C-O and C-C bonds. The reaction pathway for iodobenzene diacetate was investigated using DFT.

Chapter five contains experimental details and characterising data for the compounds reported.

Acknowledgements

"You will give us peace, LORD, because everything we have done was by your power."

Isaiah 26:12 (CEV)

I would like to thank my family for their continual support and encouragement during the PhD process. I express gratitude to my supervisors Prof. Polly L. Arnold and Prof. Melanie S. Sanford for their input and support throughout this project.

I would like to recognize the contribution of Benjamin Manga to the synthesis of ($L^{N,Ar}$)Pd(bzq) and José-Maria Muńoz-Molina in preparing (L^{N})Pd(phpy) and Pd(L^{N})$_2$. I am gratefulness to Patricia Richardson and Brannon Gary for their helpful discussions with regards to DFT calculations.

I would like to thank the post-docs Dr Stephen Liddle, Dr Christopher Carmichael, Dr Sergey Zlatogorsky, Dr Emmalina Hollis and Dr Stephen Mansell for so patiently answering my many questions. Thanks to everyone in Lab 34 for making my time in Edinburgh so enjoyable. Thanks go also to the Sanford group for making me so welcome and helping me to settle in the USA.

Important structures and abbreviations

Abbreviation	Meaning
$L^{O,R}$ ($L^{O} = L^{O,Me}$)	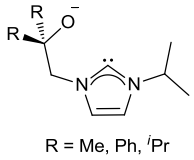 R = Me, Ph, ^{i}Pr
L^{N}	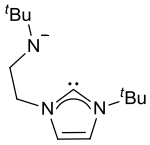
$L^{N,Ar}$	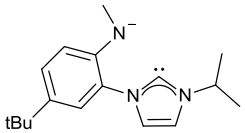
phpy	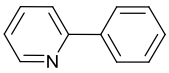
^{OMe}phpy	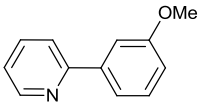
bzq	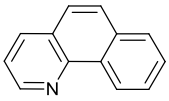
Labelling of protons in (L^{O})Pd(phpy)	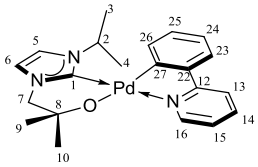
CNC	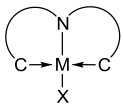 tridentate ligand
DFT	density functional theory
N''	$N(SiMe_3)_2$
OAc	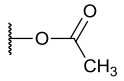

Abbreviation	Meaning
DMF	dimethylformamide
OTf	OSO_2CF_3
LDA	lithium diisopropylamide
nOe	nuclear overhauser effect
Cp	cyclopentadienyl
HOMO	highest occupied molecular orbital
LUMO	lowest unoccupied molecular orbital
NMR	nuclear magnetic resonance
ppm	parts per million
NCS	N-chlorosuccinimide
NBS	N-bromosuccinimide
bzq-Cl	10-chlorobenzo[h]quinoline
phpy-Br	2-(2-bromophenyl)pyridine
phpy-2OAc	2-(2,6-diacetoxyphenyl)pyridine
phCOpy-H	phenyl(2-pyridinyl)methanone
pypyr-H	1-phenyl-2-pyrrolidone
phpyz-H	1-phenylpyrazole
Mephpy-H	3-methyl-2-phenylpyridine
o-tolylpy-H	o-tolylpyridine
Etpy-H	2-ethylpyridine
n-BuOpy-H	2-(n-butoxy)pyridine
NHC	*N*-heterocyclic carbene
thf	tetrahydrofuran
2,6-lutidine	2,6-dimethylpyridine

Table of Contents

Chapter 1 – Introduction 2

1.1. Introduction 2

1.2. Palladium(II) NHC complexes 2

1.3. Palladium(II) alkoxide complexes 5

1.4. Palladium(II) amide complexes. 8

1.5. Organometallic palladium(IV) complexes 13

1.6. Palladium(IV) in catalysis 15

1.7. Aims of this work 18

1.8. References 19

Chapter 2 – Synthesis of starting materials 24

2.1. Introduction 24

2.2. Generating structures for calculations 24

2.3. Choosing a functional and basis set 24

2.4. Evaluating basis sets using (L^{O})Pd(phpy) 26

2.5. Simplification of ligands to reduce computational expense 30

2.6. Accounting for solvent effects 32

2.7. Ligand design 34

2.8. Alkoxide tethered N-heterocyclic carbene proligands 35

2.8.1. Synthesis of $[H_2L^{O,Ph}]I$ 35

2.8.2. Synthesis of $[H_2L^{O,iPr}]I$ 36

2.9. Aryl-amido tethered N-heterocyclic carbene proligand 37

2.9.1. Synthesis 37

2.10. Deprotonation of the NHC proligands 39

2.10.1. Preparation of $KL^{O,R}$ 39

2.10.2. Deprotonation of $[H_2L^{N,Ar}]I$ 40

2.11. Pd(II) mixed ligand complexes 41

2.11.1. Preparation of $[(L^{O})PdCl]_2$ type complexes 42

2.11.2. Preparation of (L^{O})Pd(phpy) 42

2.11.3. Synthesis of related ($L^{O,R}$)Pd(phpy) type complexes 47

2.11.4. Synthesis of (L^{N})Pd(phpy) 51

2.11.5. Synthesis of ($L^{N,Ar}$)Pd(bzq) 51

2.12. Synthesis of $M(L)_2$ complexes (M = Pd, Ni) 53

2.12.1. Preparation of $Pd(L^O)_2$ 53
2.12.2. Preparation of $Pd(L^N)_2$ 54
2.12.3. Preparation of $Ni(L^O)_2$ 55
2.13. Cyclic voltammetry 57
2.14. Conclusions 60
2.15. References 61

Chapter 3 – Pd^{IV} NHC halide complexes 65
3.1. Introduction 65
3.2. Oxidation of $(L^O)Pd(phpy)$ with NBS 66
3.2.1. Potential isomers of $(L^O)Pd(phpy)(Br)$(succinimide) 68
3.2.2. Oxidation of $(L^O)Pd(bzq)$ with NBS 70
3.2.3. Reductive elimination reactions of $(L^O)Pd(phpy)(Br)$(succinimide) 71
3.2.4. Products from decomposition of $(L^O)Pd(bzq)(Br)$(succinimide) 72
3.2.5. Analysis of NBS reaction by electrospray mass spectrometry 73
3.2.6. Reaction of $(L^O)Pd(phpy)(Br)$(succinimide) with water 75
3.3. Pd-catalysed ligand-directed oxidative halogenation 77
3.3.1. Stability of $(L^O)Pd(phpy)$ under catalytic conditions 78
3.3.2. Initial screening of $(L^O)Pd(phpy)$ catalysed halogenation 78
3.3.3. Ligand directed catalytic functionalisation using $(L^O)Pd(phpy)$ 80
3.3.4. Ligand directed catalytic bromination using $(L^O)Pd(bzq)$ and N-bromosuccinimide 82
3.4. Reaction profile $(L^O)Pd(phpy)$ and N-bromosuccinimide 85
3.4.1. Discussion 87
3.5. Oxidation of $(L^O)Pd(bzq)$ with $PhI(Cl)_2$ 89
3.5.1. Single crystal X-ray diffraction structure of $(L^O)Pd(bzq)Cl_2$ 90
3.5.2. DFT analysis of isomers of $(L^O)Pd(phpy)Cl_2$ 91
3.5.3. Products from decomposition of $(L^O)Pd(bzq)Cl_2$ 92
3.5.4. Single crystal X-ray diffraction structure of $(L^{OH})Pd(bzq)Cl$ 94
3.5.5. Formation of $(L^{OH})Pd(bzq)Cl$ and conversion to $(L^O)Pd(bzq)$. 95
3.6. Computational analysis of Pd^{IV}-based chlorination reactions 96
3.6.1. Discussion 97
3.7. Development of a new NHC ligand to stabilise Pd^{IV} 98
3.7.1. DFT analysis of a range of tethered NHC ligands 100
3.7.2. Synthesis of $(L^{N,Ar})Pd(bzq)$ 102

3.7.3. Oxidation of ($L^{N,Ar}$)Pd(bzq) with $PhI(Cl)_2$ 104
3.7.4. Decomposition of ($L^{N,Ar}$)Pd(bzq)Cl_2 105
3.7.5. Computational analysis of reductive elimination 106
3.8. Conclusions 109
3.9. References 111

Chapter 4 – Formation of C-O and C-C bonds from Pd^{IV} complexes. 114
4.1. Introduction 114
4.2. (L^{O})Pd(phpy) + $PhI(OAc)_2$ 115
4.2.1. (L^{O})Pd($phpy^{-OAc}$)OAc 115
4.2.2. [(L^{O})Pd(phpy)·$PhI(OAc)_2$] 118
4.2.3. DFT simulations of [(L^{O})Pd(phpy)]·$PhI(OAc)_2$ 119
4.2.4. (L^{OH})Pd(phpy)OH + $PhI(OAc)_2$ 121
4.2.5. (L^{O})Pd(phpy) + AcOH 122
4.2.6. Esterification of (L^{OH})Pd(phpy)OAc 123
4.3. Computational analysis of reaction between (L^{O})Pd(phpy) with $PhI(OAc)_2$ 125
4.3.1. Discussion 127
4.4. C-C bond formation 127
4.4.1. (L^{O})Pd(phpy) + $[Ph_2I]BF_4$ 127
4.4.2. Other reports of intermediates with hypervalent iodine reagents 129
4.4.3. (L^{O})Pd(phpy) + MeI 130
4.4.4. (L^{O})Pd(phpy) + $SiMe_3N_3$ 131
4.4.5. ($L^{N,Ar}$)Pd(bzq) + MeI 132
4.5. Catalysis testing 133
4.5.1. Comparison of (L^{O})Pd(phpy) and $Pd(OAc)_2$ for catalytic ligand directed acetoxylation 134
4.5.2. Effect of solvent on (L^{O})Pd(phpy) catalysed acetoxylation 135
4.5.3. (L^{O})Pd(phpy) catalysed acetoxylation of 2-ethylpyridine 136
4.5.4. (L^{O})Pd(phpy) catalysed C-C bond formation 137
4.5.5. Comparison between (L^{O})Pd(phpy) and ($L^{O,Ph}$)Pd(phpy) as precatalysts 137
4.6. Conclusions 138
4.7. References 140

General Considerations 142
Synthetic Procedures 144

1 $[H_2L^{O,Ph}]I$ 144
2 $[H_2L^{O,iPr}]I$ 144
3 $[H_2L^{N,Ar}]I$ 145
4 $KL^{O,Ph}$ 146
5 $KL^{O,Me}$ 147
6 $(L^{N})Pd(allyl)$ 147
7 $Pd(L^{O,Me})_2$ 147
8 $Pd(L^{N})_2$ 148
9 $Ni(L^{O,Me})_2$ 149
10 $Ni(L^{O,Me})_2Cl$ 149
11 $Ni(L^{O,Me})_2$ + $PhI(OAc)^2$ 150
12 $(L^{O,Me})Pd(phpy)$ 150
13 $(L^{O,Ph})Pd(phpy)$ 151
14 $(L^{O,iPr})Pd(phpy)$ 152
15 $(L^{O})Pd(^{OMe}phpy)$ 153
16 $(L^{N})Pd(phpy)$ 154
17 $(L^{O})Pd(bzq)\cdot 1/3CH_2Cl_2$ 155
18 $(L^{N,Ar})Pd(bzq)$ 156
19 $(L^{O})Pd(bzq)(Cl)_2$ 157
20 $(L^{O})Pd(bzq\text{-}Cl)Cl$ 158
21 $(L^{O})Pd(bzq)(succinimide)Br$ 159
22 $(L^{O})Pd(phpy)(succinimide)Br$ 160
23 $(L^{O})Pd(phpy^{Br})(succinimide)$ 161
24 Effect of temperature and concentration on product distribution upon reductive elimination 161
25 $(L^{OH})Pd(phpy^{Br})(succinimide)_2$ 162
26 $(L^{OH})Pd(bzq)(succinimide)(Br)OH$ 163
27 $(L^{OH})Pd(bzq)Cl$ 163
28 Deprotonation of $(L^{OH})Pd(bzq)Cl$, conversion to $(L^{O})Pd(bzq)$. 164
29 $(L^{N,Ar})Pd(bzq\ )(Cl)_2$ 164
30 Decomposition of $(L^{N,Ar})Pd(bzq)(Cl)_2$ 165
31 $[(L^{O})Pd(phpy)]PhI(OAc)_2$ 166
32 $(L^{O})Pd(phpy^{OAc})OAc$ + PhI 166
33 $(L^{OH})Pd(phpy^{OAc})(OAc)OH$ 167
34 $[(L^{O})Pd(phpy)]Ph_2IBF_4$ 168

35 [(L^{O})Pd($phpy^{Ph}$)]BF_4 + PhI 168
36 [($L^{O,Ph}$)Pd(phpy)]Ph_2IBF_4 169
37 [($L^{O,Ph}$)Pd($phpy^{Ph}$)]BF_4 + PhI 169
38 (L^{OMe})Pd(phpy)I 170
39 (L^{OTMS})Pd(phpy)N_3 170
40 (L^{OH})Pd(phpy)OH 171
41 (L^{OH})Pd(phpy)OAc 172
42 ($L^{OH,iPr}$)Pd(phpy)Cl 172
43 ($L^{N,Ar}$)Pd(bzq)(Me)(I) 173
44 Preliminary (L^{O})Pd(phpy) catalysed ligand directed C-H bond oxidative halogenation 175
45 Catalytic bromination using (L^{O})Pd(bzq) and N-bromosuccinimide 176
46 Comparison of (L^{O})Pd(phpy) and $Pd(OAc)_2$ for catalytic acetoxylation 177
47 Effect of solvent on (L^{O})Pd(phpy) catalysed acetoxylation 178
48 Comparison between (L^{O})Pd(phpy) and ($L^{O,Ph}$)Pd(phpy) as precatalysts 179
Key ^{1}H NMR spectroscopy data 180
X-ray Crystallography 183
References 190

Chapter 1

Introduction

Chapter 1 – Introduction

1.1. Introduction

Since beginning this work the fields of chemistry being explored have grown significantly. Tetravalent palladium has gone from an organometallic curiosity, unseen but invoked in catalysis to a widely accepted, accessible intermediate. *N*-Heterocyclic carbenes (NHCs) have been shown to be outstanding ligands for a variety of organometallic complexes that are key components in catalysis. Tethered NHCs have the additional advantage of being particularly suited to stabilising high oxidation state metal cations.[1, 2]

1.2. Palladium(II) NHC complexes

The frontier molecular orbital diagrams for a Fischer (**I**), Schrock (**II**), and N-heterocyclic (**III**) carbene are shown in Figure 1.

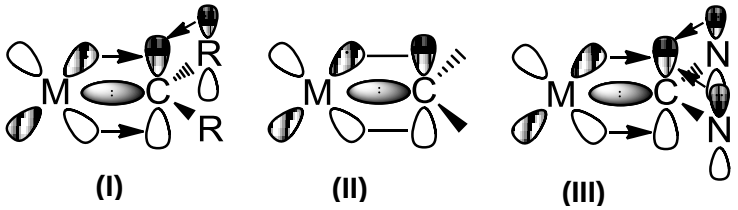

Figure 1. Orbital diagrams for a Fischer, Schrock and N-Heterocyclic carbene.[3]

Fischer carbenes σ-bond to the metal centre but have an empty p-orbital which must be sufficiently stabilised by π-donation from the metal and/or a substituent group. The stronger the π-donor on the carbene carbon the lower the M=C bond order is and lower the barrier to rotation about the M-C bond. Fischer carbenes are typically part of complexes with an a electron rich, low oxidation state metal (mid to late transition metals).

Stable complexes containing a Schrock carbene are formed when bound to early transition, high oxidation state metals. This results from better π-donation from the filled carbene p-orbital to the metal d-π orbital when the d-orbital is empty.

The stability of an NHC is mainly as a result of π-donation from the adjacent nitrogen atoms into the empty p-orbital of the carbene. NHCs are excellent σ-donors to metal centres and for a long time this was believed to be the principle mode of bonding. The nature of the metal-NHC bond is still debated but it has been demonstrated there is negligible metal-carbene back bonding in the late metal NHC bond of Pd(di-*N*-^{t}Butyl NHC)$_2$.[4]

The first example of a Pd-NHC complex was synthesised in 1972 by Lappert and co-workers (Equation 1).[5]

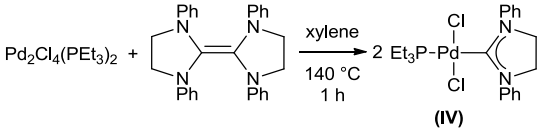

(1)

The synthetic route is not very versatile, and it took until 1997 before detailed investigation of Pd-NHC complexes began (following the publication by Arduengo *et al* of a more practical route to stable NHCs).[6] In the decade that has followed over 600 papers have been published on Pd-NHC complexes.

The area has been thoroughly reviewed, the main topics of interest are multi-dentate ligands containing two or more NHCs,[7, 8] the application of NHCs in catalysis,[9, 10] new synthetic routes to functionalised NHC ligands,[11] the development of chiral NHCs[12] along with studies to understand the associated electronic and steric factors.[13-15]

The remarkable stability of Pd-NHC complexes was demonstrated by Strassner and coworkers; complex **V** is stable in trifluoroacetic acid and in the presence of strong oxidants. It is an effective catalyst for the conversion of methane to trifluoroacetic acid methyl ester (Equation 2).[16] The choice of halide and substituent on the NHC is important. If iodide ligands are used no reaction is observed and if ^{t}Bu groups are used instead of Me the activity is halved.

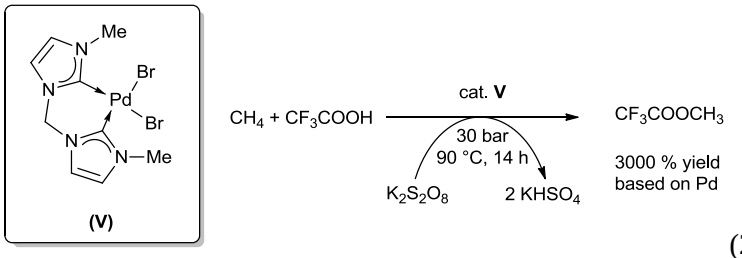

(2)

The Pd-NHC bond is not completely unreactive. Whilst no intermediates to the formation of **VI** could be found by ^{1}H NMR spectroscopy, DFT calculations suggest a five coordinate Pd^{II} intermediate from which C-C bond formation takes place.[17] This mode of reactivity is an important consideration when working with coordinatively saturated Pd complexes.

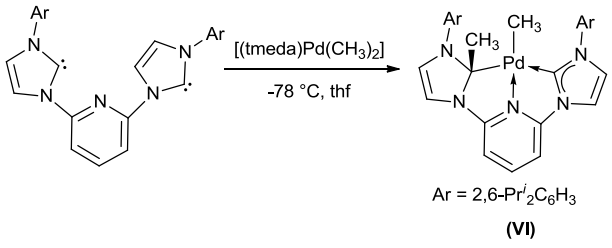

(3)

Palladium-catalysed cross-coupling reactions (such as Suzuki-Miyaura and Heck) have seen improvements with the introduction of bulky NHC ligands which are typically superior to the most active phosphane ligands. Despite this, Pd-NHC catalysts are still rarely used in the synthesis of natural products due to the expensive precursors required to synthesise the NHC ligand. Palladium-catalysed polymerisation is one area of growth for NHCs. The bis(aryloxide tethered NHC) palladium complex **VII** was found to be an excellent catalyst for the polymerisation of vinylnorbornene (10^{7} g of polynorbornene (mol of Pd)$^{-1}$ h^{-1}).[18]

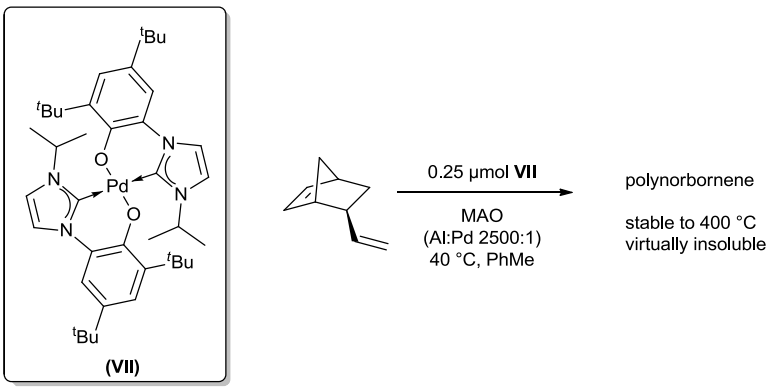

(4)

NHCs are likely to remain an important area of chemistry for many more years. The strong interest in Pd-NHC complexes in catalysis, for example, has led to improvements in asymmetric catalysis where an electron-rich metal centre is beneficial.[19]

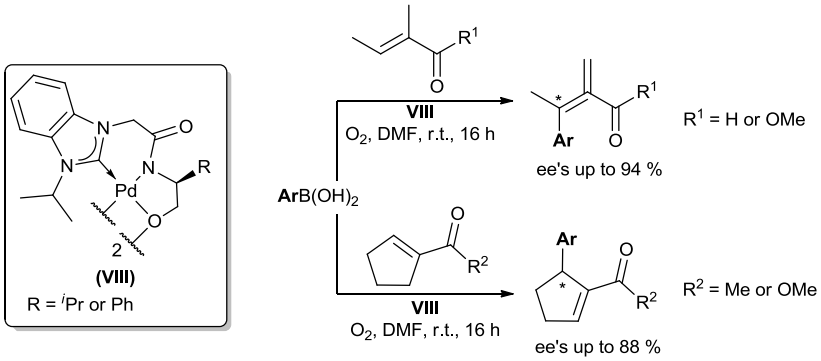

Scheme 1. Asymmetric intermolecular boron Heck-type reaction.[19]

The chiral dimeric tridentate NHC-amidate-alkoxide palladium(II) complex (**VIII**) was found to be a much more effective catalyst than previous methods. The coupled products had a high degree enantioselectivity due to non-bonding interactions in the proposed transition state.

1.3. Palladium(II) alkoxide complexes

Many palladium catalysed transformations involve Pd-O bonds including the aerobic oxidation of alcohols,[20, 21] the kinetic resolution of secondary alcohols,[22] and the oxidative functionalisation of C-H bonds.[23] These species are often transient and so the synthesis of complexes containing discrete Pd^{II}-O-R bonds can help in understanding these systems. Isolated Pd^{II} alkoxide complexes are relatively uncommon considering the interest and widespread use of Pd in modern organic synthesis. The majority of the thirty three reported complexes contain secondary alkoxide or methoxide ligands. Palladium complexes with aryloxide ligands are more common with over sixty reported examples. These will not be covered here.

Palladium alkoxide complexes are of particular interest for homogeneous palladium-catalyzed aerobic oxidation of alcohols.[24] In order to make Pd-$O_{alkoxide}$ complexes that can be studied trifluoromethyl groups are included on the same carbon the oxygen is bound to.[25-28] Complex **IX** (Equation 5) slowly decomposes in solution with the formation of Pd^0 presumably by β-hydride elimination.[25]

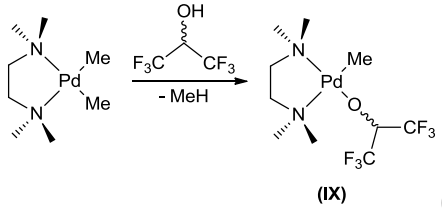

(5)

The electron-withdrawing CF_3 group disfavours the β-agostic interaction between palladium and the C-H bond that precedes β-hydride elimination. In the kinetic resolution of secondary alcohols β-hydride elimination is a key feature of the catalytic process. An excellent demonstration of this was made by Stoltz and co-workers.[29] Whilst the substrate α-(methyl)benzyl alcohol readily undergoes kinetic resolution, α-(trifluoromethyl)benzyl alcohol is unreactive. This could be exploited to form complex **X** a relevant intermediate in the oxidation reaction, Scheme 2. Addition of $AgSbF_6$ allows β-hydride to take place and oxidation of the alcohol is observed along with Pd decomposition products.

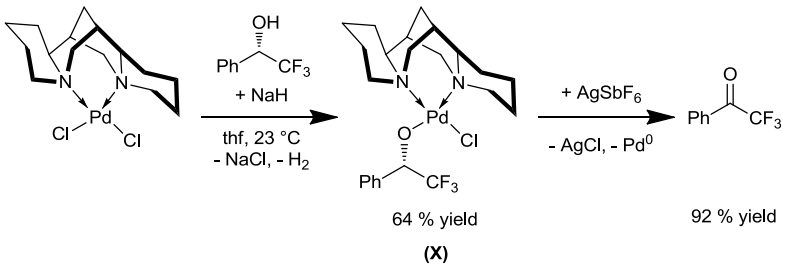

Scheme 2. Formation of a palladium-alkoxide (-)-sparteine complex.[29]

Most of the reported methoxide complexes have been synthesised whilst examining the reactivity of palladium complexes with μ-peroxo or μ-hydroxy ligands, an example of which is shown in Equation 6.[30-42]

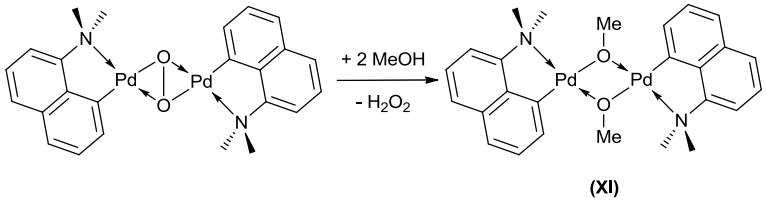

(6)

Klüfers and co-workers have synthesised a range of Pd^{II} carbohydrate complexes in which the Pd is bound by two secondary alkoxide groups to the sugar molecule (Figure 2).[43-52] A number of conformers could be observed by ^{1}H and ^{13}C NMR spectroscopy, with the type of sugar rather than palladium determining the possible structures.

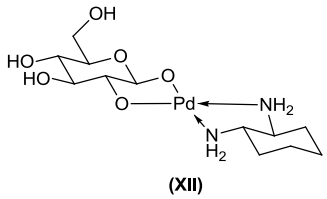

Figure 2. Palladium alkoxide complex of glucose.[52]

Where the alkoxide is part of a bidentate ligand β-hydride elimination is not a significant decomposition pathway for the complexes, presumably because the ring structures prevent the correct geometry for β-hydride elimination being obtained.

In complexes where the free alcohol is present interactions between palladium and oxygen can still be important.[53] By ^{1}H NMR spectroscopy two enantiomers of **XIII** are observed at room temperature which converge upon heating to 60 °C (Scheme 3). By replacing the bromide with nitrate an intermediate structure with the alcohol coordinated to palladium can

be isolated. A Pd-$O_{alkoxide}$ bond can be formed by addition of a base or the alcohol can be displaced by addition of a stronger donor ligand such as pyridine.

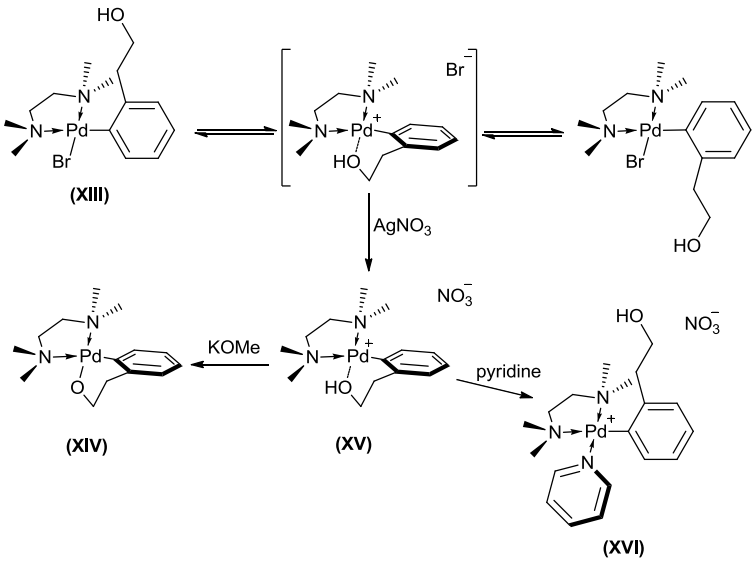

Scheme 3. Conversion between structures in a palladium alcohol complex.[53]

1.4. Palladium(II) amide complexes.

Isolated Pd^{II} amide complexes are also relatively uncommon (Pd^{II} amidate complexes (Pd-NR(COR) R = H, alkyl or aryl) are not discussed here on the basis that they behave more like acetate than amido ligands). The first example of a Pd amide complex was reported by Fryzuk and coworkers in 1981, Equation 7.[54, 55] The amide group is part of a chelating PNP ligand.

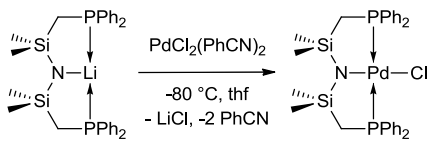

(7)

There are two main routes to synthesise palladium amide complexes; direct reaction of the amine with a hydroxide bridged Pd complex or treatment of a complex containing a Pd-Cl bond with an alkali metal salt of an amide. Most of the reported complexes are synthesised using aryl amines as the reactions proceed more cleanly and in higher yields.[30, 56-62] Where the arylamide is not part of a chelating ligand the Pd complexes formed are either monomeric or dimeric with the amide bridging two Pd centres.

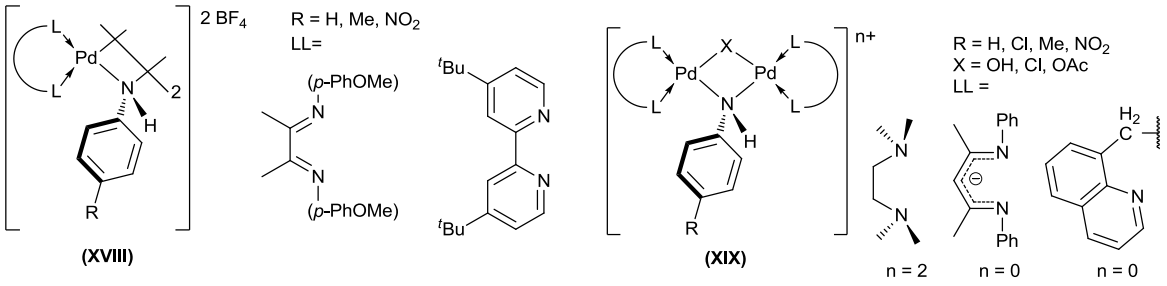

Figure 3. Examples of bridged palladium amide complexes.[30, 56-59]

It has been reported that M-NR_2 bonds are much weaker than M-OR bonds for late transition metals.[63] The weaker bond to palladium and ease of β-hydride elimination means there are very few examples of monodentate Pd-NR_2 (R = alkyl) complexes.[64, 65]

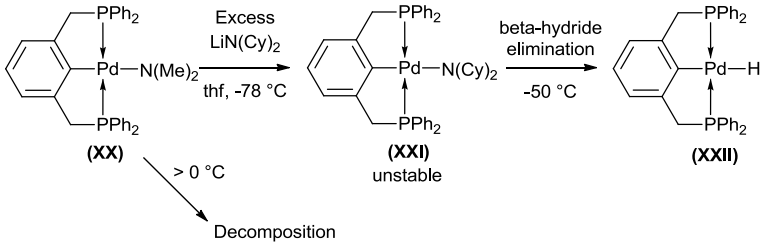

Scheme 4. Reactivity of Pd-amido complex bearing a PCP ligand.

The [(PCP)Pd(NMe_2)] complex reported by Park and coworkers (Scheme 4) is formed by deprotonation of a cationic Pd^{II} amine PCP pincer complex. The complex decomposes above 0 °C presumably as a result of β-hydride elimination. Interestingly, if the dimethyl amide is

replaced by dicyclohexyl amide a much more unstable complex is formed. This is likely due to the greater steric congestion of the dicyclohexyl amide facilitating β-hydride elimnation.

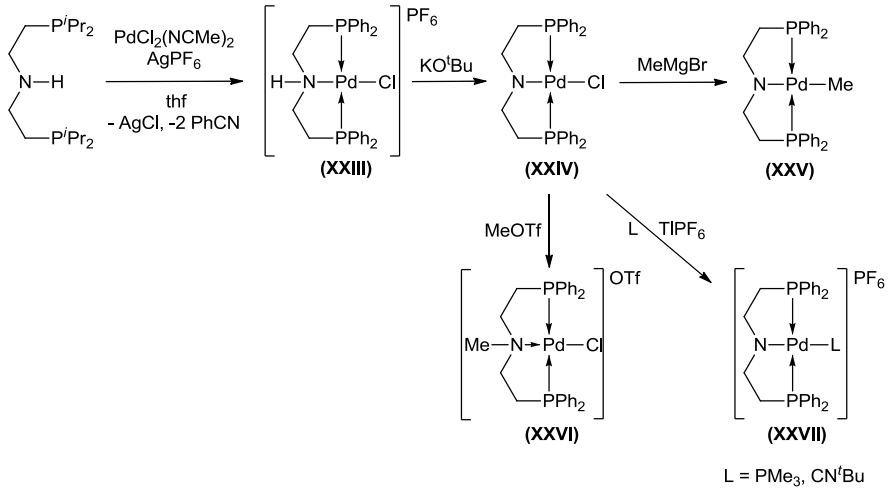

Scheme 5. Reactivity at Pd bearing a PNP ligand.

Schnieder and coworkers have investigated the reactivity of Ir^{I}, Ru^{II} and Pd^{II} complexes bearing a PNP pincer ligand, Scheme 5. The Pd^{II}-amide complex is obtained by deprotonation of a cationic Pd^{II} amine PNP pincer complex. The pincer ligand stabilises the amide against β-hydride elimination and allows for substitution of the ligand *trans*-disposed to the amide. Addition of methyl triflate leads to methylation of the amide as can be expected for a highly nucleophilic amido ligand. Starting from [Pd(I)Ph(tmeda)] the analogous phenyl complex can be obtained.

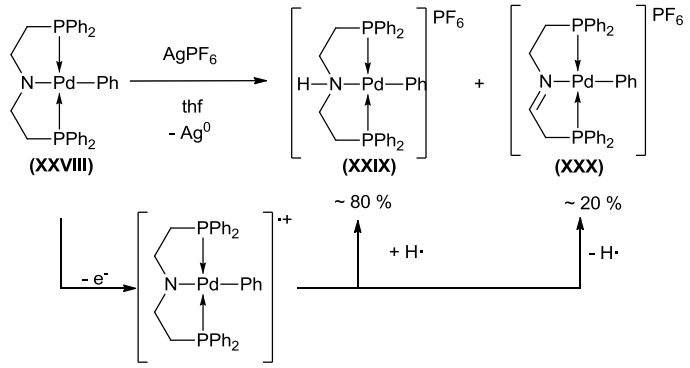

Scheme 6. Oxidation of [(PNP)Pd(Ph)] with $AgPF_6$.

Treatment of [(PNP)Pd(Ph)] with $AgPF_6$ yields $[(PNP^H)Pd(Ph)]PF_6$ as the major product. Upon oxidation $[(PNP)Pd(Ph)]^{+\cdot}$ is proposed as the intermediate species, the radical can be quenched either by abstracting a proton from the solvent (confirmed by utilising d_8-thf) or another molecule of $[(PNP)Pd(Ph)]^{+\cdot}$. This gives rise to the product mixture observed.

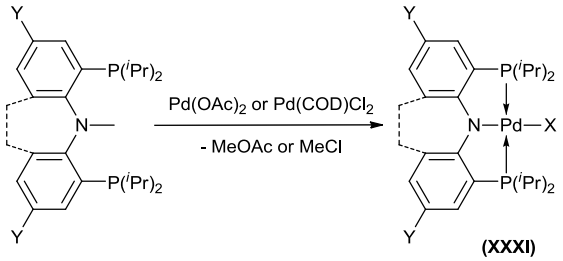

(XXXI)

Y = H, F, Br, $SiMe_3$, Me
X = H, Cl, Br, I, OAc, OTf,
OH, OMe, OEt, O^{i}Pr,
Me, Et, Bu, Ph, CH_2Ph (8)

Ozerov and coworkers extensively investigated the reactivity of related (PNP)Pd complexes (Equation 8).[66-70] They found alkoxide and alkyl fragments were remarkably thermally stable to β-hydride elimination due to the rigidity of the PNP ligand blocking the cis coordination sites. The thermal decomposition of (PNP)PdOEt (where Y = F) is slow in C_6D_6 but is hastened by addition of EtOH. It is proposed that β-hydride elimination occurs via dissociation of the alkoxide anion. PNP complexes of palladium have also been investigated for applications in Suzuki and Heck catalysis.[66-75]

Other palladium complexes containing CNC and NNN ligands have also been reported (Figure 4).[76-78] Complexes **XXIII** and **XXXIV** demonstrate the complimentary nature of NHCs as donors compared to existing PNP complexes (such as **XXIV** and **XXXI**).

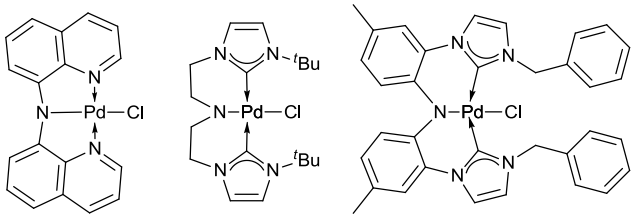

Figure 4. Other Pd^{II} amido complexes.

Hartwig and coworkers have made a major contribution to Pd amide chemistry in their studies of C-N bond formation from Pd^{II}.[62, 79-84] The electronic and steric factors governing C-N bond formation from Pd^{II} as well as the kinetic and mechanistic aspects have been thoroughly investigated.

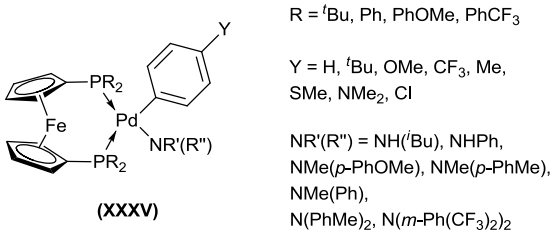

Figure 5. A variety of electronically diverse Pd^{II} amido complexes.

Heating [(dppf)Pd(Ar)(NR'(R"))] leads to direct C-N bond formation from the four-coordinate Pd-amido complex. Reductive elimination is accelerated by electron-withdrawing substituents on the Pd-bound aryl group.

If an unsymmetrical dppf ligand is used two regioisomers are obtained with the major isomer having the aryl ligand trans-disposed to the phosphine with the less electron-rich substituent. This is important as the minor regioisomer undergoes much faster reductive elimination. The substituent on the amido ligand has a much greater effect on the rate of reductive elimination than the substituent on the dppf ligand. This understanding contributed to the development of the industrially important Buchwald-Hartwig cross coupling reactions.[85]

1.5. Organometallic palladium(IV) complexes

Compared to the thermodynamically stable and kinetically inert Pt^{IV} complexes, Pd^{IV} complexes have traditionally been seen as rare and elusive. This is expected on thermodynamic grounds as the ionisation potential is greater for Pd ($Pd_{(g)} \rightarrow Pd^{4+}_{(g)}$ = 2546 kcal/mol, $Pt_{(g)} \rightarrow Pt^{4+}_{(g)}$ = 2238 kcal/mol).[86] The very first Pd^{IV} complexes containing a Pd-C bond were synthesised by Uson *et al.* in 1975, Scheme 7.[87]

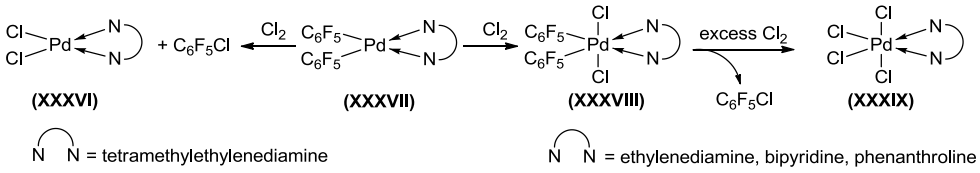

Scheme 7. First reported organometallic Pd^{IV} complexes.

Addition of chlorine to bis(pentafluorophenyl) Pd^{II} complexes bearing a bidentate nitrogen donor ligand led to formation of a Pd^{IV} intermediate; except when the more bulky tetramethylethylene diamine ligand was used. This steric factor is an important consideration in Pd^{IV} chemistry where significant crowding around an octahedral Pd^{IV} complex occurs with most choices of ligand. Interestingly, with the less bulky ligands excess chlorine was needed to promote reductive elimination. A similar effect was observed recently with (*t*-Bu-bpy)Pd^{IV}(*p*-FC_6H_4)$(F)_3$(FHF) where excess XeF_2 was needed to promote reductive elimination.[88]

Modern interest in Pd^{IV} organometallic complexes was driven initially by the work of Canty and co-workers who have published over 20 papers on the subject. The breakthrough was to demonstrate that methyl iodide could oxidatively add to (bpy)$Pd^{II}Me_2$ to yield a thermally unstable Pd^{IV} complex, Equation 9.[89]

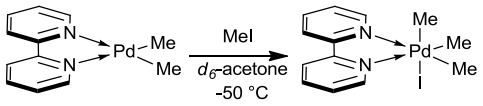

(XXXX) **(XXXXI)** (9)

More recently interest in $Pd^{II/IV}$ for catalytic applications has also lead to renewed interest in organometallic Pd^{IV} complexes. A number of recent reviews give a thorough view of this area.[86, 90-93] Pd^{IV} was identified by the Sanford group as a transient intermediate in ligand directed oxidative C-H bond functionalisation. A detailed understanding of carbon-oxygen bond formation from palladium remained elusive[94, 95] until Sanford and co-workers isolated a series of stable Pd^{IV} complexes as part of their mechanistic investigations (Scheme 7).[96, 97]

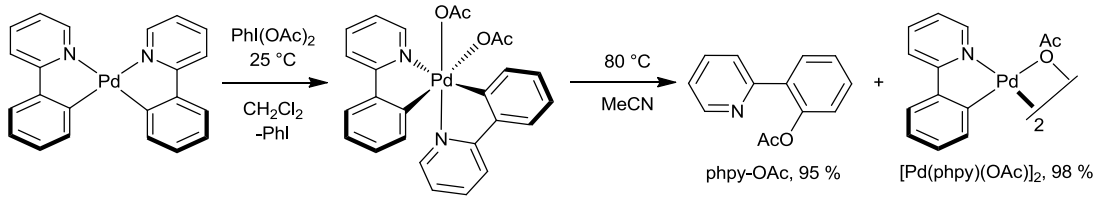

(XXXXII) **(XXXXIII)** **(XXXXIV)**

Scheme 7. Synthesis of $(phpy)_2Pd(OAc)_2$ and subsequent C-O bond formation.

Another recent report comes from the group of Ritter (Scheme 8).[98] Treatment of the aryl Pd^{II} complex **XXXXV** with Selectfluor® (1-chloromethyl-4-fluoro-1,4-diazoniabicyclo[2.2.2]octane bis-tetrafluoroborate) at room temperature yields a stable cationic Pd^{IV} complex. Alternatively XeF_2 can be used to form a stable neutral Pd^{IV} complex **XXXXVII**. When heated C-F bond formation occurs in high yield, the cationic complex undergoes reductive elimination with relative ease compared to the neutral complex. This is a helpful illustration of how much easier carbon element bond formation is at a cationic Pd^{IV} centre.

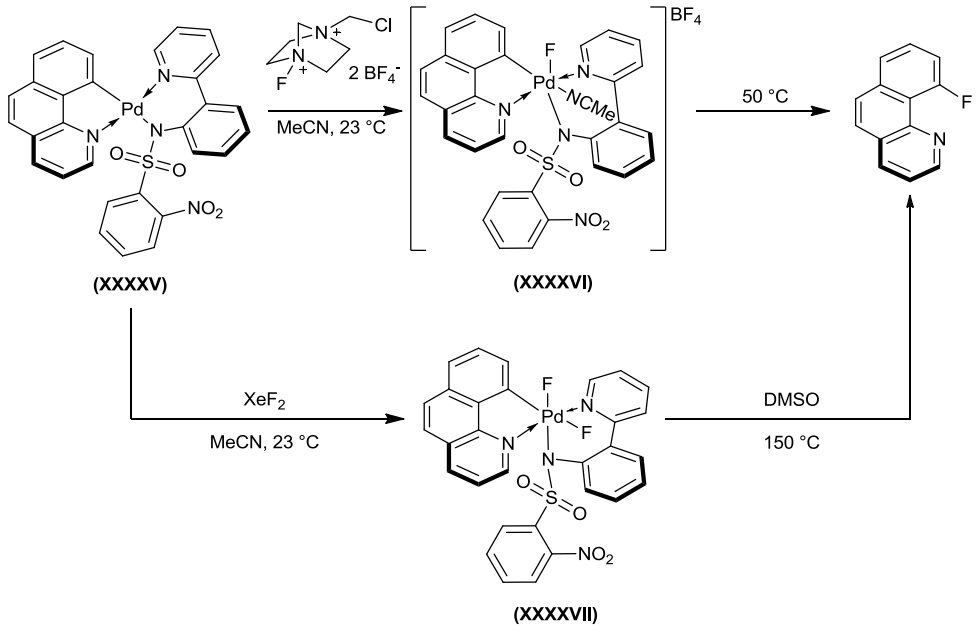

Scheme 9. Synthesis of monoarylpalladium(IV) complexes and C-F bond formation.[98]

1.6. Palladium(IV) in catalysis

The traditional approach to installing the desired functional group into an organic molecule is through functional group interconversion, Scheme 9. Palladium has made a valuable contribution to organic synthesis through $Pd^{0/II}$ cross-coupling reactions. Alternatively C-H activation to form a carbon-metal bond followed by functionalisation yields the desired molecule.

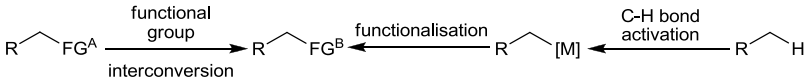

Scheme 9. Alternative approaches to functionalisation of organic substrates.

The challenge with the second approach is reactivity (C-H bonds have a high bond energy) and selectivity (C-H bonds are ubiquitous). The solution is to use substrates which contain a directing group such that only one C-H bond is held proximal to the metal centre (Scheme 10). This approach has been used successfully by many groups for C-C bond formation.[99]

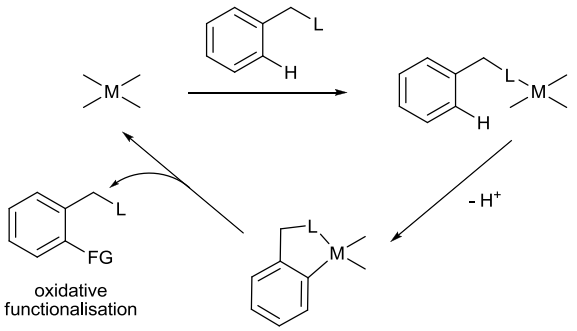

Scheme 10. Alternative approaches to functionalisation of organic substrates.

Crabtree and co-workers observed that $Pd(OAc)_2$ could catalyse the functionalisation of benzene by $PhI(OAc)_2$ (Equation 10).[100] The reaction was proposed to proceed via a Pd^{IV} intermediate.

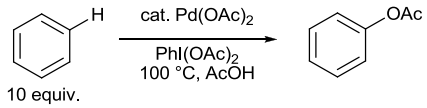

(10)

The key link made by the Sanford group was to combine the two ideas. In the proposed Pd^{II}/Pd^{IV} cycle for these transformations, ligand-directed C-H activation - step a in Scheme 11 - is followed by oxidation of Pd^{II} to Pd^{IV} in the presence of a strong oxidant (step b). The resulting Pd^{IV} complex can then undergo C-X bond-forming reductive elimination (step c) to generate the product. Recently, similar Pd^{IV} or closely related dimeric Pd^{III} intermediates have been proposed in many different Pd-catalyzed reactions, including C-H functionalisations, aminofunctionalisations of alkenes, the construction of cyclopropanes from enynes, and the arylhalogenation of olefins.[99, 101-106]

The best current methods for catalytic ligand-directed functionalisation of arene and alkane C-H bonds employ $Pd(OAc)_2$ as a catalyst in conjunction with a terminal oxidant such as $PhI(OAc)_2$, $PhICl_2$ or an *N*-halosuccinimide.[23, 107-112]

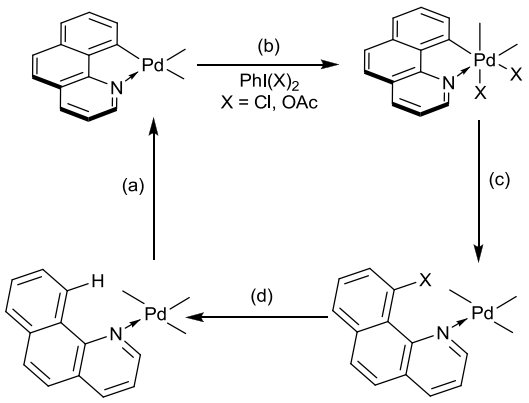

Scheme 11. $Pd(OAc)_2$ catalysed functionalisation of benzo[h]quinoline. a) ligand directed C-H activation; b) oxidation of Pd^{II} to Pd^{IV} by $PhI(X)_2$; c) C-X bond-forming reductive elimination; d) ligand exchange.

It is not possible to directly observe the proposed Pd^{IV} intermediates in the catalytic reactions due to the low stability of such species. Model Pd^{IV} complexes have been synthesised and used to study the mechanism of reductive elimination in forming C-O, C-Cl and C-F bonds.[88, 97, 113]

Selective C-H bond functionalisation has the potential to transform the way important chemicals are synthesised in the same way that the discovery of Pd cross-coupling reactions did. The attractiveness of these reactions in organic synthesis is that there is no requirement for prefunctionalisation and they allow for diversification at a late stage in the synthesis of complicated molecules.

While $Pd^{II/IV}$-catalyzed processes are efficient and selective for certain classes of substrates, significant challenges remain in this field. In particular, the development of novel catalysts with enhanced activity, broader scope, and chiral ligand environments would be highly desirable. However, catalyst design for this mechanistic manifold has been extremely limited due to the relatively small subset of ancillary ligands (predominantly sp^2 N donors and carboxylates)[88, 91, 97, 98, 113] that are known to support high oxidation state Pd centres.

1.7. Aims of this work

Several key features must be considered in the design of ancillary ligands for these oxidative transformations. First, suitable ligands should be strong σ-donors (it is unlikely that a d^6 Pd^{IV} center has orbitals low enough in energy to accept electrons *via* π-donation) and sufficiently bulky and/or chelating to help stabilize the higher palladium oxidation states.[88, 91, 97, 98, 113] Second, the ligands must be resistant to decomposition under the highly oxidizing reaction conditions. Third, it is essential that the supporting ligands do not participate in reductive elimination reactions that compete with functionalisation of the desired substrate. Finally, the ideal ancillary ligands would be modular, in order to facilitate the design of new catalysts for regio- and stereoselective reactions.[114, 115]

The Arnold group has previously used N-heterocyclic carbene (NHC) ligands functionalized with tethered anionic alkoxy or amido groups to stabilize high oxidation state metal cations.[1, 2] Such ligands are attractive candidates for accessing the target Pd^{IV} species because NHC-Pd^{II} complexes are known to be stable in acidic reaction media and in the presence of strong oxidants.[116, 117] Based on these considerations, we set out to synthesize Pd^{II} complexes containing chelating carbene ligands that could participate in key steps of the catalytic cycle in Scheme 11. To this end, variants of both the alkoxy and amido NHC ligands will be utilised.

The aim of this project is to synthesise symmetric and asymmetric Pd complexes of anionic-tethered NHC ligands that exhibit high stability under C-H activation/oxidation conditions. Isolation of a stable Pd^{IV} complex which represents a viable intermediate in the catalytic cycle is strongly desired.

To aid this process a total of nine months were spent at the University of Michigan, in the group of Prof. Melanie S. Sanford. This gave the opportunity to approach the problem from a different perspective and for the author to learn new techniques.

1.8. References

[1] P. L. Arnold and I. J. Casely, *Chem. Rev.*, 2009, **109**, 3599.

[2] P. L. Arnold, S. A. Mungur, A. J. Blake, and C. Wilson, *Angew. Chem., Int. Ed.*, 2003, **42**, 5981.

[3] F. A. W. Cotton, G.; Murillo, C. A.; Bochmann, M., in 'Advanced Inorganic Chemistry, 6th ed.' ed. F. A. Cotton, 1999.

[4] J. C. Green, R. G. Scurr, P. L. Arnold, and F. G. N. Cloke, *Chem. Commun.*, 1997, 1963.

[5] D. J. Cardin, B. Cetinkaya, E. Cetinkaya, M. F. Lappert, L. J. Manojlovic-Muir, and K. W. Muir, *J. Organomet. Chem.*, 1972, **44**, C59.

[6] A. J. Arduengo, III, R. L. Harlow, and M. Kline, *J. Am. Chem. Soc.*, 1991, **113**, 361.

[7] D. Pugh and A. A. Danopoulos, *Coord. Chem. Rev.*, 2007, **251**, 610.

[8] M. Poyatos, J. A. Mata, and E. Peris, *Chem. Rev.*, 2009, **109**, 3677.

[9] E. A. B. Kantchev, C. J. O'Brien, and M. G. Organ, *Angew. Chem., Int. Ed.*, 2007, **46**, 2768

[10] F. Boeda and S. P. Nolan, *Annual Reports Section "B" (Organic Chemistry)*, 2008, **104**, 184.

[11] F. E. Hahn and C. J. Mareike *Angew. Chem., Int. Ed. Engl.*, 2008, **47**, 3122.

[12] M. C. Perry and K. Burgess, *Tetrahedron: Asymmetry*, 2003, **14**, 951.

[13] R. A. Kelly Iii, H. Clavier, S. Giudice, N. M. Scott, E. D. Stevens, J. Bordner, I. Samardjiev, C. D. Hoff, L. Cavallo, and S. P. Nolan, *Organometallics*, 2007, **27**, 202.

[14] S. Díez-González and S. P. Nolan, *Coord. Chem. Rev.*, 2006.

[15] D. G. Gusev, *Organometallics*, 2009, **28**, 6458.

[16] M. Muehlhofer, T. Strassner, and W. A. Herrmann, *Angew. Chem., Int. Ed.*, 2002, **41**, 1745.

[17] A. A. Danopoulos, N. Tsoureas, J. C. Green, and M. B. Hursthouse, *Chem. Commun. (Cambridge, U. K.) FIELD Full Journal Title:Chemical Communications (Cambridge, United Kingdom)*, 2003, 756.

[18] Y. Kong, H. Ren, S. Xu, H. Song, B. Liu, and B. Wang, *Organometallics*, 2009, **28**, 5934.

[19] K. S. Yoo, J. O'Neill, S. Sakaguchi, R. Giles, J. H. Lee, and K. W. Jung, *J. Org. Chem.*, **75**, 95.

[20] B. A. Steinhoff, S. R. Fix, and S. S. Stahl, *J. Am. Chem. Soc.*, 2002, **124**, 766.

[21] D. R. Jensen, M. J. Schultz, J. A. Mueller, and M. S. Sigman, *Angew. Chem., Int. Ed.*, 2003, **42**, 3810.

[22] J. A. Mueller and M. S. Sigman, *J. Am. Chem. Soc.*, 2003, **125**, 7005.

[23] A. R. Dick, K. L. Hull, and M. S. Sanford, *J. Am. Chem. Soc.*, 2004, **126**, 2300.

[24] B. Karimi and A. Zamani, *J. Iran. Chem. Soc.*, 2008, **5**, S1.

[25] G. M. Kapteijn, A. Dervisi, D. M. Grove, H. Kooijman, M. T. Lakin, A. L. Spek, and G. v. Koten, *J. Am. Chem. Soc.*, 1995, 10939.

[26] J.-C. C. Yong-Joo Kim, Kohtaro Osakada, *Journal of Organometallic Chemistry* 1995, **491**, 97.

[27] R. J. Nielsen and W. A. Goddard, III, *J. Am. Chem. Soc.*, 2006, **128**, 9651.

[28] G. Marc Kapteijn, D. M. Grove, G. van Koten, W. J. J. Smeets, and A. L. Spek, *Inorg. Chim. Acta*, 1993, **207**, 131.

[29] R. M. Trend and B. M. Stoltz, *J. Am. Chem. Soc.*, 2008, **130**, 15957.

[30] S. Kannan, A. J. James, and P. R. Sharp, *Polyhedron*, 2000, **19**, 155.

[31] Y. Kobayashi, N. Nagao, S. Okeya, and Y. Fukuda, *Chem. Lett.*, 1996, 663.

[32] S. Okeya, S. Koshino, M. Namie, I. Nagasawa, and Y. Kushi, *J. Chem. Soc., Chem. Commun.*, 1995, 2123.

[33] G. Lopez, J. Ruiz, G. Garcia, J. M. Marti, G. Sanchez, and J. Garcia, *J. Organomet. Chem.*, 1991, **412**, 435.
[34] P. J. Chung, *Taehan Hwahakhoe Chi*, 1986, **30**, 516.
[35] A. R. Siedle and L. H. Pignolet, *Inorg. Chem.*, 1982, **21**, 3090.
[36] R. Sugimoto, H. Eikawa, H. Suzuki, Y. Moro-Oka, and T. Ikawa, *Bull. Chem. Soc. Jpn.*, 1981, **54**, 2849.
[37] M. Louey, P. D. Nichols, and R. Robson, *Inorg. Chim. Acta*, 1981, **47**, 87.
[38] A. B. Goel and S. Goel, *Transition Met. Chem. (Netherlands)*, 1980, **5**, 378.
[39] P. J. Chung, H. Suzuki, Y. Moro-Oka, and T. Ikawa, *Chem. Lett.*, 1980, 63.
[40] H. Suzuki, K. Mizutani, Y. Morooka, and T. Ikawa, *J. Am. Chem. Soc.*, 1979, **101**, 748.
[41] C. B. Anderson, B. J. Burreson, and J. T. Michalowski, *J. Org. Chem.*, 1976, **41**, 1990.
[42] D. A. White, *J. Chem. Soc. A* 1971, 143.
[43] M. Achternbosch and P. Klufers, *Acta Crystallogr., Sect. C: Cryst. Struct. Commun.*, 1994, **50**, 175.
[44] R. Ahlrichs, M. Ballauff, K. Eichkorn, O. Hanemann, G. Kettenbach, and P. Klüfers, *Chem.-Eur. J.*, 1998, **4**, 835.
[45] X. Kastele, P. Klufers, and T. Kunte, *Z. Anorg. Allg. Chem.*, 2001, **627**, 2042.
[46] P. Klüfers and T. Kunte, *Angew. Chem., Int. Ed. Engl.*, 2001, **40**, 4210.
[47] P. Klufers and T. Kunte, *Eur. J. Inorg. Chem.*, 2002, 1285.
[48] P. Klüfers and T. Kunte, *Eur. J. Inorg. Chem.*, 2002, **2002**, 1285.
[49] P. Klufers and T. Kunte, *Chem.-Eur. J.*, 2003, **9**, 2013.
[50] P. Klüfers and T. Kunte, *Chem.-Eur. J.*, 2003, **9**, 2013.
[51] T. Allscher, P. Klufers, and O. Labisch, *Carbohydr. Res.*, 2007, **342**, 1419.
[52] Y. Arendt, O. Labisch, and P. Klufers, *Carbohydr. Res.*, 2009, **344**, 1213.
[53] P. L. Alsters, J. Boersma, W. J. J. Smeets, A. L. Spek, and G. v. Koten, *Organometallics*, 1993, **12**, 1639.
[54] M. D. Fryzuk and P. A. MacNeil, *J. Am. Chem. Soc.*, 1981, **103**, 3592.
[55] M. D. Fryzuk, P. A. MacNeil, S. J. Rettig, A. S. Secco, and J. Trotter, *Organometallics*, 1982, **1**, 918.
[56] A. Singh, U. Anandhi, M. A. Cinellu, and P. R. Sharp, *Dalton Trans.*, 2008, 2314.
[57] J. Ruiz, V. Rodríguez, G. López, P. A. Chaloner, and P. B. Hitchcock, *J. Chem. Soc., Dalton Trans.*, 1997, 4271.
[58] J. Ruiz, N. Cutillas, J. Torregrosa, G. Garcia, G. Lopez, P. A. Chaloner, P. B. Hitchcock, and R. M. Harrison, *J. Chem. Soc., Dalton Trans.*, 1994.
[59] A. Hadzovic, J. Janetzko, and D. Song, *Dalton Trans.*, 2008, 3279.
[60] A. L. Seligson, R. L. Cowan, and W. C. Trogler, *Inorg. Chem.*, 1991, **30**, 3371.
[61] L. A. Villanueva, K. A. Abboud, and J. M. Boncella, *Organometallics*, 1994, **13**, 3921.
[62] M. S. Driver and J. F. Hartwig, *J. Am. Chem. Soc.*, 1996, **118**, 4206.
[63] H. E. Bryndza, L. K. Fong, R. A. Paciello, W. Tam, and J. E. Bercaw, *J. Am. Chem. Soc.*, 1987, **109**, 1444.
[64] Y.-J. Kim, J.-C. Choi, and K. Osakada, *J. Organomet. Chem.*, 1995, **491**, 97.
[65] S. Y. Ryu, H. Kim, H. S. Kim, and S. Park, *J. Organomet. Chem.*, 1999, **592**, 194.
[66] L. Fan, B. M. Foxman, and O. V. Ozerov, *Organometallics*, 2004, **23**, 326.
[67] L. Fan, L. Yang, C. Guo, B. M. Foxman, and O. V. Ozerov, *Organometallics*, 2004, **23**, 4778.
[68] O. V. Ozerov, C. Guo, L. Fan, and B. M. Foxman, *Organometallics*, 2004, **23**, 5573.
[69] W. Weng, C. Guo, C. Moura, L. Yang, B. M. Foxman, and O. V. Ozerov, *Organometallics*, 2005, **24**, 3487.
[70] C. M. Fafard and O. V. Ozerov, *Inorg. Chim. Acta*, 2007, **360**, 286.
[71] L.-C. Liang, P.-S. Chien, and M.-H. Huang, *Organometallics*, 2004, **24**, 353.

[72] L.-C. Liang, P.-S. Chien, and M.-H. Huang, *Organometallics*, 2005, **24**, 353.
[73] J. Storch, J. Cermák, M. Posta, J. Sýkora, and I. Císarová, *J. Organomet. Chem.*, 2008, **693**, 3029.
[74] A. N. Marziale, E. Herdtweck, J. r. Eppinger, and S. Schneider, *Inorg. Chem.*, 2009, **48**, 3699.
[75] D. Hedden and D. M. Roundhill, *Inorg. Chem.*, 1985, **24**, 4152.
[76] J. C. Peters, S. B. Harkins, S. D. Brown, and M. W. Day, *Inorg. Chem.*, 2001, **40**, 5083.
[77] R. E. Douthwaite, J. Houghton, and B. M. Kariuki, *Chem. Commun.*, 2004, 698.
[78] W. Wei, Y. Qin, M. Luo, P. Xia, and M. S. Wong, *Organometallics*, 2008, **27**, 2268.
[79] D. A. Culkin and J. F. Hartwig, *Organometallics*, 2004, **23**, 3398.
[80] M. Yamashita, J. V. Cuevas Vicario, and J. F. Hartwig, *J. Am. Chem. Soc.*, 2003, **125**, 16347.
[81] M. W. Hooper and J. F. Hartwig, *Organometallics*, 2003, **22**, 3394.
[82] M. S. Driver and J. F. Hartwig, *J. Am. Chem. Soc.*, 1997, **119**, 8232.
[83] M. S. Driver and J. F. Hartwig, *Organometallics*, 1997, **16**, 5706.
[84] G. Mann and J. F. Hartwig, *J. Am. Chem. Soc.*, 1996, **118**, 13109.
[85] N. Marion, O. Navarro, J. Mei, E. D. Stevens, N. M. Scott, and S. P. Nolan, *J. Am. Chem. Soc.*, 2006, **128**, 4101.
[86] P. Sehnal, R. J. K. Taylor, and I. J. S. Fairlamb, *Chemical Reviews*, 2010, **110**, 824.
[87] R. Uson, J. Fornies, and R. Navarro, *J. Organomet. Chem.*, 1975, **96**, 307.
[88] N. D. Ball and M. S. Sanford, *J. Am. Chem. Soc.*, 2009, **131**, 3796.
[89] A. J. Canty, *Acc. Chem. Res.*, 1992, **25**, 83.
[90] A. J. Canty, *Dalton Trans.*, 2009, 10409.
[91] A. J. Canty, in 'Palladium complexes containing Pd(I), Pd(III), or Pd(IV)', ed. E.-I. Negishi, New York, 2002.
[92] L.-M. Xu, B.-J. Li, Z. Yang, and Z.-J. Shi, *Chem. Soc. Rev.*, 2009, **39**, 712.
[93] M. Kilian, *Angew. Chem., Int. Ed. Engl.*, 2009, **48**, 9412.
[94] A. J. Canty, M. C. Denney, G. van Koten, B. W. Skelton, and A. H. White, *Organometallics*, 2004, **23**, 5432.
[95] A. J. Canty, M. C. Denney, B. W. Skelton, and A. H. White, *Organometallics*, 2004, **23**, 1122.
[96] A. R. Dick, J. W. Kampf, and M. S. Sanford, *J. Am. Chem. Soc.*, 2005, **127**, 12790.
[97] J. M. Racowski, A. R. Dick, and M. S. Sanford, *J. Am. Chem. Soc.*, 2009, **131**, 10974.
[98] T. Furuya and T. Ritter, *J. Am. Chem. Soc.*, 2008, **130**, 10060.
[99] N. R. Deprez and M. S. Sanford, *J. Am. Chem. Soc.*, 2009, **131**, 11234.
[100] T. Yoneyama and R. H. Crabtree, *J. Mol. Catal A: Chem.*, 1996, **108**, 35.
[101] D. C. Powers and T. Ritter, *Nature Chem.*, 2009, **1**, 302.
[102] T. W. Lyons and M. S. Sanford, *Tetrahedron*, 2009, **65**, 3211.
[103] K. Muniz, C. H. Hoevelmann, and J. Streuff, *J. Am. Chem. Soc.*, 2008, **130**, 763.
[104] D. Kalyani and M. S. Sanford, *J. Am. Chem. Soc.*, 2008, **130**, 2150.
[105] Y. Li, D. Song, and V. M. Dong, *J. Am. Chem. Soc.*, 2008, **130**, 2962.
[106] G. Liu and S. S. Stahl, *J. Am. Chem. Soc.*, 2006, **128**, 7179.
[107] L. V. Desai, K. L. Hull, and M. S. Sanford, *J. Am. Chem. Soc.*, 2004, **126**, 9542.
[108] D. Kalyani, A. R. Dick, W. Q. Anani, and M. S. Sanford, *Tetrahedron*, 2006, **62**, 11483.
[109] H. Kodama, T. Katsuhira, T. Nishida, T. Hino, and K. Tsubata, *Chem. Abstr.*, 2001, **135**, 344284.
[110] J. J. Li, R. Giri, and J. Q. Yu, *Tetrahedron*, 2008, **64**, 6979.
[111] D. Kalyani, N. R. Deprez, L. V. Desai, and M. S. Sanford, *J. Am. Chem. Soc.*, 2005, **127**, 7330.
[112] D. Kalyani and M. S. Sanford, *Organic Letters*, 2005, **7**, 4149.

[113] S. R. Whitfield and M. S. Sanford, *J. Am. Chem. Soc.*, 2007, **129**, 15142.
[114] B. F. Shi, N. Maugel, Y. H. Zhang, and J. Q. Yu, *Angew. Chem., Int. Ed.*, 2008, **47**, 4882.
[115] T. Tsujihara, K. Takenaka, K. Onitsuka, M. Hatanaka, and H. Sasai, *J. Am. Chem. Soc.*, 2009, **131**, 3452.
[116] D. Meyer, M. A. Taige, A. Zeller, K. Hohlfeld, S. Ahrens, and T. Strassner, *Organometallics*, 2009, **28**, 2142.
[117] M. S. Viciu, E. D. Stevens, J. L. Petersen, and S. P. Nolan, *Organometallics*, 2004, **23**, 3752.

Chapter 2
Synthesis of starting materials

Chapter 2 – Synthesis of starting materials

2.1. Introduction

DFT calculations are used throughout this thesis to complement the experimental data and sections 2.2 to 2.6 discuss how the appropriate level of theory was chosen. Detailed results for all calculations can be found on the appendix DVD.

Previous reports of palladium complexes bearing bidentate mono-anionic tethered NHCs have been limited to aryloxy,[1-4] amidate,[5-9] thio[10-12] and carboxylate[13] tethers. A number of tridentate CNC NHC-Pd complexes have also been reported.[14-16] Sections 2.7 to 2.12 expands the range of palladium complexes bearing bidentate mono-anionic tethered NHCs to alkoxide and amido tethers. The synthesis of homoleptic and heteroleptic palladium complexes utilising tethered-NHCs are also considered.

2.2. Generating structures for calculations

Initial structures were drawn using GaussView,[17] Argus Lab[18] or Gabedit[19] and a simple molecular mechanics optimisation was performed. All calculations were carried out using GAUSSIAN 03 computational chemistry program.[17] Further optimisation of these structures was carried out using RHF/LANL2DZ.[20-23] This allowed geometries close to the correct structure to be obtained with relatively low computational expense.

2.3. Choosing a functional and basis set

There are a number of recent computational papers exploring the reactivity of $Pd^{II/IV}$ systems.[24-29] The functional B3LYP[30-32] is used almost exclusively whilst a range of basis sets have been employed. The majority of papers utilise a version of LANL2DZ[20-23] whilst a few use a version of SDD.[33] Some authors add extra diffuse and polarisation functions to heavy elements (*i.e.* Pd, Br and I).

DFT can miss conformers if dispersion is important (*i.e.* induced dipole moments that cause attraction). Polarisation functions are those with higher angular momentum quantum number (*e.g.* p, d, f) and are important for delocalised charge whilst diffuse functions have higher principle quantum numbers (e.g. 3p, 4p). For light elements (*i.e.* C, H, N and O) the basis set 6-31G(d) is commonly used for geometry optimisations, with 6-311+G(2d,p) or higher used in single point calculations to gain extra accuracy.

The challenge is to balance the accuracy of the result with the computational cost. A greater number of basis functions generally lead to a better approximation to the actual wavefunction. DFT costs about the same as Hartree Fock in the time required but is of much better quality. For DFT calculations the expense increases N^3 with the number of non-hydrogen atoms. For systems containing atoms with a large number of electrons an effective core potential basis set is often used. The core electrons not involved in the bonding are modelled as a single unit, dramatically cutting the cost (*e.g.* LanL2DZ or SDD).

Four different combinations of split basis sets were considered initially:

i.) B3LYP/LanL2DZ/6-31G(d,p)

ii.) B3LYP/LanL2DZ/6-311+G(2d,p)

iii.) B3LYP/LanL2TZ/6-311+G(2d,p) with added f-polarisability on Pd

iv.) B3LYP/SDD/6-311+G(2d,p)

2.4. Evaluating basis sets using (L^O)Pd(phpy)

The suitability of the basis set combinations i-iv was considered by calculating the structure of (L^O)Pd(phpy). The availability of a single crystal X-ray structure (section 2.11.2) and I.R. spectrum of (L^O)Pd(phpy) made the task much simpler.

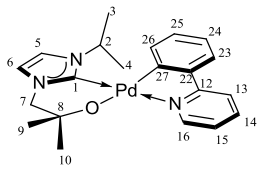

Figure 1. Numbering Scheme for the carbon atoms in (L^O)Pd(phpy).

The X-ray structure of (L^O)Pd(phpy) was first optimised using RHF/LANL2DZ before carrying out a geometry optimisation and vibrational analysis with one of the chosen basis sets (i-iv). The results shown in Figures 2 - 5 are summarised in Table 1.

Parameter	X-Ray	LanL2DZ/ 6-31G(d,p)	LanL2DZ/ 6-311+G(2d,p)	LanL2TZ/ 6-311+G(2d,p)	SDD/ 6-311+G(2d,p)
Pd-O1(Å)	2.043(2)	2.0925	2.1018	2.0878	2.0883
Pd-N3 (Å)	2.059(2)	2.0967	2.0978	2.0884	2.0908
Pd-C27(Å)	1.999(2)	2.0273	2.0224	2.0181	2.0193
Pd-C1(Å)	1.982(2)	2.0022	2.0035	1.9985	1.9981
O1-Pd-C1 (°)	91.06	88.08	88.35	88.56	88.45
C1-Pd-N3 (°)	101.15	101.35	101.53	101.44	101.47
O1-C8 (Å)	1.398(3)	1.3858	1.3877	1.3889	1.3889
Deviation C-C	-	0.96 %	0.67 %	0.66 %	0.67 %
Computational Expense (h)	-	38	569	565	632

Table 1. Selected bond lengths, angles and costs. All the calculated N-C distances fall within the standard deviation for the X-ray structure.

The geometries calculated for i-iv are very similar. Some difference between the X-ray structure and the calculated structures would be expected due to packing forces (the calculated structure is essentially gas phase). The basis sets chosen show reasonable agreement with the X-ray data. The biggest differences concern bonds and angles around palladium (Figure 3 and 4).

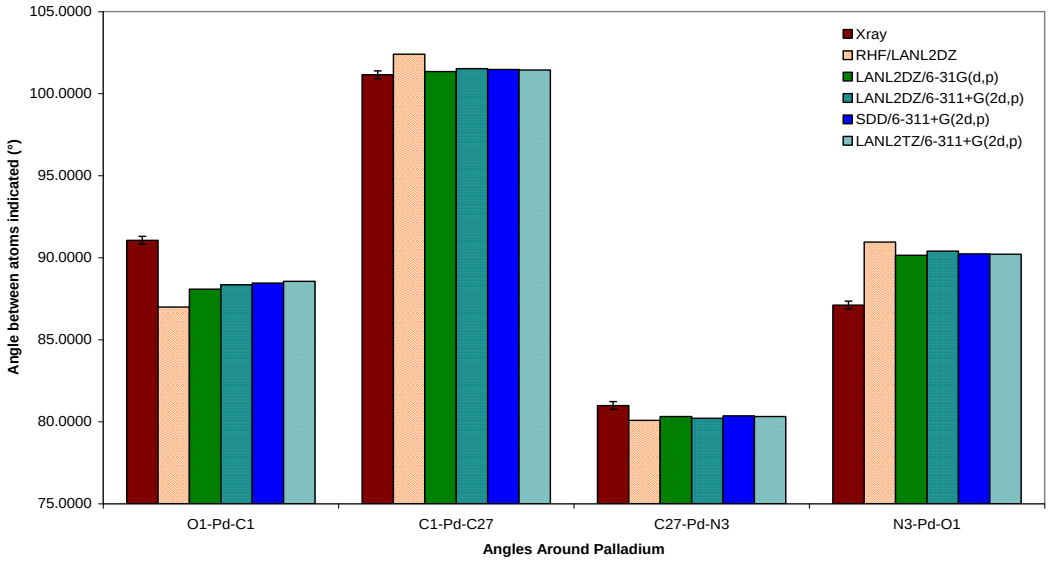

Figure 2. Comparison between experimental and calculated angles around palladium.

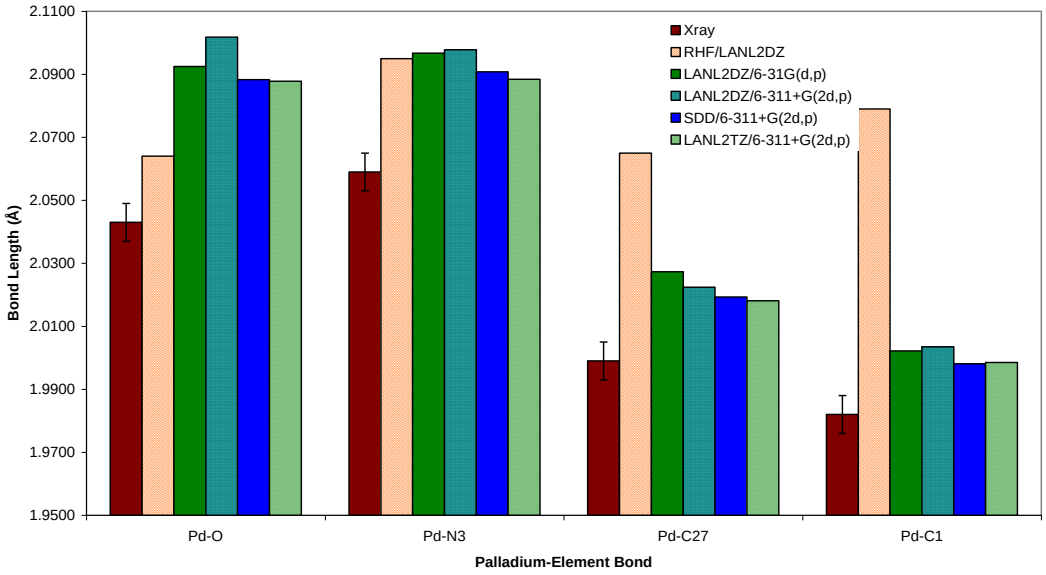

Figure 3. Comparison between experimental and calculated Pd-element bond lengths.

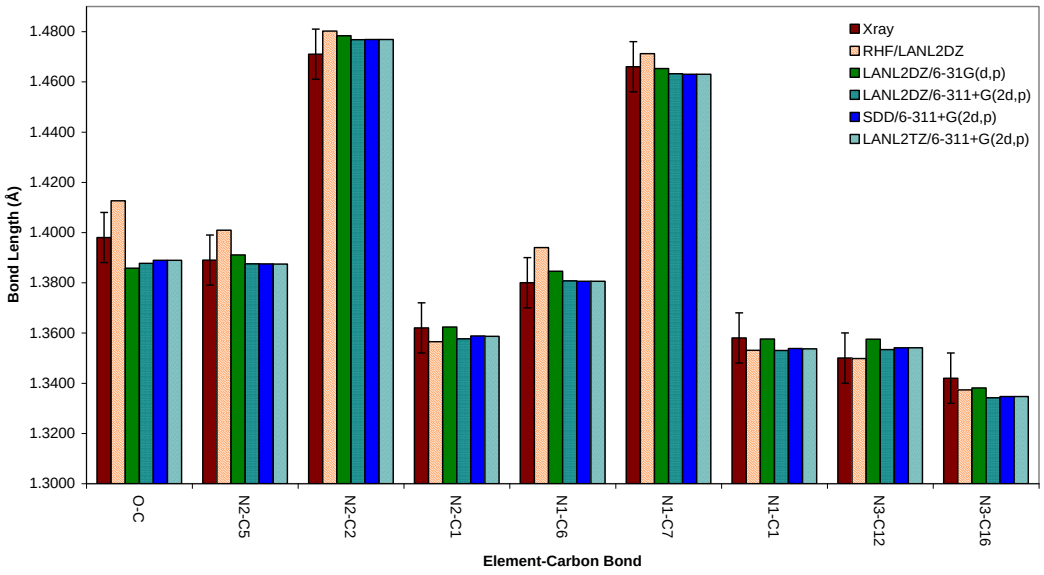

Figure 4. Comparison between experimental and calculated element-C bond lengths.

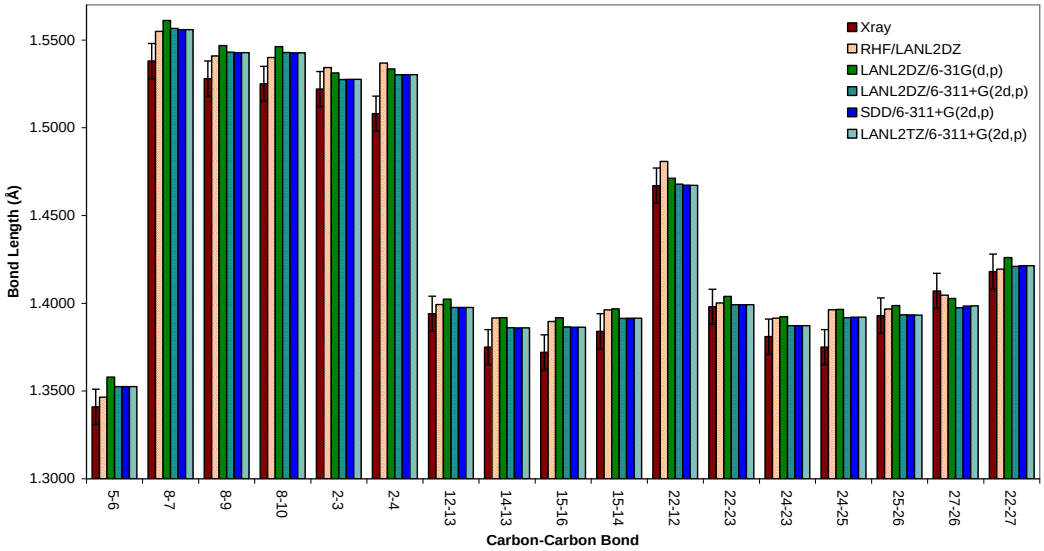

Figure 5. Comparison between experimental and calculated C-C bond lengths.

Another measure of the suitability of a given level of theory is to compare the calculated I.R. spectrum with the experimental spectrum. Vibrational calculations are based on the approximation that modes are harmonic. Deviations will occur where there may be significant anharmonicity. Commonly this occurs on very flat potential energy surfaces (such as a protein backbone), in minima separated by a very low barrier (torsional changes at a

transition state) or where there is strong anharmonic coupling. Additionally these calculations do not compute overtone or combination bands which may be present in the experimental spectra. Typically the calculated harmonic frequencies are systematically higher than the experimental data so a scaling factor is applied.[34]

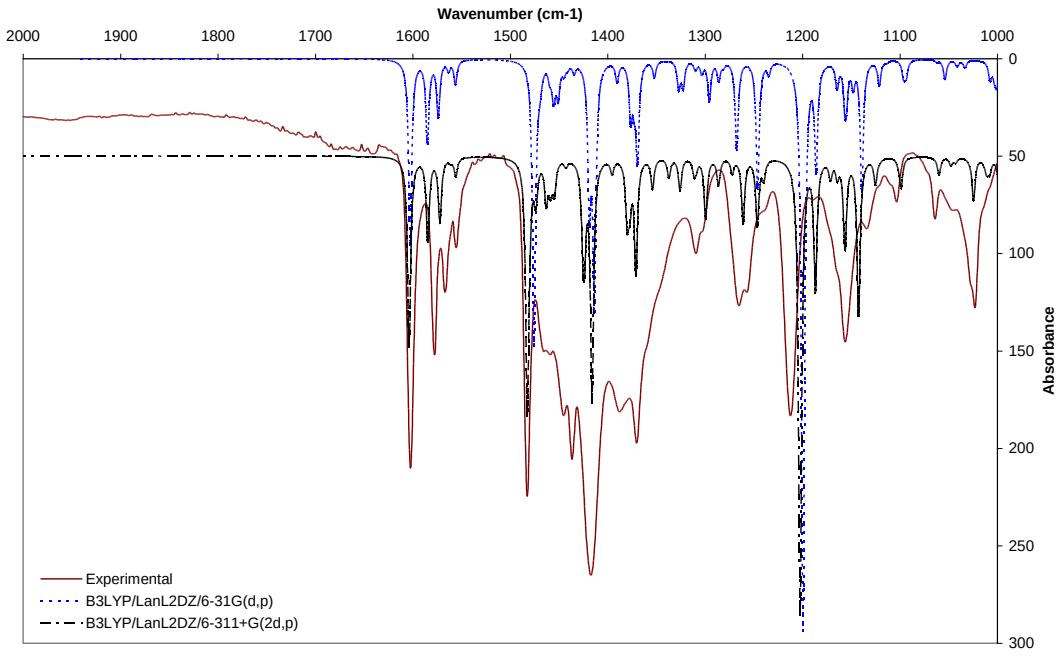

Figure 6. Comparison of calculated and experimental I.R. for (L^O)Pd(phpy). The results for basis sets ii-iv are essentially identical so only i and ii are included for comparison. The calculated I.R. spectra were scaled by 0.96 (6-31+G(2d,p)) or 0.97 (6-31G(d,p)).

The region of interest is 2000 to 1000 cm^{-1}. The computed spectra closely match the experimentally determined result allowing straightforward assignment of the vibrations which were visualised using Jmol.[35] As expected 6-311+G(2d,p) is a better fit than 6-31G(d,p) but the improvement is only marginal. The HOMO and LUMO isosurfaces of (L^O)Pd(phpy) were plotted for each of the chosen methods (i-iv). The size, shape and location of the electron density were essentially the same in each case.

The major difference between the methods investigated is the computational expense. Using the functional B3LYP in conjunction with LANL2DZ (Pd, Br and I) and 6-31G(d,p) (H, C, O, N and Cl) gives useful results in an acceptable length of time.

2.5. Simplification of ligands to reduce computational expense

To reduce the level of computational expense further the effect of replacing the *iso*-propyl group with a methyl was evaluated (Figure 8). Since the CH_3 groups in the *iso*-propyl group are pointing away from the palladium the steric effect should be minimal but the electronic effect (which is more subtle) is hard to estimate.

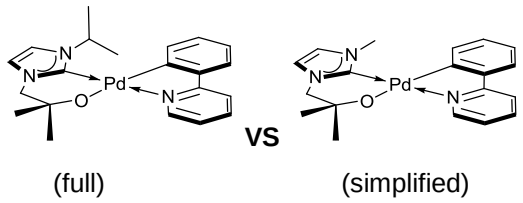

Figure 7. Two structures of (L^O)Pd(phpy) under comparison

There is very little structural change upon simplifying the ligand. The bond lengths around Pd change by only 0.002 Å whilst the angles shift by up to 0.4°. There is a significant drop in the computational cost (table 2).

Parameter	Full L^O ligand	Simplified L^O ligand
Pd-O1(Å)	2.0925	2.0938
Pd-N3 (Å)	2.0967	2.0956
Pd-C27(Å)	2.0273	2.0277
Pd-C1(Å)	2.0022	1.9992
O1-Pd-C1 (°)	88.08	88.54
C1-Pd-C27 (°)	101.35	101.50
C27-Pd-N3 (°)	80.32	80.36
N3-Pd-O1 (°)	90.15	89.98
Computational Expense (h)	38	30

Table 2. Selected bond lengths, angles and costs.

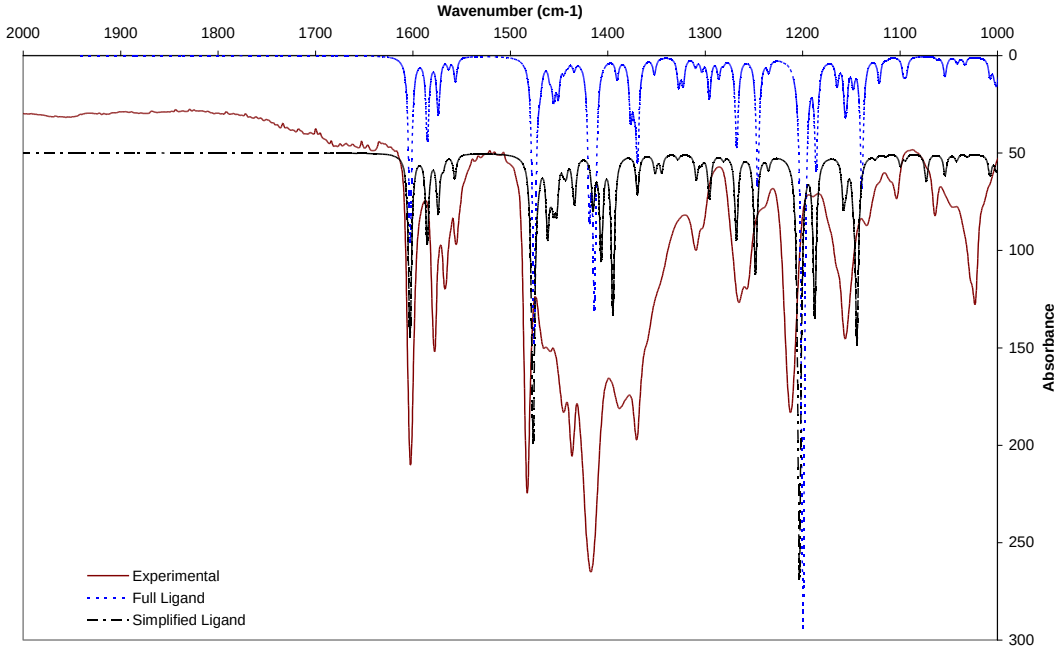

Figure 8. Comparison of calculated (full and simplified ligand) with experimental I.R. for (L^O)Pd(phpy). The calculated I.R. spectra were scaled by 0.97.

Comparing the I.R. spectra (Figure 8) there are subtle differences in the range 1300 to 1500 cm^{-1}. The differences are small enough not to interfere with assignment of the experimental data.

Complexes	Full L^O ligand (kcal/mol)	Simplified L^O ligand (kcal/mol)
(L^O)Pd($phpy^H$)(succ.) + NBS	+4.75	+5.28
(L^O)Pd(phpy) + NBS + Hsucc.	0	0
(L^O)Pd(phpy)(br)(succ.)^a + Hsucc.	-0.32	-1.77
(L^O)Pd(phpy)(br)(succ.)^b + Hsucc.	+0.33	-0.83
(L^O)Pd($phpy^{Br}$)(succ.) + Hsucc.	-20.90	-20.77

Table 3. Effect of ligand simplification on thermodynamic reaction profile for (L^O)Pd(phpy) and NBS (most stable isomers). $^aN_{succ}$-Br opposite in Pd^{IV} complex. $^bN_{succ}$-Br adjacent in Pd^{IV} complex.

The oxidations of (L^O)Pd(phpy) with NBS and with $PhI(Cl)_2$ were also considered. The most stable isomer identified for the simplified ligand was also calculated for the full ligand. As Table 3 shows there is very little difference in the thermodynamics of the two systems (with NBS). Given the comparatively simple level of theory being employed the simplified system

can be considered isoenergetic. The same was observed with the C-Cl bond forming transition state.

Complexes	Full L^O ligand (kcal/mol)	Simplified L^O ligand (kcal/mol)
$(L^O)Pd(phpy) + PhI(Cl)_2$	0	0
$(L^O)Pd(phpy)Cl_2 + PhI$	-37.48	-37.28
C-Cl bond forming TS + PhI	-15.18	-14.52
Barrier to TS	-22.30	-22.76

Table 4. Effect of ligand simplification on reaction profile for $(L^O)Pd(phpy)$ and $PhI(Cl)_2$ (most stable isomers). The calculated t½ (at 298.15 K) is 41 mins (full) or 89 mins (simplified).

Detailed analysis once the calculations were completed showed that the simplification did not always lead to computational savings. The greater number of available low energy conformers of the methyl group compared to *iso*propyl meant the potential energy surface around the minima was flatter for the simplified ligand, and hence, the geometry optimisations sometimes took longer to converge.

2.6. Accounting for solvent effects

Solvation effects can significantly change the energy of both intermediates and ground state structures. To explore what effect this might have on the calculated reaction profiles, solvation corrections were carried out for the most stable isomers calculated in the gas phase for the reaction between $(L^O)Pd(phpy)$ and $PhICl_2$.

The polarisable continuum model was used in which the cavity around the molecule is created via a series of overlapping spheres, originally devised by Tomasi and coworkers.[36] Geometry optimisations carried out in the solvent field failed to converge. As a result single point calculations were carried out (using the gas phase optimised structures) and the vibrational frequencies calculated. The reaction profile was evaluated for MeCN (the solvent used experimentally) and DCM (since the dielectric constant is significantly different). The

product of C-H activation (L^O)Pd(phpy) was normalised to zero for each case and the data is summarised in Table 5.

Step	Gas Phase (kcal/mol)	MeCN (kcal/mol)	DCM (kcal/mol)
Starting Complex	-12.60	-11.90	-12.09
C-H Activation	0.00	0.00	0.00
Oxidation	-37.28	-46.40	-45.56
C-Cl bond forming TS	-14.52	-21.61	-19.85[a]
Product of reductive elimination	-49.37	-62.99	-61.41
Barrier to TS (t½ h @ 298.15 K)	22.76 (1.5)	24.78 (45)	25.71 (217)

Table 5. Effect of solvent on calculated thermodynamic profile. [a]Two negative frequencies in calculation output, one corresponding to the transition state, the other a whole molecule flex.

Inclusion of a solvent field has a greater effect on the energies than the choice of solvent. There is a large difference in dielectric constant between MeCN and DCM ($\varepsilon = 36.64$ and $\varepsilon = 8.93$ respectively) but difference in energy is small (1 - 2 kcal/mol). The choice of method to model the solvent is likely to have a greater effect than the choice of solvent.

For charged species (especially anionic ones) extra steps need to be taken to get accurate results when using DFT. Diffuse functions would be needed to be included in the basis sets and solvent effects (implicit and/or explicit) need to be accounted for. This can be seen in the systems studied. In the gas phase solvating Cl^- with five molecules of MeCN or AcO^- with six molecules of MeCN lowers the energy by 16.6 and 14.8 kcal/mol respectively. Calculations by others on charged Pd^{IV} complexes have shown that including the solvent effects can reduce the difference in energy between charged and non-charged species by as much as 70 kcal/mol.[37]

Only six structures (in the systems studied) required this level of treatment. To be able to comment effectively solvent correction would need to be applied to each system being studied. The information gained for such a small number of structures is not worth the extra computational expense of 27 - 45 h per structure.

2.7. Ligand design

Previous work in the group,[38] based on that by Glas *et al*,[39] has shown that the combination of an epoxide, imidazole and an alkyl halide is an atom efficient, versatile and high yielding route to proligands for alkoxy- NHCs. In the initial step a substituted epoxide undergoes ring opening at the least hindered end by imidazole. The resultant N-alkyl imidazole can be quaternised by treatment with an alkyl halide to afford the imidazolium halide proligand, Scheme 1. The proligand $[H^2L^{O,Me}]I$ (R^1 = R^2 = Me, R^3 = ^{i}Pr) has been synthesised previously.[38]

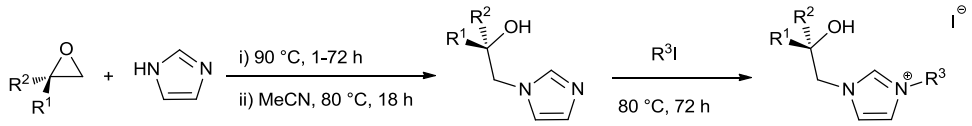

Scheme 1. Synthesis of alkoxy-tethered NHC proligands.

The flexible nature of the ligand design allows the synthesis of a wide range of bidentate anionic NHCs, Figure 9. The ligand design allows for straightforward incorporation of a variety of alkyl groups $R^{1\text{-}5}$. The incorporation of different groups at $R^{1\text{-}5}$ allows for the introduction of chirality. The anionic NHCs are obtained from imidazolium salt proligands by deprotonation with a base such as KH or *via* direct reaction with a basic transition metal salt, for example $Pd(OAc)_2$.

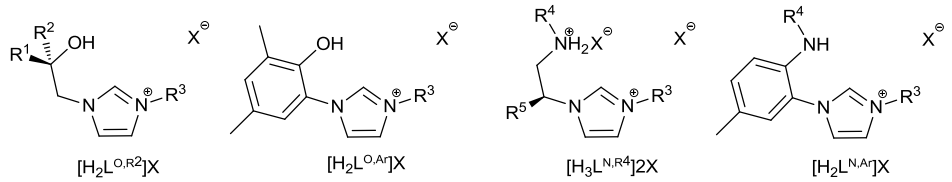

Figure 9. Alkoxy $[H_2L^{O,R2}]X$, aryloxy $[H_2L^{O,Ar}]X$, amido $[H_3L^{N,R2}]2X$, and arylamido $[H_2L^{N,Ar}]X$, NHC proligands.

2.8. Alkoxide tethered N-heterocyclic carbene proligands

The proligands $[H_2L^{O,Ph}]I$ ($R^1 = R^2 = Ph$, $R^3 = {}^iPr$) and $[H_2L^{O,iPr}]I$ ($R^1 = R^2 = R^3 = {}^iPr$) were synthesised using the same methodology as for $[H_2L^{O,Me}]I$.

2.8.1. Synthesis of $[H_2L^{O,Ph}]I$

Under an inert atmosphere $(Ph)_2COCH_2$ was combined with imidazole and heated for 1 h at 90 °C. After addition of dry MeCN the reaction mixture was heated to 80 °C for a further 18 h. (Scheme 1). One equivalent of 2-iodopropane was added to the solution before heating at 80 °C for 72 h. Workup from MeCN afforded $[HOCPh_2CH_2(1\text{-}HC\{NCHCHNPr^i\})]I$, $[H_2L^{O,Ph}]I$ as a colourless solid in 68 % yield. The ^1H NMR spectrum of $[H_2L^{O,Ph}]I$ displays a characteristic resonance at 8.61 ppm in $(CD_3)_2SO$ identified as the imidazolium proton.

Single crystals of $[H_2L^{O,Ph}]I$ were grown by slow cooling of a saturated MeCN solution. The molecular structure is depicted in Figure 10 and confirms the expected connectivity.

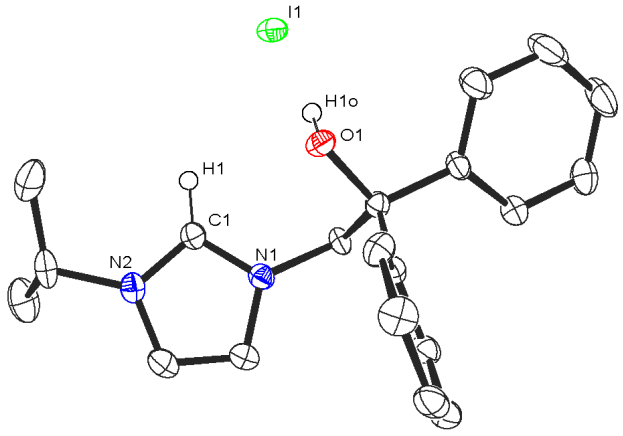

Figure 10. Thermal ellipsoid plot of the molecular structure of $[H_2L^{O,Ph}]I$ (50 % probability) with selected hydrogen atoms omitted for clarity. Selected distances (Å) and angles (°): C1-N1 1.341(4), C1-N2 1.339(4), N1-C1-N2 107.8 (3).

The hydroxyl proton was located on the differential Fourier map. A hydrogen bond to the iodide anion was found, with a O-I distance of 3.504 Å and an O-H-I angle of 174.3°. The N-C-N angle of 107.8(3)° is indicative of a cationic imidazolium system as are N-C1 bond lengths of 1.341(4) and 1.339(4) Å.

2.8.2. Synthesis of $[H_2L^{O,iPr}]I$

Di-*iso*-propyl epoxide is significantly less reactive than diphenyl epoxide and the reaction mixture to form $[H_2L^{O,iPr}]I$ was heated at 90 °C for 3 days before addition of MeCN. Slow cooling of a concentrated solution of the crude product mixture to -30 °C afforded $[HOC^iPr_2CH_2(1\text{-}HC\{NCHCHNPr^i\})]I$, $[H_2L^{O,iPr}]I$ as a waxy solid in 41 % yield after removal of the mother liquor by filtration. The ^1H NMR spectrum of $[H_2L^{O,iPr}]I$ exhibits a resonance at 10.18 ppm in $CDCl_3$, characteristic of an imidazolium proton.

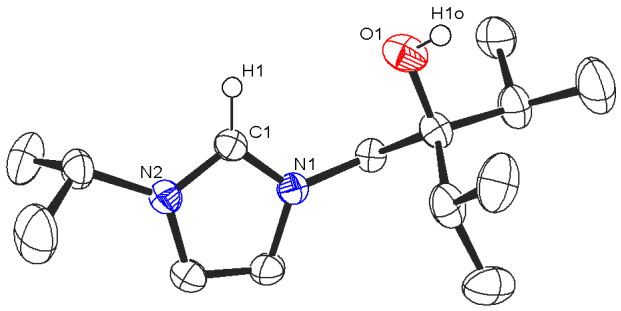

Figure 11. Thermal ellipsoid plot of the molecular structure for the cation of $[H_2L^{O,iPr}]I$ (50 % probability). The iodide anion and selected hydrogen atoms have been omitted for clarity. Selected distances (Å) and angles (°): C1-N1 1.333(3), C1-N2 1.327(3), N1-C1-N2 108.6 (2).

Single crystals of $[H_2L^{O,iPr}]I$ were grown by slow cooling of a saturated MeCN solution to -30 °C. The molecular structure is depicted in Figure 11 and confirms the expected connectivity. The hydroxyl proton was located on the differential Fourier map. A hydrogen bond to the iodide anion was found, with a O-I distance of 3.487 Å and an O-H-I angle of

157.1°. The N-C-N angle of 108.6(2)° is indicative of a cationic imidazolium system as are N-C1 bond lengths of 1.333(3) and 1.327(3) Å.

2.9. Aryl-amido tethered N-heterocyclic carbene proligand

As detailed in section 3.7 an aryl-amido tethered NHC was identified as a promising ligand to stabilise Pd^{IV}. The only other ligands of this type reported are two tridentate CNC NHC ligand by Kunz[16] and Luo[15] (Figure 12).

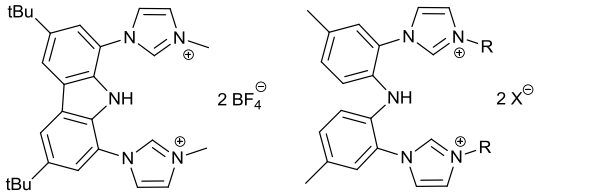

XXXXVIII **XXXXIX**

Figure 12. Previously reported arylamido NHC proligands.

2.9.1. Synthesis

The proligand $[H_2L^{N,Ar}]I$ was obtained in four steps from 4-*tert*-butylaniline (Scheme 2), using a synthetic route based on that reported by Kunz and coworkers.[16] Using KI as a source of iodide in the presence of strong acid and hydrogen peroxide, 2-iodo-4-*tert*-butylaniline was obtained in 86 % yield.[40] Subsequent *N*-methylation[41] was possible by deprotonation of one NH using one equivalent of MeLi in thf at - 78 °C, then addition of excess dimethyl sulfate. The reaction mixture was allowed to warm to room temperature and after an aqueous acid work-up *N*-methyl-2-iodo-4-*tert*-butylaniline was obtained in 66 % yield.

The substituted aniline was coupled to imidazole using standard copper coupling conditions: a catalyst mixture comprising of 12.5 mol% of CuI and 25 mol% of 1,10-phenanthroline was suspended in DMF. To this mixture, *N*-methyl-2-iodo-4-*tert*-butylaniline, 2 equivalents of imidazole and 2 equivalents of caesium carbonate were added. The reaction mixture was heated to 120 °C under a nitrogen atmosphere for 65 h.

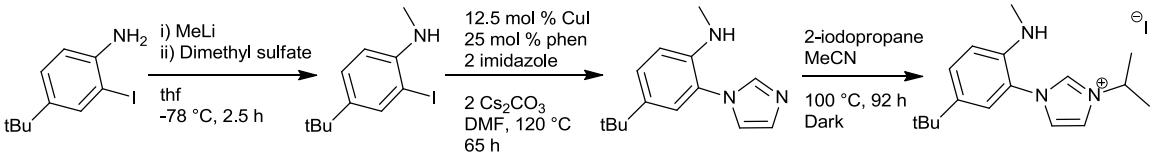

Scheme 2. Synthesis of $[H_2L^{N,Ar}]I$.

The resultant suspension was dried *in vacuo*, suspended in CH_2Cl_2 and filtered to remove the copper and caesium containing by-products. The filtrates were concentrated *in vacuo* and the coupled product [*N*-methyl-2-imidazole-4-*tert*-butyl-analine] was obtained as colourless needles in 44 % yield by evaporative crystallisation. The coupled product was combined with 1 equivalent of 2-iodopropane in MeCN and heated, in the dark, at 100 °C for 92 h. The proligand $[H_2L^{N,Ar}]I$ was obtained in 80 % yield after removal of the solvent, 20 % overall yield.

The ^1H NMR spectrum of $[H_2L^{N,Ar}]I$ exhibits a characteristic imidazolium proton resonance at 8.91 ppm in $CDCl_3$. The NH proton which appears between 3 and 4 ppm (in $CDCl_3$) for 4-*tert*-butyl-2-iodoanaline and *N*-methyl-4-*tert*-butyl-2-iodoanaline was not observed in the ^1H NMR spectrum of the proligand. The *N*-methyl and *t*-butyl groups appear as singlets and the other resonances were also assigned.

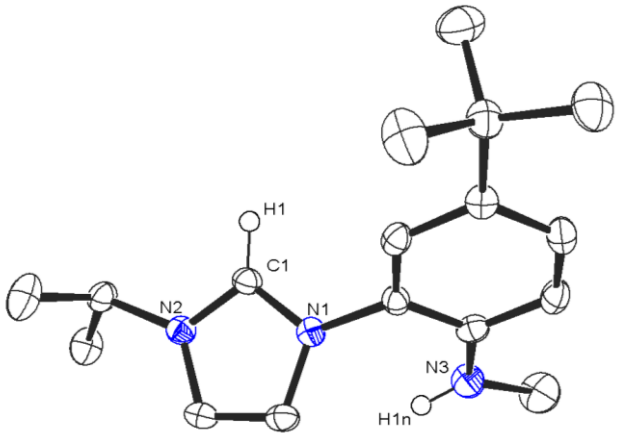

Figure 13. Thermal ellipsoid plot of the cation in the molecular structure of $[H_2L^{N,Ar}]I$ (50 % probability) with the iodide anion and selected hydrogen atoms omitted for clarity. Selected distances (Å) and angles (°): C1-N1 1.329(3), C1-N2 1.327(3), N1-C1-N2 108.6 (2).

Single crystals of $[H_2L^{N,Ar}]I$ were grown by diffusion of hexanes into a saturated CH_2Cl_2 solution. The molecular structure is depicted in Figure 13 and confirms the expected connectivity, although there is no evidence of hydrogen bonding to the iodide anion. The N-C-N angle of 108.6(2)° is typical of a cationic imidazolium system as are N-C1 bond lengths of 1.329(3) and 1.327(3) Å.

2.10. Deprotonation of the NHC proligands

2.10.1. Preparation of $KL^{O,R}$

Each of the proligands were treated with an excess of KH in thf at -78 °C, then warmed to room temperature and stirred for 18 h (Equation 1). In each case, the formation of the potassium salt $KL^{O,R}$ is accompanied by evolution of hydrogen and precipitation of KI; $KL^{O,R}$ is obtained as a colourless solid after filtration and removal of the solvent under reduced pressure.

Both $KL^{O,Me}$ and $KL^{O,Ph}$ are colourless, air- and moisture-sensitive solids obtained in high yield (~ 80 %). The product $KL^{O,iPr}$ is oily and difficult to work with. As a result $KL^{O,iPr}$ was generated *in situ* for reactions.

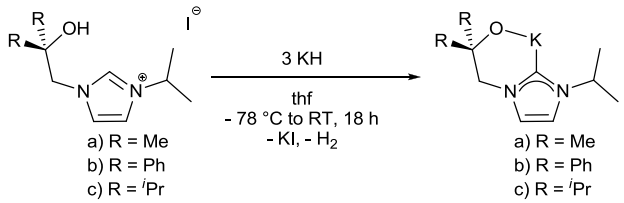

(1)

The ^{1}H NMR spectrum (C_6D_6) of $KL^{O,Ph}$ exhibits a single set of resonances and confirms removal of the imidazolium proton. The $^{13}C\{^{1}H\}$ NMR spectrum (C_6D_6) displays a resonance at 209.5 ppm attributed to the carbene centre. This is comparable with the 208.4 ppm reported for $KL^{O,Me}$.[38]

The ^{1}H NMR spectrum of $KL^{O,Me}$ (in CD_3CN) showed all the expected resonances except the backbone protons which were not observed. However when CH_3CN was used the backbone protons are observed and this H/D exchange of the backbone protons underlines their reactivity. Substitution at the backbone of NHC complexes has been noted with $N(SiMe_3)_2^-$, $B(C_6F_5)_3$, Ir nanoparticles, and CCl_3^-.[42-45]

2.10.2. Deprotonation of $[H_2L^{N,Ar}]I$

A number of bases were evaluated to deprotonate the two acidic hydrogen atoms in $[H_2L^{N,Ar}]I$ and both *n*BuLi and KN" were found to be suitable bases, Equation 2. Treatment with KH or lithium diisopropylamide (LDA) led to decomposition of the ligand.

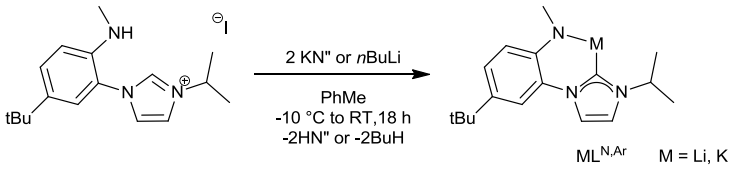

(2)

This is in contrast to the deprotonation of **XXXXVIII**[16] and **XXXXIX**[15] The mono anion of ligand **XXXXVIII** was best synthesised using three equivalents of LDA in thf solution. The bases KO^{t}Bu, KH, and MeLi were also suitable bases for deprotonation, with lithium bases giving slightly superior results. Attempts to form Pd complexes of ligand **XXXXIX** by *in situ* deprotonation with bases including *n*BuLi, LDA, KO^{t}Bu, and NaH followed by treatment with $Pd(Cl)_2$ or $Pd(OAc)_2$ were found to be unsuccessful.[15]

Analysis of the crude ^{1}H NMR spectra of the products, when *n*BuLi or KN" were used as a base, suggested that the deprotonation was successful. However, upon subsequent storage in thf solution or upon workup, the salts decomposed. Consequently $ML^{N,Ar}$ (M = Li, K) were generated *in situ* in PhMe when needed.

2.11. Pd(II) mixed ligand complexes

After consideration of the catalytic cycle, section 1.6, $[(L^O)Pd(OAc)]_2$ was selected as the simplest alkoxy-tethered Pd complex suitable for use in ligand-directed oxidative C-H bond functionalisation catalysis. (Scheme 3).

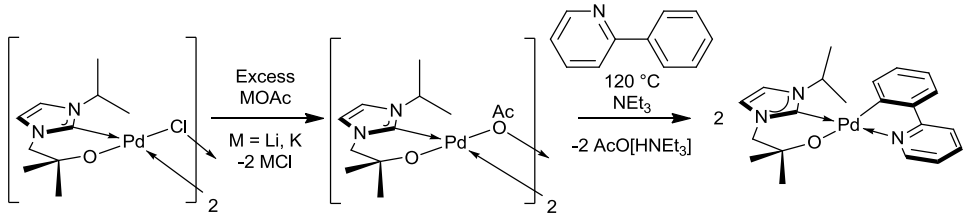

Scheme 3. Proposed precatalyst formation and species generated by substrate C-H activation.

2.11.1. Preparation of $[(L^O)PdCl]_2$ type complexes

Attempts to prepare a pure sample of $[(L^O)PdCl]_2$ were as follows:

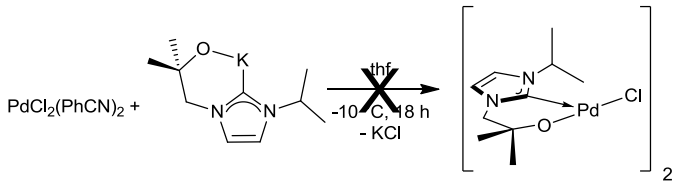

(3)

Treatment of $Pd(Cl)_2(PhCN)_2$ with an equimolar amount of KL^O in thf at -10 °C resulted in the formation of a red/brown compound (Equation 3). Analysis of the crude reaction mixture by mass spectrometry (electron impact) indicated formation of $Pd(L^O)_2$; m/z = 469 [M+H] *vide supra*.

An alternative target to $[(L^O)Pd(OAc)]_2$ is $(L^N)Pd(alkyl)$. C-H activation would occur with loss of a small molecule such as propene. Treatment of $[Pd(allyl)Cl]_2$ with two equivalents of $Li(L^N)\cdot 2LiBr$, in thf at -10 °C, yielded $(L^N)Pd(allyl)$ in quantitative yield (Equation 4).

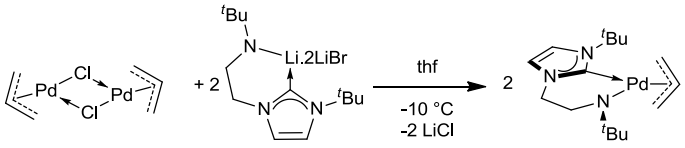

(4)

This line of investigation was discontinued because direct synthesis of $(L^{O/N})Pd(phpy)$ would allow for much simpler study of the oxidation and reductive elimination steps.

2.11.2. Preparation of $(L^O)Pd(phpy)$

There are a wide variety of reported PdL_2 complexes containing two identical bidentate mono-anionic ligands. It can be challenging to obtain pure samples of palladium complexes

containing only one bidentate mono-anionic ligand. Such heteroleptic complexes may be in equilibrium with the homoleptic alternatives (Equation 5).[46]

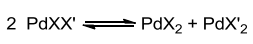

(5)

Pure samples are vital for accurate appraisal of catalytic activity. Since $[Pd(phpy)Cl]_2$ is known not to be in equilibrium with its homoleptic counterparts, the heteroleptic complex (L^O)Pd(phpy) was chosen as a more straightforward target for the isolation of pure material to study both the oxidation chemistry and catalysis, Figure 13.

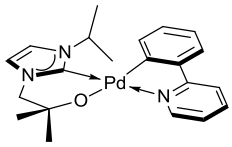

Figure 13. (L^O)Pd(phpy).

Cyclometallation at Pd^{II} has been extensively studied and a wide range of complexes have been synthesised.[47] Stirring an equimolar mixture of 2-phenylpyridine and $PdCl_2$ in $MeOH/H_2O$ for 3 days yielded $[Pd(phpy)Cl]_2$, Equation 6. If the agitation used in the synthesis of $[Pd(phpy)Cl]_2$ is insufficient formation of intractable impurities are common.[48]

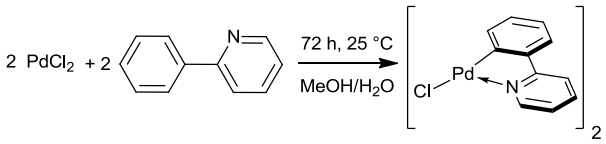

(6)

A less atom-efficient but high yielding route is available by stirring an equimolar mixture of 2-phenylpyridine and $Pd(OAc)_2$ in AcOH for 18 h. The compound $[Pd(phpy)OAc]_2$ is obtained as a pale yellow solid in excellent yield (90 %, Scheme 4). Subsequent treatment of

this solid with an excess of LiCl in acetone afforded $[Pd(phpy)Cl]_2$ in high purity (90 % yield).[49]

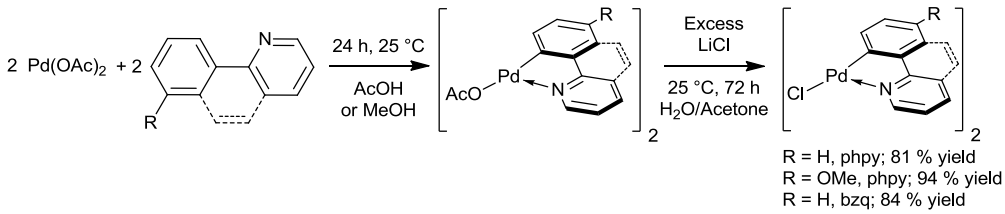

Scheme 4. Alternative route to prepare $[Pd(L)(Cl)]_2$.

By the same method the dimers $[Pd(bzq)Cl]_2$ and $[Pd(^{OMe}phpy)Cl]_2$ were obtained in high yield and purity (Scheme 4). To avoid undesirable reactions of the substrate with AcOH the cyclopalladation steps were carried out in MeOH. $[Pd(phpy)Cl]_2$ and its analogues are useful starting materials due to the potential for further reactivity of the chloride ligand.

A solution of KL^O in thf was added to a cold (-78 ºC) suspension of $[Pd(phpy)Cl]_2$ (in thf), and the reaction mixture was stirred at room temperature for 18 h. After filtration to remove KCl and removal of the volatiles, $(L^O)Pd(phpy)$ was obtained as a pale yellow solid in excellent yield (95 %, Equation 7).

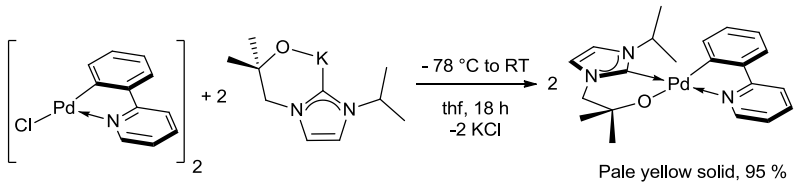

(7)

When 2,6-lutidine was added to the suspension of $[Pd(phpy)Cl]_2$ in thf before the addition of KL^O to help break up the dimer and solublise the Pd reactant. It was found that inclusion of 2,6-lutidine in the reaction significantly decreased the yield (68 % instead of 95 %).

The complex (L^O)Pd(phpy) has been characterised by ^{1}H and ^{13}C{^{1}H} NMR spectroscopy, high-resolution mass spectrometry and elemental analysis. The ^{1}H NMR spectrum (CD_3CN) contains a set of resonances attributable to a coordinated phpy and a coordinated L^O ligand in a 1:1 ratio. A resonance at 9.02 ppm (CD_3CN) for H16 (Figure 14) is ~0.4 ppm higher than that observed for other palladacyclic complexes containing phpy.[46, 49] This shift is likely due to the proximity of the electronegative alkoxy group. There is a notable shift for the *iso*-propyl resonance (H2) upon coordination to the palladium centre from 4.43 ppm in KL^O to 5.07 ppm. This effect is seen in other Pd-NHC complexes bearing *iso*-propyl groups.[50]

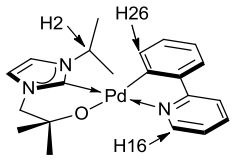

Figure 14. (L^O)Pd(phpy) illustrating the H atoms with characteristic ^{1}H NMR spectroscopy chemical shifts.

Formation of a Pd-carbene bond is evident in the ^{13}C{^{1}H} NMR spectrum by a diagnostic high frequency resonance at 175.4 ppm (CD_3CN). This is within the range previously reported for Pd^{II}-NHC complexes (182.4-149.5 ppm).[51] (L^O)Pd(phpy) is moisture sensitive but is stable in dry, aprotic solvents. (L^O)Pd(phpy) reacts readily in the solid state with one equivalent of atmospheric moisture to yield (L^{OH})Pd(phpy)OH (Equation 8). Other Pd-O NHC complexes have been demonstrated to be air- and moisture-stable.[4]

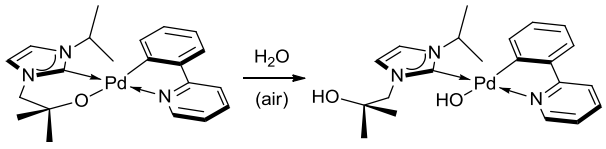

(8)

Line broadening was observed for all the resonances in the ^{1}H NMR spectrum (C_6D_6) indicative of a fluxional structure. The OH protons were observed at 6.92 and 4.16 ppm by ^{1}H NMR spectroscopy.

Single crystals of (L^O)Pd(phpy) suitable for X-ray diffraction studies were obtained by vapour diffusion of hexanes into a PhH solution at room temperature (over 3 days). The structure is illustrated in Figure 15.

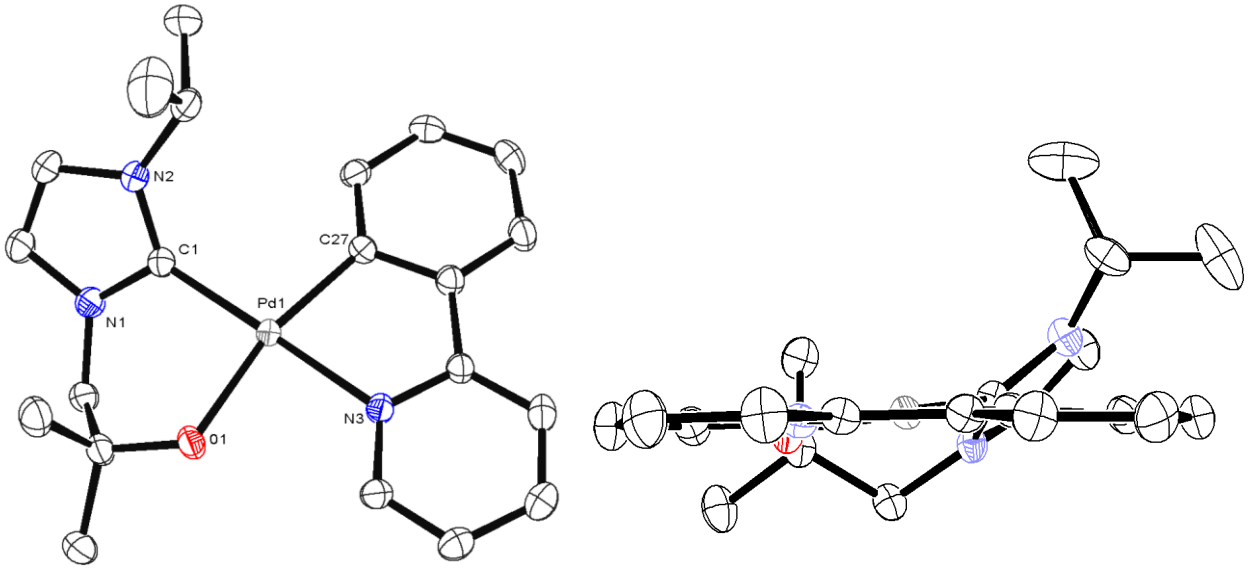

(top) (side)

Figure 15. Thermal ellipsoid plot of the molecular structure of (L^O)Pd(phpy) (50 % probability). Hydrogen atoms have been omitted for clarity.

Analysis of the structure reveals a square planar environment around the palladium atom. The Pd-C1, Pd-C27 and Pd-N3 bond lengths fall within the range reported for Pd^{II}-NHC, and Pd^{II}-phpy complexes.[52, 53] The Pd^{II}-O_{alkyl} bond length is at the longer end of the range of Pd-alkoxide complexes reported.[54] The alkoxide tether constrains the C27-Pd1-C1-N1 torsion angle to 142.9°. In Pd-NHC complexes without a tether the preferred angle is 90° to minimise the steric interaction between the NHC side arms and other ligands on the metal.

2.11.3. Synthesis of related ($L^{O,R}$)Pd(phpy) type complexes

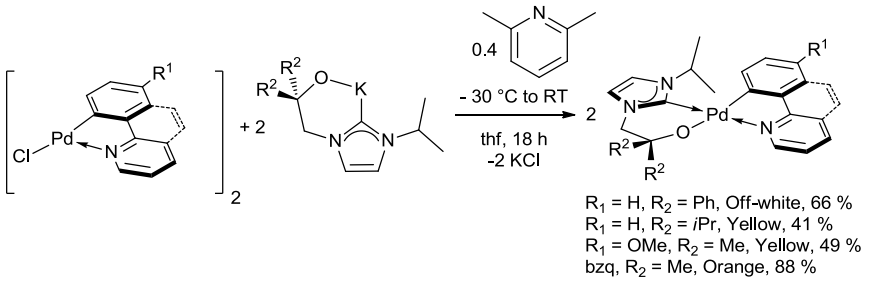

(9)

Using an analogous method to that for the preparation of (L^{O})Pd(phpy) it was possible to prepare a number of similar complexes in fair to good yields (Equation 9). The complexes are also moisture sensitive and vary in colour from off-white to orange. They are readily soluble in common organic solvents apart from ($L^{O,Ph}$)Pd(phpy) which is essentially insoluble in MeCN and PhH. The characteristic ^{1}H and $^{13}C\{^{1}H\}$ NMR spectroscopic data is summarised in Table 6.

Compound	$^{13}C\{^{1}H\}$ NMR ($\delta_{carbene}$)	^{1}H NMR (δ_{H2})	^{1}H NMR (δ_{H16})
(L^{O})Pd(phpy)	176.5 (C_6D_6)	5.30	9.72
	175.4(CD_3CN)	5.07	9.02
($L^{O,Ph}$)Pd(phpy)	174.6 (CD_2Cl_2)	5.14	9.18
($L^{O,iPr}$)Pd(phpy)	170.6 (C_6D_6)	5.33	9.73
(L^{O})Pd(^{OMe}phpy)	174.9 (CD_2Cl_2)	5.12	9.06
(L^{N})Pd(phpy)	171.5 (C_6D_6)	-	10.11
(L^{O})Pd(bzq)	174.1 (CD_3CN)	5.45	9.77
($L^{N,Ar}$)Pd(bzq)	168.4 (C_6D_6)	5.47	9.00

Table 6. Comparison of characteristic NMR spectroscopy data.

Single crystals of ($L^{O,Ph}$)Pd(phpy) suitable for X-ray diffraction studies were obtained by vapour diffusion of acetone into a dimethoxyethane solution of ($L^{O,Ph}$)Pd(phpy) at room temperature, and the molecular structure is shown in Figure 16. The carbene-, aryl- and pyridine-palladium bonds are the same length as in (L^{O})Pd(phpy) whist the alkoxide-Pd bond is longer in ($L^{O,Ph}$)Pd(phpy).

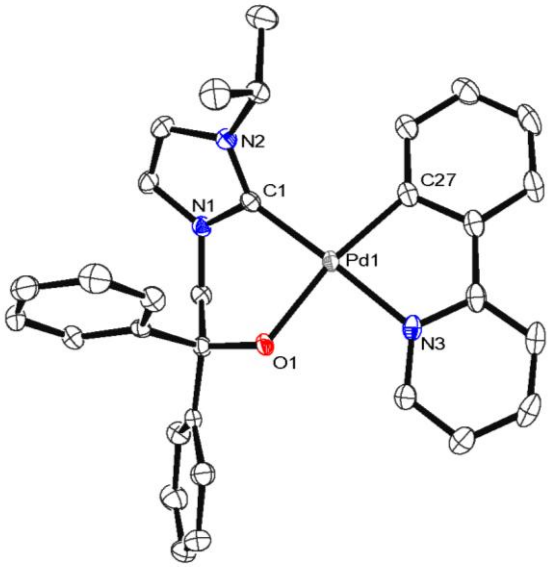

Figure 16. Thermal ellipsoid plot of the molecular structure of ($L^{O,Ph}$)Pd(phpy) (50 % probability). Hydrogen atoms have been omitted for clarity.

Single crystals of ($L^{O,iPr}$)Pd(phpy) suitable for X-ray diffraction studies were obtained by vapour diffusion of hexanes into a C_6D_6 solution of ($L^{O,iPr}$)Pd(phpy) at room temperature and the molecular structure is shown in Figure 17.

There are two independent molecules of ($L^{O,iPr}$)Pd(phpy) in the unit cell. The torsion angle C27-Pd1-C1-N1 in the two molecules are very different; 134.51(2)° and 145.65(2)°, but the average 140.80° is similar to that in (L^{O})Pd(phpy). The only other difference between the two molecules is that the packing forces have resulted in slight (~1°) variations in the geometry around palladium. The carbene-, aryl- and pyridine-palladium bonds are the same length as in (L^{O})Pd(phpy) whilst the alkoxide-Pd bond is longer in ($L^{O,iPr}$)Pd(phpy).

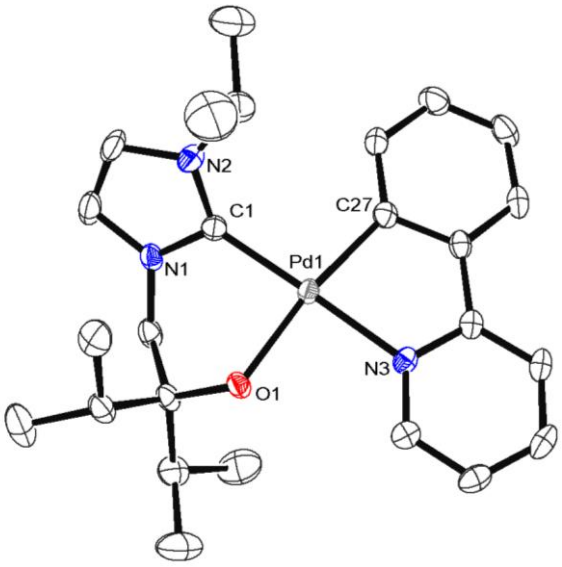

Figure 17. Thermal ellipsoid plot of the molecular structure of ($L^{O,iPr}$)Pd(phpy) (50 % probability). Hydrogen atoms have been omitted for clarity, and only one molecule of the crystallographically independent molecules are shown.

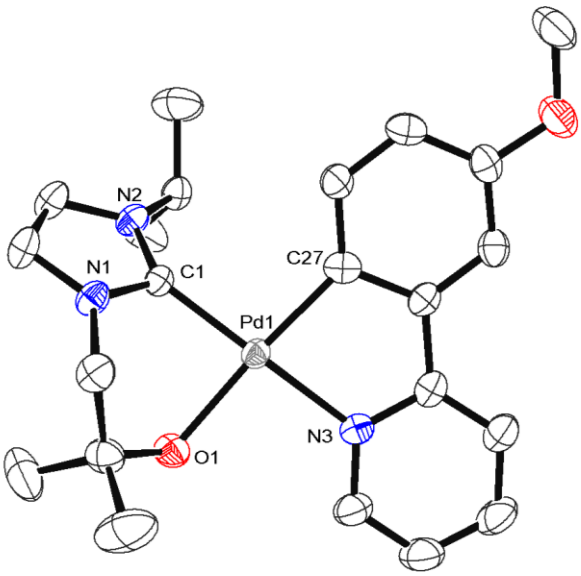

Figure 18. Thermal ellipsoid plot of the molecular structure of (L^{O})Pd(^{OMe}phpy) (50 % probability). Hydrogen atoms and solvate molecules of hexane and diacetone alcohol have been omitted for clarity.

Single crystals of (L^{O})Pd(^{OMe}phpy) suitable for X-ray diffraction studies were obtained by vapour diffusion of hexanes into an acetone solution at -20 °C over 4 days and the molecular

structure is shown in Figure 18. Both Pd-C1 and Pd-C27 are shorter than in (L^{O})Pd(phpy) [1.982(2) *versus* 1.960(4) and 1.999(2) *versus* 1.976(4)] whilst Pd-O1 is longer [2.043(2) *versus* 2.069(3)].

Single crystals of (L^{O})Pd(bzq) suitable for X-ray diffraction studies were obtained by vapour diffusion of hexanes into a CH_2Cl_2/C_6D_6 solution of ($L^{O,iPr}$)Pd(phpy) at -35 °C over two weeks. The quality of the data was too poor to allow further discussion of bonding, but the basic connectivity of the structure was established and is shown in Figure 19.

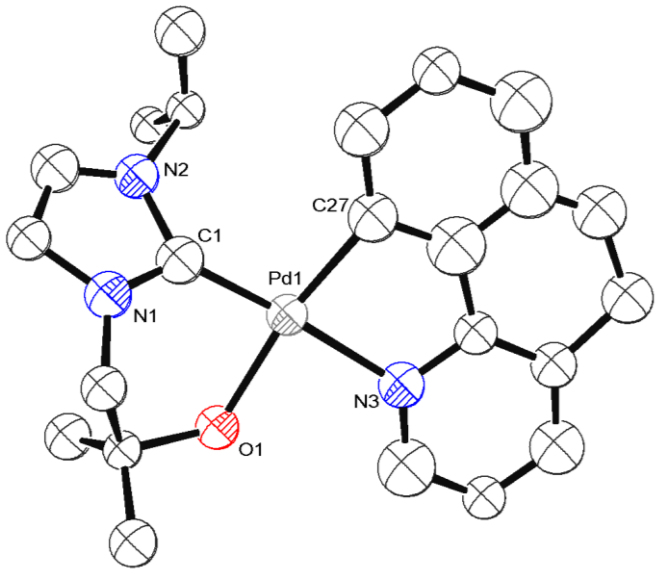

Figure 19. Molecular structure of (L^{O})Pd(bzq) demonstrating connectivity.

	(L^{O})Pd(phpy)	($L^{O,Ph}$)Pd(phpy)	($L^{O,iPr}$)Pd(phpy)	(L^{O})Pd(^{OMe}phpy)
Pd1-C1	1.982(2)	1.983(2)	1.973(2) / 1.976(2)	1.960(4)
Pd1-O1	2.043(2)	2.058(1)	2.065(1) / 2.067(2)	2.069(3)
Pd1-N3	2.059(2)	2.057(1)	2.061(2) / 2.061(2)	2.064(4)
Pd1-C27	1.999(2)	2.001(2)	2.000(2) / 1.997(2)	1.976(4)
N1-C1-N2	104.30(2)	104.43(1)	105.11(2) / 104.43(19)	105.40(4)
C1-Pd1-O1	91.06(8)	88.91(5)	86.96(7) / 90.01(7)	85.65(2)
O1-Pd1-N3	87.11(7)	88.66(5)	90.74(6) / 89.97(7)	94.63(1)
C27-Pd1-N3	80.99(8)	81.00(6)	81.23(8) / 81.01(9)	81.83(2)
C1-Pd1-C27	101.15(9)	101.44(7)	101.20(9) / 99.12(9)	98.18(2)
C27-Pd1-C1-N1	142.91(2)	137.41(12)	134.51(2) / 145.65(2)	132.1(3)

Table 7. Comparison of selected distances (Å) and angles (°) in ($L^{O,R}$)Pd(phpy) complexes.

2.11.4. Synthesis of (L^N)Pd(phpy)

A solution of Li(L^N)·2LiBr in thf was added to a cold (-78 ºC) suspension of $[Pd(phpy)Cl]_2$ (in thf) and the reaction mixture was then stirred at room temperature for 18 h. After workup (L^N)Pd(phpy) was obtained as a pale yellow solid in good yield (75 %, Equation 10).

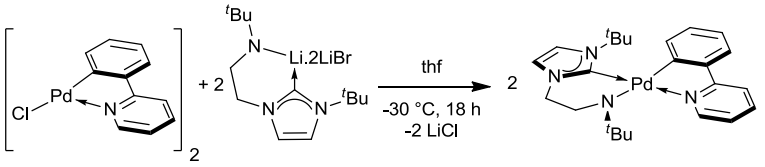

(10)

The complex (L^N)Pd(phpy) has been characterised by ^{1}H and ^{13}C{^{1}H} NMR spectroscopy and mass spectrometry. The ^{1}H NMR spectrum (C_6D_6) contains a set of resonances attributable to a coordinated phpy and a coordinated L^N ligand in a 1:1 ratio. A resonance at 10.11 ppm (C_6D_6) for H16 (see Figure 14) is higher than for the other ($L^{O,R}$)Pd(phpy) complexes synthesised (table 6). This could be a result of the steric bulk of the N-bound *tert*-butyl group. Formation of a Pd-carbene bond is evident in the ^{13}C{^{1}H} NMR spectrum by a high frequency diagnostic resonance at 171.5 ppm (C_6D_6).

2.11.5. Synthesis of ($L^{N,Ar}$)Pd(bzq)

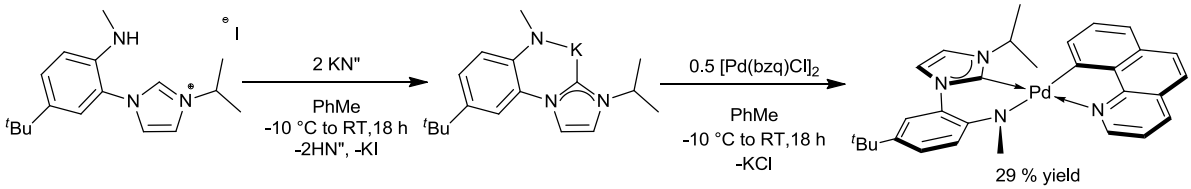

Scheme 5. Preparation of ($L^{N,Ar}$)Pd(bzq).

A solution of KN" was added to a suspension of $[H_2L^{N,Ar}]I$ in PhMe at -10 °C, Scheme 5. After stirring for 18 h at room temperature, the reaction mixture was added slowly to a suspension of $[Pd(bzq)Cl]_2$ in PhMe at -10 °C. The reaction mixture was allowed to warm

slowly to RT and stirred for 24 h. After work up from PhMe/hexane, ($L^{N,Ar}$)Pd(bzq) was isolated as a dark red solid in low yield (29 %).

The conformation of ($L^{N,Ar}$)Pd(bzq) was confirmed by ^{1}H NMR spectroscopy; nOe interactions were observed between H16 and the methyl group of the amide (Figure 20). No nOe interaction was observed for H2⋯H26.

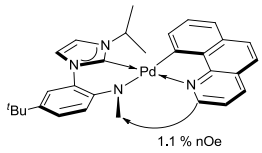

Figure 20. nOe observations in ($L^{N,Ar}$)Pd(bzq).

The resonance for H16 was observed at 9.00 ppm by ^{1}H NMR spectroscopy (C_6D_6). This is at much lower frequency than for (L^{O})Pd(bzq) (9.76 ppm, C_6D_6) and (L^{N})Pd(phpy) (10.11 ppm). Comparing L^{N} with $L^{N,Ar}$, the difference can be attributed to the greater steric influence of the *N-tert*-butyl group compared to the *N*-methyl. When comparing L^{O} and $L^{N,Ar}$ the location of the electron lone pair(s) on the sp^2 hybridised oxygen and sp^3 hybridised nitrogen must be considered. In the calculated structure of ($L^{N,Ar}$)Pd(phpy) the N-H16 distance is 2.99 Å and the nitrogen lone-pair points away from H16 compared to (L^{O})Pd(phpy) with a O-H16 distance of 2.24 Å where the oxygen lone-pairs point towards H16. The $^{13}C\{^{1}H\}$ NMR spectrum (C_6D_6) exhibits a resonance at 168.4 ppm attributable to the carbene carbon.

In the absence of a crystal structure the compound was modelled by DFT, the geometry optimised structure is shown in Figure 21.

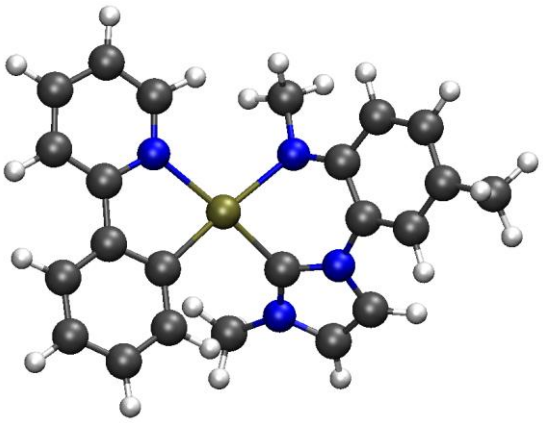

Figure 21. Calculated structure for ($L^{N,Ar}$)Pd(phpy). The *trans*-isomer (shown) is more stable by 7.5 kcal/mol. Selected bond distances: H16····NMe 2.02 Å, H2····H26 2.64 Å.

The *trans*-isomer of ($L^{N,Ar}$)Pd(phpy) was calculated to be 7.5 kcal/mol more stable, in agreement with the experimental data. The distance between H16 and the closest proton on the amido methyl group is 2.02 Å. The H2-H26 distance of 2.64 Å is larger than in (L^{O})Pd(phpy) (2.43 Å) where nOe interactions are seen. These data is in good agreement with the observed nOe interactions (H16····NMe but not H2····H26).

2.12. Synthesis of M(L)$_2$ complexes (M = Pd, Ni)

Given the apparent formation of Pd(L^{O})$_2$ during the attempted synthesis of [(L^{O})PdCl]$_2$ complexes, efforts were made to purposely make Pd(L^{O})$_2$, Pd(L^{N})$_2$ and Ni(L^{O})$_2$.

2.12.1. Preparation of Pd(L^{O})$_2$

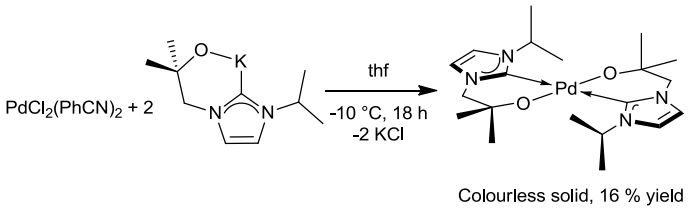

Colourless solid, 16 % yield

(11)

Treatment of $PdCl_2(PhCN)_2$ with two equivalents of KL^O afforded $Pd(L^O)_2$ in poor yield (16 %), after work up to remove an oligomeric by-product (Equation 11). The compound is a colourless solid that is sparingly soluble in C_5D_5N. The ^1H NMR spectrum of $Pd(L^O)_2$ exhibits a single set of resonances indicating a symmetrical ligand environment. The methylene protons appear as a singlet and the resonance for H2 was observed at an unusually high frequency of 6.77 ppm. To determine which isomer of $Pd(L^O)_2$ was synthesised, both were modelled using DFT, Figure 22. The *trans*-isomer was found to be 13.4 kcal/mol more stable. The high chemical shift of H2 (*iso*-propyl proton) can be explained by the short H2⋯O1 distance of 1.97 Å in the *trans*-isomer.

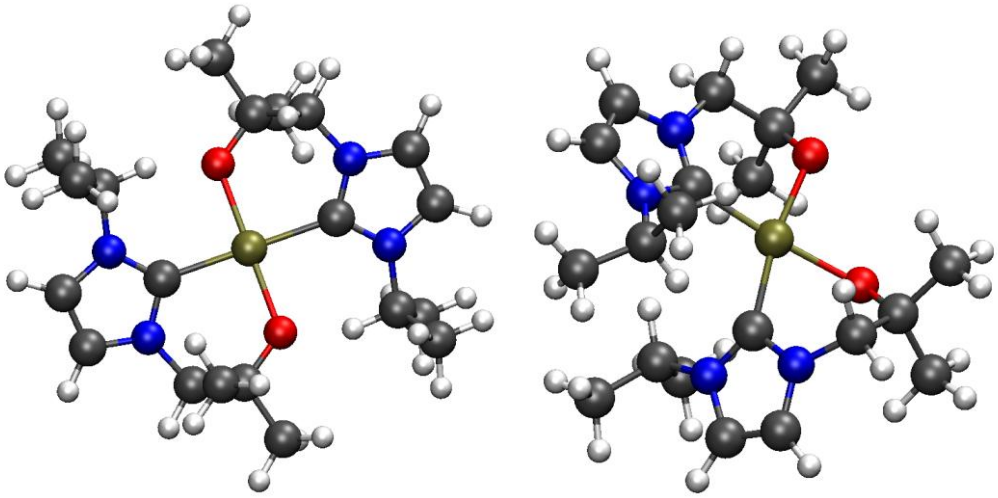

(trans) (cis)

Figure 22. Calculated structures for $Pd(L^O)_2$. The *trans*-isomer is more stable by 13.4 kcal/mol.

2.12.2. Preparation of $Pd(L^N)_2$

Treatment of $PdCl_2(MeCN)_2$ in thf with two equivalents of $Li(L^N)\cdot 2LiBr$ at -30 °C afforded $Pd(L^N)_2$ in a quantitative yield after workup (Equation 12). The complex was analysed by ^1H and $^{13}C\{^1H\}$NMR spectroscopy as well as mass spectrometry.

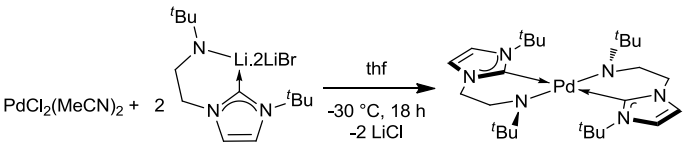

(12)

The ^{1}H NMR spectrum of Pd(L^{N})$_2$ exhibits a single set of resonances indicating a symmetrical ligand environment. Resonances for the backbone protons are absent from the ^{1}H NMR spectrum, presumably due to H-D exchange as seen previously, highlighting their acidic nature. Formation of a Pd-carbene bond is evident in the ^{13}C{^{1}H} NMR spectrum by a high frequency diagnostic resonance at 182.4 ppm (CD_3CN). This value is in agreement with closely related Pd-NHC complexes with an alkyl-amido tether.[14]

2.12.3. Preparation of Ni(L^{O})$_2$

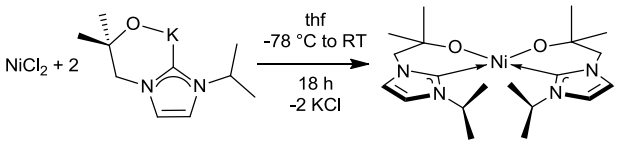

Yellow solid, 55 % yield

(13)

Treatment of Ni(Cl)$_2$ with two equivalents of KL^{O} in thf afforded Ni(L^{O})$_2$·0.5KI as a yellow microcrystalline solid, after recrystallisation from PhMe (55 % yield, Equation 13). The KI must have come from improperly purified KL^{O}. The ^{1}H NMR spectrum exhibits a single set of resonances for the backbone and *iso*-propyl protons, and two sets of the resonances for the methyl and methylene resonances suggesting the structure has different symmetry elements to Pd(L^{O})$_2$. The ^{13}C{^{1}H} NMR spectrum (C_5D_5N) exhibits a resonance at 167.5 ppm attributable to the carbene carbon. This is in line with other reported Ni^{II}-NHC complexes.[55-58]

The yellow solid appears to be stable in air for a few days but rapidly decomposes in $CDCl_3$. It is stable in solution (dry thf/hexane) at -20 °C for 2 years, with single crystals suitable for X-ray diffraction studies grown from this solution.

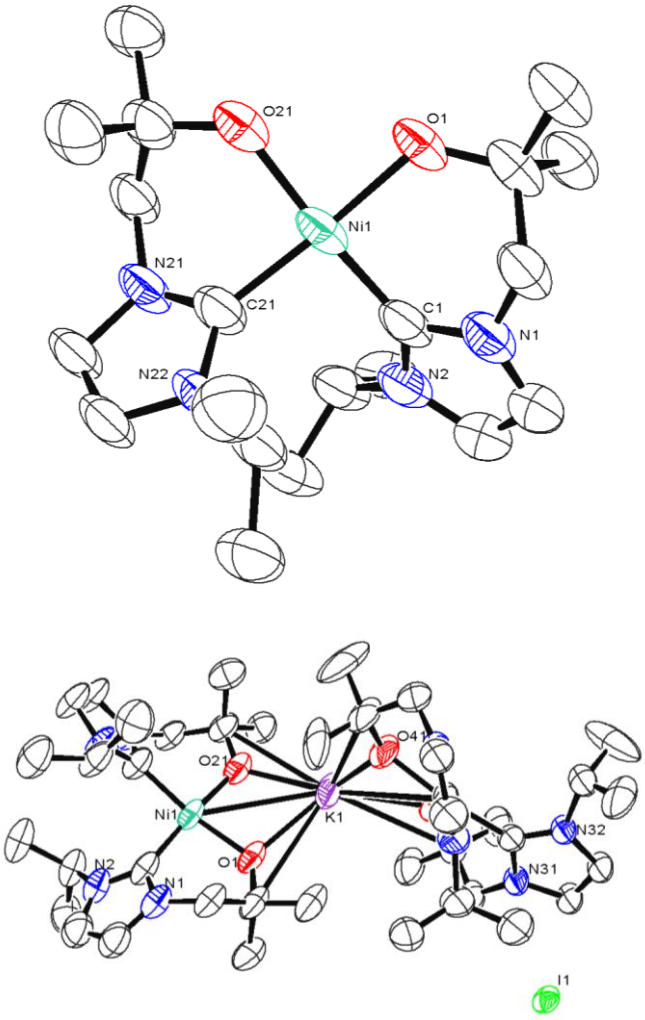

Figure 23. Thermal ellipsoid plot of the molecular structure of KI·2[Ni(L^O)$_2$] (50 % probability) - right hand side. Hydrogen atoms, K cation, I anion and second molecule of Ni(L^O)$_2$ have been omitted for clarity - left hand side. Selected bond lengths (Å) and angles (°): Ni1-C1 1.857(4), Ni1-O1 1.887(2), N1-C1-N2 104.7(3). O1-K1 2.586(3), O21-K1 2.509(2), O31-K1 2.661(2), O41-K1 2.544(3), O1-K1-O21 60.49(8), O31-K1-O41 59.40(8).

The molecular structure obtained (Figure 23) is in agreement with the evidence obtained by NMR spectroscopy. The NHC ligands are *cis*-disposed in a square planar arrangement

around Ni. The Ni-$C_{carbene}$ and Ni-O bond lengths are within the range previously reported for other tethered-NHC Ni complexes.[1, 12, 55, 59-62] Two molecules of $Ni(L^O)_2$ are bridged by a potassium cation coordinated through the oxygen atoms. The structure also contained extensively disordered hexane molecules which could not be effectively modelled individually so were modelled using the squeeze methodology included in the Platon package.[63]

It appears the inclusion of KI (carried over in the synthesis of KL^O) maybe important, as subsequent attempts to make $Ni(L^O)_2$ afforded an intractable mixture as well as Ni black. Difficulties in synthesising large quantities of pure $M(L^O)_2$ restricted detailed investigation of their oxidation chemistry. Initial investigations have demonstrated that $Ni(L^O)_2 \cdot 0.5KI$ forms a paramagnetic species upon treatment with $PhICl_2$. The ^1H NMR spectrum contains resonances from +20 to -10 ppm (CH_2Cl_2), suggesting the formation of $Ni(L^O)_2Cl$ and this compound is stable in solution for at least a week. Treatment of $Ni(L^O)_2 \cdot 0.5KI$ with $PhI(OAc)_2$ forms a mixture of diamagnetic Ni complexes.

2.13. Cyclic voltammetry

The electrochemical properties of the complexes were examined by cyclic voltammetry, and the results are reported in Table 8. All the cyclometallated complexes (entries a-f) exhibit an irreversible oxidation wave between +0.55 and + 0.42 V. Such irreversibility has been observed by others[64] in the free ligands phpy-H and bzq-H. Additionally an irreversible reduction wave between -2.30 and -2.66 V is observed (entries a-f). According to the work of Gehdini *et al.* complexes of phpy tend to show reversible or quasi reversible reduction, where as complexes of bzq have a tendency for irreversible behaviour; whilst free phpy-H and bzq-H always show irreversible reductions.[64]

Entry	Compound	Oxidation E^{Ox} / V [a]	Reduction E^{Red} / V [a]
a	$(L^{O})Pd(phpy)$	+0.42[c]	-2.66[b]
b	$(L^{O,Ph})Pd(phpy)$	+0.55[c]	-2.61[b]
c	$(L^{O,iPr})Pd(phpy)$	+0.37[c]	-2.52[b]
d	$(L^{O})Pd(bzq)$	+0.52[c]	-2.59[c]
e	$(L^{N,Ar})Pd(bzq)$	-0.44[c], +0.46[c]	-2.49[c]
f	$[Pd(phpy)OAc]_2$	+0.49[b]	-2.30[c]
g	$[H_2L^{N,Ar}]I$	-0.20[c]	-0.93[c]

Table 8. [a]Potentials were obtained in dry 1,2-dimethoxyethane solution using tetrabutylammonium tetrafluoroborate (0.2 M) as supporting electrolyte; values are reported relative to the oxidation or reduction peak of Cp_2Fe/Cp_2Fe^+, using a platinum working electrode vs. Ag wire as a pseudo reference electrode. [b]Quasi-reversible. [c]Irreversible.

Several trends are apparent between the oxidation potentials and ligand structures. For the three $(L^{O,R})Pd(phpy)$ complexes the more electron donating the ligand (as predicted by chemical intuition) the lower the oxidation potential (entry c < a < b). Comparison of entries d and e suggests that $L^{N,Ar}$ is more electron donating than L^{O} (see section 3.7.1 for a computational comparison). Changing the substituent on the NHC ligand can have as much of an impact on the oxidation potential as changing the aryl-pyridine ligand (entry a and b *versus* a and d). No trends are observed for the reduction potentials.

The HOMO and LUMO orbitals of $(L^{O})Pd(phpy)$ and $(L^{N,Ar})Pd(phpy)$ have been calculated using DFT and are illustrated in Figure 16. It can be seen that the HOMO is mainly located on the Pd and heteroatom tether. Thus it is not surprising that changes in the alkoxy-tether have a moderate impact on the oxidation potential.

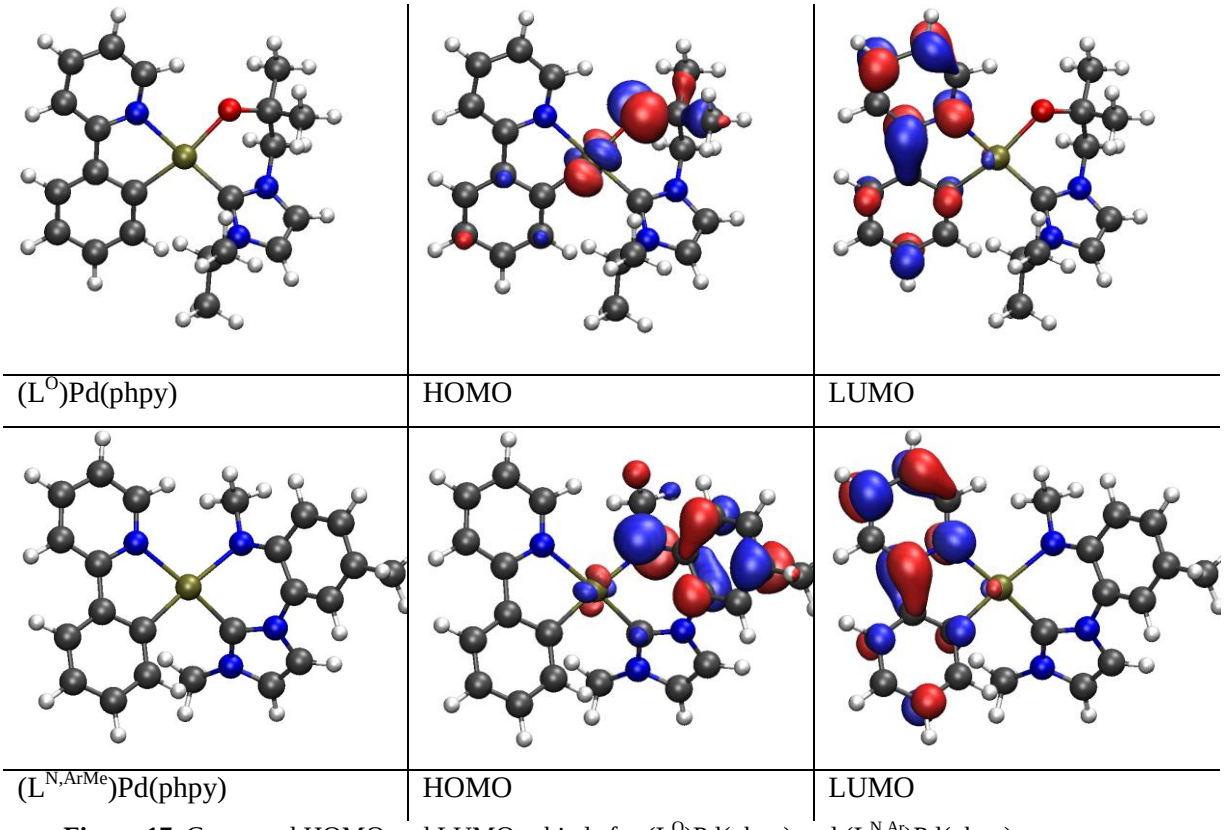

(L^{O})Pd(phpy)	HOMO	LUMO
($L^{N,ArMe}$)Pd(phpy)	HOMO	LUMO

Figure 17. Computed HOMO and LUMO orbitals for (L^{O})Pd(phpy) and ($L^{N,Ar}$)Pd(phpy).

The oxidation seen at -0.44 V for ($L^{N,Ar}$)Pd(bzq) is likely based on the aryl ring. This result is unsurprising given the rich electrochemistry of anilines. The oxidation potential of +0.46 V for ($L^{N,Ar}$)Pd(bzq) is comparable to the other complexes tested provided that oxidation of the ligand has no effect on the oxidation potential at palladium. The LUMO is principally located on the phpy ligand in both cases and the reduction of these compounds is mainly phpy based.

2.14. Conclusions

Two new alkoxy-tethered NHC proligands have been synthesised, $[H_2L^{O,Ph}]I$ and $[H_2L^{O,iPr}]I$, as well as a new arylamido-tethered NHC proligand $[H_2L^{N,Ar}]I$. Isolation of pure alkali metal salts of these compounds was only possible for $[H_2L^{O,Ph}]I$.

Treatment of chloride bridged dimers $[Pd(L)Cl]_2$ (L = phpy, ^{OMe}phpy or bzq) with alkali metal salts of tethered-NHC ligands yielded six new alkoxy tethered NHC palladium complexes and two new amido-tethered NHC palladium complexes. (L^O)Pd(phpy), $(L^{O,iPr})$Pd(phpy) and (L^O)Pd(^{OMe}phpy) have also been structurally characterised. The carbene resonances were observed in the range 177-168 ppm by $^{13}C\{^1H\}$ NMR spectroscopy and cyclic voltammetry measurements showed a link between the observed oxidation potential and ligand donor ability.

The synthesis of NiL^O_2 is only possible in the presence of KI and the ligands are *cis*-disposed about the metal centre. Single crystal X-ray diffraction studies confirmed the geometry and demonstrated that the potassium cation stabilises the complex by coordinating to the alkoxide oxygen atoms. By comparison of the ^1H NMR spectra it can be seen that the ligands in PdL^O_2 and PdL^N_2 are *trans*-disposed about the metal centre.

DFT calculations on these systems using a relatively simple level of theory are able to accurately predict the geometries of the products; providing complimentary information to the experimentally determined data.

2.15. References

[1] A. W. Waltman and R. H. Grubbs, *Organometallics*, 2004, **23**, 3105.

[2] T. Yagyu, S. Oya, M. Maeda, and K. Jitsukawa, *Chem. Lett.*, 2006, **35**, 154.

[3] H. Ren, P. Yao, S. Xu, H. Song, and B. Wang, *J. Organomet. Chem.*, 2007, **692**, 2092.

[4] Y. Kong, H. Ren, S. Xu, H. Song, B. Liu, and B. Wang, *Organometallics*, 2009, **28**, 5934.

[5] S. Satoshi, Y. Kyung Soo, O. N. Justin, L. Joo Ho, S. Timothy, and J. Kyung Woon, *Angew. Chem., Int. Ed.*, 2008, **47**, 9326.

[6] C.-Y. Liao, K.-T. Chan, J.-Y. Zeng, C.-H. Hu, C.-Y. Tu, and H. M. Lee, *Organometallics*, 2007, **26**, 1692.

[7] S. Sakaguchi, K. S. Yoo, J. O'Neil, J. H. Lee, T. Stewart, and K. W. Jung, *Angew. Chem., Int. Ed.*, 2008, **47**, 9326.

[8] J. H. Lee, K. S. Yoo, C. P. Park, J. M. Olsen, S. Sakaguchi, G. K. S. Prakash, T. Mathew, and K. W. Jung, *Adv. Synth. & Cat.*, 2009, **351**, 563.

[9] J. Jarusiewicz, Y. Choe, K. S. Yoo, C. P. Park, and K. W. Jung, *J. Org. Chem.*, 2009, **74**, 2873.

[10] J. A. Cabeza, I. Del Rio, M. G. Sanchez-Vega, and M. Suarez, *Organometallics*, 2006, **25**, 1831.

[11] D. Sellmann, C. Allmann, F. Heinemann, F. Knoch, and J. Sutter, *J. Organomet. Chem.*, 1997, **541**, 291.

[12] D. Sellmann, W. Prechtel, F. Knoch, and M. Moll, *Inorg. Chem.*, 1993, **32**, 538.

[13] A. A. Danopoulos, P. Cole, S. P. Downing, and D. Pugh, *J. Organomet. Chem.*, 2008, **693**, 3369.

[14] R. E. Douthwaite, J. Houghton, and B. M. Kariuki, *Chem. Commun.*, 2004, 698.

[15] W. Wei, Y. Qin, M. Luo, P. Xia, and M. S. Wong, *Organometallics*, 2008, **27**, 2268.

[16] M. Moser, B. Wucher, D. Kunz, and F. Rominger, *Organometallics*, 2007, **26**, 1024.

[17] M. J. Frisch, G. W. Trucks, H. B. Schlegel, G. E. Scuseria, M. A. Robb, J. R. Cheeseman, J. A. Montgomery, T. Vreven, K. N. Kudin, J. C. Burant, J. M. Millam, S. S. Iyengar, J. Tomasi, V. Barone, B. Mennucci, M. Cossi, G. Scalmani, N. Rega, G. A. Petersson, H. Nakatsuji, M. Hada, M. Ehara, K. Toyota, R. Fukuda, J. Hasegawa, M. Ishida, T. Nakajima, Y. Honda, O. Kitao, H. Nakai, M. Klene, X. Li, J. E. Knox, H. P. Hratchian, J. B. Cross, V. Bakken, C. Adamo, J. Jaramillo, R. Gomperts, R. E. Stratmann, O. Yazyev, A. J. Austin, R. Cammi, C. Pomelli, J. W. Ochterski, P. Y. Ayala, K. Morokuma, G. A. Voth, P. Salvador, J. J. Dannenberg, V. G. Zakrzewski, S. Dapprich, A. D. Daniels, M. C. Strain, O. Farkas, D. K. Malick, A. D. Rabuck, K. Raghavachari, J. B. Foresman, J. V. Ortiz, Q. Cui, A. G. Baboul, S. Clifford, J. Cioslowski, B. B. Stefanov, G. Liu, A. Liashenko, P. Piskorz, I. Komaromi, R. L. Martin, D. J. Fox, T. Keith, A. Laham, C. Y. Peng, A. Nanayakkara, M. Challacombe, P. M. W. Gill, B. Johnson, W. Chen, M. W. Wong, C. Gonzalez, and J. A. Pople, in 'Gaussian 03, Revision C.02', 2003.

[18] M. A. Thompson, *ArgusLab 4.0.1, Planaria Software LLC, Seattle, WA* http://www.arguslab.com.

[19] A. R. Allouche, *Gabedit is a free Graphical User Interface for computational chemistry packages. It is available from* http://gabedit.sourceforge.net/.

[20] P. J. Hay and W. R. Wadt, *J. Chem. Phys.*, 1985, **82**, 299.

[21] P. J. Hay and W. R. Wadt, *J. Chem. Phys.*, 1985, **82**, 270.

[22] W. R. Wadt and P. J. Hay, *J. Chem. Phys.*, 1985, **82**, 284.

[23] T. H. D. Jr. and P. J. Hay, in ' Modern Theoretical Chemistry', ed. H. F. S. III, New York, 1976.

[24] A. J. Mota and A. Dedieu, *J. Org. Chem.*, 2007, **72**, 9669.

[25] V. P. Ananikov, D. G. Musaev, and K. Morokuma, *J. Am. Chem. Soc.*, 2002, **124**, 2839.

[26] D. J. Cardenas, B. Martin-Matute, and A. M. Echavarren, *J. Am. Chem. Soc.*, 2006, **128**, 5033.

[27] Y. Fu, Z. Li, S. Liang, Q. X. Guo, and L. Lui, *Organometallics*, 2008, **27**, 3736.

[28] A. J. Mota and A. Dedieu, *Organometallics*, 2006, **25**, 3130.

[29] H. Z. Yu, Y. Fu, Q. X. Guo, and Z. Lin, *Organometallics*, 2009, **28**, 4507.

[30] A. D. Becke, *Phys. Rev. A*, 1988, **38**, 3098.

[31] C. Lee, W. Yang, and R. G. Parr, *Physical Review B*, 1988, **37**, 785.

[32] A. D. Becke, *J. Chem. Phys.*, 1993, **98**, 5648.

[33] D. Andrae, U. Haeussermann, M. Dolg, H. Stoll, and H. Preuss, *Theor. Chim. Acta*, 1990, **77**, 123.

[34] A. P. Scott and L. Radom, *J. Phys. Chem.*, 1996, **100**, 16502.

[35] *Jmol: an open-source Java viewer for chemical structures in 3D.* http://www.jmol.org/.

[36] J. Tomasi, B. Mennucci, and R. Cammi, *Chemical Reviews*, 2005, **105**, 2999.

[37] Y. Fu, Z. Li, S. Liang, Q.-X. Guo, and L. Liu, *Organometallics*, 2008, **27**, 3736.

[38] P. L. Arnold, M. Rodden, K. M. Davis, A. C. Scarisbrick, A. J. Blake, and C. Wilson, *Chem. Commun.*, 2004, 1612.

[39] H. Glas, E. Herdtweck, M. Spiegler, A.-K. Pleier, and W. R. Thiel, *J. Organomet. Chem.*, 2001, **626**, 100.

[40] J. Iskra, S. Stavber, and M. Zupan, *Synthesis*, 2004, 1869.

[41] R. C. Larock and L. W. Harrison, *J. Am. Chem. Soc.*, 1984, **106**, 4218.

[42] P. L. Arnold and S. T. Liddle, *Chem. Commun.*, 2005, 5638.

[43] D. Holschumacher, T. Bannenberg, C. G. Hrib, P. G. Jones, and M. Tamm, *Angew. Chem., Int. Ed. Engl.*, 2008, **47**, 7428.

[44] J. D. Scholten, G. Ebeling, and J. Dupont, *Dalton Trans.*, 2007, 5554.

[45] A. J. Arduengo, F. Davidson, H. V. R. Dias, J. R. Goerlich, D. Khasnis, W. J. Marshall, and T. K. Prakasha, *J. Am. Chem. Soc.*, 1997, **119**, 12742.

[46] P. Jolliet, M. Gianini, A. von Zelewsky, G. Bernardinelli, and H. Stoeckli-Evans, *Inorg. Chem.*, 1996, **35**, 4883.

[47] M. Ghedini, I. Aiello, A. Crispini, A. Golemme, M. La Deda, and D. Pucci, *Coord. Chem. Rev.*, 2006, **250**, 1373.

[48] M. S. Sanford, in 'Unpublished results'.

[49] T. Pugliese, N. Godbert, I. Aiello, M. Ghedini, and M. La Deda, *Inorg. Chem. Commun.*, 2006, **9**, 93.

[50] H. V. Huynh, Y. Han, J. H. H. Ho, and G. K. Tan, *Organometallics*, 2006, **25**.

[51] L. Ray, M. M. Shaikh, and P. Ghosh, *Organometallics*, 2007, **26**, 958.

[52] M. S. Viciu, R. A. Kelly, E. D. Stevens, F. Naud, M. Studer, and S. P. Nolan, *Org. Lett.*, 2003, **5**, 1479.

[53] Y.-J. Kim, X. Chang, J.-T. Han, M. S. Lim, and S. W. Lee, *Dalton Trans.*, 2004, 3699.

[54] P. Klüfers and T. Kunte, *Angew. Chem., Int. Ed. Engl.*, 2001, **40**, 4210.

[55] C.-Y. Liao, K.-T. Chan, Y.-C. Chang, C.-Y. Chen, C.-Y. Tu, C.-H. Hu, and H. M. Lee, *Organometallics*, 2007, **26**, 5826.

[56] D. S. McGuinness, W. Mueller, P. Wasserscheid, K. J. Cavell, B. W. Skelton, A. H. White, and U. Englert, *Organometallics*, 2002, **21**, 175.

[57] A. L. MacKinnon and M. C. Baird, *J. Organomet. Chem.*, 2003, **683**, 114.

[58] K. Matsubara, K. Ueno, and Y. Shibata, *Organometallics*, 2006, **25**, 3422.

[59] A. J. Boydston, J. D. Rice, M. D. Sanderson, O. L. Dykhno, and C. W. Bielawski, *Organometallics*, 2006, **25**, 6087.

[60] S. Dieter, G. Franz, and W. H. Frank, *Z. Anorg. Allg. Chem.*, 2001, **627**, 1034.

[61] W. Li, H. Sun, M. Chen, Z. Wang, D. Hu, Q. Shen, and Y. Zhang, *Organometallics*, 2005, **24**, 5925.
[62] B. E. Ketz, X. G. Ottenwaelder, and R. M. Waymouth, *Chem. Commun.*, 2005, 5693.
[63] A. L. Spek, *Acta Cryst.*, 2009, **D65**, 148.
[64] M. Ghedini, T. Pugliese, M. L. Deda, N. Godbert, I. Aiello, M. Amati, S. Belviso, F. Lelj, G. Accorsi, and F. Barigelletti, *Dalton Trans.*, 2008, 4303.

Chapter 3

Pd^{IV} NHC halide complexes

Chapter 3 – Pd^{IV} NHC halide complexes

3.1. Introduction

The majority of catalytic reactions involving palladium are based on a $Pd^{0/II}$ cycle. The Sanford group have demonstrated that a catalytic cycle based on $Pd^{II/IV}$ is feasible.[1] Catalytic cycles based on $Pd^{II/IV}$ have been put to good use by others and has been the subject of a number of recent reviews.[1-5] Prior to the start of this work none of the Pd^{IV} complexes in the literature were viable intermediates in a C-H bond functionalisation catalytic cycle. The main aim of this work was to produce a stable Pd^{IV} compound that could function as an intermediate in this catalytic cycle. The results from sections 3.3.4 and 3.5 have been published in the Journal of the American Chemical Society.[6]

A number of oxidants have been used to make organometallic Pd^{IV} complexes; MeI,[7] $[Ph_2I]OTf$,[8] $PhI(OAc)_2$,[9] NCS,[10] $PhI(Cl)_2$,[10] and XeF_2[11, 12](Scheme 1).

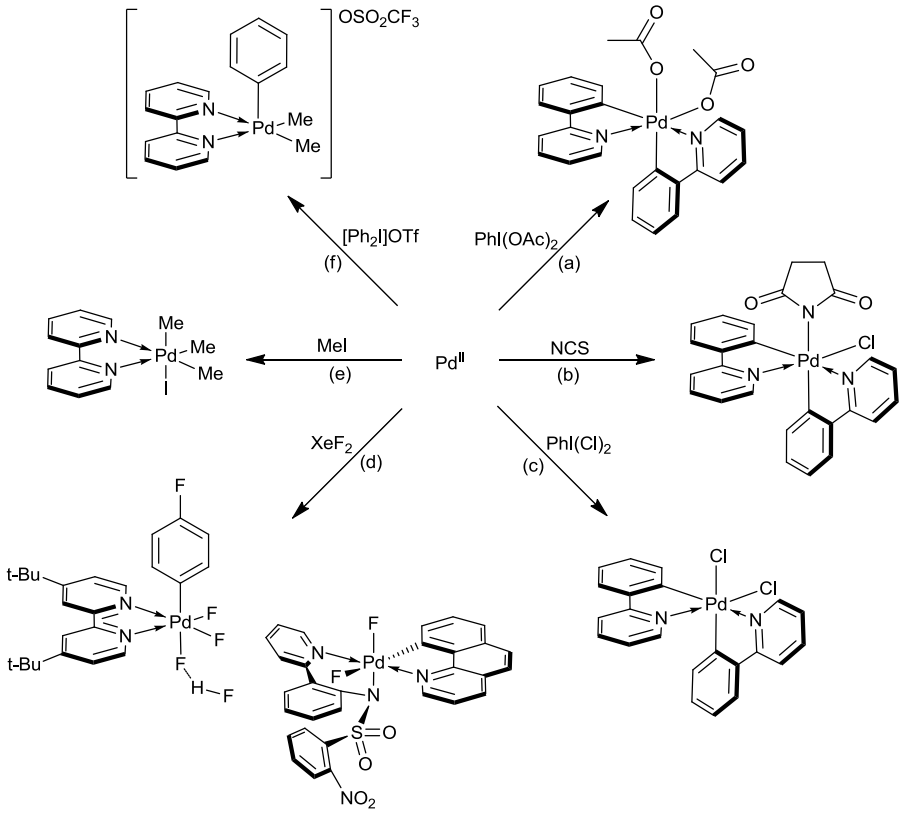

Scheme 1. A selection of Pd^{IV} complexes produced by strong oxidants; a,[9] b,[10] c,[10] d,[11, 12] e,[7] f.[8]

3.2. Oxidation of (L^O)Pd(phpy) with NBS

These reagents, and others such as $[Ph_2I]BF_4$ and NBS (*N*-bromosuccinimide), were screened for their potential to oxidise (L^O)Pd(phpy) to a Pd^{IV} complex. The reactions were monitored by solution ^1H NMR spectroscopy in CH_2Cl_2 at 25 ºC and a shift to higher frequency for H16, a strong indicator of a Pd^{IV} complex, was only observed in the case of NBS and $PhI(Cl)_2$ (see below). The oxidant NBS has been successfully used in palladium catalysed ligand-directed oxidative functionalisation catalysis.[13-15]

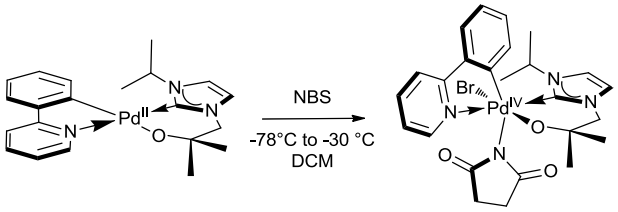

(1)

(L^O)Pd(phpy)(Br)(succinimide) was prepared by treatment of (L^O)Pd(phpy) with an equivalent of N-bromosuccinimide in CH_2Cl_2 at -78 ºC. The red solution was warmed to -30 ºC and the volatiles were removed under reduced pressure (Equation 1). (L^O)Pd(phpy)(Br)(succinimide) was characterised by ^1H and $^{13}C\{^1H\}$ NMR spectroscopy, elemental analysis and mass spectrometry. (L^O)Pd(phpy)(Br)(succinimide) is stable in solution for at least a week at -30 ºC (MeCN, PhF, thf) and for over a month at -78 ºC (CH_2Cl_2), but is insoluble in PhH. At room temperature a MeCN solution of (L^O)Pd(phpy)(Br)(succinimide) changes colour from red to yellow (Pd^{IV} to Pd^{II}) in under 10 minutes.

Extensive efforts were made to obtain single crystals of (L^O)Pd(phpy)(Br)(succinimide) for X-ray diffraction studies. Saturated solutions of (L^O)Pd(phpy)(Br)(succinimide) in a range of solvents (MeCN, PhF, thf, CH_2Cl_2) at -35 ºC were layered with hexanes or diethyl ether and kept for 2 weeks at -35 ºC to slowly mix. However, amorphous red solid was obtained from all of the solvent combinations attempted.

Inspection of the ^{1}H NMR spectrum (CD_3CN, -30 ºC) shows that the resonance for H16 has not significantly shifted (still at *c.a.* 9 ppm) whilst H2 has been deshielded (5.71 ppm compared to 5.06 ppm in the starting material). All of the resonances are sharp apart from the succinimide resonance which appears as a broad signal at 2.41 ppm. The resonance attributable to the carbene carbon has shifted to 164.7 ppm (CD_3CN) compared to 175.4 ppm in the starting material.

An nOe correlation of 1 % between H26 and H2, and between H26 and one of the methyl groups on the isopropyl and alkoxide arm of the NHC ligand allows assignment of the stereochemistry (Figure 1). Based on these data it is not possible to say whether the bromide or succinimide ligand is *trans* to the alkoxide group.

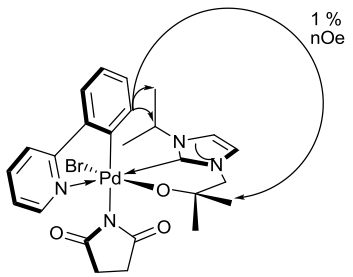

Figure 1. nOe interactions in (L^{O})Pd(phpy)(Br)(succinimide).

X-ray photoelectron spectroscopy (XPS) is a surface analysis technique and utilises a beam of photons of a fixed energy. A photon is absorbed by an atom in the sample, leading to ionisation and emission of a core electron. The binding energy of the emitted electron is characteristic for each element. The binding energy is also affected by the oxidation state of the element and, to a smaller extent, the ligands around the element. For example the value for Pd^{0} (foil) is 335.4 eV, $Pd^{II}Cl_2$ 337.8 eV and $K_2[Pd^{IV}Cl_6]$ 340.3 eV.[16-18]

XPS measurements on solid (L^{O})Pd(phpy) and (L^{O})Pd(phpy)(Br)(succinimide) both gave a value of 338 eV for Pd, corresponding to a Pd^{II} complex. The localised heating as a result of

the photons striking the sample may well have been sufficient to allow (L^O)Pd(phpy)(Br)(succinimide) to undergo decomposition.

3.2.1. Potential isomers of (L^O)Pd(phpy)(Br)(succinimide)

In the absence of a crystal structure, DFT was used to predict the possible geometric isomers of (L^O)Pd(phpy)(Br)(succinimide), Figure 2.

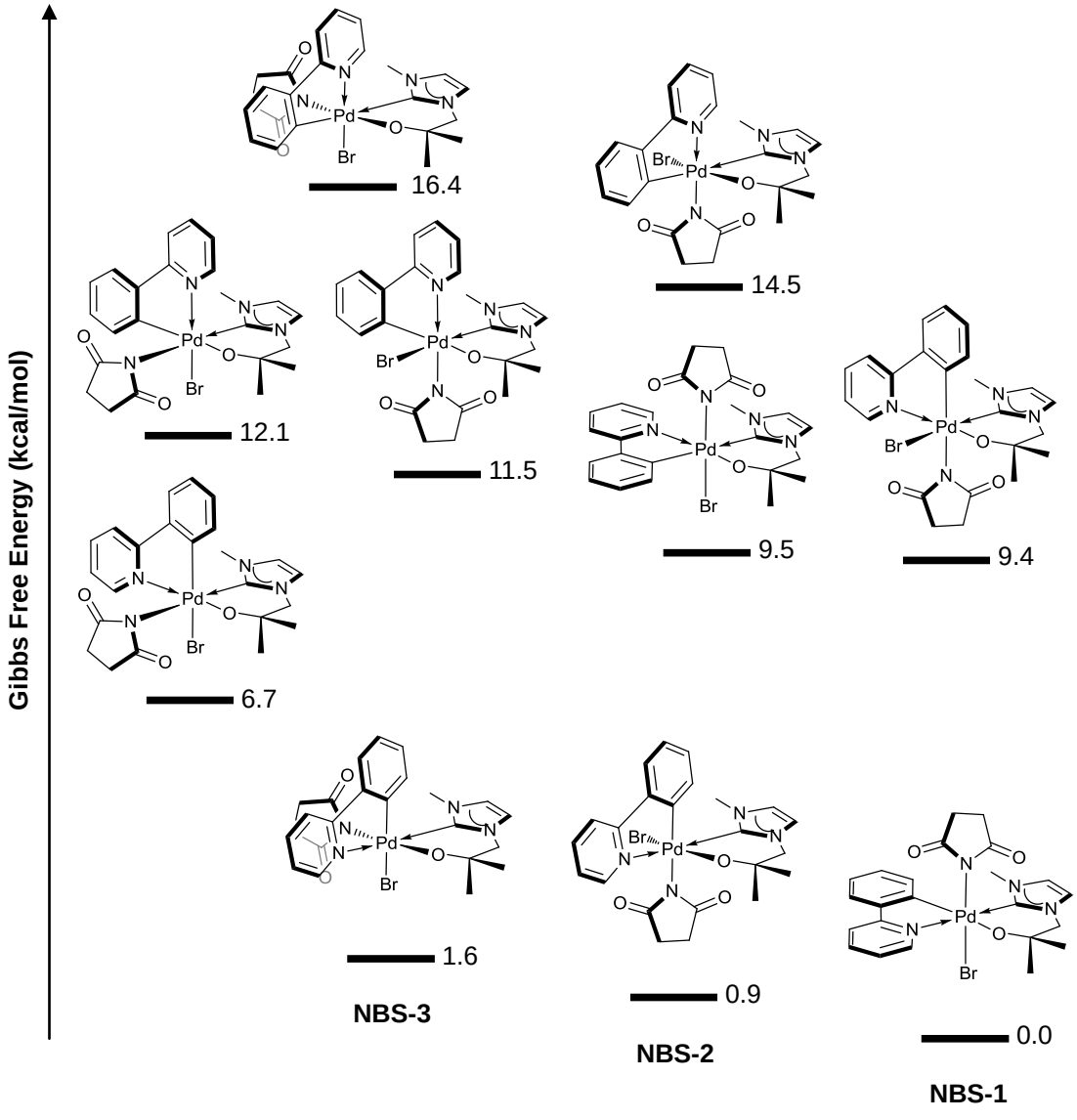

Figure 2. Calculated geometric isomers of (L^O)Pd(phpy)(Br)(succinimide); energies given relative to the lowest energy isomer.

Most of the isomers can be excluded because of their high relative energy. The inherent uncertainty in DFT calculations of ~3 kcal/mol means that structures **NBS-1**, **NBS-2** and **NBS-3** can be considered isoenergetic. Considering the nOe evidence **NBS-1** can be discounted.

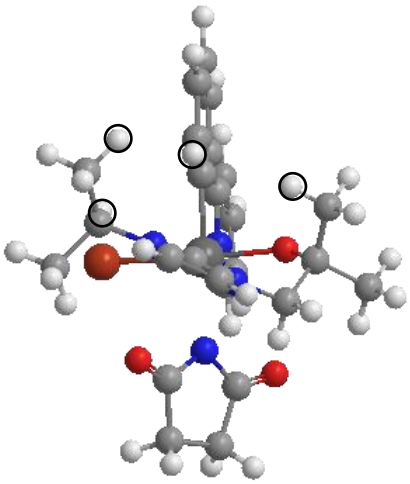

Figure 3. Calculated molecular structure of (L^O)Pd(phpy)(Br)(succinimide), isomer **NBS-2**, with protons proximal to H26 highlighted. Selected H···H distances in **NBS-2**: H26···H2 2.73 Å, H26···H4A 2.27 Å, H26···H10A 2.56 Å. **NBS-3** is structurally very similar except the succinimide group is *trans*-disposed to the alkoxide tether. Selected H···H distances in **NBS-3**: H26···H2 3.06 Å, H26···H4A 2.06 Å, H26···H10A 2.50 Å.

Complex	Succinimide C=O IR frequencies (cm^{-1})
N-bromosuccinimide	1718 (υ_{as}), 1311 (δ)
(L^O)Pd(phpy)(Br)(succinimide)	1713 (υ_{as}), 1621 (δ)
$Pd(phpy)_2(Cl)$(succinimide)[10]	1712 (υ_{as}), 1634 (δ)
NBS-1	1753 (υ_{as}), 1685 (δ)
NBS-2	1729 (υ_{as}), 1657 (δ)
NBS-3	1752 (υ_{as}), 1692 (δ)

Table 1. Selected C=O succinimide IR frequencies. Calculated frequencies scaled by 0.96 to account for systematic overestimation inherent in the DFT calculations.

The calculated structures for **NBS-2** and **NBS-3** contain short H···H distances (2-3 Å) between H26 and H2, and between H26 and one of the methyl groups on the isopropyl and alkoxide arm of the NHC ligand which match with the observed nOe data, Figure 3. Aside from the structural data, the infra-red spectra were also generated as part of the calculation process. As Table 1. shows **NBS-2** is a better match than **NBS-1** or **NBS-3**.

The experimental data for (L^O)Pd(phpy)(Br)(succinimide) is in good agreement with the other example of a Pd^{IV} complex containing a succinimide and a phpy ligand, $Pd(phpy)_2(Cl)$(succinimide).[10] As with **NBS-2** this complex has the succinimide ligand *trans*-disposed to the phenyl group.

3.2.2. Oxidation of (L^O)Pd(bzq) with NBS

In an effort to obtain single crystals suitable for X-ray diffraction studies, (L^O)Pd(bzq) was treated with NBS at -35 ºC in a variety of solvents. A variety of crystallisation techniques including vapour diffusion, layering with anti-solvent and slow evaporation at -35 ºC were tried. As with (L^O)Pd(phpy)(Br)(succinimide), an amorphous red solid was obtained in each case. Comparison of the ^{1}H NMR spectrum for (L^O)Pd(phpy)(Br)(succinimide) with that obtained for (L^O)Pd(bzq)(Br)(succinimide) demonstrates that the compounds are very similar (Table 2).

Complex	^{1}H NMR shift H2	^{1}H NMR shift H16	Succinimide IR frequencies (cm^{-1})
(L^O)Pd(bzq)(Br)(succinimide)	5.80	9.32	1713 (υ_{as}), 1615 (δ)
(L^O)Pd(phpy)(Br)(succinimide)	5.71	8.95	1713 (υ_{as}), 1621 (δ)

Table 2. Selected data for (L^O)Pd(bzq)(Br)(succinimide) and (L^O)Pd(phpy)(Br)(succinimide). The majority of the corresponding resonances in the ^{1}H NMR spectra occur at the same frequency for the two complexes.

It is probable that (L^O)Pd(bzq)(Br)(succinimide) adopts the same geometry as (L^O)Pd(phpy)(Br)(succinimide) (Equation 2). The lower solubility of (L^O)Pd(bzq)(Br)(succinimide) in CD_3CN prevented observation of a ^{13}C NMR spectrum.

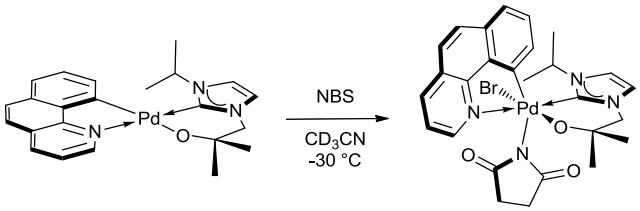

(2)

3.2.3. Reductive elimination reactions of (L^O)Pd(phpy)(Br)(succinimide)

Having established it is possible to form Pd^{IV} complexes using NBS as the oxidant, attention was turned to C-X bond formation from these Pd^{IV} complexes. When a solution of (L^O)Pd(phpy)(Br)(succinimide) is warmed to room temperature the solution changes colour from bright red to pale yellow. Analysis of the reaction mixture by ^1H NMR spectroscopy showed the presence of up to six palladium-containing complexes depending upon the concentration and rate of warming.

To separate the organic products from any Pd-containing complexes the products were stirred with basic alumina, passed through a plug of silica and then eluted with ethyl acetate. The only organic product thus obtained was confirmed to be phpy-Br by ^1H NMR spectroscopy and GC analysis. This is gratifying because many side reactions (*e.g.* C_{carb}-C_{phpy}, C_{phpy}-O, C_{phpy}-N bond-forming reductive elimination) are possible in this system.

One palladium containing complex (20 % of the eluted sample by integration) was obtained and was later found to correspond to (L^{OH})Pd(phpy)(Br), Figure 4. It is unclear how the succinimide ligand was lost or how the Pd-$O_{alkoxide}$ bond was cleaved.

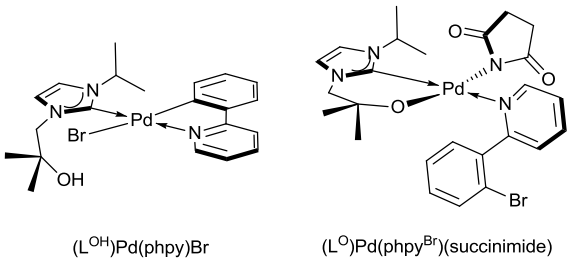

$(L^{OH})Pd(phpy)Br$ $(L^{O})Pd(phpy^{Br})(succinimide)$

Figure 4. Two of the products from the decomposition of $(L^{O})Pd(phpy)(Br)(succinimide)$.

If a dilute solution of $(L^{O})Pd(phpy)(Br)(succinimide)$ is allowed to warm slowly from -35 ºC to room temperature the major product formed is pale yellow $(L^{O})Pd(phpy^{Br})(succinimide)$, Figure 4, right-hand side. Heating a powdered sample of $(L^{O})Pd(phpy)(Br)(succinimide)$ at 90 ºC for 5 mins afforded the same major product as confirmed by ^{1}H NMR spectroscopy (90 % yield).

3.2.4. Products from decomposition of $(L^{O})Pd(bzq)(Br)(succinimide)$

When a solution of $(L^{O})Pd(bzq)(Br)(succinimide)$ is warmed to room temperature a number of palladium containing products are formed. The ratio of these products is dependant upon the concentration and rate of temperature change of the reaction. The outcome is even more complex than that for $(L^{O})Pd(phpy)(Br)(succinimide)$ as there are a number of complexes with similar solubility.

A dilute solution of $(L^{O})Pd(bzq)$ in MeCN was treated with one equivalent of NBS at -35 ºC. After allowing the solution to warm to room temperature, an aliquot was stirred with basic alumina, passed through a plug of silica and then eluted with ethyl acetate. The main product thus obtained was $(L^{OH})Pd(bzq)(Br)$, and no organic product was recovered.

Treatment of a concentrated solution of $(L^{O})Pd(bzq)$ with an equimolar amount of NBS at 25 ºC afforded $(L^{OH})Pd(bzq)(Br)$ in 19 % yield after workup. The characteristic resonances in the ^{1}H NMR spectrum (CD_3CN) are at 9.57 ppm (H16), 6.40 ppm (H26), 5.53 ppm (H2) and 3.25 (OH). The resonance for the carbene carbon is at 171.5 ppm (CD_2Cl_2).

Treatment of a dilute solution of (L^O)Pd(bzq) in MeCN at -35 ºC with an equimolar amount of NBS afforded (L^O)Pd(bzq^{-Br})(succinimide) plus four similar Pd^{II} complexes after workup. In the ^{13}C NMR spectrum (CD_3CN) the carbene resonances appear at 179.7, 155.3, 155.3 and 155.2 ppm. There are also four resonances attributable to Pd-bound succinimide, the five complexes are present in a 1:1:1:0.75:0.5 ratio (by integration) and the mixture also contains free bzq-Br and succinimide.

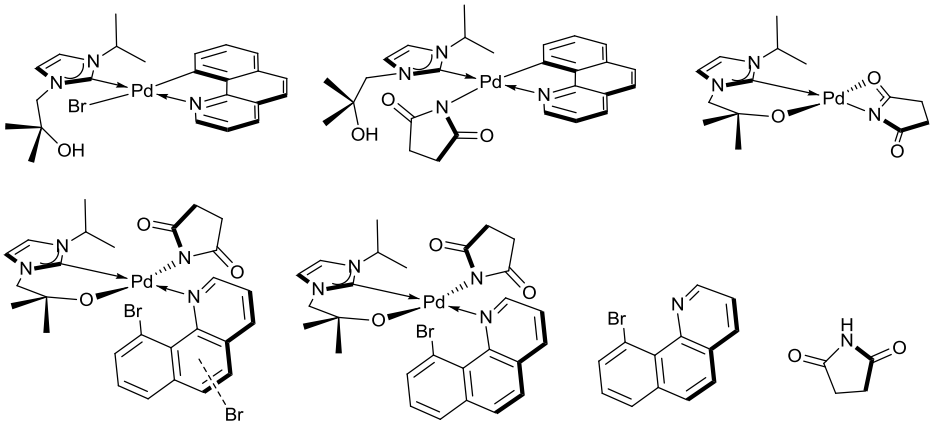

Figure 5. Possible products from treatment of (L^O)Pd(bzq) with NBS.

This prevented detailed conclusive identification of the products. Some of the possible products (based on spectroscopic observations and subsequent reactivity studies) are illustrated in Figure 5.

3.2.5. Analysis of NBS reaction by electrospray mass spectrometry

Mass spectrometry was used to study the reaction between (L^O)Pd(phpy) and NBS. The complex initially obtained upon treatment of (L^O)Pd(phpy) with NBS was compared with that obtained after 24 h at room temperature (Figure 6). As Figure 6 illustrates, phpy-Br is not present initially but is after 24 h. Looking at the palladium-containing complexes, the absence of $[(L^O)Pd(phpy)(Br)]^+$ after 24 h suggest that C-Br bond formation has taken place.

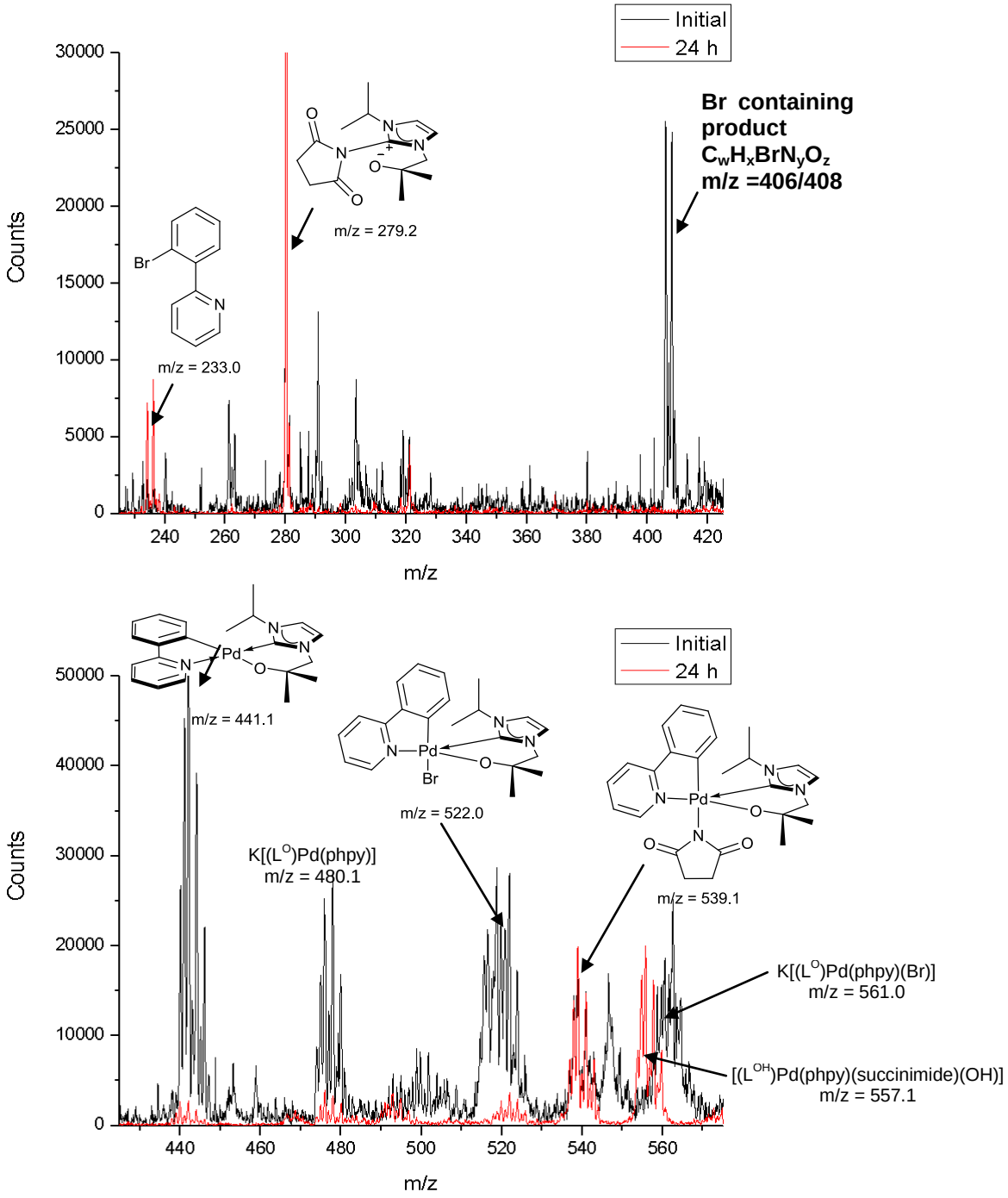

Figure 6. Comparison of (L^O)Pd(phpy)(Br)(succinimide) [black] and (L^O)Pd($phpy^{Br}$)(succinimide) [red] by mass spectrometry.

The sample was injected as a MeCN solution down a silica capillary. This can lead to incorporation of Li^+, Na^+ and K+ ions in the complexes observed.

3.2.6. Reaction of (L^O)Pd(phpy)(Br)(succinimide) with water

Failure to exclude moisture from the oxidation reaction has a significant effect. If (L^O)Pd(phpy) and NBS are combined at -20 °C in CD_3CN that has not been rigorously dried, the resonances for (L^O)Pd(phpy)(Br)(succinimide) in the ^1H NMR spectrum are replaced by two new sets of signals (in a 2:3 ratio). Monitoring the reaction by ^1H NMR spectroscopy it was clear that the two different sets of resonances correspond to two isomers of a Pd^{IV} complex, (L^{OH})Pd(phpy)(Br)(succinimide)(OH).

The characteristic resonances are 9.88 ppm (H16), 6.46 ppm (H26), 6.16 ppm (H2) and 3.94 ppm (ROH) for isomer 1 and 8.16 ppm (H16) 6.12 ppm (H26) 5.45 ppm (ROH) and 5.42 ppm (H2) for isomer 2. No Pd-OH resonances were identified. The shift of the resonance for H26 from ~7.3 ppm to 6.1-6.5 ppm combined with the appearance of OH signals is indicative of cleavage of the Pd-alkoxide bond.

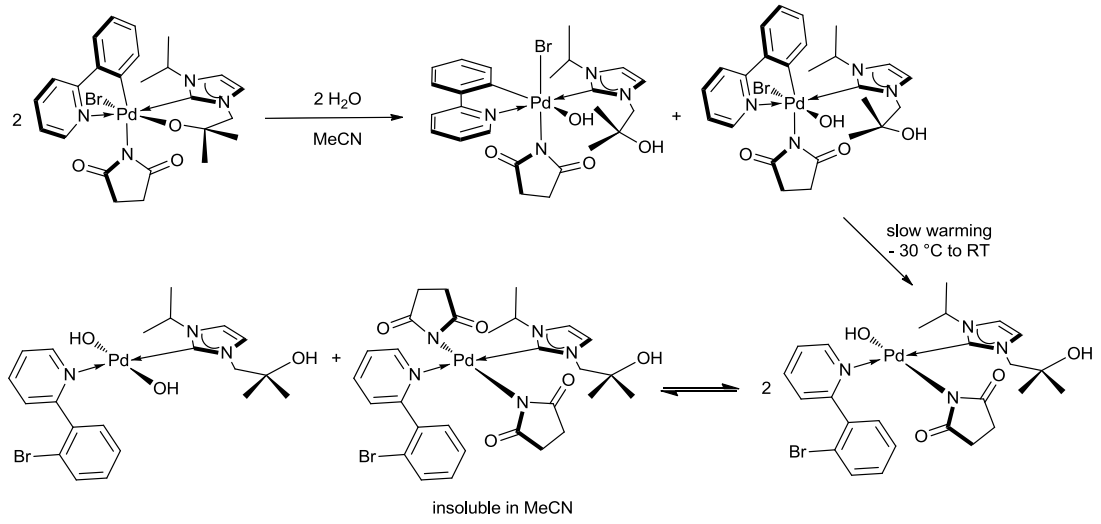

Scheme 2. Formation of (L^{OH})Pd($phpy^{Br}$)(succinimide)$_2$ in wet MeCN.

The high chemical shifts of the resonances in isomer 1 could suggest steric crowding. This would come about if the Br and succinimide ligands are in a *trans*-configuration; the NHC ligand is restricted from being orthogonal to the phpy ligand increasing the steric crowding

(Scheme 2). Upon warming to room temperature C-Br bond formation is observed (*vide infra*).

The product of C-Br bond formation can then undergo ligand exchange to give $(L^{OH})Pd(phpy^{Br})(OH)_2$ and $(L^{OH})Pd(phpy^{Br})(succinimide)_2$. The driving force for the reaction is precipitation of $(L^{OH})Pd(phpy^{Br})(succinimide)_2$ from solution. Single crystals of $(L^{O})Pd(phpy^{Br})(succinimide)_2$ suitable for X-ray diffraction studies were obtained after air was able to enter a sample of $(L^{O})Pd(phpy)(Br)(succinimide)$ in CD_3CN at -30 ºC. $(L^{O})Pd(phpy^{Br})(succinimide)_2$ is insoluble in MeCN and poorly soluble in C_5D_5N. It can be reproducibly obtained by treatment of $(L^{O})Pd(phpy)$ with NBS in wet MeCN. The molecular structure is shown in Figure 7.

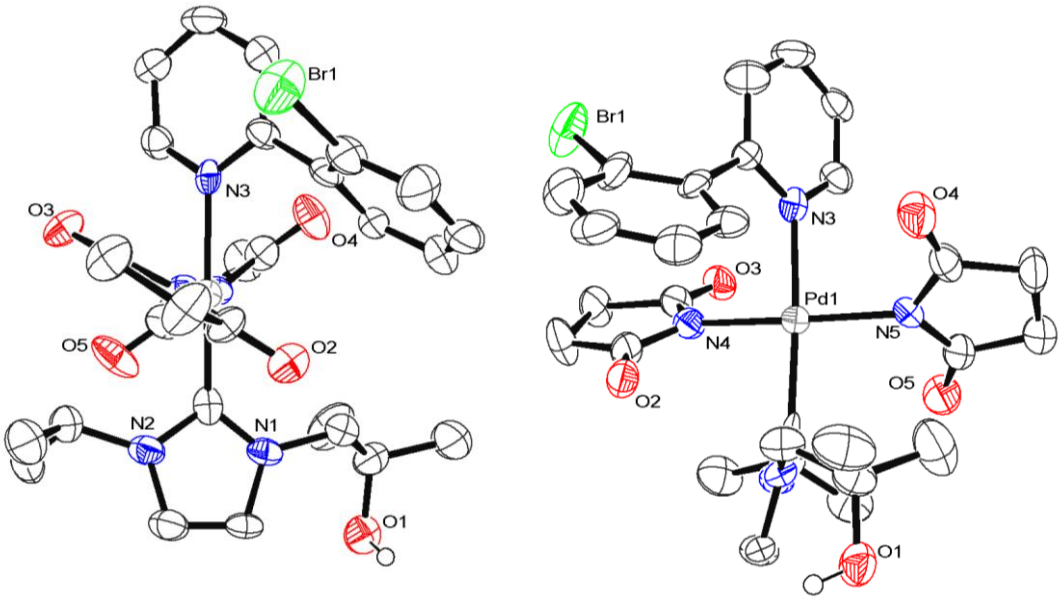

(front) (side)

Figure 7. Molecular structure of $(L^{OH})Pd(phpy^{Br})(succinimide)_2$. Ellipsoids drawn at the 50% probability level. Hydrogen atoms except alcohol omitted for clarity.

The data obtained was not of sufficient quality to accurately determine bond lengths and angles in the complex. However, structural connectivity was established and showed a

square planar palladium centre in $(L^{OH})Pd(phpy^{Br})(succinimide)_2$. The NHC and phpy-Br ligands are *trans*-disposed and are tilted away from coplanarity. The two succinimide ligands are also *trans*-disposed and the planes of the ligands are close to orthogonal.

3.3. Pd-catalysed ligand-directed oxidative halogenation

Having determined that NBS can oxidise $(L^{O})Pd(phpy)$ to make a Pd^{IV} complex which can then undergo C-Br bond formation, an appraisal of the catalytic activity was made. It was clear from the outset that $(L^{O})Pd(phpy)$ would be a poorer catalyst than $Pd(OAc)_2$ for several reasons:

- The presence of a bidentate ligand reduces the number of sites available for substrate coordination.
- The strongly electron-donating NHC ligand will also reduce the electrophilicity of the metal centre. This will slow the rate of C-H activation which is known to be the rate determining step.
- The alkoxy-tethered NHC ligand has been shown to stabilise the Pd^{IV} complexes generated, potentially increasing turn-over time.
- The requirement to carry out the reaction under air- and moisture-free conditions makes it less attractive for practical applications. Additionally, the reaction cannot be carried out in AcOH which can assist with the C-H activation step.

However, it is important to determine how much of an effect tethered-NHC ligands have under the catalytic conditions and if a catalytic cycle is indeed viable. $(L^{O})Pd(phpy)$ can be considered a precatalyst; initial oxidation by NBS followed by reductive elimination of phpy-Br yields a complex similar to $(L^{O})Pd(phpy^{Br})(succinimide)$ (Scheme 3). In the presence of excess substrate the phpy-Br would be displaced and C-H activation of this substrate would start the catalytic cycle.

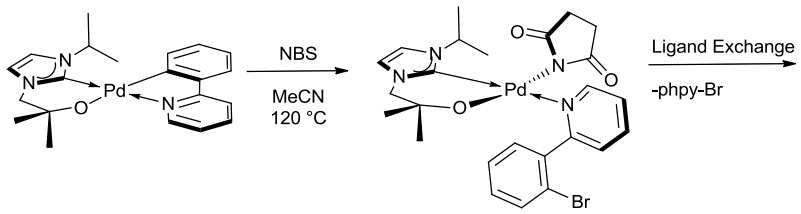

Scheme 3. Route from precatalyst (L^O)Pd(phpy) into the catalytic cycle.

3.3.1. Stability of (L^O)Pd(phpy) under catalytic conditions

The stability of the precatalyst under the catalytic conditions was evaluated. All reactions were carried out in ampoules in the dark, under air and moisture-free conditions.

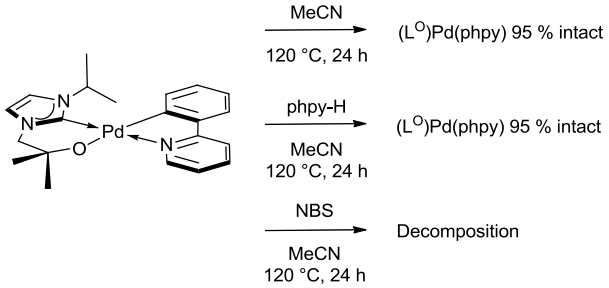

Scheme 4. Stability of precatalyst (L^O)Pd(phpy) under catalytic conditions.

(L^O)Pd(phpy) is stable in MeCN at 120 °C for 24 h (Scheme 4). It is also stable in the presence of 20 equivalents of phpy-H. With 20 equivalents of NBS, and no phpy-H, decomposition of the NHC ligand is evident in the ^{1}H NMR spectrum.

3.3.2. Initial screening of (L^O)Pd(phpy) catalysed halogenation

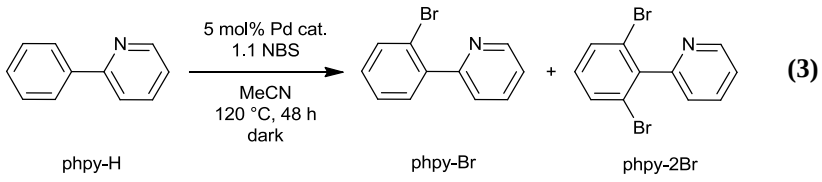

(3)

In a typical reaction the catalyst, substrate and oxidant were combined in a foil covered ampoule. MeCN was added and the reaction mixture was heated to 120 °C for 48-72 h (Equation 3). The reaction mixture was then analysed by GCMS and in each case the halogenated products were identified by the mass spectrum. No calibration curve was performed; comparisons between the results in each Table are valid although there could be a systematic error of as much as 15 % in the reported yields. A sample of the crude reaction mixture was also analysed by ^{1}H NMR spectrometry to check the fate of the catalyst.

The Sanford group were able to use a range of halogenating reagents to oxidatively functionalise 3-methyl-2-phenylpyridine.[15] This substrate was used because it can only be halogenated once. Given the expected lower reactivity of (L^O)Pd(phpy), phpy-H is suitable for an initial comparison. A number of oxidants were evaluated for the catalytic halogenation of phpy-H using (L^O)Pd(phpy) as a precatalyst under comparable conditions to $Pd(OAc)_2$ (Table 3).

Entry	Oxidant	phpy-X[a]	Reported for $Pd(OAc)_2$[b,15]
a	NBS	25 %	44 %
b	NCS	27 %	56 %
c	I_2	No reaction	40 %
d	I_2/$PhI(OAc)_2$	Decomposition	71 %

Table 3. Catalytic oxidative halogenation of phpy-H. [5 mol% (L^O)Pd(phpy), 1.0 phpy-H 1.1 oxidant, MeCN, 100 °C, 12 h] [a] GC yield based on integration of peaks. No phpy-2X was observed. [b]Results for 3-methyl-2-phenylpyridine.

Only the strong oxidants NCS and NBS were suitable for (L^O)Pd(phpy) catalysed ligand-directed C-H bond oxidative-halogenation. The lower yields compared to $Pd(OAc)_2$ are in line with slower rates of these catalysed reactions. The lack of reaction with I_2 can be explained by the iodine simply not being a strong enough oxidant. The decomposition of the

substrate observed when I_2/PhI(OAc)$_2$ was utilised could be the result of a competing non-catalysed process.

3.3.3. Ligand directed catalytic functionalisation using (L^O)Pd(phpy)

Entry	Substrate	Oxidant	Product	GC Yield[a]
e	phpy-H	NCS	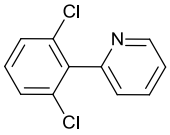	phpy-2Cl, 63 %[b]
f	bzq-H	NCS	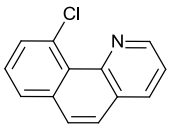	bzq-Cl, 96 %[c]
g	*n*-BuOpy-H	NCS	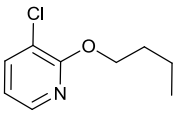	*n*-BuOpy-Cl, 56 %[d]
h	Etpy-H	NBS	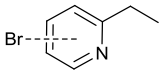	Etpy-Br, 27 %[e]
i	Etpy-H	NCS	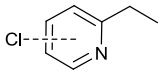	Etpy-Cl, 6 %[e]
j	*o*-tolylpy-H	NBS	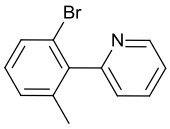	*o*-tolylpy-Br, 3 %[c]
k	*o*-tolylpy-H	NCS	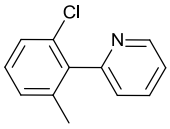	*o*-tolylpy-Cl, 17 %[c]

Table 4. Summary of halogenation [10 mol% (L^O)Pd(phpy), 1.0 substrate, 1.1 NXS, MeCN, 120 °C, 48 h] [a]GC yield based on integration of peaks, average of two runs. [b]Added 2.5 equiv. of NCS to make phpy-2Cl, also obtained 34 % of phpy-Cl. [c]5 mol % (L^O)Pd(phpy). [d]Chlorination of the aromatic ring occurred rather than alkyl chain and is Pd catalysed. [e]Halogenation of the aromatic ring occurred rather than alkyl chain and happens in absence of catalyst.

Having identified suitable oxidants, a range of substrates were evaluated, Table 4. (L^O)Pd(phpy) is a suitable precatalyst for the chlorination of bzq-H and phpy-H in good yield (96 % and 63% respectively).

The only $Pd^{II/IV}$ catalysed ligand-directed catalytic halogenation of an sp^3 C-H bond reported by the Sanford group is 8-methylquinoline.[14] The rigid aromatic system holds the methyl group in proximity to the pyridine directing group. Additionally the electronic effect of being bound to an aromatic system lowers the barrier to C-H bond activation. Consequently the lack of sp^3 halogenation for Etpy-H is not surprising.

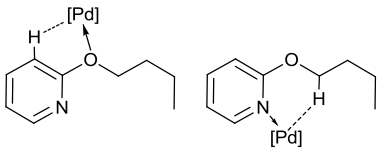

Figure 8. Possible C-H bond activation intermediates of *n*-BuOpy-H. O-directed C-H activation is preferred.

The resonances in the ^{1}H NMR spectrum for the substituted *n*-BuOpy-H show substitution on the pyridine ring proximal to the ether rather than the alkyl chain as desired. It was hoped the presence of the oxygen would help lower the barrier to C-H activation at the adjacent sp^3 centre. There is competition between the pyridine and ether heteroatom to ligate to palladium (Figure 8). Whilst pyridine is a stronger donor and so will be bound more of the time, the C-H bond on the pyridine ring proximal to the ether is significantly easier to activate.

The ^{1}H NMR spectra of the crude reaction mixtures allow the fate of the catalyst to be established. For bzq-H and phpy-H a single set of ligand resonances is observed for the catalyst. The chemical shift of H2 indicates the NHC ligand is still attached to Pd (5.7 and 6.0 ppm respectively). With *o*-tolylpy-H the NHC ligand resonances can be identified but are significantly broadened. In the catalytic halogenation of Etpy-H the resonances for H2 were

identified at 5.8 and 6.1 ppm (NBS and NCS respectively). A larger amount of decomposition products are observed in the ^{1}H NMR spectra of the crude catalytic halogenation of both *o*-tolylpy-H and Etpy-H when NBS was used compared to NCS.

3.3.4. Ligand directed catalytic bromination using (L^{O})Pd(bzq) and N-bromosuccinimide

Having identified some of the limitations of (L^{O})Pd(phpy) as a precatalyst, efforts were made to get more accurate data.

Entry	Substrate	Product	GC Yield[a]
l	bzq-H	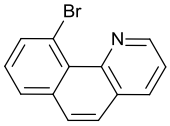	bzq-Br, 81 %
m	phpy-H	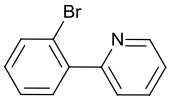	phpy-Br, 73 %[b]
n	Mephpy-H	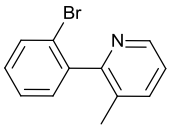	Mephpy-Br, 25 %
o	phpyr-H	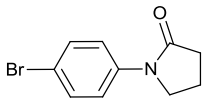	0 %[c]
p	phpyz-H	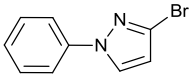	0 %[c]
q	phCOpy-H	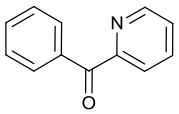	NR

Table 5. Summary of bromination with (L^{O})Pd(bzq) [5 mol% (L^{O})Pd(bzq), 1.25 NBS, MeCN, 100 °C, 48-96 h] [a] Average of two concurrent runs; [b] Additional 1.25 equiv of NBS added after 48 h, heated for 96 h. ca. 5 % of phpy-2Br was formed; [c] substrate reacts with the oxidant to brominate in a different position, so no catalytic yield can be determined.

The phpy-Br formed by initial oxidation of the precatalyst could compete with the desired substrate to bind to Pd, thus lowering the rate of reaction. To avoid this (L^O)Pd(bzq) was used as the precatalyst since bzq-Br is a much poorer ligand than phpy-Br for Pd.

In a typical reaction (L^O)Pd(bzq), NBS and substrate were combined in a foil covered ampoule. MeCN was added and the reactions were heated to 100 °C for 72 h. The reaction mixture was then analysed by gas chromatography, and in each case the brominated products were identified by comparison with GC data from genuine samples. The addition of naphthalene at the end of the reaction as a GC standard allowed accurate determination of GC yields (after a calibration curve). The crude reaction mixtures were also analysed by ^{1}H NMR spectroscopy to determine the fate of the catalyst.

As demonstrated in Table 5, excellent yields were obtained for the formation of bzq-Br and phpy-Br as expected. The lower yield for Mephpy-Br is disappointing but highlights the slower turn-over of the system (entry n and t).

Entry	Substrate	Product	GC Yield[a]
r	bzq-H	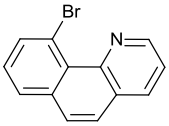	bzq-Br, 93 %
s	phpy-H	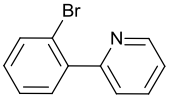	phpy-Br, 63 %[b]
t	Mephpy-H	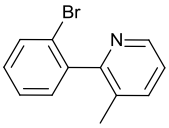	Mephpy-Br, 53 %
u	phCOpy-H	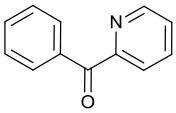	phCOpy-Br, 56 %

Table 6. Comparable data for $Pd(OAc)_2$ [Analogous reaction conditions as above, with 5 mol% Pd(OAc)2 1.5 - 2.5 NBS, AcOH or MeCN, 100 °C, 12h.][14] [a] Average of two concurrent runs; [b] Additionally 15 % phpy-2Br was formed (M. S. Sanford et. al. unpublished results).

In the bromination of phpyz-H and phpyr-H, non-catalysed processes, which compete when $Pd(OAc)_2$ is used as a catalyst, dominate. The decreased activity makes (L^O)Pd(bzq) selective towards monobromination of 2-phenylpyridine compared to $Pd(OAc)_2$ (entries m and s), but unable to functionalise phCOpy-H.Notably, these reactions are slow relative to those catalyzed by $Pd(OAc)_2$, which are complete within 12 h under identical conditions. This is not unexpected since the current system was optimized for the stabilization of Pd^{IV}, and cyclopalladation (typically the rate determining step) is expected to be sluggish at a more electron rich Pd^{II} centre.[19]

Importantly, at the end of catalytic reactions, no protonated/unbound carbene ligand was observed by ^{1}H NMR spectroscopy, suggesting the enhanced stability of the Pd-carbene bond to prolonged heating under oxidizing conditions. If the reactions are not carried out in the dark around a 15 % improvement in yield is observed. However, the resultant reaction mixtures have much higher amounts of undesired side products (by ^{1}H NMR spectroscopy).

This lower activity presents interesting opportunities with molecules with more than one site that could undergo ligand directed C-H bond functionalisation (Figure 9). Whilst $Pd(OAc)_2$ might be expected to give a complex mixture of products functionalised at H^{1-4}, the decreased activity of (L^O)Pd(bzq) is likely to result in more selective functionalisation at H^2 only.

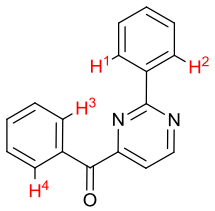

Figure 9. Substrate with multiple sites for ligand directed C-H bond activation.

3.4. Reaction profile (L^O)Pd(phpy) and N-bromosuccinimide

Having identified the probable structure for the Pd^{IV} complex produced by treatment of (L^O)Pd(phpy) with NBS it was of comparatively little extra effort to map out an entire reaction profile, Figure 10. Comparing the calculated reaction pathway with the experimental results it is clear that the actual reaction is significantly more complex. Under dilute conditions the oxidation/reductive elimination pathway considered here (intramolecular processes only) appears to be dominant. Whilst the catalysis is carried out under dilute conditions (in Pd), the evidence points to the Pd-O bond no longer being intact in the active catalyst. Taking account of this is prohibitively expensive. The number of potential isomers that would have to be considered at each stage in the reaction is at the very least doubled or tripled.

The four-coordinate Pd^{II} complex (**Reactant-E1**) initially undergoes C-H activation (**TS-E1**). Dissociation of a succinimide anion is required to yield a vacant site for C-H activation. The C-H bond undergoing activation is bound to Pd with C_{phenyl}-Pd and Pd-H bonds of 2.26 Å and 2.18 Å respectively. The C-H bond has lengthened from 1.07 to 1.27 Å and is out of the plane of the aromatic ring by 35.1°. The succinimide ligand has shifted from the Pd to form a N-H bond (1.56 Å). The free energy cost of **TS-E1** is calculated to be +39.7 kcal/mol. Loss of succinimide leads to the formation of a four-coordinate Pd^{II} complex (**Int-E1)**. The free energy change is -5.3 kcal/mol relative to **Reactant-E1**.

If oxidation were to occur *via* homolytic cleavage of the N-Br bond in NBS then formation of a Pd^{III} intermediate (**Int-E4**) might be expected. The free energy change is +17.4 kcal/mol relative to **Reactant-E1**. In **Int-E4** the C_{phenyl}-Pd and Br-Pd bonds are *trans*-disposed. Subsequent radical recombination would give an isomeric Pd^{IV} complex of **Int-E2**. This isomer of **Int-E2** where the C_{phenyl}-Pd and Br-Pd bonds are *trans*-disposed would have to go through **Int-E3** for C-Br bond formation to occur.

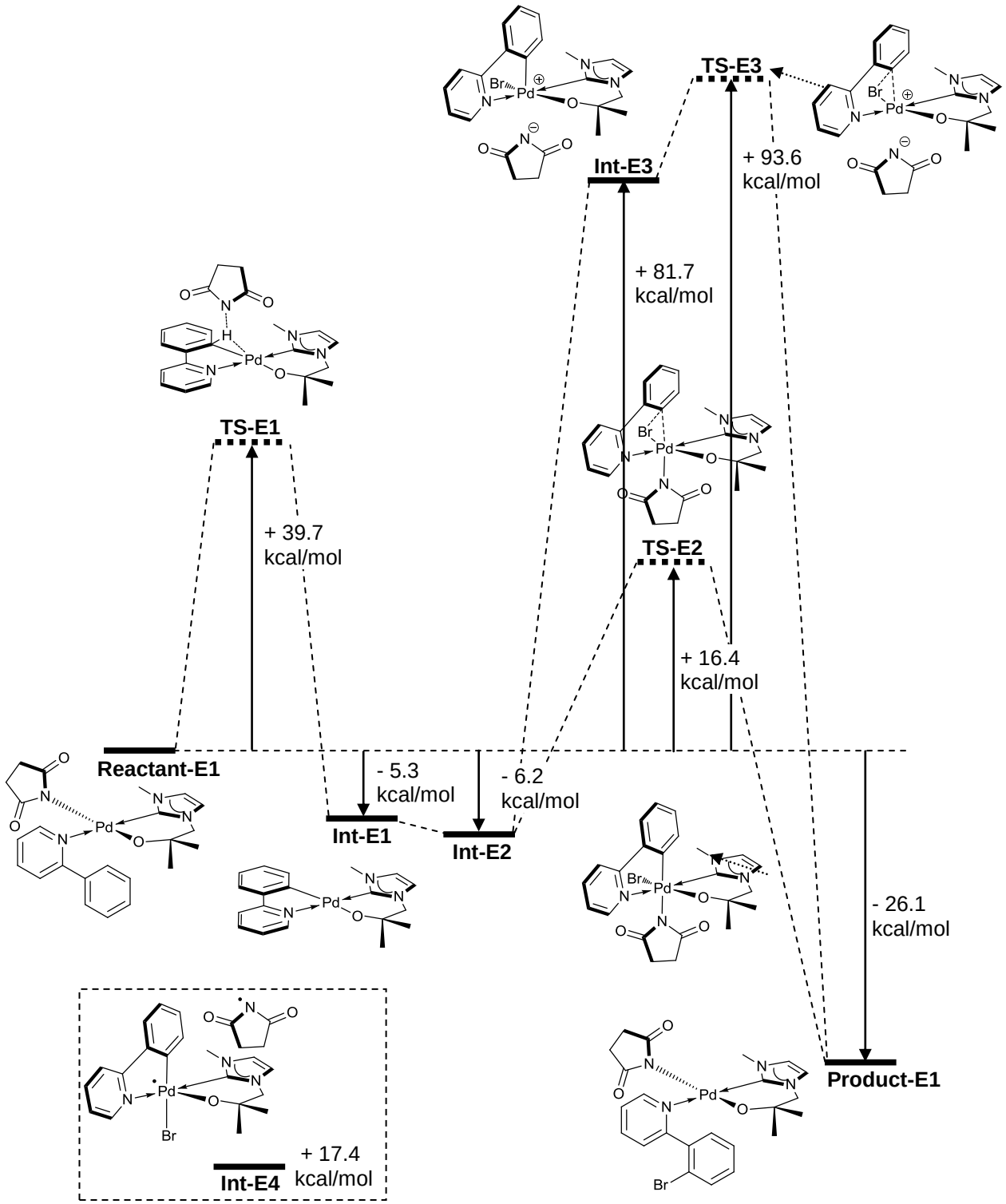

Figure 10. Free energy profile for reaction between (L^O)Pd(phpy) and NBS (all the free energies are relative to Reactant). Barrier to reductive elimination for (L^O)Pd(phpy)(Br)(Succinimide), +22.6 kcal/mol.

Int-E1 reacts with NBS to yield a six-coordinate Pd^{IV} complex (**Int-E2**). The NBS has added in a *cis* arrangement; with the succinimide *trans*-disposed to, and the bromide *cis*-disposed to, the C_{phenyl}-Pd bond. The free energy change is -6.2 kcal/mol relative to **Reactant-E1**.

From **Int-E2** there are two possible outcomes, direct reductive elimination to make a new C_{phenyl}-Br bond (**TS-E2**) or loss of the succinimide ligand to form a five-coordinate cationic Pd^{IV} complex (**Int-E3**) from which reductive elimination can occur (**TS-E3**). In **TS-E2** C-Br bond formation leads to the C_{phenyl}-Pd-Br angle decreasing from 89.7° to 52.6°. At the same time the C_{phenyl}-Pd and Br-Pd bond lengths increase from 2.02 Å to 2.26 Å and 2.57 Å to 2.86 Å respectively. The free energy cost of **TS-E2** is calculated to be +16.4 kcal/mol. Once formation of the C_{phenyl}-Br bond is complete **Product-E1** (a four coordinate Pd^{II} complex) is obtained with an overall free energy change of -26.1 kcal/mol.

Alternatively, loss of a succinimide anion yields **Int-E3** in which the Br is still *cis*-disposed to the C_{phenyl}-Pd bond. The free energy change is +81.7 kcal/mol relative to **Reactant-E1**. In **TS-E3** the C_{phenyl}-Pd-Br angle decreases from 100.0° to 57.8° to facilitate C-Br bond formation. The C_{phenyl}-Pd and Br-Pd bond lengths increase from 2.03 Å to 2.26 Å and 2.54 Å to 2.62 Å, respectively. The free energy cost of **TS-E3** is calculated to be +93.6 kcal/mol. Recombination of the succinimide anion yields the four coordinate Pd^{II} complex **Product-E1**.

3.4.1. Discussion

The catalytic cycle begins by C-H bond activation of phpy-H and loss of succinimide. As indicated in Figure 11, the process of C-H activation is multi-step, although only one transition state could be identified (**TS-E1**). Transitional structures were obtained as part of the modelling process but contained more than one negative frequency in their vibrational

modes and so are not transition state structures. The short Pd···H contact (2.18 Å) and elongated C-H distance (1.27 Å) in **TS-E1** are indicative of an agostic complex.

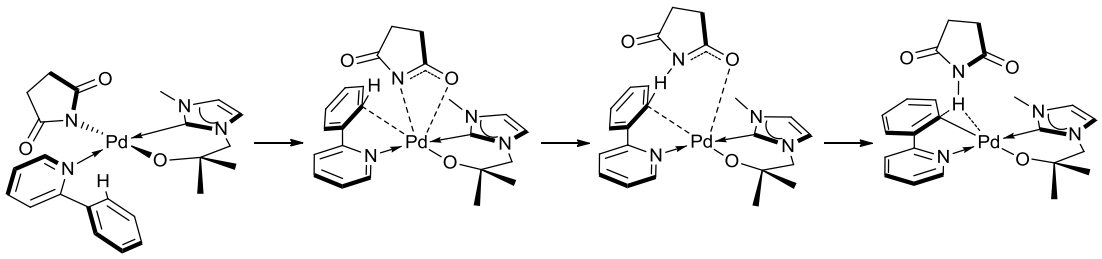

Figure 11. Possible process of C-H activation at **Reactant-E1**.

It is possible that **Int-E1** could react with NBS to make a five-coordinate Pd^{III} complex (**Int-E4**). However, the calculated barrier to reductive elimination is approximately equal to the energy of a Pd^{III} intermediate. Experimentally $(L^{O})Pd^{IV}$(phpy)(Br)(succinimide) forms readily at -30 °C upon treatment with NBS, and C-Br bond formation does not start to occur until the solution is warmed to about 0 °C. This suggests the barrier to oxidation is much lower than for reductive elimination.

From $(L^{O})Pd^{IV}$(phpy)(Br)(succinimide) it appears C-Br bond formation occurs directly. A cationic intermediate cannot be ruled out even though the calculated energies are considerably higher. The structures were calculated in the gas phase and it is well known that DFT overestimates the energies of charged complexes. Inclusion of solvent into the calculations (by utilising a solvent field and/or explicit inclusion of solvent molecules) tends to lower the calculated energies of charged complexes significantly relative to the non-charged ones. The extent to which this occurs is very dependent on the methodology used to model the solvent. There were insufficient computational resources to make a fuller appraisal of the reaction including solvent effects.

To complete the cycle from **Product-E1** back to **Reactant-E1** a ligand exchange is required. Assuming that phpy-H and phpy-Br have equal binding affinities then the exchange would be under statistical control with an overall free energy change close to 0 kcal/mol.

Formation of $(L^{OH})Pd(phpy)Br$ and succinimide from the decomposition of $(L^{O})Pd(phpy)(Br)(succinimide)$ could be explained by formation of **Int-E4**. The radicals in **Int-E4** could extract protons from the solvent to give $(L^{OH})Pd(phpy)Br$ and succinimide. The energy of **Int-E4** is only +1 kcal/mol greater than the proposed C-Br bond forming transition state. This suggests that **Int-E4** could be an alternative product present under conditions when C-Br bond formation is able to occur.

3.5. Oxidation of $(L^{O})Pd(bzq)$ with $PhI(Cl)_2$

The above evidence strongly supports the existence of a Pd^{IV} intermediate in ligand-directed oxidative functionalisation catalysis. The complex nature of the reactivity and the inability to obtain a single crystal suitable for X-ray diffraction studies was frustrating. Treatment of $(L^{O})Pd(bzq)$ with $PhI(Cl)_2$ was undertaken to confirm the intermediate presence of a Pd^{IV} complex. It was hoped the extra rigidity (compared to phpy) would help to stabilise any Pd^{IV} intermediates and the large, planar ligand produce a more crystalline product.

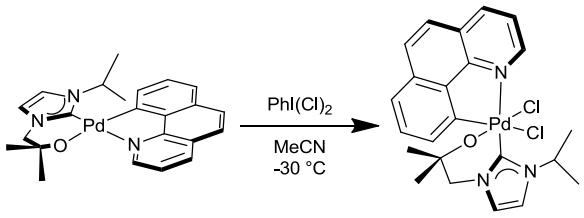

(4)

Treatment of $(L^{O})Pd(bzq)$ with an equimolar amount of $PhI(Cl)_2$ in CD_3CN at -30 °C resulted in the formation of $(L^{O})Pd(bzq)Cl_2$ from the oxidative addition of two chloride ligands to the Pd centre (Equation 4). Monitoring the reaction by ^{1}H NMR spectroscopy, rapid and essentially quantitative formation of $(L^{O})Pd(bzq)Cl_2$ can be observed. The resonance for H16 is shifted to higher frequency (9.80 ppm), and the carbene resonance is now observed at 150.6 ppm in the ^{13}C NMR spectrum. $(L^{O})Pd(bzq)Cl_2$ has been fully characterised and is stable in the solid state for at least one week at room temperature.

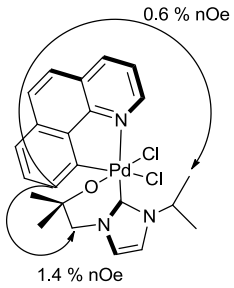

Figure 12. Observed nOe interactions in $(L^{O})Pd(bzq)Cl_2$.

An nOe interaction between H26···H7A and H26···H3A suggests that a similar structure to $(L^{O})Pd(bzq)(Br)$(succinimide) is present in solution, Figure 12.

3.5.1. Single crystal X-ray diffraction structure of $(L^{O})Pd(bzq)Cl_2$

Single crystals of $(L^{O})Pd(bzq)Cl_2$ suitable for X-ray analysis were grown by diffusion of pentanes into an acetone solution of $(L^{O})Pd(bzq)Cl_2$ at -35 °C; the molecular structure is shown in Figure 13.

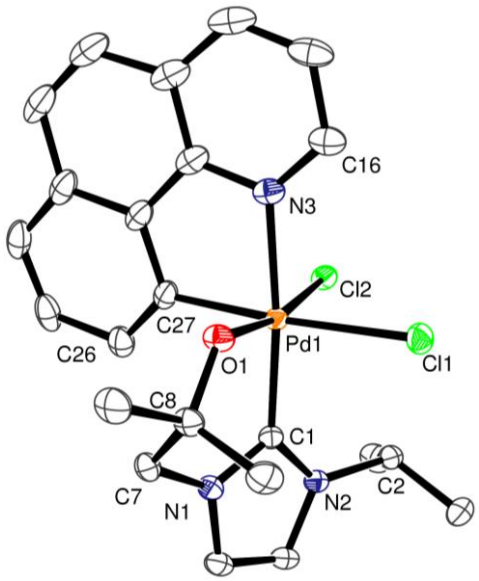

Figure 13. Molecular structure of $(L^{O})Pd(bzq)Cl_2$, ellipsoids drawn at the 50% probability level and hydrogen atoms are omitted for clarity. Selected bond lengths (Å) and angles (deg): Pd1-C1 1.993(2), Pd1-O1 1.993(1), Pd1-N3 2.105(2), Pd1-C27 2.045(2), Pd1-Cl1 2.464(2), Pd1-Cl2 2.342(1); C27-Pd1-C1-N1 60.4(2).

The palladium centre is approximately octahedral. The Pd–$C_{carbene}$ bond is long (1.993(2) Å), and comparison of the Pd–C_{aryl}, Pd–O, and Pd–Cl distances with those in the handful of other structurally characterised Pd^{IV} complexes such as $(phpy)_2Pd(OAc)_2$ and $(phpy)_2Pd(succinimide)Cl$ suggests that they are also longer in $(L^O)Pd(bzq)Cl_2$,[9-12, 20, 21] in accordance with significant steric congestion at the octahedral metal centre. This represents the first example of a structurally characterised Pd^{IV}-NHC complex and also the first Pd^{IV} alkoxide. The nOe interactions suggest that the solid state structure is retained in solution.

3.5.2. DFT analysis of isomers of $(L^O)Pd(phpy)Cl_2$

DFT was found to be suitable for modelling Pd^{II} structures and to check the applicability to Pd^{IV}, computational analysis of the potential isomers of $(L^O)Pd(phpy)Cl_2$ was carried out. It was found that the arrangement of ligands observed for $(L^O)Pd(bzq)Cl_2$ was also the most stable for $(L^O)Pd(phpy)Cl_2$ (Figure 14) with the lowest energy isomer 5.2 kcal/mol lower in energy than the next lowest. This is further confirmation that the level of theory chosen to model the system is appropriate and therefore confidence can be placed in the results of calculations where less experimental data is available.

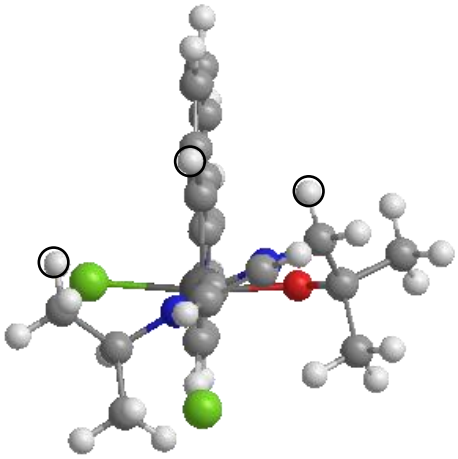

Figure 14. Calculated molecular structure for $(L^O)Pd(phpy)Cl_2$. H⋯H interactions observed by nOe highlighted; H26⋯H7A 2.6 Å and H26⋯H3A 3.8 Å.

3.5.3. Products from decomposition of $(L^O)Pd(bzq)Cl_2$

$(L^O)Pd(bzq)Cl_2$ is stable at -35 °C in acetonitrile but upon warming in solution it undergoes C–Cl bond-forming reductive elimination. As shown in Equation 5, warming a solution of $(L^O)Pd(bzq)Cl_2$ (5.3×10^{-4} M) in MeCN from -30 to 33 °C over 24 h afforded yellow $(L^O)Pd(bzq^{-Cl})Cl$ as the major product in 75% isolated yield.

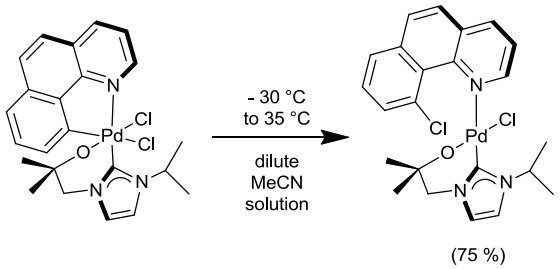

(5)

This is one of only a few examples of directly observable carbon-halogen bond-forming reductive elimination from a Pd^{IV} complex.[9-12] No reductive elimination products containing the carbene ligand were detected under any conditions. This again is surprising because many side reactions (*e.g.*, $C_{carbene}$–C_{bzq}, C_{bzq}–O, or $C_{carbene}$–Cl bond-forming reductive elimination) are possible in this system.

As with NBS, changing the reaction concentration had a significant impact on the products resulting from thermal decomposition. Gratifyingly for $(L^O)Pd(bzq)Cl_2$ only three different products are formed. When the reaction was conducted at a higher concentration (1.1×10^{-2} M), product $(L^O)Pd(bzq^{-Cl})Cl$ was formed as only 46 % of total Pd-containing products (Equation 6). Equimolar quantities of $(L^{OH})Pd(bzq)Cl$ and a complex assigned as $(L^O)Pd(bzq^{2Cl})Cl$ made up the remaining Pd-containing complexes.

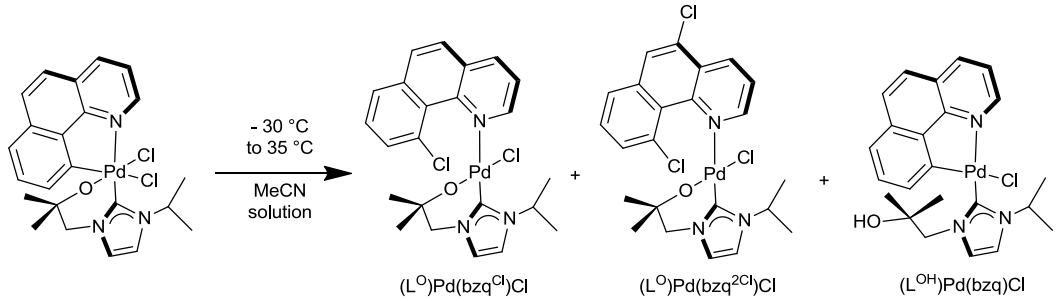

Dilute solution (5.3×10^{-4} M)	10	:	1	:	1
Conc. solution (1.1×10^{-2} M)	1.7	:	1	:	1

(6)

The ratio of these two products was readily determined by integration of the diagnostic ^1H NMR resonances for H16 (9.03 ppm and 9.42 ppm, respectively). The decomposition can be monitored by ^1H NMR spectroscopy. At 25 °C in CD_3CN the half-life of $(L^O)Pd(bzq)Cl_2$ is 40 mins (8.7×10^{-3} M); increasing the concentration approximately six-fold (5.5×10^{-2} M) reduces the half-life by a third (to 27 mins).

$(L^O)Pd(bzq^{2Cl})Cl$ has not been isolated as a sole product of any reaction. $(L^O)Pd(bzq^{2Cl})Cl$ is formulated as the 5,10-dichlorobenzoquinoline ligated isomer, as this is a more reasonable assignment than the 6,10-dichlorobenzoquinoline isomer on chemical grounds, since $PhI(Cl)_2$ is known to chlorinate benzoquinoline at the 5-position. The reaction mixture (from a high-concentration reaction) was stirred with basic alumina, poured onto a plug of silica and eluted with ethyl acetate. Analysis by mass spectrometry (ESI+) confirms the presence of bzq-Cl along with small amounts of bzq-2Cl (confirmed by HRMS).

$(L^O)Pd(bzq^{Cl})Cl$ was treated with $PhI(Cl)_2$ in CD_3CN at 25 °C. The ^1H NMR spectra indicates formation of $(L^O)Pd(bzq^{2Cl})Cl$ along with an unidentified palladium complex in equal quantities. This supports the formulation of $(L^O)Pd(bzq^{2Cl})Cl$ although the exact isomer has not been unequivocally determined.

The formation of $(L^O)Pd(bzq^{2Cl})Cl$ and $(L^{OH})Pd(bzq)Cl$ suggests that intermolecular decomposition pathways (presumably involving electrophilic aromatic substitution on the bzq ligand and protonolysis of the alkoxide) can be competitive for Pd^{IV} complex $(L^O)Pd(bzq)Cl_2$ under some conditions. This is particularly interesting because intramolecular C–X bond forming reductive elimination from Pd^{IV} has typically been assumed to be fast in such systems.[9-12, 20]

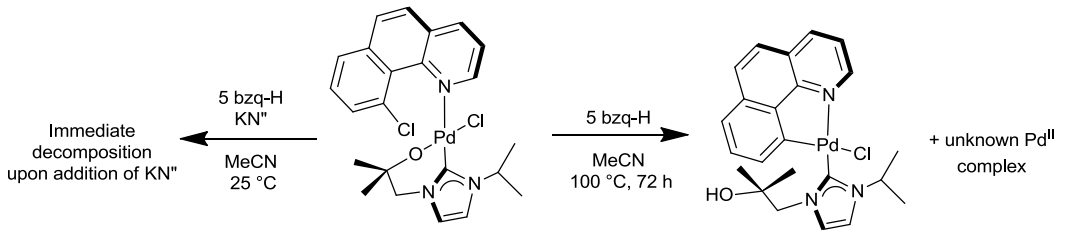

Scheme 5. Attempted C-H activation starting from $(L^{O})Pd(bzq^{Cl})Cl$.

A MeCN solution of $(L^{O})Pd(bzq^{Cl})Cl$ and excess bzq-H was heated to 100 °C for 72 h (Scheme 5). The resultant bright yellow solution was analysed by ^{1}H NMR spectroscopy and by integration of the resonances for H16 and H2 the solution was found to contain 38 % $(L^{O})Pd(bzq^{Cl})Cl$, 30 % $(L^{OH})Pd(bzq)Cl$ and 32 % of an unidentified Pd^{II} complex. The ^{1}H NMR spectrum of the unknown Pd^{II} complex is very similar to $(L^{OH})Pd(bzq)Cl$. When a MeCN solution of $(L^{O})Pd(bzq^{Cl})Cl$ and bzq-H was treated with KN" at 25 °C, with the intention of forming $(L^{O})Pd(bzq)$, decomposition was observed immediately.

3.5.4. Single crystal X-ray diffraction structure of $(L^{OH})Pd(bzq)Cl$

Moisture was able to enter a cold MeCN solution of $(L^{O})Pd(bzq)Cl_2$ and upon warming to room temperature and allowing to stand colourless crystals of $(L^{OH})Pd(bzq)Cl$ were obtained. Complex $(L^{OH})Pd(bzq)Cl$ was characterized by single crystal X-ray analysis and the structure is shown in Figure 15. The palladium centre is approximately square planar and the NHC ligand is almost orthogonal (92.8(2)°) to the plane of the bzq ligand. The Pd–C_{aryl} and Pd–N distances are in agreement with similar reported Pd^{II} complexes such as $(Ph_2\overline{PPhCO_2})\overline{Pd(bzq)}$.[22] The Pd–Cl and Pd–$C_{carbene}$ are also comparable to the related complex $(\overline{NHC})\overline{Pd(PhPhNMe_2)}Cl$ (NHC = N,N'-bis(2,6-di-isopropylphenyl)imidazol-2-ylidene).[23]

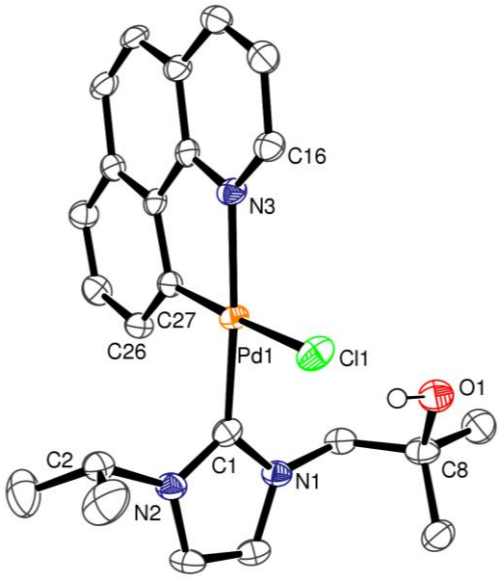

Figure 15. Molecular structure of (L^{OH})Pd(bzq)Cl. Ellipsoids are drawn at the 50% probability level and all hydrogen atoms except for the OH have been omitted for clarity. Selected bond lengths (Å) and angles (deg): Pd1-C1 1.981(3), Pd1-N3 2.085(3), Pd1-C27 2.000(3), Pd1-Cl1 2.413(4); C27-Pd1-C1-N1 92.8(2).

3.5.5. Formation of (L^{OH})Pd(bzq)Cl and conversion to (L^{O})Pd(bzq).

(L^{OH})Pd(bzq)Cl can be obtained as a colourless powder by addition of HCl to a solution of (L^{O})Pd(bzq) in MeCN, Scheme 6. Conversion back to (L^{O})Pd(bzq) is readily achieved by addition of equimolar KN" to a thf solution of (L^{OH})Pd(bzq)Cl. Likewise NaCp, $KOBu^{t}$ and KCH_2Ph were also effective for the conversion back to (L^{O})Pd(bzq) but in poorer yields.

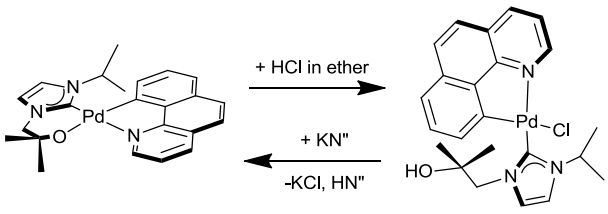

Scheme 6. Independent synthesis of (L^{OH})Pd(bzq)Cl and conversion back to (L^{O})Pd(bzq).

3.6. Computational analysis of Pd^{IV}-based chlorination reactions

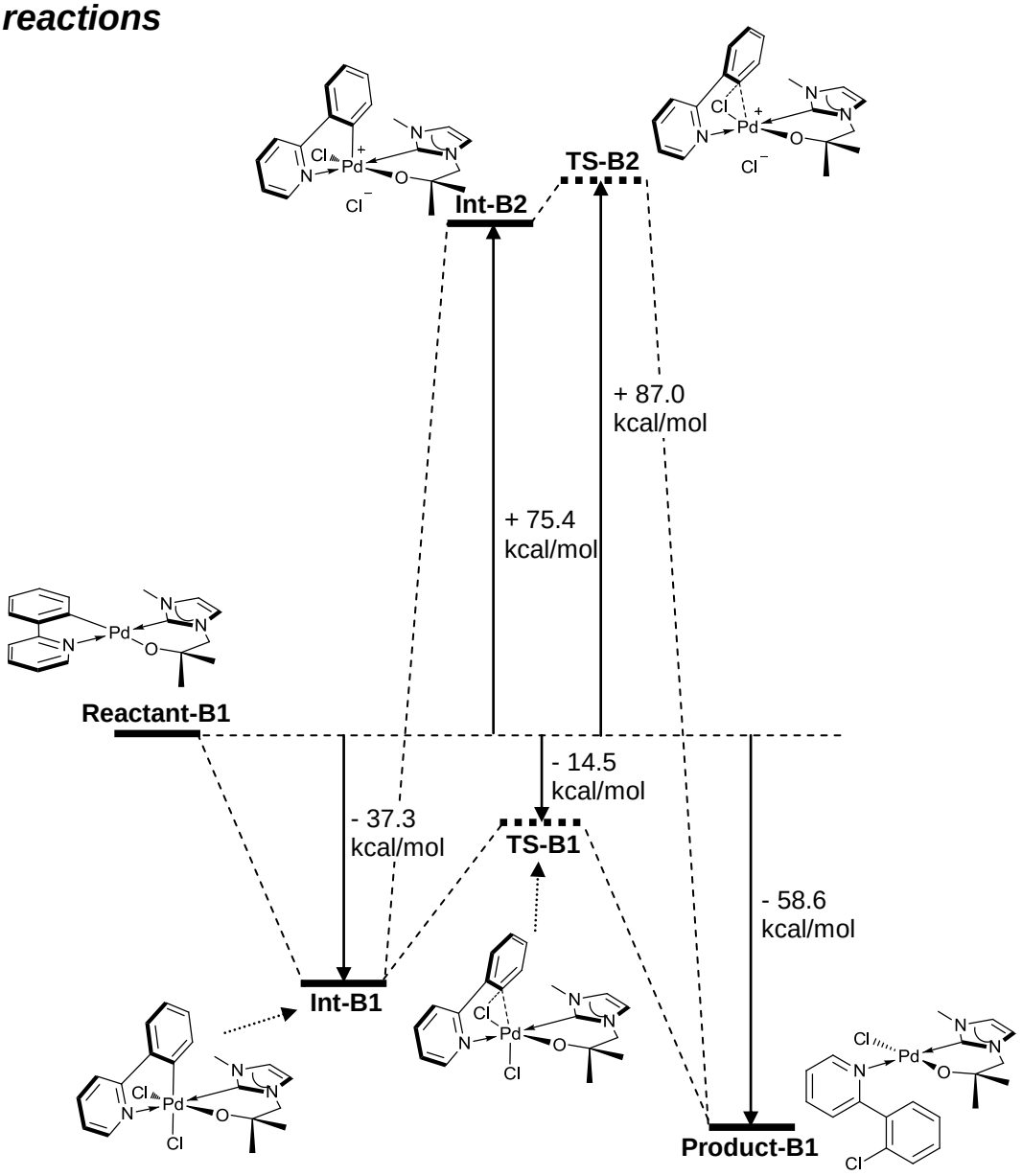

Figure 16. Free energy profile for reaction between $(L^O)Pd(phpy)$ and $PhI(Cl)_2$ (all the free energies are relative to **Reactant-B1** plus $PhI(Cl)_2$). Barrier to reductive elimination for $(L^O)Pd(phpy)Cl_2$ is +22.8 kcal/mol.

The four-coordinate Pd^{II} complex (**Reactant-B1**) reacts with $PhI(Cl)_2$ to yield a six-coordinate Pd^{IV} complex (**Int-B1**) and iodobenzene. The chlorides add in a *cis* manner to

give a structure analogous to that obtained with NBS. **Int-B1** directly undergoes reductive elimination through a single, six-coordinate transition state (**TS-B1**). In **TS-B1** the C_{phenyl}-Pd-Cl angle decreases from 84.8° to 51.4°. The C_{phenyl}-Pd bond length increases from 2.04 Å to 2.22 Å and Cl-Pd bond length increases from 2.42 Å to 2.66 Å. The free energy barrier for **TS-B1** is calculated to be +22.8 kcal/mol. The direct product of C_{phenyl}-Cl bond formation is a four coordinate Pd^{II} complex (**Product-B1**) and the overall free energy change is -58.6 kcal/mol. Reductive elimination is known to be more likely to occur at a positively charged, five-coordinate Pd^{IV} centre. The free energy change in dissociating a chloride ligand from **Int-B1** is +112.7 kcal/mol. In **TS-B2** the C_{phenyl}-Pd-Cl angle decreases from 97.4° to 58.0°, while the C_{phenyl}-Pd bond length increases from 2.03 Å to 2.22 Å and Cl-Pd bond length increases from 2.36 Å to 2.42 Å, respectively. The barrier for **TS-B2** is calculated to be +11.6 kcal/mol. The product after recombination of the chloride anion is the four coordinate Pd^{II} complex **Product-B1**.

3.6.1. Discussion

The oxidation of (L^O)Pd(phpy) appears to be essentially barrierless. No intermediates to oxidation could be determined. The calculated structure, **Int-B1**, is in good agreement with the results obtained experimentally for (L^O)Pd(bzq). The barrier to reductive elimination is calculated to be similar to (L^O)Pd(phpy)(Br)(Succinimide). This is not entirely surprising as the transition state is very similar. A limited assessment of solvent effects was made (section 2.6), for **Reactant-B1** going to **Product-B1** through **TS-B1**, in both CH_2Cl_2 and MeCN. Despite the large difference in dielectric constants (ε = 8.93 and 35.69 respectively) no significant effect on the energy profile was observed compared to the gas phase or each other. There were insufficient computational resources to fully extend this study to **Int-B2** or **TS-B2** but it should be noted that solvating the chloride anion with five molecules of MeCN (in the gas phase) reduces the energy of **Int-B2** and **TS-B2** by about 19 kcal/mol. Again this

suggests a charged intermediate cannot be completely ruled out but is less likely than for NBS (**Int-B2** is ~25 kcal/mol higher in energy from the neutral Pd^{IV} complex than for **Int-E3**). This can be explained in part by the succinimide anion being able to delocalise the negative charge much more effectively than chloride. The combination of a more readily accessible cationic Pd^{IV} complex and the possibility of ligand scrambling might go some way to explaining why the decomposition of (L^O)Pd(phpy)(Br)(Succinimide) is much more complex.

3.7. Development of a new NHC ligand to stabilise Pd^{IV}

The steric, electronic and chemical nature of anionic tethered NHC ligands can be readily tuned due to their modular synthesis. The electronic and steric properties in NHCs are linked; increasing the size of the alkyl side-arms leads to an increase in donor ability as well as steric bulk.[24]

Reports have shown that the different donating powers of NHCs can be evaluated as part of metal carbonyl complexes.[24, 25] Nolan and co-workers used a series of $[(L)Ir(CO)_2Cl]$ complexes (L = NHC or PR_3) to compare the σ-donor strength of NHCs to phosphines. NHCs are stronger donors than phosphines and the order of donor strength can be ranked using IR spectroscopy (by examining the change in υ_{CO} in a series of complexes).

IR data can be calculated using DFT allowing the assessment of a much wider range of NHCs under identical conditions. Results calculated for $[(NHC)M(CO)_x]$ (M = Cr, x = 5; M = Ni, x = 3) complexes show good agreement with experimental results.[26, 27]

As detailed in section 3.2.2, treatment of (L^O)Pd(bzq) with equimolar NBS yields a Pd^{IV} complex. As a consequence (L^O)Pd(bzq) can be used as a precatalyst for the bromination of substrates such as 2-phenylpyridine. From this starting point it was clear that modifying the tethered NHC to increase the electron density at palladium could give rise to more stable Pd^{IV} complexes. Alternatively, mediating the electron donating capability of the ligand

could allow for more facile C-H activation. To assess the impact of various modifications to the NHC ligand on the electron density at Pd a DFT study was undertaken.

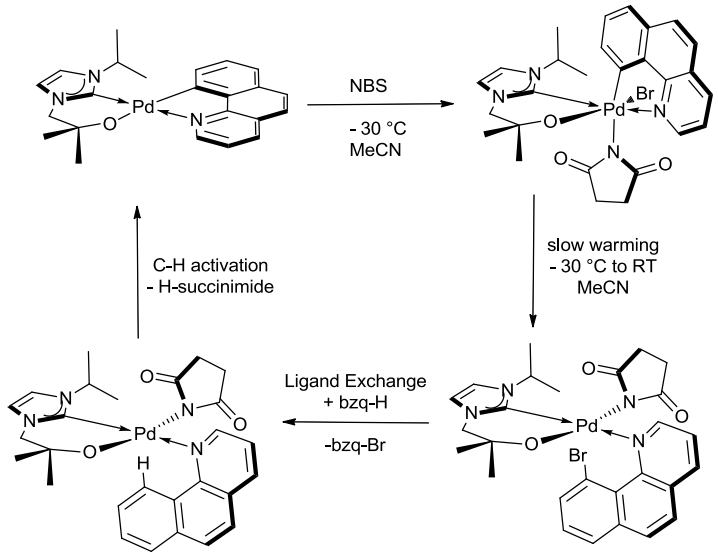

Scheme 7. Catalytic bromination of benzo[h]quinoline with NBS and (L^O)Pd(bzq).

In the catalytic cycle for NBS at the point of C-H activation the ligands around Pd are L^O, succinimide and N-bound benzo[*h*]quinoline (Scheme 7). Modification of the tethered NHC to generate analogues of (L^O)Pd(bzq-H)(succinimide) allows changes in the CO stretching frequency of the carbonyl in the succinimide ligand to be correlated with how electron-rich the Pd centre is. By replacing bzq-H with CO in these analogues of (L^O)Pd(bzq-H)(succinimide) it would be possible to comment on the electron density at Pd from the IR stretching frequencies of CO. CO is preferable since it had been used in previous studies, for example with $[Cr(CO)_5L]$ to compare computationally the relative donor strength of NHCs, phosphines and diamino carbenes.[26]

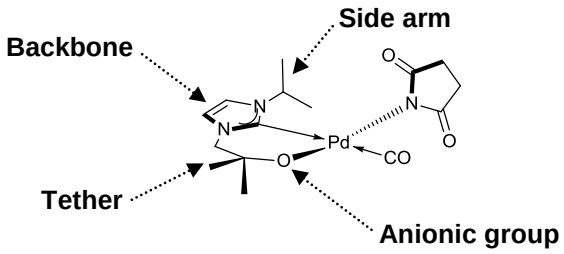

Figure 17. Options for modifying anionic-tethered NHC.

Anionic tethered NHCs can be modified in a number of ways (Figure 17). The side arm mainly affects the steric demands of the ligand,[27] the backbone can be modified to tune the electronics of the ligand,[25, 27] the tether can be flexible[28, 29] or rigid[30, 31] and a variety of anionic groups can be employed.[28-34]

3.7.1. DFT analysis of a range of tethered NHC ligands

The Pd-NHC complex needs to be stable under strongly oxidising conditions and not contain extra binding sites (such as cyano groups on the backbone) limiting the range of functional groups that can be employed.

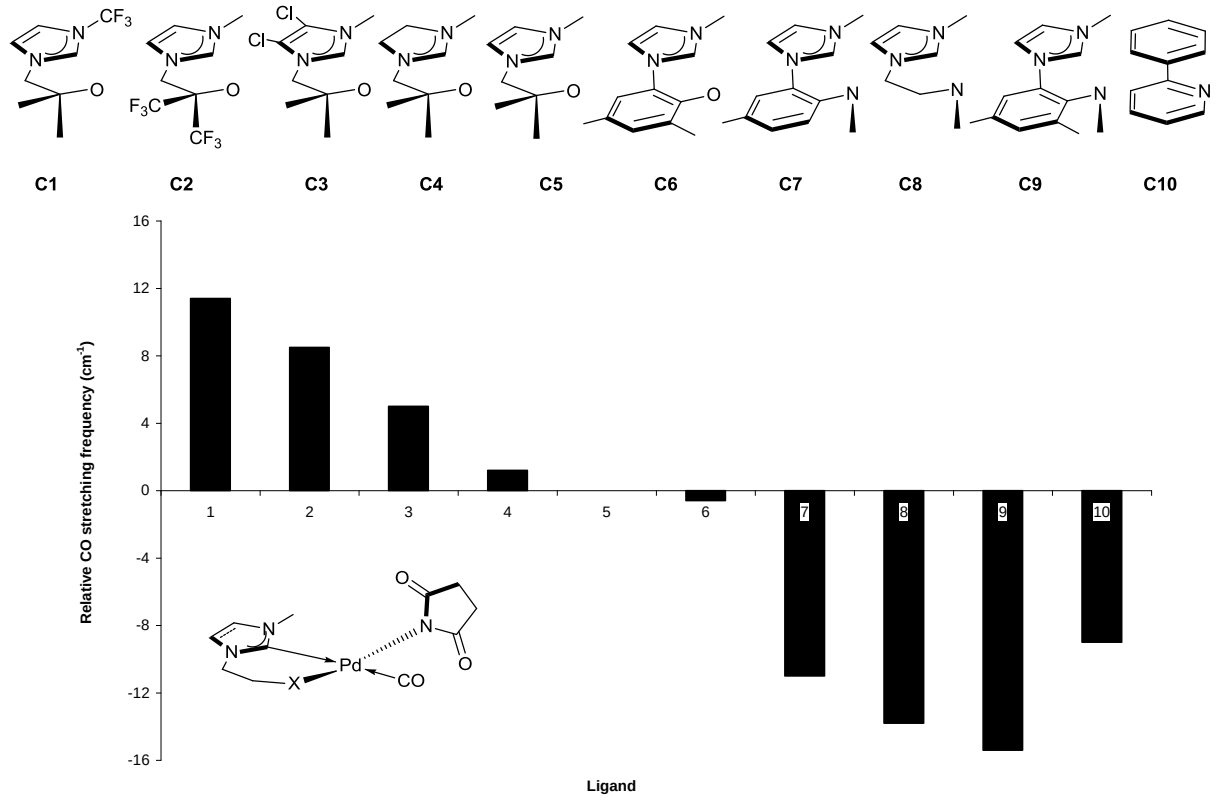

Figure 18. Calculated IR stretching frequencies for a variety of anionic tethered NHCs (relative to (L^O)Pd(succinimide)(CO): 2183 cm^{-1}, average value of cis and trans isomers). 2-phenylpyridine is included for comparison purposes.

DFT was used to calculate the IR data for [(NHC)Pd(CO)(succinimide)] with the range of tethered-NHC ligands shown in Figure 18. Differences in the totally symmetric vibrational mode for CO indirectly indicate the change in electron density at Pd for the different ligands.

The calculated change in υ_{CO} upon replacing the unsaturated backbone with an saturated one (**C5** to **C4**) is +1 cm^{-1}, or upon chlorinating the backbone (**C5** to **C3**) is +5 cm^{-1}, in agreement with previous reports.[27, 35] Entry **C5** is the standard alkoxy-NHC ligand for which Pd^{IV} catalysis data was obtained (the average υ_{CO} was calculated to be 2183 cm^{-1}). A change in υ_{CO} to higher wavenumbers indicates a decrease in back-bonding from palladium. This more electron deficient palladium should be a (slightly) faster catalyst for ligand directed $Pd^{II/IV}$ catalysis compared to **C5**. Conversely, a change in υ_{CO} to lower wavenumbers would indicate a more electron-rich palladium centre. Provided there is no significant π-electron donation by the ligand this increased electron density should help to stabilise any subsequently formed Pd^{IV} complex. The trend although not the magnitude observed could be predicted by chemical common sense.

Amido-tethered NHC ligands are significantly more electron donating than the alkoxy-tethered ligands (by -11 to -15 cm^{-1}). Recent theoretical work rules out the possibility of π-donation by the amido ligand to Pd^{II} on the basis of symmetry requirements.[36] The nitrogen based tethered NHC ligands are more electron donating than 2-phenylpyridine (as indicated by a change in υ_{CO} of -2 to -6 cm^{-1}). It is known that $[Pd(phpy)OAc]_2$ does not undergo a second C-H activation to make $Pd(phpy)_2$. These results suggest that anionic nitrogen-tethered NHCs would be completely unsuitable for ligand directed oxidative functionalisation catalysis. CNC ligands containing NHCs and an amido tether have been used previously to make electron-rich Rh^{I}, $Pd^{0/II}$ and Y^{III} complexes.[31, 37, 38]

Unsurprisingly the incorporation of electron withdrawing groups in the ligand such as CF_3 or Cl leads to a reduction in Pd-CO back-bonding. A perfluorinated NHC would make an interesting target ligand for ligand directed oxidative functionalisation catalysis. The perfluorinated epoxide required for the preparation of **C2** represents a significant synthetic challenge. *N*-trifluoromethylimidazole is commercially available but the nucleophilic attack on epoxide required to install the alkoxide arm and afford **C1** would be severely hampered by the electron-withdrawing CF_3 group. **C3** represents the best chance of reducing the donor power of the NHC as chlorination of the backbone could potentially be carried out after installation of the alkoxide arm.

Switching to a saturated backbone (**C5** to **C4**, +1 cm^{-1}) or an aryloxide for the tether (**C5** to **C6**, -0.5 cm^{-1}) has only a minor effect on the donor capability. Moving from an oxygen to a nitrogen based tether shows a significant decrease in υ_{CO} (**C5** to **C8**, -14 cm^{-1} or **C6** to **C9**, -15 cm^{-1}). However, **C8** may be susceptible to β-hydride elimination either at Pd^{II} or upon oxidation.[39] It is known that rigid ligands help stabilise Pd^{IV} complexes but this effect is not found by calculating changes in υ_{CO}.

3.7.2. Synthesis of $(L^{N,Ar})Pd(bzq)$

Having identified that a tethered-NHC ligand similar to **C9** (Figure 18) would be a strong donor, the balance between steric and electronic factors was considered (Figure 19).

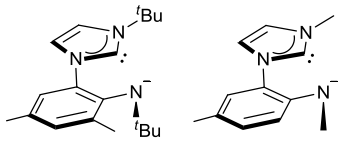

Figure 19. Balance between electronic and steric considerations in $[L^{N,Ar}]^-$

As the crystal structure of $(L^{O})Pd(bzq)Cl_2$ demonstrated (section 3.5.1) there is little room around an octahedral Pd^{IV} complex. Steric considerations are important as steric crowding can help facilitate reductive elimination.[40] As was noted by Nolan and co-workers increasing the electron donating ability of an NHC ligand results in an increase in steric bulk.[24] The $(L^{N,Ar})Pd(bzq)$ complex synthesised (Figure 20) was a compromise between donor ability and steric considerations. An *iso*-propyl side arm retains most of donor capabilities with the steric component pointing away from the Pd centre. Given the proximity of the amido group to the Pd centre an N-methyl substituent was settled upon despite introducing the potential for β-hydride elimination. A *tert*-butyl group *para* to the amine was also included to ensure good solubility of the resultant complexes.

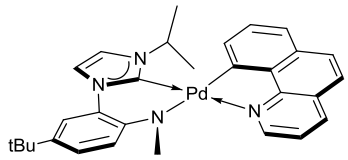

Figure 20. $(L^{N,Ar})Pd(bzq)$

The synthesis of $(L^{N,Ar})Pd(bzq)$ is described in section 2.9 and 2.11.5. The maroon complex decomposes if kept in solution for more than a day, presumably as a result of β-hydride elimination or C-N bond forming reductive elimination. The ^1H NMR spectrum of the decomposition was inconclusive but with further work it should be possible to identify the cause of the poor stability.

3.7.3. Oxidation of $(L^{N,Ar})Pd(bzq)$ with $PhI(Cl)_2$

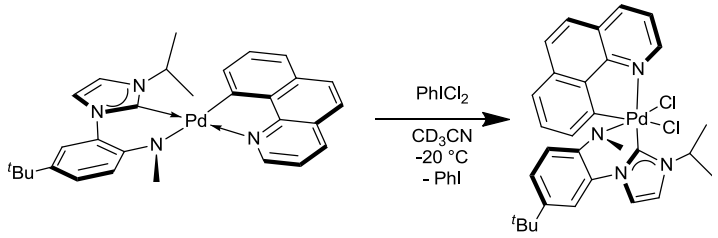

(7)

Treatment of $(L^{N,Ar})Pd(bzq)$ with an equimolar amount of $PhI(Cl)_2$ in CD_3CN at -20 °C results in the formation of $(L^{N,Ar})Pd(bzq)Cl_2$ by oxidative addition of two chloride ligands to the Pd centre (Equation 7). Monitoring the reaction by ^1H NMR spectroscopy, rapid and essentially quantitative formation of $(L^{N,Ar})Pd(bzq)Cl_2$ can be observed. The resonances for H16 and H2 have shifted to higher frequency (9.91 and 6.15 ppm respectively). The N-methyl group resonance shifts from 3.65 ppm to ~2.30 ppm and is split into three, suggesting restricted rotation. The only nOe interaction that could be found between the NHC and bzq ligand was 0.19 % for H16⋯NMe. Upon examination of the calculated structure of $(L^{N,Ar})Pd(phpy)Cl_2$ (Figure 21) the reason for the lack of observed nOe interactions is evident. The shortest distance between protons on the two ligands is 2.70 Å for H16⋯NMe.

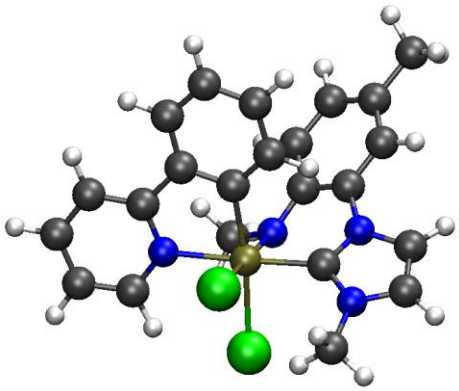

Figure 21. Calculated molecular structure for $(L^{N,Ar})Pd(phpy)Cl_2$.

The calculated Pd^{IV} structures for L^O and $L^{N,Ar}$ are very similar to each other. There is a slight elongation of the bond lengths (~0.01 Å) in $(L^{N,Ar})Pd(phpy)Cl_2$ compared to $(L^O)Pd(phpy)Cl_2$. The Pd-C1 bond is the exception and has contracted slightly (Table 7).

Treatment of $(L^{N,Ar})Pd(bzq)$ with $PhI(Cl)_2$ in CH_2Cl_2 at -78 °C, followed by removal of the solvent (at -20 °C) also yielded a slate-blue coloured solid. Elemental analysis of the solid fitted for $(L^{N,Ar})Pd(bzq)Cl_2$+PhI+KCl. The KCl was evidently carried over during the synthesis of $(L^{N,Ar})Pd(bzq)$.

	$(L^{O})Pd(phpy)Cl_2$	$(L^{N,Ar})Pd(phpy)Cl_2$
Pd-C1	2.024 Å	2.017 Å
Pd-C27	2.040 Å	2.047 Å
Pd-N3	2.117 Å	2.136 Å
Pd-Cl1	2.510 Å	2.520 Å
Pd-Cl2	2.421 Å	2.447 Å
Pd-O/N4	2.035 Å	2.105 Å
C27-Pd-C1-N1	64.3°	58.5°

Table 7. Comparison of calculated structures of $(L^{O})Pd(phpy)Cl_2$ and $(L^{N,Ar})Pd(phpy)Cl_2$.

3.7.4. Decomposition of $(L^{N,Ar})Pd(bzq)Cl_2$

The decomposition of the Pd^{IV} complex $(L^{N})Pd(bzq)Cl_2$ (in CD_3CN at 25 °C) was monitored by ^1H NMR spectroscopy. A dark blue solution was obtained initially, which changed to a maroon colour after 5 minutes and was entirely converted to this intermediate species in about 20 minutes. This unidentified maroon complex remains unchanged for about 90 minutes at room temperature before decomposing with a $t_{1/2} \approx 80$ minutes. This decomposition produces two major final products in a 2:1 ratio (by integration).

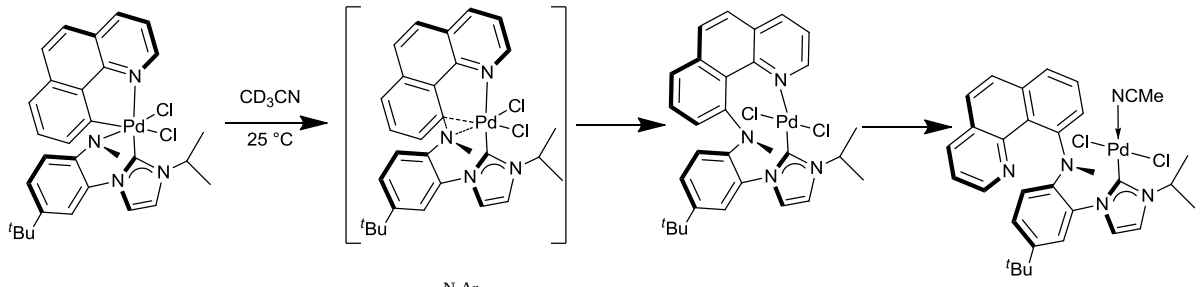

Scheme 8. Possible decomposition of $(L^{N,Ar})Pd(phpy)Cl_2$.

The resonance for H16 in the major isomer (8.40 ppm) is at a significantly lower frequency than the minor isomer (9.26 ppm) suggesting that in the major isomer H16 is not sterically encumbered (Scheme 8). The remaining resonances of the major and minor isomers are very

similar. Presumably the structure of the minor isomer is related, probably with the pyridine ring coordinated to Pd (Figure 22).

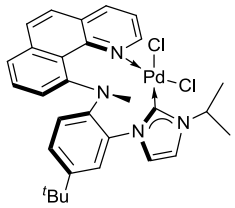

Figure 22. Possible structure of the minor isomer from the decomposition of $(L^{N,Ar})Pd(phpy)Cl_2$.

3.7.5. Computational analysis of reductive elimination

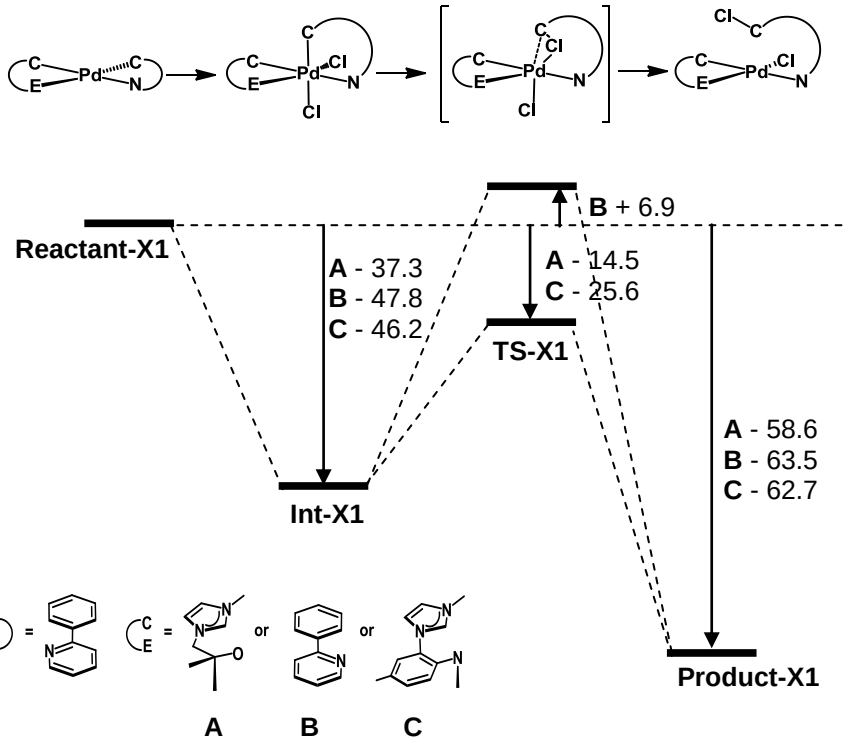

Figure 22. Free energy profile for reaction between $(L^X)Pd(phpy)$ and $PhI(Cl)_2$ (all the free energies are in kcal/mol and relative to **Reactant-X1**). Barriers to reductive elimination: $(L^O)Pd(phpy)Cl_2$, 22.8 kcal/mol; $Pd(phpy)_2Cl_2$, 54.7 kcal/mol; $(L^{N,Ar})Pd(phpy)Cl_2$, 20.6 kcal/mol.

To help understand the reactivity of $(L^{N,Ar})Pd(bzq)Cl_2$ the barrier to reductive elimination was calculated for a simplified structure (^{t}Bu and ^{i}Pr groups were replaced with Me, and

phpy was used in place of bzq) and compared to calculations on a simplified structure of $(L^O)Pd(bzq)Cl_2$[6] and to $Pd(phpy)_2Cl_2$[10] that were reported previously. Calculations were also carried out to confirm that these ligand simplifications had minimal effect on the geometry or calculated barrier. Given the uncertain nature of the transition state (via a five-coordinate cationic Pd^{IV} or directly from a six-coordinate Pd^{IV}) it was decided to compare only **TS-X1**. The four-coordinate Pd^{II} complex reacts with $PhI(Cl)_2$ to yield a six-coordinate Pd^{IV} complex (**Int-X1**) and iodobenzene. **Int-X1** directly undergoes reductive elimination through a single, six-coordinate transition state (**TS-X1**). The important bond lengths and angles are listed in Table 8 and free energy values are noted in Figure 22. The final product is a four coordinate Pd^{II} complex (**Product-X1**).

	C-Pd-Cl angle (°)		C-Pd bond (Å)		Cl-Pd bond (Å)	
Complex	Int-X1	TS-X1	Int-X1	TS-X1	Int-X1	TS-X1
A	84.8	51.4	2.04	2.22	2.42	2.66
B	88.5	50.7	2.02	2.23	2.31	2.56
C	84.6	58.5	2.05	2.27	2.44	2.68

Table 8. Important bond lengths and angles for Int-X1 and TS-X1.

As Figure 22 demonstrates, the barrier to reductive elimination for $(L^{N,Ar})Pd(phpy)Cl_2$ is very similar to $(L^O)Pd(phpy)Cl_2$ (~20 kcal/mol) and is less than half that for $Pd(phpy)_2Cl_2$. Given the very similar geometries of the transition states it would appear that it is steric crowding in the NHC based systems that is assisting the more facile C-Cl bond formation. For the complex $(L^N)Pd(phpy)Cl_2$ the calculated barrier to reductive elimination is +20.1 kcal/mol. Whilst anionic tethered-NHCs may be useful ligands for donating electron density to a transition metal, in each case the energy of the transition state is affected to the same extent as the Pd^{IV} complex leading to no net gain in stability.

Experimentally, $Pd(phpy)_2Cl_2$ does not decompose in solution at room temperature, $(L^O)Pd(bzq)Cl_2$ has a half-life of 40 minutes and $(L^{N,Ar})Pd(bzq)Cl_2$ decomposes completely within 15 minutes. Although the calculations show the transition state pathways to be of similar energy for the Pd^{IV} tethered-NHC complexes the very different lifetimes suggest another channel not modelled here is the lowest energy decomposition pathway for the aryl-imido system.

C-N bond formation is one likely alternative pathway. Modelling the transition states for carbon-heteroatom coupling in $(L^O)Pd(phpy)Cl_2$ and $(L^{N,Ar})Pd(phpy)Cl_2$ showed a clear difference. The methyl groups on the alkoxide tether clash with the aromatic ring of phpy preventing a C-O bond forming transition state from being found. For $(L^{N,Ar})Pd(phpy)Cl_2$ the C-N bond forming transition state was trivial to locate with a barrier of +22.6 kcal/mol. Whilst this is 2 kcal/mol higher in energy than direct C-Cl bond formation solvent effects could change the relative energies of these two competing pathways. It is known that C-N bond formation at Pd^{II} is faster for a more electron-rich nitrogen atom.[41]

3.8. Conclusions

Four new Pd^{IV} complexes have been synthesised; $(L^{O})Pd(phpy)(br)(succinimide)$, $(L^{O})Pd(bzq)(br)(succinimide)$, $(L^{O})Pd(bzq)Cl_2$ and $(L^{N,Ar})Pd(bzq)Cl_2$. Calculated structures and properties for simplified versions of these complexes are in good agreement with the experimental data (single crystal X-ray structures, nOe interactions and IR spectra).

The decomposition of these Pd^{IV} complexes is complicated by competing intermolecular reactions. For $(L^{O})Pd(phpy)(br)(succinimide)$ and $(L^{O})Pd(bzq)(br)(succinimide)$ the product mixture is very complex. It would require significant effort to identify the individual components which have very similar physical properties. The reactivity of $(L^{O})Pd(bzq)Cl_2$ is somewhat simpler.

Both NBS and NCS are suitable oxidants to use with $(L^{O})Pd(bzq)$ for ligand directed C-H bond functionalisation catalysis. The catalysis is much slower than with $Pd(OAc)_2$ and the range of substrates which can be functionalised is limited to substituted phenylpyridine. This lower reactivity and substrate scope could be useful for selective functionalisation in molecules with more than one directing group.

The donor strength and steric properties of NHC ligands can be readily tuned. Their potential as ligands for palladium-catalysed ligand-directed oxidative-functionalisation depends on achieving facile C-H bond activation. Finding a base compatible catalytic reaction would allow for halogenation of sp^3 centres, something that is not yet possible with $Pd(OAc)_2$. To that end it is important to unambiguously identify the Pd species at end of catalysis with $(L^{O})Pd(bzq)$ and NBS.

Given steric crowding is important in determining the stability of a Pd^{IV} complex any ligand must have minimal steric bulk close to the palladium. A traditional NHC has two groups

which point into the coordination sphere around the metal. Replacing one of the nitrogen atom adjacent to the carbene tends to lead to a reduction in the donor ability of the ligand. [42]

A tether of more than two atoms between the N of the NHC and the metal centre introduces a twist about the M-$C_{carbene}$ bond, further increasing the steric influence of the ligand. In the context of Pd^{IV} a tether ending in O, NR or C_{sp3} can result in reactivity at the Pd-element bond rather than oxidation of the metal.

Based on the work by Huynh *et al* a Werner type ligand is more electron donating than a traditional NHC ligand and significantly more so than pyridine.[42] Taking all these factors into consideration a Pd^{II} centre bearing two of the ligand depicted in Figure 23 should maximise the stability of any Pd^{IV} provided the ligand is inert under the oxidising conditions required to produce Pd^{IV}.

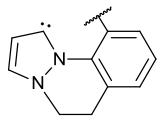

Figure 23. Tethered carbene ligand to give a more stable Pd^{IV} complex.

3.9. References

1 T. W. Lyons and M. S. Sanford, *Chemical Reviews*, 2010, **110**, 1147.
2 N. R. Deprez and M. S. Sanford, *Inorg. Chem.*, 2007, **46**, 1924.
3 P. Sehnal, R. J. K. Taylor, and I. J. S. Fairlamb, *Chemical Reviews*, 2010, **110**, 824.
4 M. Kilian, *Angew. Chem., Int. Ed. Engl.*, 2009, **48**, 9412.
5 L.-M. Xu, B.-J. Li, Z. Yang, and Z.-J. Shi, *Chem. Soc. Rev.*, 2009, **39**, 712.
6 P. L. Arnold, M. S. Sanford, and S. M. Pearson, *J. Am. Chem. Soc.*, 2009, **131**, 13912.
7 P. K. Byers, A. J. Canty, B. W. Skelton, and A. H. White, *J. Chem. Soc., Chem. Commun.*, 1986, 1722.
8 A. Bayler, A. J. Canty, J. H. Ryan, B. W. Skelton, and A. H. White, *Inorg. Chem. Commun.*, 2000, **3**, 575.
9 J. M. Racowski, A. R. Dick, and M. S. Sanford, *J. Am. Chem. Soc.*, 2009, **131**, 10974.
10 S. R. Whitfield and M. S. Sanford, *J. Am. Chem. Soc.*, 2007, **129**, 15142.
11 N. D. Ball and M. S. Sanford, *J. Am. Chem. Soc.*, 2009, **131**, 3796.
12 T. Furuya and T. Ritter, *J. Am. Chem. Soc.*, 2008, **130**, 10060.
13 A. R. Dick, K. L. Hull, and M. S. Sanford, *J. Am. Chem. Soc.*, 2004, **126**, 2300.
14 D. Kalyani, A. R. Dick, W. Q. Anani, and M. S. Sanford, *Tetrahedron*, 2006, **62**, 11483.
15 D. Kalyani, A. R. Dick, W. Q. Anani, and M. S. Sanford, *Org. Lett.*, 2006, **8**, 2523.
16 S. Kohiki and T. Hamada, *J. Mater. Sci.*, 1990, **25**, 1344.
17 V. I. Nefedov, I. A. Zakharova, I. I. Moiseev, M. A. Porai-koshits, M. N. Vargoftik, and A. P. Belov, *Zh. Neorg. Khimii*, 1973, **18**.
18 V. I. Nefedov, *Koord. Khim.*, 1978, **4**.
19 L. V. Desai, K. J. Stowers, and M. S. Sanford, *J. Am. Chem. Soc.*, 2008, **130**, 13285.
20 A. J. Canty and E. i. Negishi, 'Handbook of Organopalladium Chemistry for Organic Synthesis', 2002.
21 A. J. Canty, J. Patel, M. Pfeffer, B. W. Skelton, and A. H. White, *Inorg. Chim. Acta*, 2002, **327**, 20.
22 G. Sánchez, J. García, D. Meseguer, J. L. Serrano, L. García, J. Pérez, and G. López, *Dalton Trans.*, 2003, 4709.
23 M. S. Viciu, R. A. Kelly, E. D. Stevens, F. Naud, M. Studer, and S. P. Nolan, *Org. Lett.*, 2003, **5**, 1479.
24 R. A. Kelly III, H. Clavier, S. Giudice, N. M. Scott, E. D. Stevens, J. Bordner, I. Samardjiev, C. D. Hoff, L. Cavallo, and S. P. Nolan, *Organometallics*, 2007, **27**, 202.
25 D. M. Khramov, V. M. Lynch, and C. W. Bielawski, *Organometallics*, 2007, **26**, 6042.
26 M.-T. Lee and C.-H. Hu, *Organometallics*, 2004, **23**, 976.
27 D. G. Gusev, *Organometallics*, 2009, **28**, 6458.
28 P. L. Arnold, S. A. Mungur, A. J. Blake, and C. Wilson, *Angew. Chem., Int. Ed.*, 2003, **42**, 5981.
29 P. L. Arnold, M. Rodden, and C. Wilson, *Chem. Commun.*, 2005, 1743.
30 A. W. Waltman and R. H. Grubbs, *Organometallics*, 2004, **23**, 3105.
31 M. Moser, B. Wucher, D. Kunz, and F. Rominger, *Organometallics*, 2007, **26**, 1024.
32 B. E. Ketz, A. P. Cole, and R. M. Waymouth, *Organometallics*, 2004, **23**, 2835.
33 J. A. Cabeza, I. Del Rio, M. G. Sanchez-Vega, and M. Suarez, *Organometallics*, 2006, **25**, 1831.

[34] A. A. Danopoulos, P. Cole, S. P. Downing, and D. Pugh, *J. Organomet. Chem.*, 2008, **693**, 3369.
[35] H. M. Lee, J. Y. Zeng, C.-H. Hu, and M.-T. Lee, *Inorganic Chemistry*, 2004, **43**, 6822.
[36] S. Moncho, G. Ujaque, P. Espinet, F. Maseras, and A. Lledós, *Theoretical Chemistry Accounts: Theory, Computation, and Modeling (Theoretica Chimica Acta)*, 2009, **123**, 75.
[37] I. S. Edworthy, A. J. Blake, C. Wilson, and P. L. Arnold, *Organometallics*, 2007, **26**, 3684.
[38] W. Wei, Y. Qin, M. Luo, P. Xia, and M. S. Wong, *Organometallics*, 2008, **27**, 2268.
[39] A. N. Marziale, E. Herdtweck, J. Eppinger, and S. Schneider, *Inorg. Chem.*, 2009, **48**, 3699.
[40] R. Uson, J. Fornies, and R. Navarro, *J. Organomet. Chem.*, 1975, **96**, 307.
[41] J. F. Hartwig, *Nature*, 2008, **455**, 314.
[42] H. V. Huynh, Y. Han, R. Jothibasu, and J. A. Yang, *Organometallics*, 2009, **28**, 5395.

Chapter 4

Formation of C-O and C-C bonds from Pd^{IV} complexes

Chapter 4 – Formation of C-O and C-C bonds from Pd^{IV} complexes.

4.1. Introduction

The Sanford group have observed differences in reactivity depending upon the oxidant used for catalytic oxidative C-H bond functionalisation suggesting different mechanisms are operating in each case. In catalytic C-O and C-Cl bond formation C-H activation is rate limiting but through different mechanisms.[1] Detailed studies of the kinetic order for each reaction component as well as Hammett plots for electronically diverse 2-*o*-tolylpyridines allowed the elucidation of the reaction mechanism. . The catalyst resting state in both cases is most likely $[(L)Pd(X)]_2$ (L = *o*-tolpy^H, X = Cl, OAc).

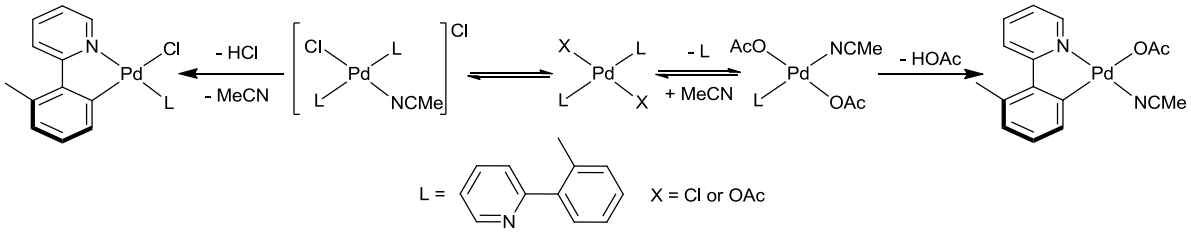

Scheme 1. Possible mechanisms for C-H activation at Pd^{II}.[1]

In the chlorination reactions pre-equilibrium chloride dissociation followed by C-H activation at a cationic complex best explains the data (Scheme 1). For acetoxylation pre-equilibrium dissociation of one *o*-tolpy-H ligand followed by C-H activation at a monomeric Pd complex or acetate-bridged Pd dimeric complex is expected.

For catalytic oxidative C-C bond formation, oxidation was found to be the rate limiting step as a result of predissociation steps involving the oxidant and excess substrate.[2]

4.2. $(L^O)Pd(phpy) + PhI(OAc)_2$

When $(phpy)_2Pd$ is combined with a stoichiometric amount of $PhI(OAc)_2$ a stable Pd^{IV} complex can be formed (Scheme 2).[3] The ^1H NMR spectrum (d_6-acetone) of $(phpy)_2Pd(OAc)_2$ contains 16 distinct aromatic signals in the range 6.29 and 9.46 ppm and two different acetate resonances at 1.63 and 1.74 ppm. This is consistent with cis-phpy and OAc ligands, and was confirmed by X-ray crystallography. Upon heating a solution of $(phpy)_2Pd(OAc)_2$ in MeCN for 30 minutes at 80 °C, clean C-O bond forming reductive elimination occurs. Consequently $PhI(OAc)_2$ was investigated as a stoichiometric oxidant for $(L^O)Pd(phpy)$.

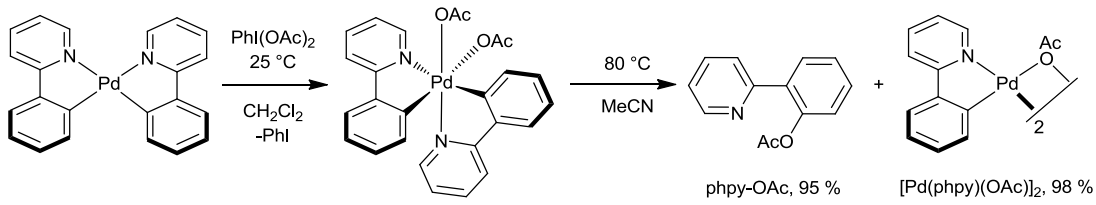

Scheme 2. Synthesis of $(phpy)_2Pd(OAc)_2$ and subsequent C-O bond formation.

4.2.1. $(L^O)Pd(phpy^{-OAc})OAc$

A solution of $(L^O)Pd(phpy)$ in CH_2Cl_2 was treated with one equivalent of $PhI(OAc)_2$ and after stirring at 25 °C for 24 h, a yellow solid was precipitated by addition of hexanes. The rate of the reaction is partially limited by the poor solubility of the starting materials in common solvents (PhH, MeCN). The ^1H NMR spectrum (C_6D_6) of the precipitate has characteristic resonances at 8.99 ppm for H16 and 5.85 ppm for H2. There are two resonances for acetate at 2.37 and 1.84 ppm. In the ^{13}C NMR spectrum (C_6D_6) the resonance for the carbene is at 164.3 ppm. The complex remains unchanged (by ^1H NMR spectroscopy) after a week in solution. From this spectroscopic data and by elemental analysis it is not

possible to determine whether the product is the Pd^{IV} complex $(L^O)Pd(phpy)(OAc)_2$ or the reductive elimination product $(L^O)Pd(phpy^{-OAc})OAc$ (Scheme 3).

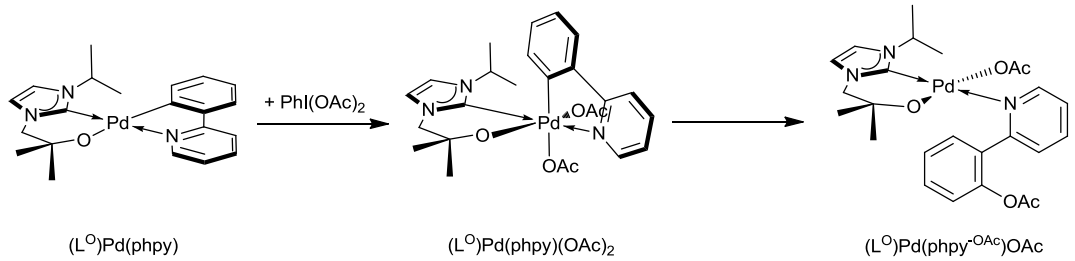

Scheme 3. Oxidation of $(L^O)Pd(phpy)$ with $PhI(OAc)_2$.

The difference between the two possible products should be evident in the infra-red spectrum; the peaks for an organic acetate group are very different from a metal-bound acetate. An absorption at 1772 cm^{-1} in the IR spectrum is due to the stretching of an acetate group bound to a phenyl group. This was assigned based on comparison with the IR spectrum of $[Pd(phpy)OAc]_2$, $(L^O)Pd(phpy)$ and the OAc containing complexes reported by the Sanford group.[4] The IR spectra for $(L^O)Pd(phpy)(OAc)_2$ and $(L^O)Pd(phpy^{OAc})OAc$ were calculated using DFT and compared to the experimental spectrum (Figure 1).

Comparing the calculated spectra to the experimental, the position rather than the intensity of the peaks should be considered. Deviations from the experimental spectrum are expected where there are strong anharmonic vibrational modes. The calculated spectrum for $(L^O)Pd(phpy^{-OAc})(OAc)$ (bottom) appears to be a better fit, in agreement with the original assignment.

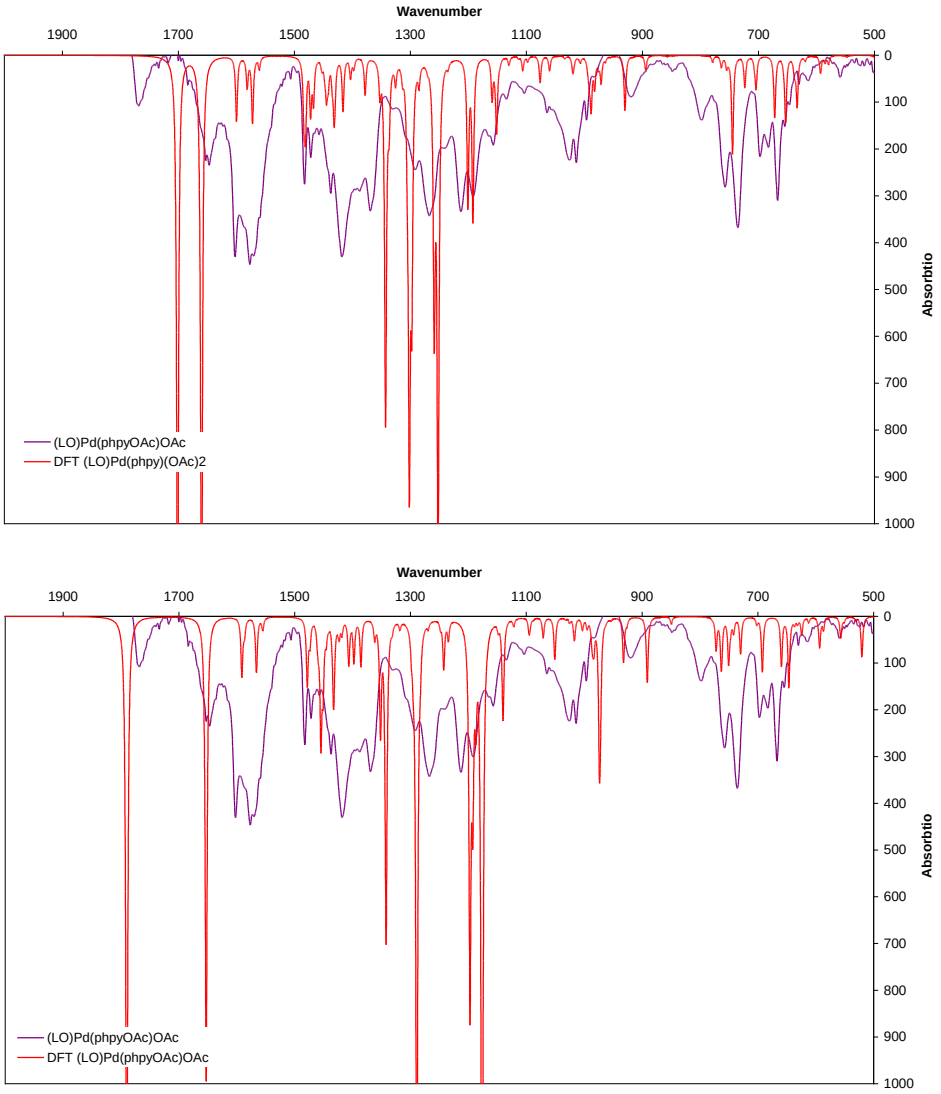

Figure 1. Calculated IR spectrum for $(L^{O})Pd(phpy)(OAc)_2$, (top) and $(L^{O})Pd(phpy^{-OAc})OAc$ (bottom) overlaid on experimental IR assigned as $(L^{O})Pd(phpy^{-OAc})OAc$. See appendix 1 for details of the calculations.

The Sanford group typically use poly-vinyl pyridine or silica to separate the organic and palladium products at the end of a stoichiometric reaction. The organic products can then be identified by GC analysis and NMR spectroscopy. To confirm phpy-OAc had indeed been formed a solution of $(L^{O})Pd(phpy^{-OAc})(OAc)$ was stirred with celite and then eluted through silica. No organic products were displaced from the Pd centre, the product eluted through the silica could be assigned as $(L^{OH})Pd(phpy^{-OAc})(OAc)OH$ (by ^{1}H NMR spectroscopy).

4.2.2. [(L^O)Pd(phpy)·PhI($OAc)_2$]

The reaction between (L^O)Pd(phpy) and PhI($OAc)_2$ was monitored by ^1H and $^{13}C\{^1H\}$ NMR spectroscopy (in CD_3CN, C_6D_6 or CH_2Cl_2). An intermediate complex was observed which showed characteristic resonances in the ^1H NMR spectrum (C_6D_6) for the intermediate at 9.15 ppm (H16), 6.09 ppm (H2), and 2.50 and 1.84 ppm (OAc). The $^{13}C\{^1H\}$ NMR spectrum (CD_3CN) has a resonance at 165.3 ppm assignable to the carbene and a resonance at 122.3 ppm corresponding to the *ipso* carbon bonded to the iodine in the oxidant.

This is interesting because it suggests oxidation has yet to take place, the chemical shift of the *ipso* carbon bonded to the iodine is indicative of the oxidation state of the iodine (Figure 2). The resonance in the ^1H NMR spectrum (C_6D_6) at 2.50 ppm also corresponds to an OAc group bound to I^{III}.

Attempts to crystallise [(L^O)Pd(phpy)·PhI($OAc)_2$] afforded single crystals that were shown by X-ray diffraction to be a polymorph of PhI($OAc)_2$. The structure has been communicated to the CCDC (CCDC 776352).

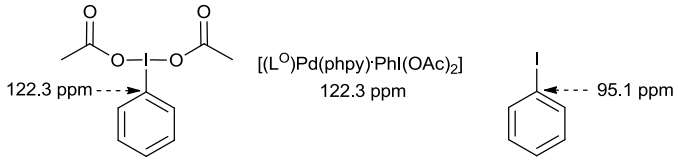

Figure 2. ^{13}C NMR spectroscopic (CD_3CN) chemical shift of *ipso* arene carbon in PhI($OAc)_2$ and PhI.

An IR spectrum was taken of the reaction mixture after all of the (L^O)Pd(phpy) had been consumed. By subtracting the IR spectrum for (L^O)Pd($phpy^{OAc}$)OAc, peaks unique to the [(L^O)Pd(phpy)·PhI($OAc)_2$] were found (1713 and 1385 cm^{-1}).

The Sanford group have successfully used electronically diverse acetoxylating reagents to manipulate the rate of C-O bond formation from Pd^{IV} complexes.[3, 4] A *p*-nitrobenzoate ligand has been shown to slow the rate of reductive elimination from Pd^{IV}. In the hope of stabilising the intermediate (L^O)Pd(phpy) was treated with equimolar PhI($O_2C(C_6H_4)NO_2)_2$. The rate of intermediate formation is limited by the poor solubility of PhI($O_2C(C_6H_4)NO_2)_2$ in common

organic solvents; so significant quantities of $[(L^O)Pd(phpy)\cdot PhI(O_2C(C_6H_4)NO_2)_2]$ could not be obtained. Monitoring the reaction between $(L^O)Pd(phpy)$ and one equivalent of $PhI(O_2C(C_6H_4)OMe)_2$ (known to increase the rate of reductive elimination from Pd^{IV}) by ^1H NMR spectroscopy no $[(L^O)Pd(phpy)\cdot PhI(O_2C(C_6H_4)OMe)_2]$ complex was observed (Scheme 4).

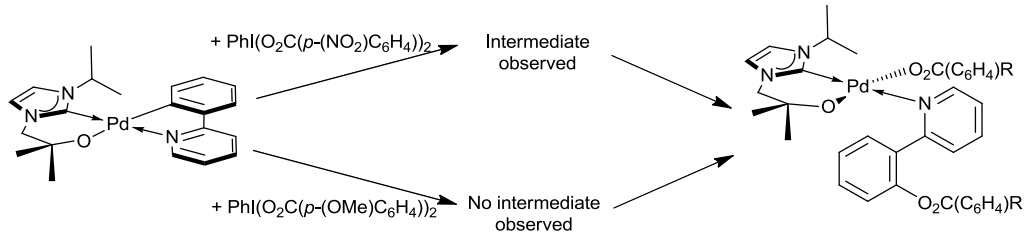

Scheme 4. Oxidation of $(L^O)Pd(phpy)$ with electronically diverse $PhI(O_2C(C_6H_4)R)_2$.

4.2.3. DFT simulations of $[(L^O)Pd(phpy)]\cdot PhI(OAc)_2$

To help understand the nature of $[(L^O)Pd(phpy)\cdot PhI(OAc)_2]$, possible structures were modelled using DFT. Starting from the calculated structure for $(L^O)Pd(phpy)(OAc)_2$, removing the OAc groups and placing $PhI(OAc)_2$ nearby in space led to barrierless formation of $(L^O)Pd(phpy)(OAc)_2$ (plus PhI).

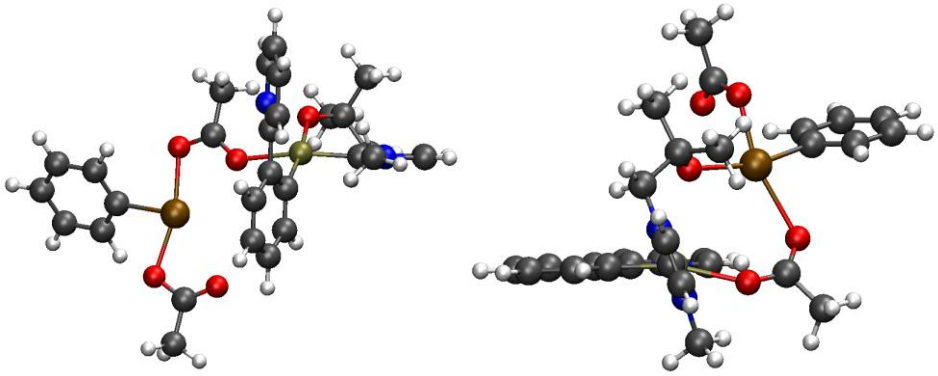

Figure 3. Computational analysis of possible intermediates in the reaction between $[(L^O)Pd(phpy)]$ and $PhI(OAc)_2$.

One of the mechanisms considered for C-O bond formation from $(phpy)_2Pd(OAc)_2$ is dissociation of a pyridyl arm of one cyclometalated ligand followed by internal coupling.[4] A

stable intermediate was found by dissociation of the pyridyl arm of the cyclometalated ligand and coordination of $PhI(OAc)_2$ in its place (Figure 3).

Considering $PhI(OAc)_2$ instead as [PhI(OAc)]OAc it is conceivable that reaction with the alkoxide arm of $(L^O)Pd(phpy)$ could occur in an analogous manner to other ionic species such as H_2O (section 2.11.2) and HCl (section 3.5.5). Gratifyingly a stable complex was found in which an acetate group is bound to Pd and the alkoxide arm to I^{III}, Figure 3.

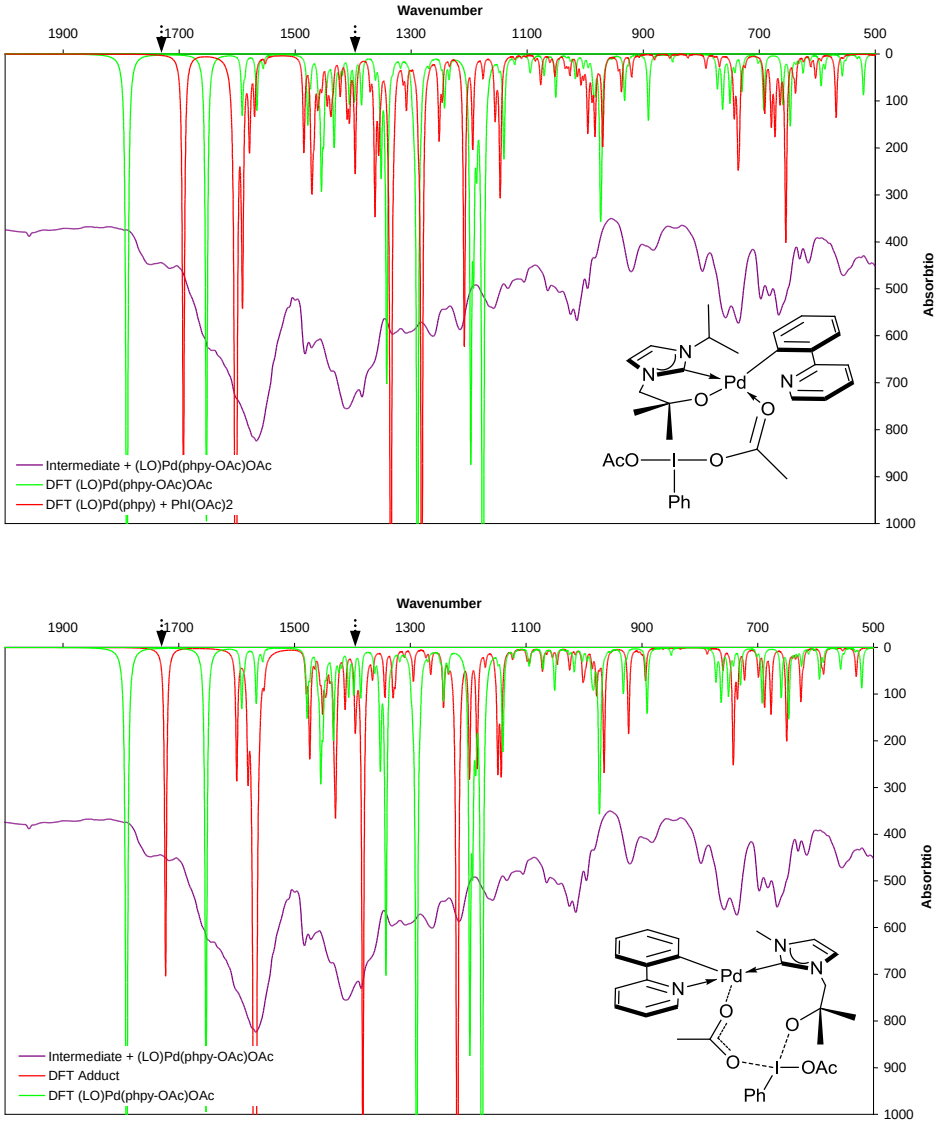

Figure 4. Calculated IR spectra for $(L^O)Pd(phpy^{-OAc})OAc$ (green) and intermediate (red), overlaid on experimental data (purple) containing mixture of $[(L^O)Pd(phpy)\cdot PhI(OAc)_2]$ and $(L^O)Pd(phpy^{-OAc})OAc$. The arrows denote the characteristic peaks identified for the intermediate.

The calculated IR spectrum for each of these potential intermediates along with the calculated spectrum for (L^{O})Pd(phpy^{-OAc})OAc was overlaid with the experimentally obtained IR spectrum (Figure 4.). The calculated IR spectrum where the alkoxide ligand has exchanged places with an acetate is a much better match to the experimental data (Figure 4).

4.2.4. (L^{OH})Pd(phpy)OH + PhI(OAc)$_2$

(L^{O})Pd(phpy) readily reacts with any available moisture to afford (L^{OH})Pd(phpy)OH (section 2.11.2). The reaction between (L^{OH})Pd(phpy)OH and equimolar PhI(OAc)$_2$ was monitored by ^{1}H NMR spectroscopy (in C_6D_6 or MeCN at 10 °C) and no intermediate complexes were observed (Scheme 5).

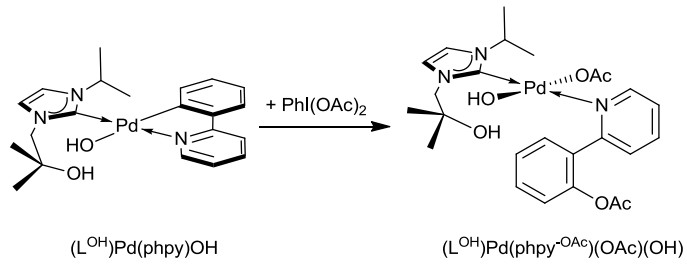

(L^{OH})Pd(phpy)OH (L^{OH})Pd(phpy^{-OAc})(OAc)(OH)

Scheme 5. Oxidation of (L^{OH})Pd(phpy)OH with PhI(OAc)$_2$.

The resonance for H16 was used to monitor loss of starting material and product formation. The reaction is significantly faster with (L^{OH})Pd(phpy)OH (t½ = 2 mins, C_6D_6; t½ = 17.5 mins, MeCN) than with (L^{O})Pd(phpy) (t½ greater than 5 h at 25 °C, C_6D_6 and MeCN). Failure to exclude water (leading to cleavage of the Pd-$O_{alkoxide}$ bond) might lead to an increase in the rate of turnover in catalysis (since no stable intermediate will be formed). A complex similar to [(L^{O})Pd(phpy)·PhI(OAc)$_2$] may form when [Pd(phpy)OAc]$_2$ is treated with PhI(OAc)$_2$ but without a bridging ligand to help stabilise the complex it is likely any intermediate will not be observable.

4.2.5. (L^O)Pd(phpy) + AcOH

As part of the proposed cycle for catalytic acetoxylation the C-H activation step would liberate AcOH. It has already been shown in section 3.5.5 that (L^O)Pd(bzq) reacts readily with acids such as HCl. Treatment of a solution of (L^O)Pd(phpy) in MeCN with stoichiometric glacial AcOH at 25 °C afforded (L^{OH})Pd(phpy)OAc in quantitative yield after removal of the solvent under reduced pressure (Equation 1).

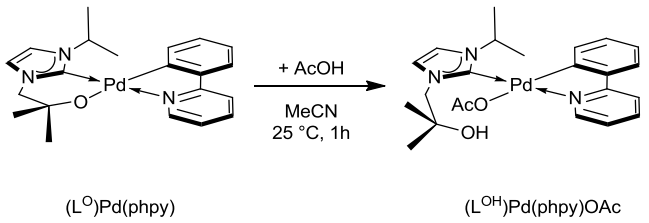

(L^O)Pd(phpy) (L^{OH})Pd(phpy)OAc **(1)**

The complex was characterised by ^1H and ^{13}C NMR spectroscopy, elemental analysis and IR spectroscopy. The major peaks in the IR spectrum (for the acetate) are at 1601, 1566, 1482 and 1416 cm^{-1} (versus 1758, 1414 and 1360 cm^{-1} in free AcOH). The OH resonance is visible in the ^1H NMR spectrum at 6.39 ppm (C_6D_6). The ^{13}C NMR spectrum has a resonance at 173.6 ppm attributable to the carbene carbon. This is good evidence that the phpy is still cyclometalated; the $\delta C_{carbene}$ appears at > 170 ppm in cyclometalated Pd^{II} complexes and < 165 ppm in complexes where phpy is coordinated only by the pyridine. It seems probable that if (L^O)Pd(phpy) was used for catalytic ligand-directed acetoxylation the catalyst resting state would be (L^{OH})$Pd(OAc)_2$. To regenerate (L^O)Pd(phpy) as the active species in C-H activation the AcOH produced by C-H activation would need to be removed with a base. If a chiral version of the alkoxide ligand was used, this would allow a chiral environment to be maintained close to the Pd centre. However the rate of turnover may be slowed by the formation of complexes similar to [(L^O)Pd(phpy)·$PhI(OAc)_2$] competing with C-H activation.

4.2.6. Esterification of (L^{OH})Pd(phpy)OAc

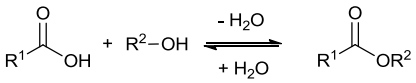

(2)

Carboxylic acids react with alcohols to produce esters (Equation 2). It is possible esterification of the free OH in (L^{OH})Pd(phpy)OAc could take place under conditions similar to those used in catalysis (Scheme 6). Treatment of (L^{O})Pd(phpy) with excess AcOH at 100 °C did not result in esterification, only (L^{OH})Pd(phpy)OAc was observed. The tertiary nature of the alcohol in (L^{OH})Pd(phpy)OAc makes esterification difficult. A Fisher esterification was also tried and catalytic sulphuric acid is added to activate the carbonyl and aid removal of the water produced in the reaction to drive the equilibrium to the product.[5] However, only (L^{OH})Pd(phpy)OAc was produced in the reaction.

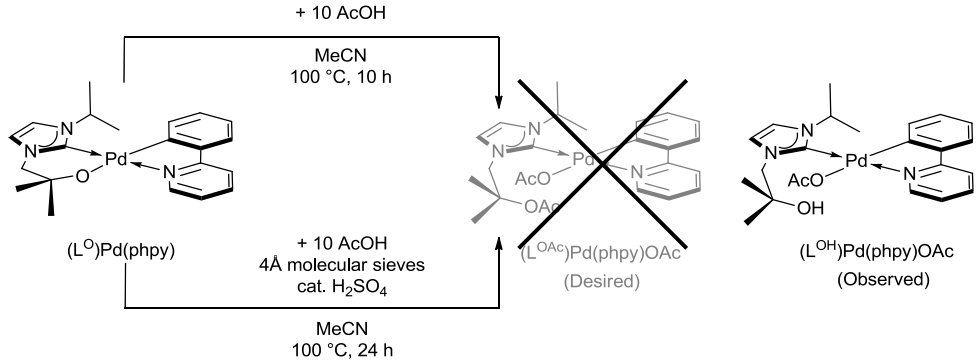

Scheme 6. Attempted esterification of (L^{OH})Pd(phpy)OAc.

If the alcohol arm in (L^{OH})Pd(phpy)OAc could be reversibly esterified with benzoic acid it might be possible for selective C-H activation of the captured benzoic acid to take place. There are a number of reported methods for the esterification of tertiary alcohols at -10 °C in CH_2Cl_2 (Scheme 7).

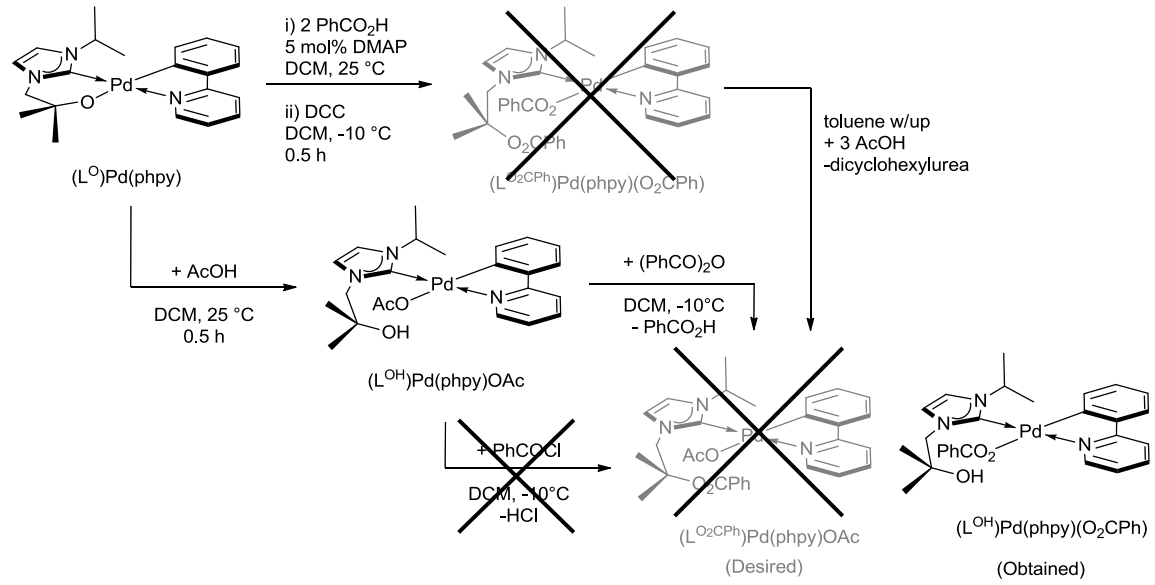

Scheme 7. Further attempts to esterify (L^{OH})Pd(phpy)OAc. DMAP = 4-N,N-dimethylaminopyridine. DCC = dicyclohexylcarbodiimide.

A Steglich esterification was attempted.[6] A mixture of (L^{O})Pd(phpy), two equivalents of $PhCO_2H$ and 5 mol% of DMAP in CH_2Cl_2 were cooled to -10 °C. DCC was added to promote esterification and the reaction mixture was allowed to warm to room temperature. After workup (L^{OH})Pd(phpy)(O_2CPh) was obtained. Treatment of (L^{OH})Pd(phpy)OAc (in CH_2Cl_2 at -10 °C) with $(PhCO)_2O$ also afforded (L^{OH})Pd(phpy)(O_2CPh).

No reaction occurred when a CH_2Cl_2 solution of (L^{OH})Pd(phpy)OAc was treated with PhCOCl at -10 °C. The tertiary alcohol in (L^{OH})Pd(phpy)OAc is very resistant to substitution.

4.3. Computational analysis of reaction between (L^O)Pd(phpy) with $PhI(OAc)_2$

To gain further insight a computational analysis of the reaction between (L^O)Pd(phpy) and $PhI(OAc)_2$ was carried out using DFT. The reaction space was explored computationally in order to construct the reaction chart shown in Figure 5.

The four-coordinate Pd^{II} complex reacts initially with $PhI(OAc)_2$ to afford a four-coordinate Pd^{II} complex (**Int-D1**) [(L^O)Pd(phpy)·$PhI(OAc)_2$], in which one acetate group is bridging the Pd^{II} and I^{III} centres and the alkoxide tether is now bound to I^{III}. The calculated $O_{alkoxide}$-Pd bond has increased in length from 2.11 to 2.94 Å. The N_{pyr}-Pd bond length has decreased from 2.90 Å to 2.12 Å. The C_{phenyl}-Pd-$C_{carbene}$-N2 torsion angle has increased from 50.5° to 112.7° as the NHC has rotated around the $C_{carbene}$-Pd bond (with respect to the plane of the molecule).

A five-coordinate cationic Pd^{IV} complex (**Int-D2**) is obtained upon loss of iodobenzene. The $O_{alkoxide}$-Pd bond has decreased from 2.94 Å to 1.99 Å. The acetate ligand adopts a κ^2 binding mode with $O_{acetate}$-Pd bond lengths of 2.10 Å and 2.33 Å. The free energy change is + 63.6 kcal/mol relative to **Reactant-D1** in the gas phase (the energy of a DFT gas phase structure of a charged complex is overestimated).

From **Int-D2** there are two possible reaction pathways; direct reductive elimination from a five-coordinate cationic Pd^{IV} complex (**TS-D2**) or formation of a six-coordinate Pd^{IV} complex (**Int-D3**) from which direct reductive elimination can occur (**TS-D3**). In **TS-D2** the C_{phenyl}-Pd-$O_{acetate}$ angle decreases from 101.6° to 53.7°. The C_{phenyl}-Pd bond length increases from 2.02 Å to 2.19 Å whilst the $O_{acetate}$-Pd bond length decreases from 2.14 Å to 2.10 Å. **TS-D2** is calculated to lie + 84.8 kcal/mol above the **Reactant-D1**. The product after recombination of the acetate anion is a four coordinate Pd^{II} complex (**Product-D1**). The overall free energy change is -56.6 kcal/mol.

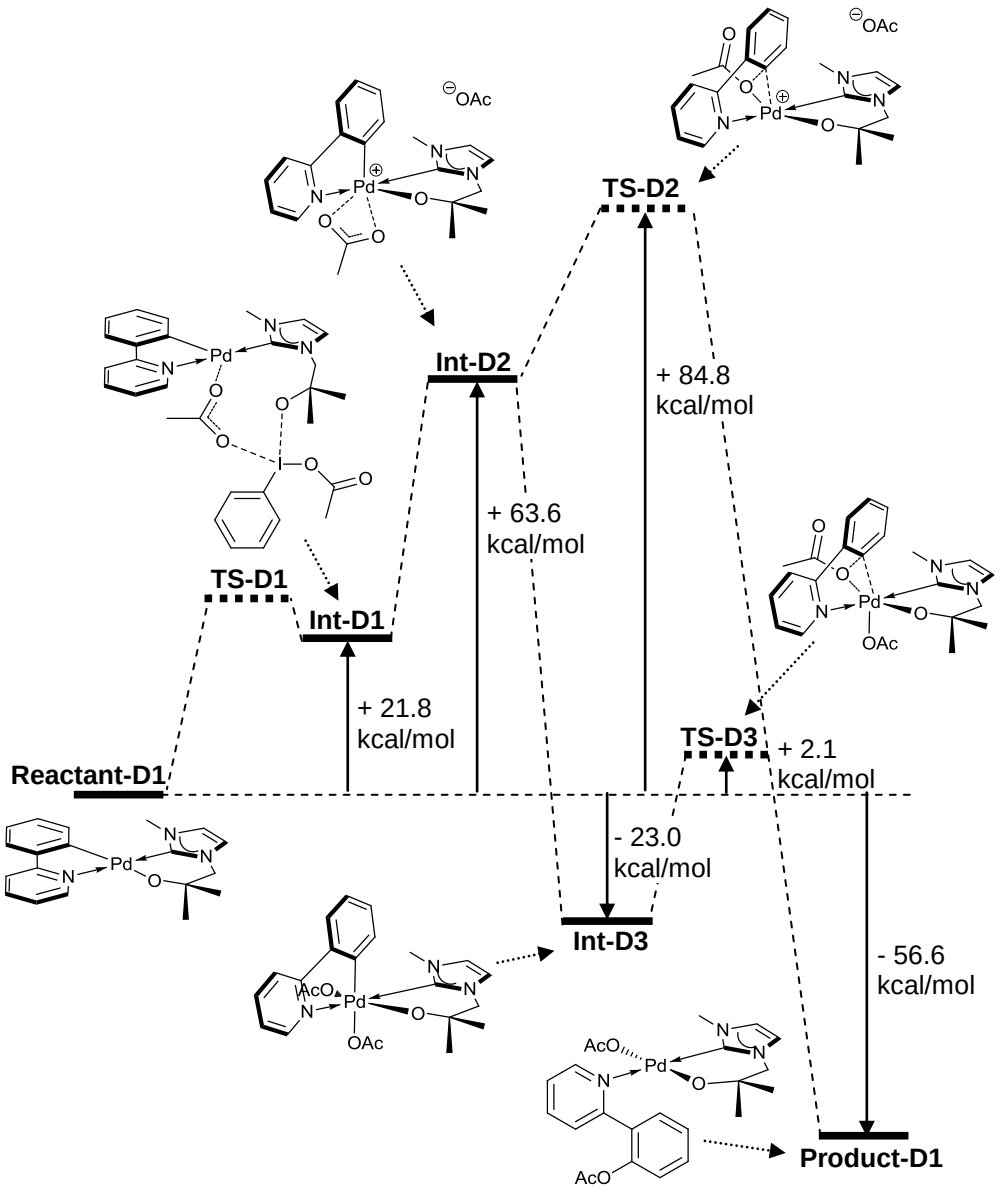

Figure 5. Free energy profile for reaction between (L^O)Pd(phpy) and $PhI(OAc)_2$ (all the free energies are relative to Reactant). Due to the conformational flexibility of the ligands it was not possible to calculate all the possible transition states and intermediates.

Int-D3 is formed upon recombination of the acetate anion to afford a six-coordinate Pd^{IV} complex with the acetate ligands in a cis arrangement. The free energy change is - 23.0 kcal/mol relative to **Reactant-D1** in the gas phase. In **TS-D3** the C_{phenyl}-Pd-$O_{acetate}$ angle decreases from 84.1° to 52.0°, while the C_{phenyl}-Pd and $O_{acetate}$-Pd bond lengths increase from

2.03 Å to 2.16 Å and 2.02 Å to 2.17 Å, respectively. The free energy cost of **TS-D3** is calculated to be + 2.1 kcal/mol relative to **Reactant-D1** in the gas phase. The product is a four coordinate Pd^{II} complex (**Product-D1**). The overall free energy change is -56.6 kcal/mol.

4.3.1. Discussion

If the mechanism of Pd-oxidation was similar to that seen for NBS and $PhICl_2$ then the calculated reaction profile suggests it should be possible to observe a Pd^{IV} intermediate (since going from **Reactant-D1** to **Int-D3** is exothermic by 23.0 kcal/mol). If a direct route from **Int-D1** to **Int-D3** exists the barrier must be significant. Experimentally the reaction required heating to 75 °C or extended time (12 h) at 25 °C to convert $[(L^O)Pd(phpy)\cdot PhI(OAc)_2]$ to $(L^O)Pd(phpy^{OAc})(OAc)$.

The calculated reaction profile supports the absence of an observable Pd^{IV} complex experimentally even though it is a key intermediate in the reaction. If sufficient energy is available to overcome the barrier to oxidation, the barrier to reductive elimination can also be overcome. This also helps explain why the reactions proceed so cleanly; a short lived Pd^{IV} complex only has time to undergo intramolecular reactions.

4.4. C-C bond formation

Both $[Ph_2I]OTf$[7] and MeI[8] have been used for the stoichiometric preparation of Pd^{IV} complexes.

4.4.1. $(L^O)Pd(phpy) + [Ph_2I]BF_4$

CD_3CN was frozen onto a mixture of the powders $(L^O)Pd(phpy)$ and $[Ph_2I]BF_4$ at -78 °C. The reaction mixture was warmed to -10 °C and monitored by ^1H and ^{13}C NMR spectroscopy. Clean formation of an intermediate complex was observed with analogous

resonances to that seen for $[(L^{O})Pd(phpy)\cdot PhI(OAc)_2]$, Scheme 8. This supports the formulation of $[(L^{O})Pd(phpy)\cdot PhI(OAc)_2]$ as the result of exchange between an acetate and the alkoxide.

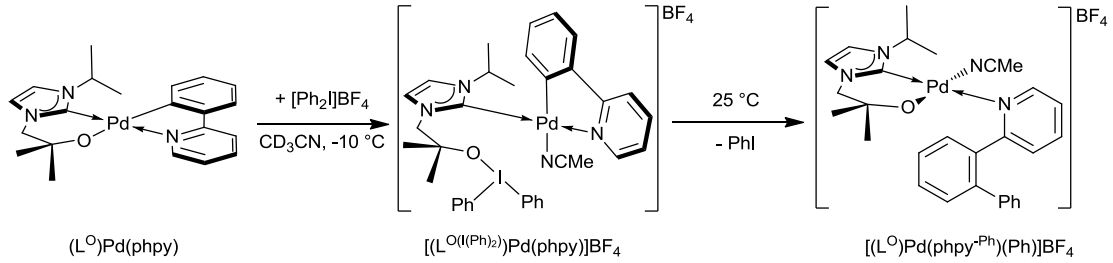

Scheme 8. Oxidation of $(L^{O})Pd(phpy)$ with $[Ph_2I]BF_4$.

A shift to lower frequency for the characteristic resonance H16 (8.34 ppm) indicates a reduction in the steric crowding around Pd. The existence of I^{III} was inferred by the presence of a resonance at 117.7 ppm in the ^{13}C NMR spectrum (CD_3CN). Upon warming to 25 °C slow formation of $[(L^{O})Pd(phpy^{-Ph})]BF_4$ + PhI was observed over 24 h. The $C_{carbene}$ resonance is at 150.6 ppm in the ^{13}C NMR spectrum suggesting C-C bond formation has occurred.

The reaction was repeated with $(L^{O,Ph})Pd(phpy)$ and monitored by ^{1}H and ^{13}C NMR spectroscopy. Formation of $[(L^{O,Ph})Pd(phpy)\cdot(Ph_2I)BF_4]$ was also observed. The poor solubility of $(L^{O,Ph})Pd(phpy)$ in CD_3CN along with substantial line broadening in the ^{1}H and ^{13}C NMR spectra hampered characterisation of the intermediate.

Attempts to grow single crystals suitable for X-ray diffraction studies by diffusion of hexanes in to a saturated CH_2Cl_2 solution of $[(L^{O,Ph})Pd(phpy)\cdot(Ph_2I)BF_4]$ (or Et_2O in to MeCN) yielded a brown oil.

4.4.2. Other reports of intermediates with hypervalent iodine reagents

The Sanford group have not reported observing any intermediates prior to oxidation. Malinakova and coworkers report formation of an intermediate, **XXXXXI,** when the palladacycle **XXXXX** (Scheme 9) was treated with 1-*n*-octene-yl(phenyl)iodonium tetrafluoroborate at -50 °C in $CDCl_3$.[9] The complex was putatively assigned as the Pd^{IV} complex **XXXXXI**.

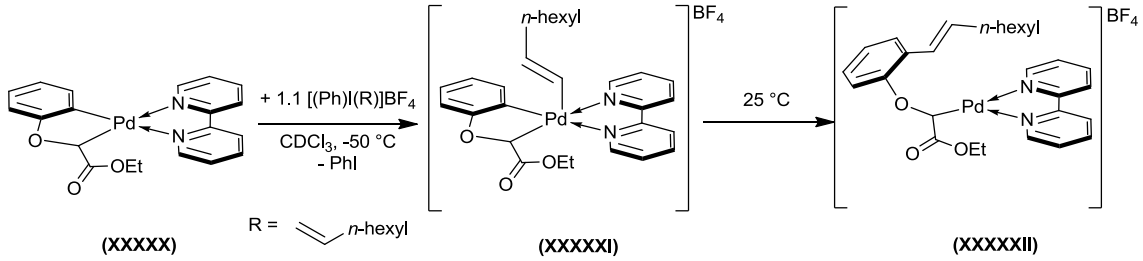

Scheme 9. Proposed oxidation of **XXXXX** with [(Ph)I(1-n-octene-yl)]BF_4.

Examining the ^1H NMR spectra provided (all taken at -50 °C in $CDCl_3$) it is clear to us that the chemical shifts of the resonances assigned to PhI are not at the same frequency in the spectra of **XXXXXI** and **XXXXXII**. This leads us to conclude that free PhI has not been eliminated in **XXXXXI**. A complex similar to [(L^O)Pd(phpy)·(Ph_2I)BF_4] could be envisaged (Figure 6). The δ^- alkyl fragment has been transferred from Pd to I^{III} and the cationic Pd centre generated is stabilised by donation from the carbonyl group.

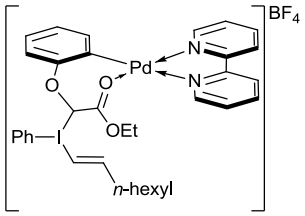

Figure 6. Alternative structure for complex **XXXXXI**.

No ^{13}C NMR spectroscopic data for **XXXXXI** are provided and without the chemical shifts of the phenyl group bound to iodine, it is not possible to rule out either structure. From the intermediate in Figure 6 oxidation to an undetected Pd^{IV} complex would occur followed by C-C bond-forming reductive elimination to afford **XXXXXII**.

4.4.3. (L^O)Pd(phpy) + MeI

The reaction between (L^O)Pd(phpy) and MeI, in MeCN at 0 °C, was monitored by ^1H NMR spectroscopy. No evidence of a Pd^{IV} complex was observed (based on the absence of the characteristic chemical shift of a Pd^{IV} Me group). Instead, slow formation of a new Pd^{II} complex occurred.

The new Pd^{II} complex was subsequently prepared by treatment of (L^O)Pd(phpy) with one equivalent of MeI at 25 °C (Equation 3) to afford (L^{OMe})Pd(phpy)I after removal of the volatiles under reduced pressure.

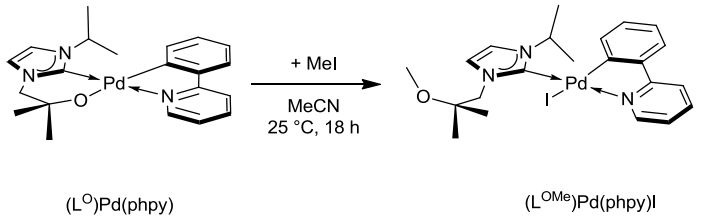

(3)

The complex (L^{OMe})Pd(phpy)I has been fully characterised. In the ^1H NMR spectrum (C_6D_6), the observation of nOe interactions between the Me group derived from MeI (2.80 ppm) and one of the carbene backbone hydrogen atoms supports the proposal that cleavage of the Pd-O bond has occurred (Figure 7).

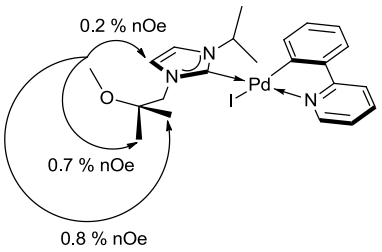

Figure 7. nOe interactions in (L^{OMe})Pd(phpy)I.

In the ^{1}H NMR spectrum (C_6D_6) a resonance at 10.30 ppm (H16) indicates significant steric bulk or the presence of an electronegative element close to H16; for example an iodide bound to Pd. The $C_{carbene}$ resonance is at 172.9 ppm in the ^{13}C NMR spectrum (C_6D_6) suggesting that the phpy is still cyclometalated. The complex was stirred with basic alumina and eluted through silica with ethyl acetate. By ^{1}H NMR spectroscopy (L^{OMe})Pd(phpy)I was unchanged lending further support to the notion that the Pd-O bond has already been cleaved.

This reaction doesn't appear to occur via a Pd^{IV} intermediate. If it did C-C bond formation would be expected with elimination of phpy-Me (perhaps with competing C-O bond formation). Electrophilic attack by MeI has been observed for palladalactones[10] and zinc alkoxides.[11, 12] The ease with which the Pd-O bond is cleaved in the presence of complexes with highly ionic bonds prevents formation of Pd^{IV} by a reliable classical route.[8]

4.4.4. (L^{O})Pd(phpy) + $SiMe_3N_3$

Treatment of (L^{O})Pd(phpy) with one equivalent of $SiMe_3N_3$ at 25 °C afforded (L^{OTMS})Pd(phpy)N_3 after removal of the volatiles under reduced pressure (Equation 4).

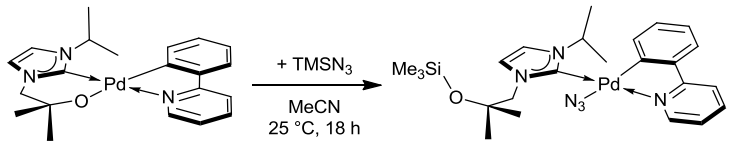

$(L^{O})Pd(phpy)$ $(L^{OTMS})Pd(phpy)N_3$ **(4)**

The complex was characterised by ^{1}H and ^{13}C NMR and IR spectroscopy, and elemental analysis. A peak at 2035 cm^{-1} in the IR spectrum is indicative of a Pd^{II}-N_3 complex rather than a phenyl-N_3.[13, 14] The carbene resonance is at 173.4 ppm in the ^{13}C NMR spectrum (CH_2Cl_2). The complex was unchanged after heating to 90 °C for 18 h in C_6D_6 (or by stirring with basic alumina and eluting through silica with ethyl acetate).

4.4.5. $(L^{N,Ar})Pd(bzq)$ + MeI

The reaction between $(L^{N,Ar})Pd(bzq)$ and MeI, in MeCN at 25 °C, was monitored by ^{1}H NMR spectroscopy. Over 18 h slow formation of three new complexes was observed in a ratio of 1.7:1:1 (Equation 5). The two lesser isomers have coincident resonances for the $L^{N,Ar}$ ligand but differing bzq resonances.

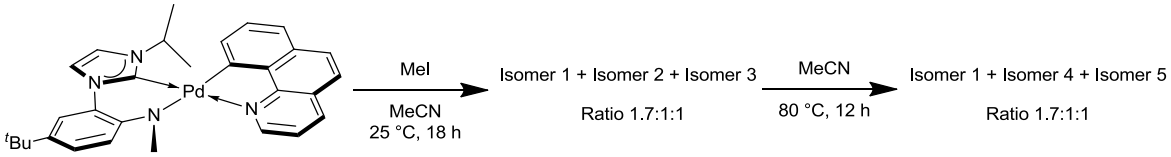

(5)

Heating the mixture to 80°C for 12 h no change is observed in the major isomer (by ^{1}H NMR spectroscopy). The other two isomers yield a new product each and again the resonances for the $L^{N,Ar}$ ligand are coincident but the bzq resonances are split out. The mixture was analysed by mass spectrometry (electrospray) and peaks for bzq-Me and $[(L^{N,Ar})Pd(bzq)(Me)]^{+}$ were observed. Without ^{13}C NMR spectra (or single crystal X-ray diffraction studies) of the different isomers it is only possible to speculate on what the structures might be (Figure 8).

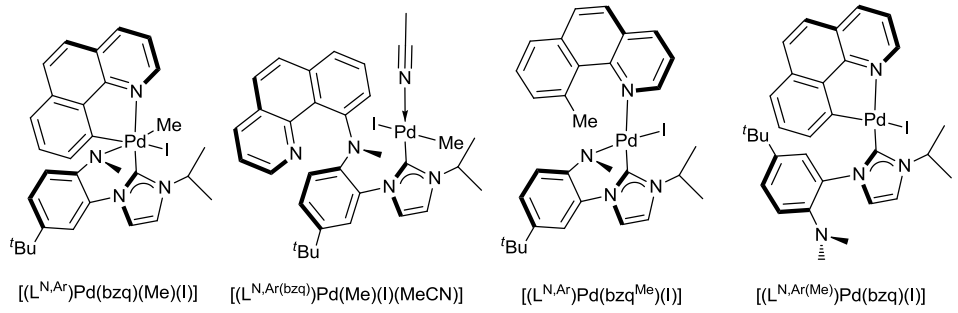

Figure 8. Possible products of the reaction between $(L^{N,Ar})Pd(bzq)$ and MeI.

4.5. Catalysis testing

Having studied the stoichiometric reaction of $(L^{O})Pd(phpy)$ with $PhI(OAc)_2$ and $[Ph_2I]BF_4$, a brief assessment of the catalytic activity was made. In a typical reaction 5 mol% of Pd catalyst was combined with the substrate, 1.1 equivalents of oxidant, and MeCN in an ampoule under dinitrogen gas. The reaction mixture was heated to 100 °C with stirring for 24 h (Equation 6).

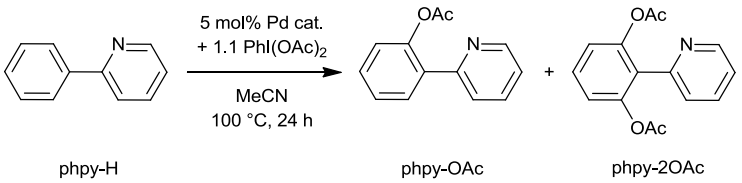

(6)

An aliquot of the reaction mixture was taken and analysed by GCMS and ^1H NMR spectroscopy. The amount of product formed was identified by comparison of the area of the separated peaks in the GC. Since no calibration curve was performed, comparisons between the results in each Table are valid although there could be a systematic error of as much as 15 % in the reported yields.

4.5.1. Comparison of $(L^O)Pd(phpy)$ and $Pd(OAc)_2$ for catalytic ligand directed acetoxylation

Initial investigations focused on the reactivity of $(L^O)Pd(phpy)$ relative to $Pd(OAc)_2$. As demonstrated in Table 1, at low temperatures $Pd(OAc)_2$ is a much better catalyst. Given that the intermediate seen in the stoichiometric reaction between $(L^O)Pd(phpy)$ and $PhI(OAc)_2$ only undergoes slow conversion to $(L^O)Pd(phpy^{-OAc})OAc$ at this temperature, the result is not unsurprising. At higher temperatures $Pd(OAc)_2$ is again faster. Interestingly though using $(L^O)Pd(phpy)$ leads to a greater proportion of phpy-2OAc being formed.

Entry	Substrate	Temp.	Catalyst	GC yield phpy-OAc[a]	GC yield phpy-2OAc[a]
a	phpy-H	40 °C	$(L^O)Pd(phpy)$	0 %	-
b	phpy-H	40 °C	$Pd(OAc)_2$	83 %	9 %
c	phpy-H	80 °C	$(L^O)Pd(phpy)$	34 %	44 %
d	phpy-H	80 °C	$Pd(OAc)_2$	73 %	15 %
e	phpy-H	100 °C	$(L^O)Pd(phpy)$	32 %[b]	36 %[b]
f	phpy-H	100 °C	$Pd(OAc)_2$	69 %	24 %
g	etpy-H	80 °C	$(L^O)Pd(phpy)$	0 %	-
h	etpy-H	80 °C	$Pd(OAc)_2$	58 %	-

Table 1. Comparison of $Pd(OAc)_2$ and $(L^O)Pd(phpy)$ for catalytic acetoxylation [5 mol% Pd source, 1.0 phpy-H, 1.1 $PhI(OAc)_2$, MeCN, 24 h] [a]Yield based on integration of peaks in GC. [b]Addition of Cs_2CO_3 (10 equiv.) under these conditions prevents catalytic acetoxylation from occurring.

For $Pd(OAc)_2$ the amount of phpy-2OAc produced is controlled solely by the statistical availability of phpy-H and phpy-OAc in the reaction mixture. With complete consumption of $PhI(OAc)_2$ this leads to formation of a 2:1 ratio of phpy-OAc to phpy-2OAc.[15]

For $(L^O)Pd(phpy)$ under identical conditions the production of phpy-2OAc does not seem to be controlled by the same factors. This could be a result of the NHC ligand restricting access to the Pd-centre reducing the rate at which newly functionalised phpy-OAc can be replaced

by phpy-H. Alternatively if $(L^{OH})Pd(OAc)_2$ is the active catalyst the OH group could slow the rate at which phpy-OAc is replaced by forming a H-bond with the recently installed OAc group. Both processes would increase the residence time of phpy-OAc at Pd thus increasing the chances of a second C-H activation occurring. This result is in contrast to the catalytic bromination of phpy-H. Formation of phpy-2Br was disfavoured with $(L^{O})Pd(bzq)$ as the catalyst compared to $Pd(OAc)_2$.[16]

To mop up any AcOH formed by C-H activation and hence prevent cleavage of the Pd-O_{alkoxy} bond, Cs_2CO_3 was added as a base. Unfortunately in doing so no catalytic acetoxylation was observed.

$(L^{OH})Pd(OAc)_2$ is the likely active catalyst in the above reactions where $(L^{O})Pd(phpy)$ was used as a precatalyst. It was expected that the incorporation of a strongly electron-donating ligand, such as an NHC, to palladium would result in a reduction in the rate of reaction. The rate limiting step in catalytic acetoxylation has been determined to be C-H activation[1] and is more facile at an electron-deficient metal centre. The significantly reduced reactivity compared to $Pd(OAc)_2$ lends support to the idea that the NHC remains attached to the Pd during catalysis. In addition the ^1H NMR spectra of the crude reaction mixtures appear to show the NHC ligand still coordinated to Pd.

4.5.2. Effect of solvent on $(L^{O})Pd(phpy)$ catalysed acetoxylation

A number of alternative solvents for catalytic acetoxylation were investigated. The reaction requires elevated temperature and the solvent should be aprotic to avoid cleavage of the Pd-O_{alkoxy} bond. As Table 2 illustrates coordinating solvents are not suitable for this reaction, presumably because they prevent the substrate from binding to Pd long enough for C-H activation to occur. Whilst reasonable results are obtained with PhMe, acetoxylation of the solvent is a concern.[17]

Entry	Solvent	phpy-OAc[a]	phpy-2OAc[a]
i	MeCN	49 %	25 %
j	PhMe	50 %	14 %
k	thf	-	-
l	pyr	-	-

Table 2. Catalytic acetoxylation of phpy-H in different solvents [5 mol% (L^O)Pd(phpy), 1.0 phpy-H, 1.1 $PhI(OAc)_2$, 100 °C, 12 h]. [a]Yield based on integration of peaks in GC.

4.5.3. (L^O)Pd(phpy) catalysed acetoxylation of 2-ethylpyridine

Using $Pd(OAc)_2$ as a catalyst, only acetoxylation (rather than halogenation) of unactivated sp^3 centres is possible.[18] To see if catalytic acetoxylation of an sp^3 centre was possible with an NHC bound to Pd, Etpy-H was treated with $PhI(OAc)_2$ in the presence of (L^O)Pd(phpy) (Equation 7).

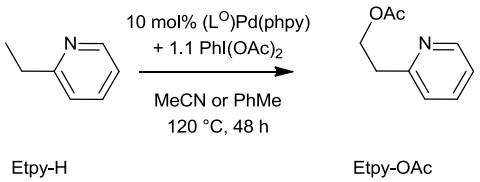

(7)

When the reaction was carried out in PhMe a small amount of Etph-OAc (*c.a.* 5 %) was formed with no evidence of Pd black. However significant quantities of 1,2- 1,3- and 1,4-acetoxytoluene were also formed in the reaction. In the absence of Etpy-H acetoxylation of PhMe still occurs but formation of Pd black is observed within 6 h. In MeCN no Etpy-OAc was formed and the ^1H NMR spectrum of the reaction mixture revealed complete decomposition of the catalyst.

4.5.4. (L^O)Pd(phpy) catalysed C-C bond formation

No catalytic reaction was observed when catalytic phenylation (of Etpy-H or *o*-tolylpy) was attempted using (L^O)Pd(phpy) and $[Ph_2I]BF_4$, Equation 8. ^{1}H NMR spectroscopic analysis of both crude catalysis mixtures (MeCN) showed only a single set of resonances for the catalyst matching $[(L^O)Pd(phpy^{Ph})]BF_4$.

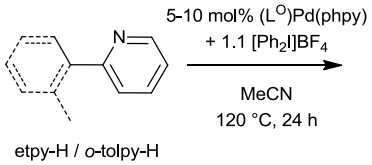

(8)

This result is not entirely unexpected as $Pd(OAc)_2$ catalysed ligand-directed C-C bond formation reactions are usually carried out in acetic acid, benzene/acetic anhydride or toluene/$NaHCO_3$.[19] The acid (anhydride or $NaHCO_3$) can assist with the C-H activation step.

4.5.5. Comparison between (L^O)Pd(phpy) and $(L^{O,Ph})$Pd(phpy) as precatalysts

To determine what effect (if any) changing the substituent on the alkoxide tether has on the catalytic activity the complexes (L^O)Pd(phpy) and $(L^{O,Ph})$Pd(phpy) were compared (Table 3). For the limited range of oxidants and substrates tested changing the group on the alkoxide tether has little to no effect on yields obtained.

Entry	Substrate	Oxidant	Product	GC Yield [a] 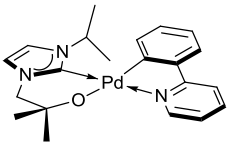	GC Yield [a] 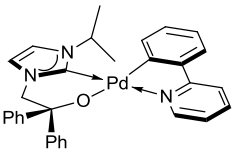
m	phpy-H	NCS	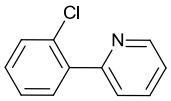	63 %	64 %
n	*o*-tolylpy-H	$PhI(OAc)_2$	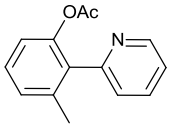	> 95 %[b]	> 95 %[b]
o	*n*-BuOpy-H	NCS	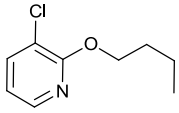	47 %[c]	57 %[c]

Table 3. Comparison of catalysts for ligand-directed acetoxylation [5 mol% ($L^{O,R}$)Pd(phpy), 1.0 substrate, 1.1 oxidant, 120 °C, 48 h]. [a]GC yield based on integration of peaks, average of two runs. [b]12 h. [c]Chlorination occurred on pyridine rather than alkyl chain and is Pd catalysed.

4.6. Conclusions

Different reactivity is observed when (L^O)Pd(phpy) is treated with $PhI(OAc)_2$, $[Ph_2I]BF_4$, NBS or $PhI(Cl)_2$. Treatment of (L^O)Pd(phpy) with $PhI(OAc)_2$ or $[Ph_2I]BF_4$ yields new Pd^{II} complexes. The structure was deduced from the experimental data and DFT calculations. Reactivity at the Pd-alkoxide bond was also observed when (L^O)Pd(phpy) was treated with AcOH, MeI or $TMSN_3$.

No evidence of Pd^{IV} was observed although calculations suggest it is a likely intermediate. The complex (L^O)Pd(phpy) appears to be an effective precatalyst for palladium-catalysed ligand-directed C-H bond acetoxylation of substituted pyridines. Heteroleptic complexes of the type (L^O)Pd(phpy) are straightforward to synthesise and a wide range of structures are possible. It is questionable how useful PdL_2 ($L = L^O$ or L^N) would be in synthesising stable

Pd^{IV} complexes given the alternative reactivity and decomposition observed when $(L^O)Pd(phpy)$ was treated with $PhI(OAc)_2$, MeI or $PhI(Cl)_2$.

The preliminary catalysis results suggest that NHCs can be viable ligands for palladium-catalysed oxidative C-H bond functionalisation. Since NHCs are tuneable ligands that appear to be inert to the strongly oxidizing reaction conditions, related systems that can impart regio- or stereocontrol over the C-H functionalisation reaction should be accessible. In substrates without a traditional directing group is selectivity possible? The addition of a tethered NHC will increase the thermodynamic requirements of the C-H activation (since the Pd is more electron rich). Starting from a complex such as $(L^O)Pd(Me)(py)$ would allow for more facile C-H activation. The process would not be catalytic but it could allow investigation of the selectivity of C-H bond activation with substrates such as naphthalene, PhCOMe, R_2BPh and $PhCH_2SiMe_3$. The selective C-H activation of oxazoles also represents an interesting challenge.

4.7. References

1 K. J. Stowers and M. S. Sanford, *Org. Lett.*, 2009, **11**, 4584.
2 N. R. Deprez and M. S. Sanford, *J. Am. Chem. Soc.*, 2009, **131**, 11234.
3 J. M. Racowski, A. R. Dick, and M. S. Sanford, *J. Am. Chem. Soc.*, 2009, **131**, 10974.
4 A. R. Dick, J. W. Kampf, and M. S. Sanford, *J. Am. Chem. Soc.*, 2005, **127**, 12790.
5 H. D. Durst and G. W. Gokel, 'Experimental organic chemistry', ed. G. W. Gokel, McGraw-Hill, 1987.
6 N. Bernhard and S. Wolfgang, *Angew. Chem., Int. Ed. Engl.*, 1978, **17**, 522.
7 A. Bayler, A. J. Canty, J. H. Ryan, B. W. Skelton, and A. H. White, *Inorg. Chem. Commun.*, 2000, **3**, 575.
8 P. K. Byers, A. J. Canty, B. W. Skelton, and A. H. White, *J. Chem. Soc., Chem. Commun.*, 1986, 1722.
9 P. D. Chaudhuri, R. Guo, and H. C. Malinakova, *J. Organomet. Chem.*, 2008, **693**, 567.
10 R. Kakino, K. Nagayama, Y. Kayaki, I. Shimizu, and A. Yamamoto, *Chem. Lett.*, 1999, 685.
11 J. T. Hoffman and C. J. Carrano, *Inorg. Chim. Acta*, 2006, **359**, 1248.
12 H. Brombacher and H. Vahrenkamp, *Inorg. Chem.*, 2004, **43**, 6042.
13 J. J. MacDougall and J. H. Nelson, *Inorg. Nucl. Chem. Lett.*, 1979, **15**, 315.
14 Y.-J. Kim, X. Chang, J.-T. Han, M. S. Lim, and S. W. Lee, *Dalton Trans.*, 2004, 3699.
15 A. R. Dick, K. L. Hull, and M. S. Sanford, *J. Am. Chem. Soc.*, 2004, **126**, 2300.
16 P. L. Arnold, M. S. Sanford, and S. M. Pearson, *J. Am. Chem. Soc.*, 2009, **131**, 13912.
17 T. Yoneyama and R. H. Crabtree, *J. Mol. Catal. A.*, 1994, **108**, 35.
18 D. Kalyani, A. R. Dick, W. Q. Anani, and M. S. Sanford, *Tetrahedron*, 2006, **62**, 11483.
19 D. Kalyani, N. R. Deprez, L. V. Desai, and M. S. Sanford, *J. Am. Chem. Soc.*, 2005, **127**, 7330.

Chapter 5
Experimental details

General Considerations

All manipulations were carried out using standard Schlenk or glovebox techniques under a dinitrogen atmosphere unless otherwise indicated. Solvents were dried by passage through towers of activated alumina or 4Å molecular sieves (pentanes, hexanes, thf, toluene, dichloromethane and diethyl ether)[1]. Acetone, acetonitrile and 2,6-lutidine were distilled from CaH_2 and degassed before use. Dioxane, dimethylformamide, benzene and pyridine were distilled from potassium and degassed before use. All solvents were stored over activated 4Å molecular sieves with the exception of pentanes, hexanes and toluene which were stored over potassium mirrors. Deuterated solvents purchased from Aldrich were dried, degassed by three freeze-pump-thaw cycles and stored under nitrogen. Deuterated benzene and pyridine were distilled from potassium; whilst deuterated acetonitrile and dichloromethane were distilled from CaH_2. Deuterated solvents purchased from Cambridge Isotope Laboratories, Inc., were used as received.

Imidazole, 2-iodopropane, 4-*t*-butyl-aniline, 1,10-phenanthroline, copper iodide, caesium carbonate, deuterated dimethyl sulfoxide, deuterated chloroform, nickel chloride, potassium bis(trimethylsilyl)amide, *n*-butyllithium (2.5 M solution in hexanes), HCl (2.0 M in dry diethyl ether), iodobenzene diacetate, glacial acetic acid, *N*-bromosuccinimide, *N*-chlorosuccinimide, 1-phenyl-2-pyrrolidone, 1-phenylpyrazole, phenyl(2-pyridinyl)methanone and anhydrous decane were purchased from Aldrich and used without further purification. Benzo[*h*]quinoline and naphthalene were also purchased from Aldrich and sublimed before use. The compounds 2-phenylpyridine and 2-ethylpyridine were purchased from Aldrich and dried over activated 4Å molecular sieves before use. Potassium hydride was purchased from Aldrich as a dispersion in oil, which was removed by hexane washing before use. Palladium acetate was purchased from either Aldrich or Strem and used without further purification. The compounds potassium *t*-amylate, iodobenzene dichloride, sodium cyclopentadienyl, potassium *t*-butoxide, potassium benzyl, trimethylsilylazide and

methyl iodide were available in the laboratory. The compounds $PdCl_2(PhCN)_2$,[2] $PdCl_2(MeCN)_2$,[3] $[Pd(phpy)Cl]_2$,[4] 2-(3-methoxyphenyl)pyridine,[5] $[Ph_2I]BF_4$,[6] *o*-tolylpyridine,[5] 3-methyl-2-phenylpyridinine,[5] iodobenzene di-*p*-nitrobenzoate,[7] iodobenzene di-*p*-methoxybenzoate,[7] the lithium complex $LiL^N \cdot 2LiBr$,[8] and the potassium salt $KL^{O,Me}$,[9] were synthesised according to literature procedures. The compounds 2,2-diphenyl-oxirane,[10] 2,2-di-*iso*-propyl-oxirane,[10] $[Pd(OMe\text{-}phpy)Cl]_2$[4] and $[Pd(bzq)Cl]_2$[4] were synthesised by modified literature procedures.

The NMR spectra [spectrometer (operating at ^1H and $^{13}C\{^1H\}$ MHz)] were recorded on a Brucker arx250 (250 and 63), dpx300 (300 and 75), dpx360 (360 and 91), dmx500 (500 and 126), ava600 (600, 151) as well as Varian Inova 400 (400 and 100) and Varian MR400 (401 and 101) spectrometers. Chemical shifts are reported in ppm and were referenced to the residual solvent resonance. Data are reported as follows: s = singlet, br = broad, d = doublet, t = triplet, sept = septet, m = multiplet; coupling constants in Hz; integration. Infra-red spectra were obtained using a JASCO FTIR-410. Gas chromatography was performed on a Shimadzu GC-17A equipped with a Restek Rtx-5 column (15 m, 0.25 mm ID, 0.25 mm df) and a FID detector. GC yields are reported as corrected GC yields based on a calibration curve against naphthalene as an internal standard. Typical errors associated with GC yields are approximately ±5 %. GC/MS analysis was performed on a FISONS GC 8000 series connected to a FISONS TRIO 1000 mass spectrometer. Electrospray mass spectra were recorded on Finnigan MAT LCQ and electron impact mass spectra were recorded on a Thermo MAT 900 XP spectrometer at the University of Edinburgh mass spectrometer facilities. High-resolution mass spectra were obtained on Micromass AutoSpec Ultima spectrometer at the University of Michigan mass spectrometry facilities. Elemental analyses were performed by Atlantic Microlab, Inc., Norcross, GA and by Mr. Stephen Boyer at the London Metropolitan University. XPS measurements were made by Dr Ron Brown at the University of Edinburgh.

Synthetic Procedures

1 $[H_2L^{O,Ph}]I$

In an ampoule $(Ph)_2COCH_2$ (4.98 g, 25.37 mmol) was combined with imidazole (1.73 g, 25.37 mmol) and heated to 90 °C for 1 h with vigorous stirring. After addition of MeCN (60 mL) the reaction mixture was heated to 80 °C for a further 18 h. One equivalent of 2-iodopropane (4.31 g, 25.37 mmol) was added to the solution before heating at 80 °C for 72 h. The volume of MeCN was reduced (~25 mL) *in vacuo* and $[HOCPh_2CH_2(1\text{-}HC\{NCHCHNPr^i\})]I$, $[H_2L^{O,Ph}]I$ was isolated as a colourless solid by removal of the solution *via* filtration (7.55 g, 68 %).

Characterising data: ^1H NMR (300 MHz, $(CD_3)_2SO$, 27 °C, δ) 8.61 (s, 1H), 7.70 (s, 1H), 7.37 (m, 10H), 6.53 (s, 1H), 5.04 (s, 2H), 4.61 (sept, J = 6.7 Hz, 1H), 1.49 (d, J = 6.7 Hz, 6H). ^{13}C NMR (75 MHz, $(CD_3)_2SO$, 27 °C, δ) 143.7, 135.1, 128.1, 127.3, 125.9, 123.8, 119.1, 76.2, 57.7, 51.8, 22.2.

Crystals suitable for X-ray analysis were grown by slow cooling of a saturated MeCN solution from 80 °C to 25 °C over 72 h.

2 $[H_2L^{O,iPr}]I$

In an ampoule $(^iPr)_2COCH_2$ (2.26 g, 17.63 mmol) was combined with imidazole (1.20 g, 17.63 mmol) and heated to 85 °C for 72 h with vigorous stirring. After addition of MeCN (60 mL) the reaction mixture was heated to 80 °C for a further 18 h. One equivalent of 2-iodopropane (4.31 g, 25.37 mmol) was added to the solution before heating at 80 °C for 24 h. The volume of MeCN was reduced (~20 mL) *in vacuo*. Slow cooling of a concentrated solution of the crude product mixture to -30 °C afforded $[HOC^iPr_2CH_2(1\text{-}$

HC{NCHCHNPr^{i}})]I, [$H_2L^{O,iPr}$]I as a pale waxy solid after removal of the mother liquor by filtration (2.69 g, 42 %).

Characterising data: ^{1}H NMR (250 MHz, $CDCl_3$, 25 °C, δ) 10.18 (m, 1H), 7.46 (m, 1H), 7.31 (m, 1H), 4.79 (m, 1H), 4.50 (s, 2H), 2.69 (b, 1H), 1.93 (sept, *J* = 7.0 Hz, 2H), 1.64 (d, *J* = 6.7 Hz, 6H), 1.01 (d, *J* = 6.7 Hz, 6H), 0.94 (d, *J* = 6.7 Hz, 6H). ^{13}C NMR (126 MHz, $CDCl_3$, 25 °C, δ) 137.2, 124.9, 118.6, 76.7, 54.0, 53.9, 33.7, 23.7, 18.5, 18.3. Anal. Calcd for $C_{14}H_{27}IN_2O$: C, 45.91; H, 7.43; N, 7.65. Found: C, 46.02; H, 7.47; N, 7.59.

Crystals suitable for X-ray analysis were grown by slow cooling of a saturated MeCN solution over 12 h to -30 °C.

3 [$H_2L^{N,Ar}$]I

4-*tert*-butyl-2-iodoaniline was synthesised according to a literature method.[11] *N*-methylation to afford *N*-methyl-4-*tert*-butyl-2-iodoanaline was carried out using a reported procedure, yield 1.31g (79 %).[12]

Characterising data: Colourless oil, b.p. > 100 °C under high vacuum (0.01-0.05 Torr). ^{1}H NMR (600 MHz, $CDCl_3$, 25 °C, δ) 7.67 (d, *J* = 2.2 Hz, 1H), 7.27 (dd, *J* = 8.5, 2.2 Hz, 1H), 6.51 (d, *J* = 8.5 Hz, 1H), 4.06 (br, 1H), 2.86 (s, 3H), 1.25 (s, 9H). ^{13}C NMR (151 MHz, $CDCl_3$, 25 °C, δ) 146.2, 141.7, 137.5, 136.0, 126.5, 109.9, 85.7, 31.65, 31.3.

In a high pressure ampoule equipped with a stirrer bar CuI (150 mg, 0.788 mmol, 0.11 equiv) and 1,10-phenanthroline (285 mg, 1.58 mmol, 0.21 equiv) were slurried in DMF (10 mL). Imidazole (1012 mg, 14.86 mmol, 2.00 equiv), *N*-methyl-4-*tert*-butyl-2-iodoanaline (2149 mg, 7.43 mmol, 1.00 equiv), caesium carbonate (4843 mg, 8.40 mmol, 2.00 equiv) and DMF (30 mL) were added. The reaction mixture was heated at 120 °C for 65 h before drying *in vacuo*. In air the reaction mixture was suspended in CH_2Cl_2 (~15 mL) and filtered. Hexanes (45 mL) was added to the filtrates, stirred and a dark tar was removed from a red solution using a separating funnel. The red solution was evaporated in air to ca. 5 mL to

yield colourless needles and red oil. The colourless crystals were washed with hexanes, to remove the red oil, giving 761 mg of coupled product as colourless needles (44 %).

Characterising data: ^{1}H NMR (360 MHz, $CDCl_3$, 25 °C, δ) 7.68 (s, 1H), 7.36 (dd, *J* = 8.4, 2.5 Hz, 1H), 7.25 (s, 1H), 7.10 (s, 1H), 7.09 (d, *J* = 2.5 Hz, 1H), 6.70 (d, *J* = 8.4 Hz, 1H), 3.48 (s, 1H), 2.77 (d, *J* = 4.8 Hz, 3H), 1.27 (s, 9H). ^{13}C NMR (91 MHz, $CDCl_3$, 25 °C, δ) 142.3, 140.1, 138.1, 129.9, 127.2, 124.2, 122.7, 120.7, 110.9, 34.1, 31.6, 30.6.

To a foiled covered ampoule containing substituted imidazole [(N{H}Me)C_6H_4(1-HC{NCHCHN})] (430 mg, 1.88 mmol, 1.00 equiv) and 2-iodopropane (670 mg, 3.94 mmol, 2.10 equiv) was added dry MeCN (5 mL). The reaction was heated at 100 °C for 92 h with stirring. The resultant mixture was dried *in vacuo*. Diethyl ether (2 mL) was added and the suspension stirred for 2 h before the volatiles were removed under reduced pressure to yield 750 mg of [$H_2L^{N,Ar}$]I as a colourless solid (100 %).

Characterising data: ^{1}H NMR (600 MHz, $CDCl_3$, 22 °C, δ) 9.03 (s, 1H), 7.62 (s, 1H), 7.37 (dd, J = 2.2, 8.6 Hz, 1H), 7.33 (s, 1H), 7.06 (s, 1H), 6.68 (d, J = 8.6 Hz, 1H), 4.99 (sept, J = 6.7 Hz, 1H), 2.72 (s, 3H), 1.68 (d, J = 6.7 Hz, 6H), 1.24 (s, 9H). ^{13}C NMR (151 MHz, CD_3Cl_3, 22 °C, δ) 142.2, 139.8, 135.2, 129.3, 124.2, 123.6, 121.4, 119.9, 112.6, 54.0, 34.1, 31.6, 30.0, 23.0. Anal: Calcd. for $C_{17}H_{26}N_3I$: C, 51.13; H, 6.56; N, 10.52; Found C, 51.17; H, 6.51; N, 10.48.

4 $KL^{O,Ph}$

Potassium hydride (0.83 g, 20.72 mmol) and [$H_2L^{O,Ph}$]I (3.00 g, 6.91 mmol) were combined in a Schlenk and cooled to -78 °C before thf (60 mL) was added slowly with stirring. The mixture was allowed to warm to room temperature with stirring. After 24 h the reaction was filtered and the filtrate was dried *in vacuo* to yield an off-white solid. The solid was stirred with hexane overnight and the colourless solid isolated by filtration (1.22 g, 51 %).

Characterising data: ^{1}H NMR (300 MHz, C_6D_6, 27 °C, δ) 7.35 (m, 10H), 6.15 (d, *J* = 1.5 Hz, 1H), 5.56 (d, *J* = 1.5 Hz, 1H), 4.72 (s, 2H), 3.78 (sept, *J* = 6.7 Hz, 1H), 1.10 (d, *J* = 6.7 Hz, 6H). ^{13}C NMR (75 MHz, C_6D_6, 27 °C, δ) 209.5, 157.0, 2 aromatic resonances under the solvent resonance, 125.2, 121.3, 113.7, 82.6, 66.5, 51.8, 24.6. Anal: Calcd. for $C_{20}H_{21}N_2OK$: C, 69.53; H, 6.42; N, 8.11; Found C, 69.84; H, 6.17; N, 8.20.

5 $KL^{O,Me}$

The synthesis of this compound has been described previously.[9] The data below was collected to demonstrate the acidic nature of the backbone protons.

Characterising data: ^{1}H NMR (400 MHz, CD_3CN, 23 °C, δ) 4.43 (sept, *J* = 6.6 Hz, 1H), 3.80 (s, 2H), 1.41 (d, *J* = 6.6 Hz, 6H), 1.03 (s, 6H). The resonances for the backbone protons are not observed presumably as a result of H/D exchange. If the spectrum is collected in CH_3CN resonances for the backbone protons are observed as singlets at 6.96 and 6.89 ppm.

6 $(L^N)Pd(allyl)$

A solution of $Li(L^N)\cdot 2LiBr$ (32 mg, 0.078 mmol) in thf (25 mL) was added dropwise to a solution of $[Pd(allyl)Cl]_2$ (14 mg, 0.039 mmol) in thf (15 mL) at -10 °C. The mixture was allowed to warm to room temperature before removal of the volatiles under reduced pressure. The resultant solid was triturated with pentane (~5 mL).

Characterising data: ^{1}H NMR (300 MHz, C_6D_5N, 27 °C, δ) 7.48 (s, 1H), 7.42 (s, 1H), 5.31 (b, 2H), 4.66 (b, 1H), 4.45 (b, 1H), 4.31 (b, 1H), 3.51 (b, 1H), 3.32 (b, 1H), 3.20 (b, 1H), 2.69 (b, 0.5H), 2.43 (b, 0.5H), 1.80 (s, 3H), 1.68 (s, 6H), 1.07 (s, 9H).

7 $Pd(L^{O,Me})_2$

To a solution of $PdCl_2(PhCN)_2$ (100 mg, 0.259 mmol, 1.00 equiv) in thf (10 mL) was added $KL^{O,Me}$ (114 mg, 0.519 mmol, 2.00 equiv) in thf (10 mL) at 0 °C. The volatiles were removed under reduced pressure before triturating with ether (10 mL) to remove any remaining PhCN. The resultant solid was dissolved in thf (10 mL) to which PhMe (5 mL)

was added to afford a precipitate. $Pd(L^O)_2$ was isolated as a colourless solid after removal of the solution by filtration (20 mg, 16 %).

Characterising data: ^{1}H NMR (250 MHz, C_6D_5N, 27 °C, δ) 7.10 (d, J = 1.9 Hz, 2H), 6.96 (d, J = 1.9 Hz, 2H), 6.77 (sept, J = 6.8 Hz, 2H), 3.82 (s, 2H), 1.37 (d, J = 6.8 Hz, 12H), 1.11 (s, 12H). Mass Spectrometry: HRMS-ESI (m/z) Calcd for $[C_{20}H_{34}N_4O_2Pd + H]$, 469.1797. Found, 469.1778. The poor solubility of $Pd(L^O)_2$ in common organic solvents precluded acquisition of a ^{13}C NMR spectra.

Alternative synthesis: $Pd(OAc)_2$ (25 mg, 0.11 mmol), $[H_2L^O]I$ (69 mg, 0.22 mmol) and Cs_2CO_3 (218 mg, 0.67 mmol) were combined in an ampoule with dioxane (4 mL). The mixture was heated at 100 °C for 24 h. After filtration away from a black precipitate and removal of the volatiles under reduced pressure a brown oil was obtained.

Characterising data: ^{1}H NMR (360 MHz, $CDCl_3$, 19 °C, δ) Major isomer: 6.96 (s, 4H), 5.53, (sept, *J* = 6.8 Hz, 2H), 4.41 (s, 4H), 1.51 (d, *J* = 6.8 Hz, 6H), 1.49 (d, *J* = 6.8 Hz, 6H), 1.31 (s, 12H). Minor isomer: 7.06 (s, 4H), 5.68 (sept, *J* = 6.8 Hz, 2H), 4.38 (s, 4H), 1.51 (d, *J* = 6.8 Hz, 6H), 1.49 (d, *J* = 6.8 Hz, 6H), 1.31 (s, 12H). Ratio 2:1.

8 $Pd(L^N)_2$

A solution of $Li(L^N)\cdot 2LiBr$ (10.1 mg, 0.025 mmol) in thf (0.4 mL) was added to a solution of $PdCl_2(MeCN)_2$ (3.3 mg, 0.013 mmol) in thf (0.4 mL) at -30 °C. The orange solution was stirred for 18 h at room temperature and then the volatiles were removed under reduced pressure. The pale solid was suspended in CD_3CN and then filtered before analysis.

Characterising data: ^{1}H NMR (250 MHz, CD_3CN, 25 °C, δ) 4.14 (m, 2H) 2.88 (m, 2H) 1.61 (s, 9H), 0.98 (s, 9H). The two resonances for the backbone protons are absent, probably due to H-D exchange. ^{13}C NMR (91 MHz, CD_3CN, 25 °C, δ) 182.4, 136.1, 129.6, 61.0, 52.2, 51.0, 42.9, 30.2, 29.6. Mass Spectrometry: EI (m/z) 550.3 [M+].

9 $Ni(L^{O,Me})_2$

To a suspension of $NiCl_2$ (0.40 g, 3.086 mmol, 1.00 equiv) in thf (60 mL) was added a solution of KL^O (1.36 g, 6.172 mmol, 2.00 equiv) in thf (60 mL) at -78 °C. After stirring at room temperature for 18 h a brown solution was isolated by filtration. The volatiles were removed under reduced pressure to yield a glassy red brown solid. A minimum of thf (30 mL) was added to dissolve up the bulk of the solid and then PhMe (15 mL) was added to precipitate the yellow product. The solution was separated from the precipitate via cannula and placed in the freezer (-35 °C). A second crop of yellow solid was obtained. The pale yellow precipitate was isolated by filtration and dried in vacuo. (0.711 g, 55 %).

Characterising data: ^{1}H NMR (300 MHz, C_6D_5N, 25 °C, δ) 7.27 (s, 2H), 7.24 (s, 2H), 4.41 (d, J = 12.1 Hz, 2H) 4.20 (sept, J = 6.6 Hz, 2H) 3.98 (d, J = 12.1 Hz, 2H) 1.55 (d, J = 6.6 Hz, 6H) 1.46 (s, 6H), 0.93 (d, J = 6.6 Hz, 6H), 0.48 (s, 6H). ^{13}C NMR (75 MHz, C_6D_5N, 25 °C, δ) 167.5, 123.4, 117.5, 67.7, 65.3, 52.0, 30.5, 28.7, 25.6, 21.3. Anal. Calcd for $C_{40}H_{68}N_8Ni_2O_4K_2I_2 \cdot 0.5C_5H_{12}$: C, 42.17; H, 6.16; N, 9.26. Found: C, 42.74; H, 6.69; N, 9.73.

Single crystals suitable for X-ray diffraction studies were grown by diffusion of hexanes into a saturated thf solution over a year at -20 °C.

10 $Ni(L^{O,Me})_2Cl$

To a mixture of $Ni(L^O)_2 \cdot 2KI$ (10.5 mg, 0.014 mmol) and $PhI(Cl)_2$ (6.5 mg, 0.027 mmol) was added CH_2Cl_2 (0.6 mL) at 25 ºC. The paramagnetic compound was characterised by ^{1}H NMR spectroscopy. Green/brown crystals suitable for X-ray diffraction studies were grown by vapour diffusion of hexanes in to a CH_2Cl_2 solution at -20 °C over 4 days. The crystals rapidly desolvated before they could be mounted preventing data collection.

Characterising data: ^{1}H NMR (300 MHz, CH_2Cl_2, 25 °C, δ) 20.27 (s, 1H), 18.43 (s, 1H), 1.82 (m, 3H), 1.50 (d, J = 6.6 Hz, 1H), 1.26 (d, J = 7.0 Hz, 1H), -3.21 (d, J = 94.0 Hz, 3H),

-3.93 (d, J = 50.0 Hz, 3H), -9.94 (m, 1H). The resonance for one methyl group is obscured by the solvent resonance.

11 $Ni(L^{O,Me})_2$ + $PhI(OAc)^2$

To a mixture of $Ni(L^O)_2 \cdot 2KI$ (10.5 mg, 0.014 mmol) and $PhI(OAc)_2$ (8.5 mg, 0.027 mmol) was added CH_2Cl_2 (0.6 mL) at 25 ºC. The diamagnetic complex was characterised by ^1H NMR spectroscopy.

Characterising data: ^1H NMR (300 MHz, CH_2Cl_2, 25 °C, δ) 7.84 (d, *J* = 7.5 Hz, 1H), 7.71 (d, *J* = 7.5 Hz, 1H), 7.12 (m, 2H), 4.22 (m, 2H), 3.67 (s, 2H), 1.97 (s, 6H obscured by excess $PhI(OAc)_2$) 1.81 (s, 3H), 1.32 (s, 3H), 1.15 (d, *J* = 5.7 Hz, 6H), 0.92 (d, *J* = 7.2 Hz, 3H), 0.90 (d, *J* = 7.2 Hz, 3H), 0.80 (s, 3H), 0.67 (s, 3H).

12 $(L^{O,Me})Pd(phpy)$

To a suspension of $[Pd(phpy)Cl]_2$ (535 mg, 0.90 mmol) in thf (20 mL) was added $[KL^O]$ (398 mg, 1.81 mmol) in thf (40 mL) dropwise at -78 °C. The reaction mixture was allowed to warm to 25 °C with stirring. After 18 h the yellow solution was separated from the pale precipitate by filtration and dried *in vacuo*. The resultant glassy solid was stirred with hexanes (10 mL) for 4 h before drying in vacuo to afford 760 mg of $(L^O)Pd(phpy)$ as a pale yellow solid (95 % yield).

The addition of lutidine to $[Pd(phpy)Cl]_2$ affords the solvated complex Pd(phpy)Cl(lutidine). The use of this in the reaction to form $(L^O)Pd(phpy)$ however results in significantly lower yields (~45 %), and the product is contaminated with a red oil, which is removed most easily by dissultion of the mixture in CH_2Cl_2/hexanes (in which the oil is insoluble) before the product can be precipitated from CH_2Cl_2 by hexanes addition.

Characterising data: ^1H NMR (250 MHz, CD_3CN, 25 °C, δ) 9.02 (d, J= 5.3 Hz, 1H), 7.90 (m, 1H), 7.82 (m, 1H), 7.62 (m, 1H), 7.28 (m, 1H), 7.23 (d, J= 2.0, 1H), 7.14 (m, 2H), 7.01 (d, J= 2.0 1H), 7.01 (m, 1H), 5.07 (sept, J= 6.6 Hz, 1H), 3.95 (s, 1H), 3.93 (s, 1H), 1.57 (d, J= 6.6

Hz, 3H), 1.27 (s, 3H), 1.27 (d, J= 6.6 Hz, 3H), 0.51 (s, 3H). ^{13}C NMR (91 MHz, CD_3CN, 25 °C, δ) 175.0, 165.8, 161.4, 148.1, 147.8, 140.1, 139.8, 129.5, 124.4, 124.1, 123.8, 122.3, 118.8, 117.1, 68.7, 67.6, 52.8, 31.4, 28.4, 25.7, 21.7.

^{1}H NMR (250 MHz, C_6D_6, 25 °C, δ) 9.66 (ddd, *J* = 0.8, 1.8, 5.4 Hz, 1H), 7.44 (m, 2H), 7.11 (m, 3H), 6.93 (ddd, *J* = 1.8, 7.4, 8.0 Hz, 1H), 6.52 (ddd, *J* = 1.3, 5.4, 7.4 Hz, 1H), 6.34 (d, *J* = 1.9 Hz, 1H), 6.30 (d, *J* = 1.9 Hz, 1H), 5.26 (sept, *J* = 6.7 Hz, 1H), 4.15 (d, *J* = 12.5 Hz, 1H), 3.47 (d, *J* = 12.5 Hz, 1H), 1.70 (s, 3H), 1.10 (d, *J* = 6.7 Hz, 3H), 0.91 (s, 3H), 0.87 (d, *J* = 6.7 Hz, 3H). ^{13}C NMR (63 MHz, C_6D_6, 25 °C, δ) 176.5, 165.8, 162.4, 148.9, 148.0, 140.2, 138.4, 129.1, 124.2, 123.4, 122.9, 121.2, 117.7, 115.6, 68.9, 67.7, 53.8, 52.2, 32.1, 29.1, 25.6, 21.9.

^{1}H NMR (400 MHz, $CDCl_3$, 30 °C, δ) 9.11 (ddd, *J* = 0.7, 1.6, 5.4 Hz, 1H), 7.73 (td, *J* = 1.7, 8.0 Hz, 1H), 7.64 (d, *J* = 8.0 Hz, 1H), 7.54 (dd, *J* = 8.0 Hz, 1H), 7.17 (m, 2H), 7.02 (dd, *J* = 1.6, 7.3 Hz, 1H), 6.99 (d, *J* = 2.0 Hz, 1H), 6.99 (dd, *J* = 1.8, 7.0 Hz, 1H), 6.94, (d, *J* = 1.9 Hz, 1H), 5.16 (sept, *J* = 6.7 Hz, 1H), 4.21 (d, *J* = 12.7 Hz, 1H), 3.81 (d, *J* = 12.7 Hz, 1H), 1.57 (d, *J* = 6.7 Hz, 3H), 1.37 (s, 3H), 1.34 (d, *J* = 6.7 Hz, 3H), 0.73 (s, 3H). ^{13}C NMR (101 MHz, $CDCl_3$, 30 °C, δ) 174.8, 164.7, 159.5, 148.4, 139.3, 138.4, 128.8, 123.6, 123.3, 122.6, 121.5, 117.5, 115.6, 67.7, 67.0, 52.1, 31.1, 28.7, 25.8, 22.3. Mass Spectrometry: HRMS-ESI (m/z) Calcd for [$C_{21}H_{25}N_3OPd$ + H], 442.1111. Found, 442.1117. Anal: Calcd for $C_{21}H_{25}N_3OPd$: C, 57.08; H, 5.70; N, 9.51; Found C, 56.98; H, 5.39; N, 9.38. Melting point (Decomp) 234-240 °C.

Single crystals of (L^O)Pd(phpy) suitable for X-ray diffraction studies were obtained by vapour diffusion of hexanes into a PhH solution at room temperature (over 3 days).

13 ($L^{O,Ph}$)Pd(phpy)

To a mixture of $[Pd(phpy)Cl]_2$ (447 mg, 0.75 mmol) and 2,6-lutidine (162 mg, 1.51 mmol) in thf (30 mL) was added [$KL^{O,Ph}$] (520 mg, 1.51 mmol) in thf (15 mL) dropwise at -78 °C. The reaction mixture was allowed to warm to 25 °C with stirring over 18 h. The dark yellow

reaction mixture was dried *in vacuo* before washing with toluene (3 x 5 mL) to remove impurities. CH_2Cl_2 (10 mL) was added and after filtering hexanes (10 mL) was added to the filtrates before drying *in vacuo*. Further washing of the solid with MeCN (2 x 5 mL) afforded 563 mg of ($L^{O,Ph}$)Pd(phpy) as an off-white powder after removal of the volatiles under reduced pressure (66 % yield).

Characterising data: ^{1}H NMR (401 MHz, CD_2Cl_2, 23 °C, δ): 9.18 (ddd, *J* = 0.8, 1.7, 5.4 Hz, 1H), 7.83 (ddd, *J* = 1.7, 7.34 8.1 Hz, 1H) , 7.76 (m, 3H), 7.61 (dd, *J* = 1.6, 7.5 Hz, 1H), 7.40-7.32 (m, 4H), 7.24-7.18 (m, 3H), 7.11-6.99 (m, 5H), 6.69 (d, *J* = 2.0 Hz), 6.55 (d, *J* = 2.0 Hz), 5.14 (sept, *J* = 6.7 Hz, 1H), 4.83 (d, *J* = 12.6 Hz, 1H), 4.74 (d, *J* = 12.6 Hz, 1H), 1.51 (d, *J* = 6.7 Hz, 3H), 1.23 (d, *J* = 6.7 Hz, 3H). ^{13}C NMR (101 MHz, CD_2Cl_2, 23 °C, δ): 174.6, 165.2, 159.9, 152.1, 150.2, 148.3, 147.5, 146.5, 139.6, 139.0, 129.1, 128.2, 127.6, 127.3, 127.2, 126.2, 125.6, 124.0, 123.6, 123.1, 122.1, 118.2, 115.7, 77.8, 66.2, 54.5, 54.3, 54.0, 53.7, 53.5, 52.4, 25.6, 22.0. Mass Spectrometry: HRMS-ESI (m/z) Calcd for [$C_{31}H_{29}N_3OPd$ + H], 566.1424. Found, 566.1413. Anal: Calcd for $C_{31}H_{29}N_3OPd$: C, 65.78; H, 5.16; N, 7.42. Found: C, 65.71; H, 5.16; N, 7.39.

Single crystals of ($L^{O,Ph}$)Pd(phpy) suitable for X-ray diffraction studies were obtained by vapour diffusion of acetone into a dimethoxyethane solution of ($L^{O,Ph}$)Pd(phpy) at room temperature over two weeks.

14 ($L^{O,iPr}$)Pd(phpy)

To a mixture of [$H_2L^{O,iPr}$]I (284 mg, 0.78 mmol) and KH (93 mg, 2.33 mmol) cooled to -78 °C was added thf (20 mL) dropwise with stirring. The reaction mixture was allowed to warm to 25 °C and then stirred for a further 18 h. The yellow solution was filtered away from a colourless precipitate onto a suspension of [Pd(phpy)Cl]$_2$ (230 mg, 0.39 mmol) in thf (10 mL) at -10 °C. The reaction mixture was allowed to warm to 25 °C with stirring. After 18 h the reaction mixture was dried *in vacuo*. The reaction mixture was extracted with toluene (20 mL) and filtered. The filtrates were concentrated (~ 5 mL) and hexanes were added slowly (5

mL). Initially an orange waxy solid was obtained that coated the stirrer bar. After decanting the solution away from the waxy solid more hexanes was added (15mL) to afford a bright yellow precipitate. The solution was removed by filtration to yield 159 mg of ($L^{O,iPr}$)Pd(phpy) as an bright yellow powder after drying *in vacuo* (41 % yield).

Characterising data: ^{1}H NMR (401 MHz, C_6D_6, 23 °C, δ): 9.73 (dd, *J* = 1.0, 5.3 Hz, 1H), 7.49 (m, 2H), 7.16 (m, 2H), (dd, *J* = 1.5, 7.6 Hz, 1H), 6.61 (ddd, *J* = 0.7, 5.2, 7.3 Hz, 1H), 6.39 (d, *J* = 1.9 Hz, 1H), 6.37 (d, *J* = 1.9 Hz, 1H), 5.33 (sept, *J* = 6.7 Hz, 1H), 4.25 (d, *J* = 13.1 Hz, 1H), 3.73 (d, *J* = 13.1 Hz, 1H), 2.21 (sept, *J* = 6.7 Hz, 1H), 1.96 (sept, *J* = 7.0 Hz, 1H), 1.55 (d, *J* = 6.7 Hz, 3H), 1.34 (d, *J* = 7.0 Hz, 3H), 1.16 (d, *J* = 6.7 Hz, 3H), 1.07 (d, *J* = 6.7 Hz, 3H), 0.95 (d, *J* = 6.7 Hz, 3H), 0.89 (d, *J* = 7.0 Hz, 3H). ^{13}C NMR (101 MHz, C_6D_6, 23 °C, δ): 170.6, 165.9, 162.5, 148.1, 140.26, 138.3, 129.1, 124.2, 123.3, 122.5, 121.3, 117.7, 115.7, 75.1, 59.2, 36.3, 36.1, 35.3, 25.9, 21.8, 19.8, 19.7, 19.2, 18.4. Anal: Calcd for $C_{25}H_{33}N_3OPd$: C, 60.30; H, 6.68; N, 8.44. Found: C, 60.39; H, 6.60; N, 8.42.

Single crystals of ($L^{O,iPr}$)Pd(phpy) suitable for X-ray diffraction studies were obtained by vapour diffusion of hexanes into a C_6D_6 solution of ($L^{O,iPr}$)Pd(phpy) at room temperature over a week.

15 (L^{O})Pd(^{OMe}phpy)

To a mixture of [Pd(^{OMe}phpy)Cl]$_2$ (536 mg, 0.90 mmol) and 2,6-lutidine (40 mg, 0.38 mmol, 0.42 equiv) in thf (10 mL) was added KL^{O} (396 mg, 1.80 mmol, 2.00 equiv) in thf (10 mL) dropwise at -35 °C. The reaction mixture was allowed to warm to 33 °C with stirring. After 18 h the reaction mixture was dried *in vacuo*. A minimum of pentanes (10 mL) was added to the glassy orange solid and removed *in vacuo* (to eliminate traces of thf). The mixture was suspended in CH_2Cl_2 (10 mL) and filtered through a 1 cm plug of celite. The celite plug was washed with CH_2Cl_2 (2 x 10 mL). The resultant orange solution was concentrated under reduced pressure, (to *ca.* 10 mL) then pentane was added dropwise with stirring to induce crystallisation of (L^{O})Pd(OMe-phpy) as a yellow powder. The powder was isolated by

filtration, and a second crop was isolated from the filtrate by addition of more pentane (5 mL) and then filtered. The two crops of powders were combined and washed with pentane (10 mL). After removal of the volatiles under reduced pressure, 415 mg of (L^O)Pd(OMe-phpy) was afforded as an pale yellow solid (49 % yield).

Characterising data: ^{1}H NMR (500 MHz, C_6D_6, 25 °C, δ) 9.06 (dq, *J* = 0.4, 1.7, 5.5 Hz, 1H), 7.79 (td, *J* = 1.7, 7.7 Hz, 1H), 7.66 (d, *J* = 8.1 Hz, 1H), 7.21 (ddd, *J* = 1.2, 2.0, 5.5 Hz, 1H), 7.14 (d, *J* = 2.8 Hz, 1H), 7.03 (m, 2H), 6.99 (d, *J* = 1.9 Hz, 1H), 6.64 (dd, *J* = 2.7, 8.1 Hz, 1H), 5.12 (sept, *J* = 6.7 Hz, 1H), 4.06 (d, *J* = 12.7 Hz, 1H), 3.84 (d, *J* = 12.7 Hz, 1H), 3.79 (s, 3H), 1.56 (d, *J* = 6.7 Hz, 3H), 1.32 (s, 3H), 1.30 (d, *J* = 6.7 Hz, 3H), 0.57 (s, 3H). ^{13}C NMR (101 MHz, CH_2Cl_2, 25 °C, δ): 174.9, 165.1, 157.0, 150.2, 148.2, 147.8, 139.9, 138.9, 123.2, 122.0, 118.1, 116.1, 115.4, 109.8, 68.3, 67.5, 55.8, 52.4, 31.3, 20.5, 26.0, 22.2. Anal: Calcd for [$C_{22}H_{27}N_3O_2Pd \cdot 0.66CH_2Cl_2$]: C, 51.41; H, 5.58; N, 7.94; Found C, 51.42; H, 5.42; N, 7.85.

No nOe interactions were observed between the two ligands as has been seen for similar complexes. Saturation of the resonance for H16 or H26 resulted in the spin being transferred to the methoxy group rather than the NHC ligand. Single crystals of (L^O)Pd(^{OMe}phpy) suitable for X-ray diffraction studies were obtained by vapour diffusion of hexanes into an acetone solution at -20 °C over 4 days.

16 (L^N)Pd(phpy)

A solution of Li(L^N)·2LiBr (100 mg, 0.25 mmol) in thf (20 mL) was added to a suspension of [Pd(phpy)Cl]$_2$ (74 mg, 0.25 mmol) in thf (20 mL) at -78 °C. The reaction mixture was allowed to warm to room temperature with stirring. After 18 h the volatiles were removed under reduced pressure. A minimum of CH_2Cl_2 (10 mL) was added to the glassy solid and removed *in vacuo* (to eliminate traces of thf). The solid was washed with PhMe (3 x 20 mL) and then filtered. The filtrates were dried *in vacuo* to yield a yellow oil. Addition of Et_2O

(10 mL) yielded a yellow solid after removal of the volatiles under reduced pressure (90 mg, 75 %).

Characterising data: ^{1}H NMR (360 MHz, C_6D_6, 25 °C, δ) 10.11 (ddd, *J* = 0.8, 1.8, 5.6 Hz, 1H), 7.32 (dd, *J* = 2.0, 7.3 Hz, 1H), 7.06 (m, 1H), 6.99 (dd, *J* = 1.8, 10.3 Hz, 1H), 6.97 (dd, *J* = 1.7, 10.0 Hz, 1H), 6.85 (d, *J* = 2.1 Hz, 1H), 6.85 (dd, *J* = 1.7, 7.4 Hz, 1H), 6.59 (d, *J* = 2.1 Hz, 1H), 6.39 (dd, *J* = 1.6, 7.3 Hz, 1H), 6.37 (dd, *J* = 1.4, 5.6 Hz, 1H), 4.74 (m, 1H), 4.34 (m, 1H), 3.12 (m, 1H), 2.91 (m, 1H), 1.73 (s, 9H), 0.92 (s, 9H). ^{13}C NMR (91 MHz, C_6D_6, 25 °C, δ) 171.5, 165.6, 159.5, 153.0, 147.7, 138.5, 138.2, 130.4, 128.7, 124.6, 124.5, 122.6, 122.3, 119.5, 118.5, 59.2, 55.5, 51.0, 43.1, 32.6, 30.0. Mass Spectrometry: EI (m/z) 482.2 [M+].

17 $(L^O)Pd(bzq)\cdot 1/3CH_2Cl_2$

To a mixture of $[Pd(bzq)Cl]_2$ (600 mg, 0.94 mmol, 1.00 equiv) and 2,6-lutidine (40 mg, 0.38 mmol, 0.40 equiv) in thf (10 mL) was added $[KL^O]$ (413 mg, 1.88 mmol, 2.00 equiv) in thf (10 mL) dropwise at -35 °C. The reaction mixture was allowed to warm to 33 °C with stirring. After 18 h the reaction mixture was dried *in vacuo*. A minimum of CH_2Cl_2 (10 mL) was added to the glassy red solid and removed *in vacuo* (to eliminate traces of thf). Addition of CH_2Cl_2 (10 mL) and filtration through a 1 cm plug of celite was followed by two CH_2Cl_2 (10 mL) washes. The resultant blood red solution was concentrated under reduced pressure, (to *ca.* 10 mL) then pentane was added dropwise with stirring to induce precipitation of an oily byproduct, which was removed, by decanting. Further addition of pentane induced crystallisation of $(L^O)Pd(bzq)$ as a red powder. The powder was isolated by filtration, and a second crop isolated from the filtrate by addition of more pentane (1 mL) and filtration. The combined powders were was washed with pentane (10 mL) and dried *in vacuo* to afford 820 mg of $(L^O)Pd(bzq)\cdot 1/3CH_2Cl_2$ as an orange solid (88 % yield).

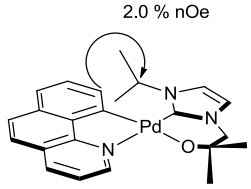

Characterising data: ^{1}H NMR (400 MHz, CD_3CN, 22 °C, δ) 9.17 (dd, *J* = 5.0, 1.6 Hz, 1H), 8.41 (dd, *J* = 8.1, 1.6 Hz, 1H), 7.79 (d, *J* = 8.8 Hz, 1H), 7.69 (d, *J* = 8.8 Hz, 1H), 7.64 (dd, *J* = 8.1, 5.0 Hz, 1H), 7.56 (m, 1H), 7.38 (m, 2H), 7.28 (d, *J* = 2.0 Hz, 1H), 7.18 (d, *J* = 2.0 Hz, 1H), 5.23 (sept, *J* = 6.8 Hz, 1H), 4.00 (m, 2H), 1.63 (d, *J* = 6.8 Hz, 3H), 1.32 (s, 3H), 1.27 (d, *J* = 6.8 Hz, 3H), 0.56 (s, 3H). ^{13}C NMR (100 MHz, CD_3CN, 22 °C, δ) 174.1, 159.5, 147.6, 143.8, 138.4, 137.2, 134.7, 130.2, 129.6, 127.5, 124.7, 124.4, 122.6, 122.3, 117.7, 69.1, 68.2, 53.3, 31.7, 28.8, 26.2, 22.2 (1 aromatic carbon is obscured the solvent MeCN resonance). Mass Spectrometry: HRMS-ESI (m/z) Calcd for [$C_{23}H_{25}N_3OPd$ + H], 466.1111. Found, 466.1122. Anal: Calcd. For [$C_{23}H_{25}N_3OPd \cdot 0.33CH_2Cl_2$]: C, 56.59; H, 5.43; N, 8.49; Found C, 56.97; H, 5.36; N, 8.50. Integration of the dichloromethane resonance observed in the ^{1}H NMR spectrum of (L^{O})Pd(bzq) gives the same ratio as measured by elemental analysis.

Single crystals of (L^{O})Pd(bzq) suitable for X-ray diffraction studies were obtained by vapour diffusion of hexanes into a CH_2Cl_2/C_6D_6 solution of ($L^{O,iPr}$)Pd(phpy) at -35 °C over two weeks.

18 ($L^{N,Ar}$)Pd(bzq)

A solution of KN" (250 mg, 1.25 mmol) in PhMe (10 mL) was added to a suspension of [$H_2L^{N,Ar}$]I (250 mg, 0.63 mmol) in PhMe (10 mL) at -10 °C. The reaction mixture was allowed to warm to RT and stirred for 18 h. The reaction was cooled back to -10 °C and added slowly to a suspension of $[Pd(bzq)Cl]_2$ in PhMe (10 mL) at -10 °C. The reaction mixture was allowed to warm to RT and stirred for 24 h. The dark suspension was filtered and the volatiles removed (from the filtrates) under reduced pressure. After addition of PhMe (10 mL) and stirring for 2 h the reaction was filtered again. The volatiles were removed from the filtrates under reduced pressure and the dark red solid was dried at 70 °C *in vacuo* to afford 100 mg of (L^{N})Pd(bzq) (29 %).

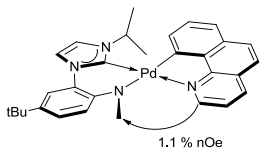

Characterising data: ^{1}H NMR (600 MHz, C_6D_6, 25 °C, δ) 9.00 (dd, *J* = 5.2, 0.8 Hz, 1H), 7.53 (dd, *J* = 7.2, 0.7 Hz, 1H), 7.50 (m, 2H), 7.45 (d, *J* = 8.6, 2.4 Hz, 1H), 7.41 (dd, *J* = 8.0, 1.1 Hz, 1H), 7.38 (t, *J* = 7.3 Hz, 1H), 7.33 (d, *J* = 2.4 Hz, 1H), 7.14 (d, *J* = 8.7 Hz, 1H), 7.10 (d, *J* = 8.7 Hz, 1H), 6.94 (d, *J* = 2.0 Hz, 1H), 6.63 (dd, *J* = 8.0, 5.2 Hz, 1H), 6.47 (d, *J* = 2.0 Hz, 1H), 5.47 (sept, *J* = 6.7 Hz, 1H), 3.65 (s, 3H), 1.46 (s, 9H), 1.15 (d, *J* = 6.7 Hz, 3H), 1.10 (d, *J* = 6.7 Hz, 3H). ^{13}C NMR (151 MHz, C_6D_6, 25 °C, δ) 168.4, 160.4, 155.8, 151.5, 150.2, 143.2, 137.1, 136.9, 134.1, 132.0, 129.8, 129.6, 127.0, 125.9, 123.5, 122.4, 120.9, 120.8, 117.6, 117.4, 113.6, 52.9, 42.6, 34.2, 32.6, 25.7, 21.3 (1 aromatic carbon is obscured by the solvent C_6D_6 resonance). Anal: Calcd. for $C_{30}H_{32}N_4Pd$: C, 64.92; H, 5.81; N, 10.09; Found C, 64.84; H, 5.74; N, 10.14.

19 $(L^O)Pd(bzq)(Cl)_2$

To a mixture of $(L^O)Pd(bzq)\cdot 1/3CH_2Cl_2$ (50.0 mg, 0.101 mmol) and $PhI(Cl)_2$ (29.5 mg, 0.107 mmol) was added anhydrous acetone (0.5 mL) at -35 °C. After 1 h at -35 °C the resultant red solution was layered with pentanes (2.0 mL) and kept at -35 °C. The resultant orange microcrystalline solid was dried *in vacuo* to afford 29.0 mg of $(L^O)Pd(bzq)Cl_2$ (53 % isolated yield). Reactions in CD_3CN at -35 °C afforded $(L^O)Pd(bzq)Cl_2$ in quantitative yield, but suitable single crystals for X-ray analysis could not be grown from this solvent.

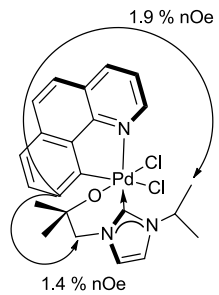

Characterising data: ^{1}H NMR (400 MHz, CD_3CN, -30 °C, δ) 9.80 (dd, *J* = 5.2, 1.2 Hz, 1H), 8.62 (dd, *J* = 8.1 1.6 Hz, 1H), 7.97 (d, *J* = 8.8 Hz, 1H), 7.92 (d, *J* = 8.8 Hz, 1H), 7.86 (dd, *J* = 8.2, 5.4 Hz, 1H), 7.84 (d, *J* = 7.9Hz, 1H), 7.59 (d, *J* = 2.0 Hz, 1H), 7.52 (t, *J* = 7.8 Hz, 1H), 7.38 (td, *J* = 7.4, 1.0, 1H), 6.86 (d, *J* = 7.5 Hz, 1H), 6.12 (br, 1H), 4.18 (br, 1H), 3.94 (d, *J* = 13.22 Hz, 1H), 1.54 (m, 6H), 0.76 (s, 3H), 0.62 (s, 3H). ^{13}C NMR (100 MHz, CD_3CN, -30 °C, δ) 150.6, 148.4, 147.6, 139.9, 139.4, 137.5, 136.3, 131.4, 130.7, 129.4,

129.1, 128.7, 126.1, 125.5, 124.2, 120.9, 74.7, 63.9, 54.0, 27.0, 26.5, 24.4, 23.6. Anal: Calcd. for $C_{23}H_{25}N_3OCl_2Pd$: C, 51.46; H, 4.69; N, 7.83; Found C, 51.50; H, 4.69; N, 7.67.

20 (L^O)Pd(bzq-Cl)Cl

To a 5.1 x10^{-4} M solution of (L^O)Pd(bzq)·1/3CH_2Cl_2 (50.0 mg, 0.101 mmol) in MeCN (20 mL) was added $PhI(Cl)_2$ (29.5 mg, 0.107 mmol) at -35 °C. The reaction mixture was allowed to warm to 33 °C over 24 h with stirring. After 72 h the reaction mixture was dried *in vacuo*. The resultant solid was purified by crystallisation from MeCN layered with Et_2O, at -35 °C to remove small quantities of (L^O)Pd(bzq^{2Cl})Cl and (L^{OH})Pd(bzq)Cl made as impurities (*vide infra*). From this mother liquor, (L^O)Pd(bzq^{Cl})Cl could be isolated by drying *in vacuo* and trituration with Et_2O (1 mL) to afford 41.4 mg as a yellow solid (75 % yield).

Characterising data, (L^O)Pd(bzq^{Cl})Cl: $_1$H NMR (401 MHz, CD_3CN, 25 °C, δ) 9.03 (dd, *J* = 4.3, 1.9 Hz, 1H), 8.31 (dd, *J* = 8.0, 1.8 Hz, 1H), 8.10 (d, *J* = 2.0 Hz, 1H), 7.89 (d, *J* = 8.8 Hz, 1H), 7.78 (d, *J* = 9.1 Hz, 1H), 7.77 (dd, *J* = 7.8, 1.30 Hz, 1H), 7.63 (m, 1H), 7.60 (dd, *J* = 8.0, 4.3 Hz, 1H), 7.44 (dd, *J* = 7.8, 1.2 Hz, 1H), 7.18 (d, *J* = 2.0 Hz, 1H), 5.79 (sept, *J* = 6.8 Hz, 1H), 5.15 (s, 2H), 1.53 (d, *J* = 6.8 Hz, 6H), 1.48 (s, 6H). ^{13}C NMR (101 MHz, CD_3CN, 25 °C, δ) 155.4, 149.4, 145.7, 138.8, 137.9, 137.5, 131.9, 129.7, 129.4, 128.7, 127.7, 127.1, 125.8, 124.7, 123.1, 118.9 71.5, 66.7, 61.4, 54.4, 26.0, 23.5. Anal: Calcd for $C_{23}H_{25}N_3OCl_2Pd$: C, 51.46; H, 4.69; N, 7.83; Found C, 51.40; H, 4.54; N, 7.79.

To a 5.3 x10^{-4} M solution of (L^O)Pd(bzq)·1/3CH_2Cl_2 (5.2 mg, 0.011 mmol) in MeCN (20 mL) was added $PhI(Cl)_2$ (3.1 mg, 0.011 mmol) at -35 °C. The reaction mixture was allowed to warm to 33 °C over 24 h with stirring. After 72 h, analysis of the ^{1}H NMR spectra (MeCN) showed a ratio ((L^O)Pd(bzq^{Cl})Cl **:** (L^O)Pd(bzq^{2Cl})Cl **:** (L^{OH})Pd(bzq)Cl) of 10:1:1.

A 1.1 x10^{-2} M solution of (L^O)Pd(bzq)Cl_2 (17.3 mg, 0.032 mmol) in MeCN (3 mL) was made at -35 °C. The reaction mixture was allowed to warm to 25 °C with stirring. After 24 h

the reaction was dried *in vacuo*. Analysis of the ^{1}H NMR spectra (CD_2Cl_2) showed a ratio ($(L^{O})Pd(bzq^{Cl})Cl$ **:** $(L^{O})Pd(bzq^{2Cl})Cl$ **:** $(L^{OH})Pd(bzq)Cl$) of 1.7:1:1.

$(L^{O})Pd(bzq^{2Cl})Cl$ is formed in the same quantity as $(L^{OH})Pd(bzq)Cl$, and has not been isolated as a sole product of any reaction. Starting from higher initial concentrations of $(L^{O})Pd(bzq)Cl_2$ results in formation of greater amounts of $(L^{O})Pd(bzq^{2Cl})Cl$ and $(L^{OH})Pd(bzq)Cl$ relative to $(L^{O})Pd(bzq^{Cl})Cl$. $(L^{O})Pd(bzq^{2Cl})Cl$ is formulated as the 5,10-dichlorobenzoquinoline ligated isomer, as this is a more reasonable assignment than the 6,10-dichlorobenzoquinoline isomer on chemical grounds, since $PhI(Cl)_2$ is known to chlorinate benzoquinoline at the 5-position. The reaction mixture was stirred with basic alumina (200 mg) and poured onto a plug of silica (2 cm in a pipette) to release the organic products from the Pd. After elution with ethyl acetate (5 mL) the solution was dried *in vacuo*. Analysis by mass spectrometry (ESI+) shows the presence of bzq-Cl along with small amounts of dichlorobenzoquinoline (confirmed by HRMS). HRMS-ESI (m/z) for dichlorobenzoquinoline: Calcd for $[C_{13}H_7NCl_2]$, 246.9950. Found, 246.9955.

To $(L^{O})Pd(bzq^{Cl})Cl$ (18.0 mg, 0.034 mmol) in CD_3CN (0.75 mL) was added $PhI(Cl)_2$ (9.2 mg, 0.034 mmol) at 25 °C. The ^{1}H NMR spectra indicates formation of $(L^{O})Pd(bzq^{2Cl})Cl$ along with an unidentified palladium complex in equal quantities, supporting the formulation of $(L^{O})Pd(bzq^{2Cl})Cl$. The absolute structure of $(L^{O})Pd(bzq^{2Cl})Cl$ cannot be determined from the NMR data.

21 $(L^{O})Pd(bzq)(succinimide)Br$

To mixture of $(L^{O})Pd(bzq)$ (33 mg, 0.071 mmol) and N-bromosuccinimide (12.6 mg, 0.071 mmol) was added CH_2Cl_2 (10 mL) and hexanes (5 mL) at -18 °C. The bright red solution

was kept at -18 °C whilst the volatiles were removed by evaporation under a dinitrogen atmosphere, to afford (L^O)Pd(bzq)(succinimide)Br as a red powder in quantitative yield.

Characterising data: ^{1}H NMR (400 MHz, CD_3CN, -30 °C, δ) 9.32 (dd, *J* = 5.5, 1.4 Hz, 1H), 8.54 (dd, *J* = 8.1, 1.4 Hz, 1H), 7.95-7.25 (m, 7H), 7.13 (d, *J* = 7.7 Hz, 1H), 5.80 (sept, *J* = 6.7 Hz, 1H), 4.00 (s, 2H), 2.47 (br, 4H), 1.71 (d, *J* = 6.7 Hz, 3H), 1.61 (d, *J* = 6.7 Hz, 3H), 0.91 (s, 3H), 0.31 (s, 3H). It was not possible to obtain a carbon NMR due to poor solubility of (L^O)Pd(bzq)(succinimide)Br in standard solvents. FTIR (KBr disc, cm^{-1}): 1713(s), 1615(s). Anal: Calcd for [$C_{27}H_{30}N_4O_3BrPd \cdot 0.25CH_2Cl_2$]: C, 49.13; H, 4.62; N, 8.41; Found C, 49.14; H, 4.58; N, 8.23.

22 (L^O)Pd(phpy)(succinimide)Br

To a mixture of (L^O)Pd(phpy) (95.0 mg, 0.215 mmol) and N-bromosuccinimide (38.3 mg, 0.215 mmol) at -40 °C was added cold MeCN (3 mL) to give a red solution. The mixture was frozen. Diethyl ether (10 mL) was added to the thawing mixture, with stirring. Cooling of the resultant solution to -70 °C afforded (L^O)Pd(phpy)(succinimide)Br as a red powder after removal of the supernatant by decanting, in 60 % yield.

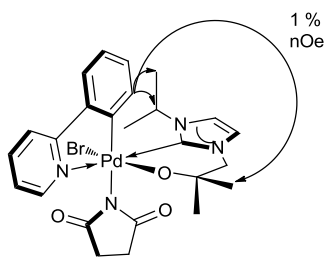

Characterising data: ^{1}H NMR (360 MHz, CD_3CN, -30 °C, δ) 8.95 (dd, *J* = 0.8, 5.7 Hz, 1H), 8.03 (d, *J* = 8.0 Hz, 1H), 7.97 (m, 1H), 7.84 (m, 1H), 7.46 (d, *J* = 2.0 Hz, 1H), 7.31 (dd, *J* = 1.3, 5.9 Hz, 1H), 7.24 (d, *J* = 2.0 Hz, 1H), 7.18 (m, 2H), 6.91 (m, 1H), 5.71 (sept, *J* = 6.5 Hz, 1H), 3.95 (d, *J* = 16.9 Hz, 1H), 3.91 (d, *J* = 16.9 Hz, 1H), 2.41 (br, 4H) 1.65 (d, *J* = 6.5 Hz, 3H), 1.60 (d, *J* = 6.5 Hz, 3H) , 0.97 (s, 3H), 0.32 (s, 3H). ^{13}C NMR (91 MHz, CD_3CN, -30 °C, δ) 189.7, 160.7, 157.4, 152.7, 151.8, 143.6, 140.6, 135.5, 131.6, 127.3, 126.4, 124.0, 123.9, 121.3, 120.2, 74.3, 63.6, 54.1, 32.3, 32.1, 26.7, 26.0, 24.2, 22.8. FTIR (Film, cm^{-1}): 1713, 1621. Anal: Calcd for [$C_{25}H_{30}N_4O_3BrPd$]: C, 48.36; H, 4.87; N, 9.02; Found C, 48.47; H, 4.64; N, 8.89.

23 (L^O)Pd($phpy^{Br}$)(succinimide)

A solution of (L^O)Pd(phpy)(succinimide)Br (25 mg, 0.040 mmol) in MeCN (20 mL) at -30 °C was allowed to warm slowly to room temperature with stirring. The volatiles were removed under reduced pressure to give a pale yellow solid.

Characterising data: ^{1}H NMR (360 MHz, CD_3CN, 25 °C, δ) 8.66 (s, 1H), 7.79 (m, 1H), 7.67 (m, 1H), 7.65 (m, 1H), 7.56 (m, 1H), 7.44 (m, 1H), 7.33 (m, 1H), 7.25 (m, 1H), 7.01 (d, *J* = 2.0 Hz, 1H), 6.99 (d, *J* = 2.0 Hz, 1H), 4.61 (sept, *J* = 6.6 Hz, 1H), 4.34 (s, 1H), 4.15 (s, 1H), 2.38 (s, 4H), 1.27 (d, *J* = 6.6 Hz, 6H), 1.15 (s, 3H), 0.85 (s, 3H). ^{13}C NMR (91 MHz, CD_3CN, 25 °C, δ) The spectrum was difficult to assign due to presence of decomposition products, data in **bold** taken from hsqc. 189.0, 158.1, 150.4, 146.3, **138.1,** 137.1, **132.1, 128.7, 124.9, 124.7, 123.9 123.7, 122.9,** 117.3, 69.8, 65.2, 51.6, 31.6, 27.7, 23.4. It was not possible to obtain an elementally pure sample of (L^O)Pd($phpy^{Br}$)(succinimide). To confirm C-Br bond formation, a solution of (L^O)Pd($phpy^{Br}$)(succinimide) (20 mg) in CH_2Cl_2 (3 mL) was stirred with basic alumina (200 mg) for 1 h. The suspension was poured onto a 1 cm plug of silica in a pipette and then eluted with ethyl acetate (2 x 5 mL). The only organic product thus obtained was confirmed to be phpy-Br by ^{1}H NMR spectroscopy and GC analysis.

24 Effect of temperature and concentration on product distribution upon reductive elimination

In a typical experiment MeCN (1 mL) was added to a mixture of (L^O)Pd(phpy) (10 mg, 0.023 mmol) and N-bromosuccinimide (4 mg, 0.023 mmol) at -30 °C. After 24 h the solution was analysed by ^{1}H NMR spectroscopy.

Key ^{1}H NMR spectroscopic resonances (401 MHz, CH_3CN, 25 °C, δ): **A** 9.34, 5.42, 4.84, 4.19; **B** 9.39, 5.45, 4.49, 4.01; **C** 9.78, 5.66, 4.40, 4.31.

Temp.	Conc.	Equivalents of NBS	Ratio of products (A:B:C)
-30 °C	0.023 M	1	9.0:4.5:1.0
-30 °C	0.023 M	2	0.3:0.3:1.0
-30 °C	0.013 M	1	5.6:3.9:1.0
-30 °C	0.046 M	1	1.3:1.6:1.0
30 °C	0.023 M	1	1.0:1.3:1.0
60 °C	0.023 M	1	1.2:1.3:1.0

Table 1. Effect of temperature, concentration and equivalents of oxidant on product ratio.

25 $(L^{OH})Pd(phpy^{Br})(succinimide)_2$

In an NMR tube equipped with a Young's tap, a mixture of $(L^{O})Pd(phpy)$ (14 mg, 0.032 mmol) and NBS (6 mg, 0.032 mmol) was treated with CD_3CN (0.5 mL, contained trace amounts of water) at -20 °C. The red solution was allowed to warm slowly to room temperature. Microcrystalline $(L^{OH})Pd(phpy^{Br})(succinimide)_2$ precipitated from the solution upon standing for 18 h.

Characterising data: ^{1}H NMR (250 MHz, C_5D_5N, 25 °C, δ) 8.82 (d, *J* = 4.95, 1H), 8.11 (d, *J* = 1.98, 1H), 7.75-7.62 (m, 4H), 7.42-7.36 (m, 2H), 7.27-7.20 (m, 3H), 6.70 (sept, *J* = 6.6 Hz, 1H), 6.56 (s, 1H), 5.54 (s, 2H), 2.43 (s, 8H), 1.60 (d, *J* = 6.6 Hz, 6H), 1.55 (s, 6H). ^{13}C NMR (91 MHz, C_5D_5N, 25 °C, δ) 188.6, 159.1, 155.2, 142.4, 136.9, 136.5, 134.0, 132.6, 130.6, 128.3, 125.4, 123.3, 122.5, 117.7, 70.8, 62.2, 53.5, 32.0, 28.1, 24.1. Mass Spectrometry: HRMS-ESI (m/z) Calcd for $[C_{29}H_{34}N_5O_5BrPd]$, 717.0781. Found, 717.0773.

Some of the $(L^{OH})Pd(phpy^{Br})(succinimide)_2$ obtained was of suitable quality for X-ray analysis.

26 (L^{OH})Pd(bzq)(succinimide)(Br)OH

In an NMR tube equipped with a Young's tap, a mixture of (L^{O})Pd(bzq) (15 mg, 0.032 mmol) and NBS (6 mg, 0.032 mmol) was treated with CD_3CN (0.5 mL, contained trace amounts of water) at -78 °C. The sample was analsysed at -30 °C by ^{1}H NMR spectrscopy.

Characterising data: ^{1}H NMR (400 MHz, CD_3CN, -30 °C, δ) 10.05 (d, *J* = 5.3 Hz, 1H), 8.62 (d, *J* = 8.0 Hz, 1H), 8.00-7.00 (m, 7H), 6.74 (d, *J* = 7.6 Hz, 1H), 6.22 (sept, *J* = 6.7 Hz, 1H), 4.06 (d, *J* = 13.3 Hz, 1H), 3.84 (d, *J* = 13.3 Hz, 1H), 2.47 (m, 4H), 1.61 (d, *J* = 6.7Hz, 3H), 1.56 (d, *J* = 6.7Hz, 3H), 0.74 (s, 3H), 0.60 (s, 3H).

27 (L^{OH})Pd(bzq)Cl

a) from (L^{O})Pd(bzq) *via* oxidation

$PhI(Cl)_2$ (29.5 mg, 0.107 mmol) was added to (L^{O})Pd(bzq)·1/3CH_2Cl_2 (50.0 mg, 0.101 mmol) in thf (*ca.* 2 mL) at 33 °C. The characteristic red-orange colour of (L^{O})Pd(bzq)Cl_2 was observed immediately, which decolorized slowly as the reaction mixture was stirred for 72 h before drying *in vacuo*. The resultant solid was triturated with Et2O (3 mL) and dried *in vacuo*. The pale solid was purified by crystallisation from MeCN, layered with Et_2O, at -35 °C to afford 25.0 mg of (L^{OH})Pd(bzq)Cl as a colourless solid (75 % yield).

b) from (L^{O})Pd(bzq) and HCl

HCl (2.0 M in diethyl ether, 0.075 mL, 0.150 mmol) was added to (L^{O})Pd(bzq)·1/3CH_2Cl_2 (50.0 mg, 0.101 mmol) in MeCN (*ca.* 5 mL) at 25 °C. The reaction mixture was stirred for 5 minutes before the resultant suspension was concentrated *in vacuo* (*ca.* 3 mL). The solution was decanted off and the colourless solid washed with MeCN (*ca.* 1 mL). The solid was dried *in vacuo* to afford 47.0 mg of (L^{OH})Pd(bzq)Cl as a colourless solid (85 % yield).

Characterising data: ^{1}H NMR (401 MHz, CD_2Cl_2, 23 °C, δ) 9.42 (dd, *J* = 5.1, 1.5 Hz, 1H), 8.34 (dd, *J* = 8.1, 1.5 Hz, 1H), 7.77 (d, *J* = 8.8 Hz, 1H), 7.66 (d, *J* = 8.8 Hz, 1H), 7.61 (dd, *J* = 8.1, 5.1 Hz, 1H), 7.57 (dd, *J* = 8.0, 0.9 Hz, 1H), 7.27 (d, *J* = 2.0 Hz, 1H), 7.26 (dd, *J* = 8.0,

7.2 Hz, 1H), 7.21 (d, *J* = 2.0 Hz, 1H), 6.38 (dd, *J* = 7.2, 0.9 Hz, 1H), 5.63 (sept, *J* = 6.8 Hz, 1H), 4.69 (d, *J* = 14.2 Hz, 1H), 4.12 (d, *J* = 14.2 Hz, 1H), 3.39 (s, 1H), 1.57 (d, *J* = 6.8 Hz, 3H), 1.40 (d, *J* = 6.8 Hz, 3H), 1.25 (s, 3H), 1.20 (s, 3H). ^{13}C NMR (101 MHz, CD_2Cl_2, 23 °C, δ) 171.9, 154.8, 153.3, 149.1, 142.6, 137.8, 134.2, 129.4, 129.3, 127.1, 124.1, 124.1, 123.1, 122.1, 122.0, 117.5, 70.9, 66.2, 62.6, 28.7, 28.1, 23.7, 23.1. HRMS-ESI (m/z) Calcd for [$C_{23}H_{27}N_3OClPd$ + Na], 525.0770. Found, 525.0776. Anal: Calcd. for $C_{23}H_{27}N_3OClPd$: C, 54.88; H, 5.41; N, 8.35; Found C, 64.35; H, 4.49; N, 9.51. Satisfactory analysis could not be obtained due to contamination with a complex that we formulate as a solvated adduct which has extremely similar chemical behaviour.

28 Deprotonation of (L^{OH})Pd(bzq)Cl, conversion to (L^{O})Pd(bzq).

To a mixture of (L^{OH})Pd(bzq)Cl (3 mg, 6.4 x 10^{-3} mmol) and $KN(SiMe_3)_2$ (KN") (1.1 mg, 5.3 x 10^{-3} mmol) in a Young's tap NMR tube equipped with a sealed capillary containing C_6D_6 as an internal reference) was added thf. Upon dissolution the reaction mixture became yellow-orange, and ^{1}H NMR spectroscopic analysis confirmed the formation of (L^{O})Pd(bzq) and HN", from comparison of the spectra of authentic samples. Likewise, a mixture of (L^{OH})Pd(bzq)Cl (3 mg, 6.4 x 10^{-3} mmol) and NaCp (0.6 mg, 6.4 x 10^{-3} mmol) in thf afforded a yellow solution that was confirmed by ^{1}H NMR spectroscopic analysis to contain only (L^{O})Pd(bzq) and HCp. The bases $KOBu^t$ and KCH_2Ph were also effective for the conversion of (L^{OH})Pd(bzq)Cl back to (L^{O})Pd(bzq) but in poorer yields.

29 ($L^{N,Ar}$)Pd(bzq)$(Cl)_2$

A mixture of (L^{N})Pd(bzq) (17.9 mg, 0.032 mmol) and $PhICl_2$ (8.9 mg, 0.032 mmol) was cooled to -78 °C. CH_2Cl_2 (3 mL) was added slowly with stirring kept at -78 °C for 0.5 h once addition was complete. The solution was warmed slowly to -10 °C, and the volatiles removed under reduced pressure over 2.5 h (keeping temperature between -30 and -10 °C). The slate blue solid obtained was warmed briefly (~15 minutes) to room temperature when it was transferred into the glovebox freezer (the solid was stored at -20 °C).

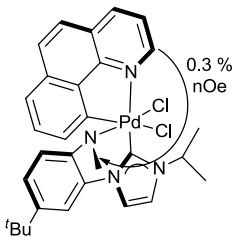

Characterising data: ^{1}H NMR (600 MHz, CD_3CN, 0 °C, δ) 9.91 (d, *J* = 4.9 Hz, 1H), 8.76 (d, *J* = 7.6 Hz, 1H), 8.26 (d, *J* = 6.1 Hz, 1H), 7.94 (m, 5H), 7.74 (d, *J* = 7.4 Hz, 2H), 7.63 (m, 2H), 7.38 (m, 1H), 7.17 (m, 2H), 7.11 (t, *J* = 8.0 Hz, 1H), 6.54 (d, *J* = 7.8 Hz, 1H), 6.36 (br, 1H) 6.15 (sept, *J* = 6.2 Hz, 1H), 2.30 (m, 3H), 1.71 (d, *J* = 6.2 Hz, 3H), 1.59 (d, *J* = 6.2 Hz, 3H), 1.28 (s, 9H). Attempts to observe a ^{13}C NMR spectrum gave only resonances for the solvent and iodobenzene. Anal: Calcd. for $C_{30}H_{33}N_4Cl_2Pd \cdot C_6H_5I \cdot KCl$: C, 47.80; H, 4.12; N, 6.19; Found C, 47.77; H, 4.12; N, 6.27.

30 Decomposition of $(L^{N,Ar})Pd(bzq)(Cl)_2$

In an NMR tube equipped with a Young's tap, CD_3CN (0.6 mL) was added to $(L^N)Pd(bzq)Cl_2 \cdot PhI \cdot KCl$ (4.1 mg, 4.1 x 10^{-3} mmol) at 25 °C. The decay of $(L^N)Pd(bzq)Cl_2$ was monitored by ^{1}H NMR spectroscopy. Colourless precipitate consistent with KCl (*vide infra*) was seen upon dissolving $(L^{N,Ar})Pd(bzq)(Cl)_2$. A dark blue solution was obtained initially, which changed to a maroon colour after 5 minutes. The Pd^{IV} complex $(L^N)Pd(bzq)Cl_2$ decomposes to an intermediate species in about 20 minutes. This unidentified complex remains unchanged for about 90 minutes before decomposing with a $t_{1/2} \approx 80$ minutes.

Characterising data (final products): ^{1}H NMR (600 MHz, CD_3CN, 25 °C, δ) Major isomer 8.39 (dd, *J* = 1.5, 8.0 Hz, 1H), 7.74 (d, *J* = 8.6 Hz, 1H), 7.66 (d, *J* = 8.6 Hz, 1H), 7.62 (dd, *J* = 5.1, 8.1 Hz, 1H), 7.54 (m, 1H), 7.30 (m, 1H), 7.17 (m, 1H), 6.68 (dd, *J* = 0.7, 7.2 Hz, 1H), 5.70 (sept, *J* = 6.8 Hz, 1H), 2.68 (s, 3H), 1.62 (d, *J* = 6.8 Hz, 3H), 1.42 (d, *J* = 6.8 Hz, 3H), 1.38 (s, 3H), 1.02 (br, 6H). Minor isomer 9.26 (br, 1H), 6.63 (br, 1H), 5.70 (sept, *J* = 6.8 Hz, 1H), 1.56 (d, *J* = 6.8 Hz, 3H), 1.50 (d, *J* = 6.8 Hz, 3H), the remaining resonances are obscured by the major isomer.

31 [(L^O)Pd(phpy)]PhI($OAc)_2$

To a mixture of (L^O)Pd(phpy) (22.5 mg, 0.051 mmol) and PhI($OAc)_2$ (16.4 mg, 0.051 mmol) at 25 °C was added CD_3CN (0.6 mL). The reaction mixture was warmed to 40 °C for 15 minutes and then analysed by ^1H and ^{13}C NMR spectroscopy.

Characterising data: ^1H NMR (600 MHz, C_6D_6, 25 °C, δ) 9.15 (ddd, *J* = 1.0, 5.8, 13.3 Hz, 1H), 8.10 (td, *J* = 1.5, 6.4 Hz, 1H), 7.79 (dd, *J* = 1.1, 7.6 Hz, 1H), 7.5-6.4 (m, 10H), 6.09 (sept, *J* = 6.7 Hz, 1H), 4.77 (dd, *J* = 13.7 Hz, 1H), 4.58 (dd, *J* = 13.7 Hz, 1H), 2.50 (s, 3H), 1.84 (s, 3H), 1.20 (dd, *J* = 6.7 Hz, 3H), 1.19 (dd, *J* = 6.7 Hz, 3H), 1.14 (s, 3H), 1.13 (s, 3H). ^{13}C NMR (91 MHz, CD_3CN, 25 °C, δ) Significant line broadening makes assignments in the aromatic region uncertain.177.8 (OAc), 177.2 (OAc), 165.3, 155.1, 150.6, 149.7, 148.0, 140.6, 139.3, 136.6, 134.8 (PhI), 133.4, 132.4 (PhI), 130.6 (PhI), 125.2, 125.1, 124.7, 123.7, 122.3 (PhI), 119.8, 118.1, 78.8, 61.5, 61.2, 54.2, 28.8, 25.3, 24.0, 23.0, 21.9 (OAc), 20.8 (OAc). FTIR (Film, cm^{-1}): 1713, 1385.

32 (L^O)Pd($phpy^{OAc}$)OAc + PhI

A solution of [(L^O)Pd(phpy)]·PhI($OAc)_2$ (28.6 mg, 0.030 mmol) in CD_3CN (0.6 mL) was heated at 75 °C for 2 h before being characterised.

Characterising data: ^1H NMR (360 MHz, CD_3CN, 25 °C, δ) 8.61 (d, *J* = 4.7 Hz, 1H), 7.97 (t, *J* = 7.4 Hz, 1H), 7.90 (d, *J* = 8.0 Hz, 1H), 7.64 (d, *J* = 7.6 Hz, 1H), 7.40-7.20 (m, 3H), 7.06 (m, 1H), 6.89 (t, *J* = 7.5 Hz, 1H), 6.15 (d, *J* = 7.2 Hz, 1H), 5.47 (sept, *J* = 6.7 Hz, 1H), 4.48 (d, *J* = 13.7 Hz, 1H), 3.91 (d, *J* = 13.7 Hz, 1H), one OAc resonance is obscured by the solvent, 1.86 (br, 3H), 1.43 (d, *J* = 6.7 Hz, 3H), 1.33 (d, *J* = 6.7 Hz, 3H), 1.14 (s, 3H), 1.12 (s, 3H). Significant line broadening and the inability to obtain the product free of starting materials and intermediate made assignments in the aromatic region uncertain. 177.8, 170.5, 165.2, 154.8, 150.8, 149.4, 142.5, 140.8, 138.8 (PhI), 138.7, 137.6, 131.9 (PhI), 130.9, 129.1

(PhI), 126.4 125.4, 125.3 125.2, 123.9, 122.4, 120.0, 117.8, 95.1 (PhI), 70.4, 63.9, 54.2, 28.9, 26.6, 24.0, 23.0, 21.2, 20.8. Mass Spectrometry: ESI (m/z) 559.0 [M+].

To a mixture of (L^O)Pd(phpy) (25 mg, 0.057 mmol) and $PhI(OAc)_2$ (18.2 mg, 0.057 mmol) was added CH_2Cl_2 (10 mL) at 25 °C. The resultant yellow solution was stirred for 18 h before drying *in vacuo*. The product was characterised by NMR spectroscopy.

Characterising data: ^{1}H NMR (500 MHz, C_6D_6, 25 °C, δ) 8.99 (d, *J* = 5.4 Hz, 1H), 7.80 (d, *J* = 8.3 Hz, 1H), 7.44 (d, *J* = 7.6 Hz, 1H), 7.14 (t, *J* = 8.8 Hz, 1H), 7.07 (t, *J* = 7.4 Hz, 1H), 7.02 (t, *J* = 7.4 Hz, 1H), 6.89 (t, *J* = 7.5 Hz, 1H), 6.69 (s, 1H), 6.59 (s, 1H), 6.51 (t, *J* = Hz, 1H), 5.85 (sept, *J* = 6.7 Hz, 1H), 5.05 (d, *J* = 13.7 Hz, 1H), 3.56 (d, *J* = 13.7 Hz, 1H), 2.37 (br, 3H), 1.84 (s, 3H), 1.37 (s, 3H), 1.33 (d, *J* = 6.7 Hz, 3H), 1.29 (s, 3H), 1.13 (d, *J* = 6.7 Hz, 3H). ^{13}C NMR (126 MHz, C_6D_6, 25 °C, δ) 176.2, 175.1, 164.3, 155.3, 149.1, 147.9, 138.6, 138.1, 135.6, 131.5, 130.9, 130.0, 124.4, 124.3, 123.8, 122.1, 118.2, 116.0, 69.8, 63.8, 53.1, 29.1, 27.6, 25.4, 23.8, 22.7, 20.4. FTIR (Film, cm^{-1}): 1772, 1653, 1196.

Stirring a solution of (L^O)Pd($phpy^{OAc}$)OAc (in C_6D_6 or CD_2Cl_2) with poly(vinyl pyridine) for 1 h failed to bind the palladium and liberate phpy-OAc.

33 (L^{OH})Pd($phpy^{OAc}$)(OAc)OH

A solution of (L^O)Pd($phpy^{OAc}$)OAc (10.1 mg, 0.018 mmol) in C_6D_6 (0.6 mL) was exposed to air for 3 days. Analysis by ^{1}H NMR spectroscopy indicated quantitative formation of (L^{OH})Pd($phpy^{OAc}$)(OAc)OH.

Characterising data: ^{1}H NMR (600 MHz, C_6D_6, 35 °C, δ) 9.01 (d, *J* = 5.2 Hz, 1H), 8.10 (dd, *J* = 1.1, 8.2 Hz, 1H), 7.79 (dd, *J* = 1.1, 7.9 Hz, 1H), 7.61 (dd, *J* = 1.1, 7.9 Hz, 1H), 7.45 (dd, *J* = 1.1, 7.7 Hz, 1H), 7.32 (s, 5H), 7.16 (m, 2H), 7.10 (dd, *J* = 1.1, 7.4 Hz, 1H), 7.03 (m, 1H), 6.92 (m, 1H), 6.77 (t, *J* = 7.8 Hz, 1H), 6.74 (d, *J* = 1.1 Hz, 1H), 6.61 (d, *J* = 1.8 Hz, 1H), 6.60 (d, *J* = 7.5 Hz, 1H), 6.55 (t, *J* = 6.4 Hz, 1H), 5.88 (sept, *J* = 6.7 Hz, 1H), 5.08 (dd, *J* =

13.7 Hz, 1H), 3.63 (dd, *J* = 13.7 Hz, 1H), 2.29 (s, 4H), 1.88 (s, 2H), 1.42 (dd, *J* = 6.7 Hz, 3H), 1.39 (s, 3H), 1.33 (s, 3H), 1.19 (dd, *J* = 6.7 Hz, 3H). ^{13}C NMR (151 MHz, C_6D_6, 35 °C, δ) 176.1, 164.7, 149.2, 147.9, 138.6, 138.1, 138.1 (PhI), 135.6, 131.5, 130.8, 130.7 (PhI), 129.9 (PhI), 128.7, 128.3, 127.8, 124.4, 124.3, 123.7, 122.1, 118.2, 116.1, 95.0 (PhI), 69.9, 63.7, 53.2, 29.0, 27.7, 23.8, 22.7, 20.3.

34 [(L^O)Pd(phpy)]Ph_2IBF_4

To a mixture of (L^O)Pd(phpy) (20 mg, 0.045 mmol, 1.00 equiv) and [Ph_2I]BF_4 (16.7 mg, 0.045 mmol, 1.00 equiv) cooled to -196 °C was added CD_3CN (0.6 mL). The reaction mixture was warmed to -10 °C inside the spectrometer over 20 minutes and monitored by ^{1}H and ^{13}C NMR spectroscopy.

Characterising data: ^{1}H NMR (360 MHz, CD_3CN, -10 °C, δ) 8.34 (d, *J* = 5.1 Hz, 1H), 7.93 (d, *J* = 7.6 Hz, 4H), 7.84 (m, 2H), 7.63 (dd, *J* = 1.0, 7.3 Hz, 1H), 7.50 (m, 2H), 7.36 (m, 2H), 7.32 (m, 3H), 7.28 (d, *J* = 1.4 Hz, 1H), 7.09 (m, 2H), 5.05 (sept, *J* = 6.7 Hz, 1H), 4.24 (d, *J* = 13.1 Hz, 1H), 3.93 (d, *J* = 13.1 Hz, 1H), 1.66 (d, *J* = 6.7 Hz, 3H), 1.52 (d, *J* = 6.7 Hz, 3H), 1.13 (s, 3H), 0.89 (s, 3H). ^{13}C NMR (91 MHz, CD_3CN, -10 °C, δ) 172.8, 164.7, 157.5, 148.7, 147.8, 140.1, 138.4, 135.7 (PhI), 132.6 (PhI), 132.5 (PhI), 131.6, 130.5, 130.0, 129.8, 129.3, 129.1, 124.8, 123.97, 123.3, 121.1, 119.2, 118.7, 117.7 (PhI), 70.7, 65.7, 53.0, 30.5, 28.7, 26.1, 22.5.

35 [(L^O)Pd($phpy^{Ph}$)]BF_4 + PhI

A solution of [(L^O)Pd(phpy)]Ph_2IBF_4 (27.5 mg, 0.045 mmol) in CD_3CN (0.6 mL) was warmed from -10 °C to 25 °C and held at 25 °C for 18 h. The reaction mixture was then heated at 75 °C for 20 minutes.

Characterising data: ^{1}H NMR (360 MHz, CD_3CN, 25 °C, δ) 8.66 (br, 1H), 8.01 (m, 1H), 7.93 (d, *J* = 8.0 Hz, 1H), 7.75 (m, 2H), 7.67 (dd, *J* = 1.1, 7.8 Hz, 1H), 7.49 (br, 2H), 7.39 (m, 3H), 7.24 (br, 1H), 7.19 (m, 1H), 7.17 (m, 1H), 7.14 (m, 1H), 7.11 (dt, *J* = 0.8, 7.7 Hz, 2H), 6.93

(dt, *J* = 1.3, 7.5 Hz, 2H), 6.05 (d, *J* = 7.2 Hz, 1H), 5.38 (sept, *J* = 6.7 Hz, 1H), 4.45 (d, *J* = 14.2 Hz, 1H), 4.10 (d, *J* = 14.2 Hz, 1H), 1.51 (d, *J* = 6.7 Hz, 3H), 1.39 (d, *J* = 6.7 Hz, 3H), 1.19 (s, 6H). ^{13}C NMR (91 MHz, CD_3CN, 25 °C, δ) 150.6 (br), 148.3 (br), 138.8 (PhI), 138.4 (br), 136.7, 134.3 (br), 133.8, 131.9 (PhI), 131.4 (br), 131.3, 130.9 (br), 130.3, 129.6, 129.4 (br), 129.1 (PhI), 128.8, 128.3, 125.8 (br), 125.7 (br), 124.8, 120.5 (br), 120.1, 119.0 (br), 95.1 (PhI), 62.6, 54.7, 28.6, 23.8, 23.2. There was significant line broadening (also seen in the ^{1}H spectra) denoted by (br). ESI:MS (m/z) 518.0 [M – BF_4].

36 [($L^{O,Ph}$)Pd(phpy)]Ph_2IBF_4

To a mixture of ($L^{O,Ph}$)Pd(phpy) (20 mg, 0.035 mmol) and [Ph_2I]BF_4 (13.0 mg, 0.035 mmol) was added CD_3CN (0.6 mL) at 25 °C. The reaction was monitored by ^{1}H NMR spectroscopy. ($L^{O,Ph}$)Pd(phpy) is poorly soluble in C_6D_6 and CD_3CN, and the intermediate showed substantial line broadening preventing accurate characterisation.

Characterising data: ^{1}H NMR (360 MHz, CD_3CN, 25 °C, δ) 9.19 (br, 1H), 8.10-6.70 (m, 29H), 5.07 (br, 2H), 4.56 (br, 1H), 1.46 (br, 3H), 1.14 (br, 3H).

37 [($L^{O,Ph}$)Pd($phpy^{Ph}$)]BF_4 + PhI

To a mixture of ($L^{O,Ph}$)Pd(phpy) (20 mg, 0.035 mmol, 1.00 equiv) and [Ph_2I]BF_4 (13.0 mg, 0.035 mmol, 1.00 equiv) was added CD_3CN (0.6 mL) at 25 °C. The reaction was monitored by ^{1}H and ^{13}C NMR spectroscopy. [($L^{O,Ph}$)Pd($phpy^{Ph}$)]BF_4 was formed in quantitative yield.

Characterising data: ^{1}H NMR (360 MHz, CD_3CN, 25 °C, δ) 8.51 (br, 1H), 8.02 (m, 3H), 7.94 (m, 1H), 7.75 (m, 3H), 7.68 (m, 2H), 7.52 (m, 2H), 7.48 (br, 2H), 7.39 (m, 4H), 7.24 (m, 6H), 7.15 (m, 4H), 6.96 (m, 1H), 6.01 (d, *J* = 7.4 Hz, 1H), 5.38 (d, *J* = 13.7 Hz, 1H), 5.26 (sept, *J* = 6.7 Hz, 1H), 4.95 (br, 1H), 1.43 (d, *J* = 6.7 Hz, 3H), 1.32 (d, *J* = 6.7 Hz, 3H). ^{13}C NMR (91 MHz, CD_3CN, 25 °C, δ) 150.6, 148.4, 146.3, 141.5, 138.8 (PhI), 138.5, 136.7, 134.4, 133.8, 133.6, 131.9 (PhI), 131.5, 131.1, 130.9, 130.7, 130.3, 129.8, 129.7, 129.4,

129.1 (PhI), 128.8, 128.7, 128.3, 127.5, 127.4, 127.3, 126.6, 125.8, 124.8, 124.7, 120.6, 114.9, 95.1 (PhI), 61.5, 54.7, 23.6.

38 (L^{OMe})Pd(phpy)I

To a solution of (L^{O})Pd(phpy) (25.2 mg, 0.057 mmol) in MeCN (10 mL) was added MeI (3.6 µL, 0.057 mmol) at 25 °C. After stirring for 18 h a dark yellow solution was obtained. The reaction was dried *in vacuo*, Et_2O (2 mL) was added and the reaction mixture was stirred for 1 h before drying *in vacuo* to afford ($L^{O,Me}$)Pd(phpy)I as an orange solid in quantitative yield by ^{1}H NMR spectroscopy.

Characterising data: ^{1}H NMR (500 MHz, C_6D_6, 25 °C, δ) 10.30 (dd, *J* = 0.7, 5.4 Hz, 1H), 7.34 (d, *J* = 1.7 Hz, 1H), 7.32 (dd, *J* = 0.8, 7.7 Hz, 1H), 7.03 (m, 2H), 6.95 (dt, *J* = 1.2, 7.5 Hz, 1H), 6.80 (dt, *J* = 1.5, 7.7 Hz, 1H), 6.48 (d, *J* = 1.7 Hz, 1H), 6.36 (dd, *J* = 0.8, 7.5 Hz, 1H), 6.30 (dt, *J* = 1.0, 6.0 Hz, 1H), 5.68 (sept, *J* = 6.8 Hz, 1H), 4.62 (d, *J* = 14.3 Hz, 1H), 4.41 (d, *J* = 14.3 Hz, 1H), 2.80 (s, 3H), 1.33 (d, *J* = 6.8 Hz, 3H), 1.10 (s, 3H), 0.99 (d, *J* = 6.8 Hz, 3H), 0.82 (s, 3H). ^{13}C NMR (126 MHz, C_6D_6, 25 °C, δ) 172.9, 165.1, 159.4, 155.3, 147.9, 138.2, 137.2, 130.1, 124.7, 124.5, 123.5, 123.0, 118.5, 117.0, 75.7, 60.3, 53.4, 49.1, 23.4, 23.3, 23.1, 22.8. FTIR (Film, cm^{-1}): 1417, 1075, 756. Anal: Calcd for $C_{22}H_{28}IN_3OPd$: C, 45.26; H, 4.83; N, 7.20; Found C, 45.22; H, 4.91; N, 7.18.

39 (L^{OTMS})Pd(phpy)N_3

To a solution of (L^{O})Pd(phpy) (25.2 mg, 0.057 mmol) in MeCN (10 mL) was added $Si(Me)_3N_3$ (7.5 µL, 0.057 mmol) at 25 °C. After stirring for 18 h a colourless solution was obtained. The reaction was dried *in vacuo*, Et_2O (2 mL) was added and the reaction mixture was stirred for 1 h before drying *in vacuo* to yield (L^{OTMS})Pd(phpy)N_3 as a colourless solid in quantitative yield by ^{1}H NMR spectroscopy.

Characterising data: ^{1}H NMR (500 MHz, CH_2Cl_2, 25 °C, δ) 8.68 (d, *J* = 4.0 Hz, 1H), 7.85 (m, 1H), 7.74 (m, 1H), 7.55 (m, 1H), 7.47 (d, *J* = 1.8 Hz, 1H), 7.28 (m, 1H), 7.17 (d, *J* = 1.8

Hz, 1H), 7.05 (m, 1H), 6.90 (m, 1H), 6.30 (m, 1H), 5.50 (sept, *J* = 6.7 Hz, 1H), 4.59 (d, *J* = 13.6 Hz, 1H), 4.26 (d, *J* = 13.6 Hz, 1H), 1.64 (d, *J* = 6.7 Hz, 3H), 1.42 (d, *J* = 6.7 Hz, 3H) , 1.39 (s, 3H), 1.27 (s, 3H) 0.16 (s, 3H), 0.09 (s, 6H). ^{13}C NMR (126 MHz, CH_2Cl_2, 25 °C, δ): 173.5, 164.8, 156.3, 149.2, 147.4, 139.4, 138.1, 130.0, 124.4, 124.2, 124.1, 123.8, 122.8, 118.7, 117.2, 74.7, 63.1, 28.6, 27.1, 24.1, 23.4, 2.6, 1.3. Minor isomer: ^{1}H NMR (500 MHz, CH_2Cl_2, 25 °C, δ) 8.68 (d, *J* = 4.0 Hz, 1H), 7.85 (m, 1H), 7.74 (m, 1H), 7.55 (m, 1H), 7.37 (d, *J* = 1.3 Hz, 1H), 7.28 (m, 1H), 7.21 (d, *J* = 1.9 Hz, 1H), 7.05 (m, 1H), 6.90 (m, 1H), 6.30 (m, 1H), 5.54 (sept, *J* = 6.7 Hz, 1H), 4.62 (d, *J* = 14.2 Hz, 1H), 4.21 (d, *J* = 14.2 Hz, 1H), 1.64 (d, *J* = 6.7 Hz, 3H), 1.42 (d, *J* = 6.7 Hz, 3H) , 1.33 (s, 3H), 1.25 (s, 3H) 0.16 (s, 3H), 0.09 (s, 6H). ^{13}C NMR (126 MHz, CH_2Cl_2, 25 °C, δ): 173.4, 164.8, 155.8, 149.3, 147.4, 139.4, 138.0, 130.1, 124.6, 124.2, 123.8, 122.9, 118.8, 117.7, 71.1, 62.1, 28.2, 27.6, 24.1, 23.4, 2.6, 1.3. FTIR (Film, cm^{-1}): 2035, 1260, 1026. Anal: Calcd for $C_{24}H_{34}N_6OPdSi$: C, 51.75; H, 6.15; N, 15.09; Found C, 51.83; H, 6.10; N, 15.08.

40 (L^{OH})Pd(phpy)OH

Solid (L^{O})Pd(phpy) was exposed to air for 3 days to afford (L^{OH})Pd(phpy)OH in quantitative yield by ^{1}H NMR spectroscopy.

Characterising data: ^{1}H NMR (500 MHz, C_6D_6, 25 °C, δ) 10.12 (s, 1H), 7.99 (m, 1H), 7.94 (br, 1H), 7.75 (s, 2H), 7.67 (m, 3H), 7.53, (m, 1H), 6.96 (s, 1H), 6.92 (br, 1H), 5.86 (br, 1H), 4.80 (br, 1H), 4.16 (br, 1H), 4.03 (d, *J* = 9.6 Hz, 1H), 2.20 (s, 3H), 1.69 (d, *J* = 6.7 Hz, 3H), 1.58 (br, 3H), 1.53 (s, 3H). ^{13}C NMR (126 MHz, C_6D_6, 25 °C, δ) 175.8, 165.2, 149.4, 148.0, 139.8, 138.5, 129.3, 124.2, 123.7, 123.0, 121.8, 117.8, 115.8, 68.9, 52.5, 31.2, 28.4, 25.2, 22.2 (2 aromatic resonances are obscured by the solvent resonance). FTIR (Film, cm^{-1}): 3427, 1417. Anal: Calcd for $C_{21}H_{27}N_3O_2Pd$: C, 54.85; H, 5.92; N, 9.14; Found C, 54.91; H, 6.00; N, 9.12.

41 (L^{OH})Pd(phpy)OAc

To a solution of (L^{O})Pd(phpy) (10.0 mg, 0.023 mmol) in MeCN (1 mL) was added AcOH (13.6 µL, 0.226 mmol) at 25 °C. Immediately a pale yellow solution was obtained. The reaction was dried *in vacuo* to afford (L^{OH})Pd(phpy)OAc as a colourless solid in quantitative by ^{1}H NMR spectroscopy.

Characterising data: ^{1}H NMR (500 MHz, C_6D_6, 25 °C, δ) 8.63 (dq, *J* = 0.7, 1.6, 5.5 Hz, 1H), 7.85 (ddd, *J* = 0.4, 1.7, 7.7 Hz, 1H), 7.75 (d, *J* = 8.1 Hz, 1H), 7.54 (dd, *J* = 1.3, 7.7 Hz, 1H), 7.24 (ddd, *J* = 0.4, 1.3, 5.5 Hz, 1H), 7.08 (d, *J* = 2.0 Hz, 1H), 7.06 (d, *J* = 2.0 Hz, 1H), 7.03 (td, *J* = 1.2, 7.5 Hz, 1H), 6.85 (td, *J* = 1.4, 7.5 Hz, 1H), 6.39 (s, 1H), 6.14 (dd, *J* = 1.0, 7.5 Hz, 1H), 5.51 (sept, *J* = 6.7 Hz, 1H), 4.63 (d, *J* = 13.8 Hz, 1H), 3.75 (d, *J* = 13.8 Hz, 1H), 1.90 (s, 3H), 1.44 (d, *J* = 6.7 Hz, 3H), 1.34 (d, *J* = 6.7 Hz, 3H), 1.16 (s, 6H). ^{13}C NMR (126 MHz, C_6D_6, 25 °C, δ) 177.2, 173.6, 164.1, 153.4, 148.3, 146.8, 139.0, 137.4, 129.6, 123.8, 123.7 (Two coincident peaks), 122.4, 118.3, 116.1, 69.3, 63.2, 53.0, 28.2, 26.8, 24.4, 23.6, 22.4. FTIR (Film, cm^{-1}): 3399, 1566, 1415. Anal: Calcd for $C_{23}H_{29}N_3O_3Pd$: C, 55.04; H, 5.82; N, 8.37; Found C, 54.87; H, 5.93; N, 8.24.

42 ($L^{OH,iPr}$)Pd(phpy)Cl

To a mixture of [$H_2L^{O,iPr}$]I (40 mg, 0.11 mmol) and KH (13 mg, 0.31 mmol) cooled to -78 °C was added thf (20 mL) dropwise with stirring. The reaction mixture was allowed to warm to 25 °C over 2 h and then stirred for a further 2 h. The yellow solution was filtered away from a colourless precipitate onto a suspension of Pd(phpy)Cl(2,6-lutidine) (44 mg, 0.11 mmol) in thf (10 mL) at -78 °C. The reaction mixture was allowed to warm to 25 °C with stirring. After 6 h the reaction mixture was filtered and the filtrates were dried *in vacuo*. The solid was dissolved in C_6H_6 (15 mL) and filtrated through a 1cm plug of celite to afford a bright yellow solution. The solution was layered with pentanes (15 ml) and colourless crystals suitable for X-ray analysis grew from this solution.

Characterising data: ^{1}H NMR (400 MHz, $CDCl_3$, 25 °C, δ) 9.32 (d, *J* = 5.6 Hz, 1H), 7.78 (tdd, *J* = 0.7, 1.6, 7.7, 1H), 7.68 (d, *J* = 7.8 Hz, 1H), 7.53 (d, *J* = 7.8 Hz, 1H), 7.34 (s, 1H), 7.23 (s, 1H), 7.18 (d, *J* = 6.4 Hz, 1H), 7.06 (s, 1H), 7.04 (t, *J* = 7.6 Hz, 1H), 6.88 (t, *J* = 7.3 Hz, 1H), 6.14 (d, *J* = 7.7 Hz, 1H), 5.56 (sept, J = 6.7 Hz, 1H), 4.64 (d, J = 14.6 Hz, 1H), 4.37 (d, J = 14.6 Hz, 1H), 2.77 (s, 1H), 2.05, 1.94, 1.52 (d, J = 6.7 Hz, 3H), 1.37 (d, J = 6.7 Hz, 3H), 1.01 (d, J = 6.7 Hz, 3H), 0.94 (d, J = 6.7 Hz, 3H), 0.93 (d, J = 6.7 Hz, 3H), 0.91 (d, J = 6.7 Hz, 3H). ^{13}C NMR (101 MHz, $CDCl_3$, 25 °C, δ) 173.1, 164.1, 154.8, 149.8, 146.5, 138.4, 136.7, 129.5, 124.0, 123.6, 123.5, 122.1, 117.8, 116.5, 54.3, 53.1, 33.4, 33.2, 29.7, 23.6. Anal: Calcd for [$C_{25}H_{34}ClN_3OPd \cdot 0.25C_6H_6$]: C, 57.46; H, 6.46; N, 7.59; Found C, 57.13; H, 6.60; N, 7.56.

43 ($L^{N,Ar}$)Pd(bzq)(Me)(I)

A suspension of ($L^{N,Ar}$)Pd(bzq) (2 mg, 0.0036 mmol) in CH_3CN (0.6 mL) was frozen at -78 °C. Under a flow of nitrogen MeI (0.3 μL, 0.0048 mmol) was added. The reaction mixture was allowed to warm slowly to 25 °C. The reaction was monitored by ^{1}H NMR spectroscopy and all the starting material was consumed after 18 h at 25 °C. Three isomers were obtained in a 1:0.6:0.6 ratio.

Characterising data: ^{1}H NMR (600 MHz, CH_3CN, 25 °C, δ) Isomer 1: 9.78 (d, *J* = 4.7 Hz, 1H), 8.41 (dd, *J* = 1.4, 4.6 Hz, 1H) 8.39 (m, 1H), 7.86 (m, 1H), 7.81 (d, *J* = 8.7 Hz, 1H), 7.71 (d, *J* = 8.7 Hz, 1H), 7.65 (d, *J* = 7.9 Hz, 1H), 7.56 (dd, *J* = 5.2, 8.1 Hz, 1H), 7.50 (d, *J* = 2.2 Hz, 1H), 7.36 (br, 1H), 7.24 (m, 1H), 7.18 (m, 1H), 7.14 (m, 1H), 7.01 (d, *J* = 8.4 Hz, 1H), 6.60 (d, *J* = 7.1 Hz, 1H), 5.68 (sept, *J* = 6.7 Hz, 1H), 2.59 (s, 3H), 1.93 (s, 3H), 1.59 (d, *J* = 6.7 Hz, 3H), 1.44 (d, *J* = 6.7 Hz, 3H), 0.67 (s, 9H). Isomer 2 & 3: 9.67 (d, *J* = 3.8 Hz, 1H), 8.36 (d, *J* = 8.0 Hz, 1H), 7.86 (m, 1H), 7.78 (d, *J* = 2.1 Hz, 1H), 7.76 (s, 1H), 7.74 (s, 1H), 7.66 (d, *J* = 8.7 Hz, 1H), 7.60 (d, *J* = 7.9 Hz, 1H), 7.54 (m, 1H), 7.52 (m, 1H), 7.40 (m, 1H), 7.36 (m, 1H), 7.31 (br, 1H), 7.24 (m, 1H), 7.18 (m, 1H), 7.14 (m, 1H), 6.65 (d, *J* = 7.1 Hz,

1H), 6.58 (d, *J* = 8.2 Hz, 1H), 5.62 (sept, *J* = 6.7 Hz, 1H), 4.27 (s, 3H), 2.62 (s, 3H), 1.60 (d, *J* = 6.7 Hz, 3H), 1.44 (d, *J* = 6.7 Hz, 3H), 0.89 (s, 9H).

The reaction mixture was heated to 80 °C for 12 h. Isomer 1 was unchanged whilst isomer 2 & 3 yielded two new products. Three isomers were obtained in a 1:0.6:0.6 ratio.

Characterising data: ^{1}H NMR (600 MHz, CH_3CN, 25 °C, δ) Isomer 4 & 5: 9.25 (dd, *J* = 2.0, 7.4 Hz, 1H), 8.97 (dd, *J* = 1.6, 4.3 Hz, 1H), 8.90 (d, *J* = 2.3 Hz, 1H), 8.29 (ddd, *J* = 1.8, 6.4, 7.1 Hz, 1H), 7.98 (dd, *J* = 2.0, 7.1 Hz, 1H), 7.89 (d, *J* = 8.8 Hz, 1H), 7.86 (m, 1H), 7.74 (dd, *J* = 1.8, 5.1 Hz, 1H), 7.69 (d, *J* = 2.0Hz, 1H), 7.59 (dd, *J* = 1.3, 5.8 Hz, 1H), 7.39 (d, *J* = 3.9 Hz, 1H), 7.37 (d, *J* = 2.5 Hz, 1H), 7.33 (d, *J* = 2.2 Hz, 1H), 7.24 (m, 1H), 7.18 (m, 1H), 7.14 (m, 1H), 7.08 (d, *J* = 8.4 Hz, 1H), 5.56 (sept, *J* = 6.7 Hz, 1H), 2.54 (s, 3H), 1.51 (d, *J* = 6.7 Hz, 6H), 1.40 (s, 9H). One methyl resonance is obscured by the solvent peak. Mass Spectrometry: EI (m/z) 193.0 [bzq-Me], 569.0 [M - I].

44 Preliminary (L^O)Pd(phpy) catalysed ligand directed C-H bond oxidative halogenation

Substrate (0.023 mmol, 1.0 equiv), oxidant (0.024 mmol, 1.1 equiv) and (L^O)Pd(phpy) (0.5 mg, 0.001 mmol, 0.05 equiv) were combined in a foil-covered 5 mL ampoule. MeCN (1 mL) was added and the reaction was heated to 100 °C for 12 h. The reaction mixture was then stirred with polyvinyl pyridine for 1 h before being analysed by GC/MS.

Oxidant	phpy-X[a]	Reported for $Pd(OAc)_2$[b 13]
NBS	25 %	44 %
NCS	27 %	56 %
I_2	No reaction	40 %
I_2/PhI$(OAc)_2$	Decomposition	71 %

Table 2. Catalytic oxidative halogenation of phpy-H. [5 mol% (LO)Pd(phpy), 1.0 phpy-H 1.1 oxidant, MeCN, 100 °C, 12 h] a GC yield based on integration of peaks. No phpy-2X was observed. bResults for 3-methyl-2-phenylpyridine.

Typical procedure: Substrate (0.2 mmol, 1.0 equiv), oxidant (0.22 mmol, 1.1 equiv) and (L^O)Pd(phpy) (4.4 mg, 0.01 mmol, 0.05 equiv) were combined in a foil-covered 5 mL ampoule. MeCN (3.4 mL) was added and the reaction was heated to 120 °C for 48 h. The reaction mixture was then analysed by GC/MS.

Substrate	Oxidant	Product	GC Yield[a]
phpy-H	NCS	2-(2,6-dichlorophenyl)pyridine	phpy-2Cl, 63 %[b]
bzq-H	NCS	10-chlorobenzo[h]quinoline	bzq-Cl, 96 %[c]
n-BuOpy-H	NCS	3-chloro-2-(n-butoxy)pyridine	*n*-BuOpy-Cl, 56 %[d]
Etpy-H	NBS	bromo-2-ethylpyridine	Etpy-Br, 27 %[e]
Etpy-H	NCS	chloro-2-ethylpyridine	Etpy-Cl, 6 %[e]
o-tolylpy-H	NBS	2-(2-bromo-6-methylphenyl)pyridine	*o*-tolylpy-Br, 3 %[c]
o-tolylpy-H	NCS	2-(2-chloro-6-methylphenyl)pyridine	*o*-tolylpy-Cl, 17 %[c]

Table 3. Summary of halogenation [10 mol% (LO)Pd(phpy), 1.0 substrate, 1.1 NXS, MeCN, 120 °C, 48 h] aGC yield based on integration of peaks, average of two runs. bAdded 2.5 equiv. of NCS to make phpy-2Cl, also obtained 34 % of phpy-Cl. c5 mol % (LO)Pd(phpy). dChlorination occurred on pyridine rather than alkyl chain and is Pd catalysed. eHalogenation occurred on pyridine rather than alkyl chain and happens in absence of catalyst.

45 Catalytic bromination using (L^O)Pd(bzq) and N-bromosuccinimide

Typical procedure: Substrate (0.687 mmol, 1.00 equiv), N-bromosuccinimide (152.8 mg, 0.858 mmol, 1.25 equiv) and (L^O)Pd(bzq) (16.4 mg, 0.034 mmol, 0.05 equiv) were combined in a 25 mL foil-covered ampoule. Acetonitrile (5.80 mL) was added and the reaction was heated for 72 h at 100 °C. At the end of a reaction, an aliquot was removed and analysed by ^{1}H NMR spectroscopy, (with a sealed capillary containing C_6D_6 as an internal reference) to determine the fate of the catalyst. The sample was returned to the reaction flask, and naphthalene in MeCN (1.00 mL, 0.23 M) was added as a GC standard. The reaction mixture was then analysed by gas chromatography, and in each case, the brominated products were identified by comparison with GC data from genuine samples.

Substrate	Product	GC Yield[a]
bzq-H	10-bromobenzo[h]quinoline	bzq-Br, 81 %
phpy-H	2-(2-bromophenyl)pyridine	phpy-Br, 73 %[b]
Mephpy-H	3-methyl-2-(2-bromophenyl)pyridine	Mephpy-Br, 25 %
phpyr-H	1-(4-bromophenyl)-2-pyrrolidone	0 %[c]
phpyz-H	1-phenyl-3-bromopyrazole	0 %[c]
phCOpy-H	No reaction	NR

Table 4. Summary of bromination with (LO)Pd(bzq) [5 mol% (LO)Pd(bzq), 1.25 NBS, MeCN, 100 °C, 48-96 h] a Average of two concurrent runs; b Additional 1.25 equiv of NBS added after 48 h, heated for 96 h. ca. 5 % of phpy-2Br was formed; c substrate reacts with the oxidant to brominate in a different position, so no catalytic yield can be determined.

46 Comparison of (L^O)Pd(phpy) and $Pd(OAc)_2$ for catalytic acetoxylation

Typical procedure: Substrate (0.024 mmol, 1.0 equiv), Iodobenzene diacetate (8.4 mg, 0.026 mmol, 1.1 equiv) and (L^O)Pd(phpy) (0.5 mg, 0.001 mmol, 0.05 equiv) or $Pd(OAc)_2$ (0.3 mg, 0.001 mmol, 0.05 equiv) were combined in a 5 mL ampoule. MeCN (3.0 mL) was added and the reaction was heated for 24 h. The reaction mixture was then analysed by GC/MS, and in each case, the acetoxylated products were identified by the mass spectrum of the separated peaks.

Substrate	Temp.	Catalyst	GC yield Rpy-OAc[a]	GC yield phpy-2OAc[a]
phpy-H	40 °C	(L^O)Pd(phpy)	0 %	-
phpy-H	40 °C	$Pd(OAc)_2$	83 %	9 %
phpy-H	80 °C	(L^O)Pd(phpy)	34 %	44 %
phpy-H	80 °C	$Pd(OAc)_2$	73 %	15 %
phpy-H	100 °C	(L^O)Pd(phpy)	32 %[b]	36 %[b]
phpy-H	100 °C	$Pd(OAc)_2$	69 %	24 %
Etpy-H	80 °C	(L^O)Pd(phpy)	0 %	-
Etpy-H	80 °C	$Pd(OAc)_2$	58 %	-

Table 5. Comparison of $Pd(OAc)_2$ and (L^O)Pd(phpy) for catalytic acetoxylation [5 mol% Pd source, 1.0 phpy-H, 1.1 $PhI(OAc)_2$, MeCN, 24 h] [a]Yield based on integration of peaks in GC. [b]Addition of Cs_2CO_3 (10 equiv.) under these conditions prevents catalytic acetoxylation from occurring.

47 Effect of solvent on (L^O)Pd(phpy) catalysed acetoxylation

2-phenylpyridine (3.2 mg, 0.023 mmol, 1.0 equiv), Iodobenzene diacetate (7.8 mg, 0.024 mmol, 1.1 equiv) and (L^O)Pd(phpy) (0.5 mg, 0.001 mmol, 0.05 equiv) were combined in a 5 mL ampoule. Solvent (2.0 mL) was added and the reaction was heated at 100 °C for 12 h. The reaction mixture was then analysed by GC/MS, and in each case, the acetoxylated products were identified by the mass spectrum of the separated peaks.

Solvent	phpy-OAc[a]	phpy-2OAc[a]
MeCN	49 %	25 %
PhMe	50 %	14 %
thf	-	-
pyr	-	-

Table 6. Catalytic acetoxylation of phpy-H in different solvents [5 mol% (LO)Pd(phpy), 1.0 phpy-H, 1.1 PhI(OAc)2, 100 °C, 12 h]. [a]Yield based on integration of peaks in GC.

48 Comparison between (L^{O})Pd(phpy) and ($L^{O,Ph}$)Pd(phpy) as precatalysts

Typical procedure: Substrate (0.2 mmol, 1.0 equiv), oxidant (0.22 mmol, 1.1 equiv) and ($L^{O,R}$)Pd(phpy) (0.01 mmol, 0.05 equiv) were combined in a foil-covered 5 mL ampoule. MeCN (3.4 mL) was added and the reaction was heated to 120 °C for 48 h. The reaction mixture was then analysed by GC/MS.

Substrate	Oxidant	Product	GC Yield (L^{O})Pd(phpy)[a]	GC Yield ($L^{O,Ph}$)Pd(phpy)[a]
phpy-H	NCS	2-(2-chlorophenyl)pyridine	63 %	64 %
o-tolylpy-H	$PhI(OAc)_2$	2-(2-acetoxy-6-methylphenyl)pyridine	> 95 %[b]	> 95 %[b]
n-BuOpy-H	NCS	3-chloro-2-(n-butoxy)pyridine	47 %[c]	57 %[c]

Table 7. Comparison of catalysts for ligand-directed acetoxylation [5 mol% ($L^{O,XX}$)Pd(phpy), 1.0 substrate, 1.1 oxidant, 120 °C, 48 h]. [a]GC yield based on integration of peaks, average of two runs. [b]12 h. [c]Chlorination occurred on pyridine rather than alkyl chain and is Pd catalysed.

Key ^{1}H NMR spectroscopy data

Complex	Solvent	H16	H2	H7A	H7B
$H_2L^{O}I$	CD_3CN	-	4.66	4.21	4.21
KL^{O}	CD_3CN	-	4.42	3.80	3.80
$Pd(L^{O})_2$	C_6D_5N	-	6.77	3.82	3.82
$Ni(L^{O})_2$	C_6D_5N	-	4.20	3.98	3.98
(L^{O})Pd(phpy)	CD_3CN	9.02	5.07	3.95	3.93
	C_6D_6	9.66	5.26	4.15	3.47
$(L^{O,Ph})$Pd(phpy)	CD_2Cl_2	9.18	5.14	4.83	4.74
$(L^{O,iPr})$Pd(phpy)	C_6D_6	9.73	5.33	4.25	3.73
(L^{O})Pd(^{OMe}phpy)	C_6D_6	9.06	5.12	4.06	3.84
(L^{N})Pd(phpy)	C_6D_6	10.11	-	3.12	2.91
(L^{O})Pd(bzq)	CD_3CN	9.17	5.23	4.00	4.00
$(L^{N,Ar})$Pd(bzq)	C_6D_6	9.00	5.47	-	-
(L^{O})Pd(bzq)Cl_2	CD_3CN	9.80	6.12	4.18	3.94
(L^{O})Pd(bzq^{Cl})Cl	CD_3CN	9.03	5.79	5.15	5.15
(L^{O})Pd(bzq)(Br)(succinimide)	CD_3CN	9.32	5.80	4.00	4.00
(L^{O})Pd(bzq^{Br})(succinimide) + unknowns	CD_3CN	9.00 8.97 8.95	5.82 5.72 5.71 5.64 5.51	-	-
(L^{O})Pd(phpy)(Br)(succinimide)	CD_3CN	8.95	5.71	3.95	3.91
(L^{O})Pd(phpy^{Br})(succinimide)	CD_3CN	8.66	4.61	4.34	4.15
(L^{OH})Pd(phpy^{Br})(succinimide)$_2$	C_6D_5N	8.82	6.70	5.54	5.54
(L^{OH})Pd(bzq)(Br)OH	CD_3CN	10.05	6.22	4.06	3.84
(L^{OH})Pd(bzq)(Cl)	CD_2Cl_2	9.42	5.63	4.69	4.12

Table 8. Diagnostic ^{1}H NMR spectroscopic resonances.

Complex	Solvent	H16	H2	H7A	H7B
$[(L^{O})Pd(phpy)]\cdot PhI(OAc)_2$	C_6D_6	9.15	6.09	4.77	4.58
	CD_3CN				
$(L^{O})Pd(phpy^{OAc})OAc$	C_6D_6	8.99	5.85	5.05	3.56
	CD_3CN	8.61	5.47	4.48	3.91
$[(L^{O})Pd(phpy)]\cdot Ph_2IBF_4$	CD_3CN	8.34	5.05	4.24	3.93
$[(L^{O})Pd(phpy^{Ph})]BF_4$	CD_3CN	8.66	5.38	4.45	4.10
$[(L^{O,Ph})Pd(phpy)]\cdot Ph_2IBF_4$	CD_3CN	9.19	5.07	5.07	4.56
$[(L^{O,Ph})Pd(phpy^{Ph})]BF_4$	CD_3CN	8.51	5.26	5.38	4.95
$(L^{OMe})Pd(phpy)I$	C_6D_6	10.30	5.68	4.62	4.41
$(L^{OTMS})Pd(phpy)N_3$	CD_2Cl_2	8.68	5.50	4.59	4.26
		8.68	5.54	4.62	4.21
$(L^{OH})Pd(phpy)OH$	C_6D_6	10.12	4.80	4.16	4.03
$(L^{OH})Pd(phpy)OAc$	C_6D_6	8.63	5.51	4.63	3.75
$(L^{OH,iPr})Pd(phpy)$	$CDCl_3$	9.32	5.56	4.64	4.37
$(L^{N,Ar})Pd(bzq)Cl_2$	CD_3CN	9.91	6.15	-	-
$(L^{N,Ar})Pd(bzq)Cl_2$	CD_3CN	8.39	5.70	-	-
decomposition	CD_3CN	9.26	5.70	-	-
$(L^{N,Ar})Pd(bzq)(Me)(I)$	CD_3CN	9.78	5.68	-	-
		9.67	5.62	-	-
$(L^{N,Ar})Pd(bzq)(Me)(I)$	CD_3CN	9.78	5.68	-	-
decomposition		9.25	5.56	-	-
$(L^{O})Pd(phpy)$ + NBS, 25 °C	CD_3CN	8.17	5.48	4.53	4.03
		9.38	5.47	4.38	4.21
$(L^{O})Pd(phpy)$ + NBS, -30 °C	CH_3CN	9.34	5.42	4.84	4.19
		9.39	5.45	4.49	4.01
		9.78	5.66	4.40	4.31

Table 9. Diagnostic ^1H NMR spectroscopic resonances.

Complex	Solvent	H16	H2	H7A	H7B
After catalytic bromination of bzq-H with (L^O)Pd(bzq) and NBS	CD_3CN	-	5.71	4.29	4.09
		-	5.63	4.45	4.45
		-	5.63	5.14	4.79
15 mol% (L^O)Pd(phpy), phpy-H and NBS, 18 h at 80 °C	CD_3CN	9.66	5.37	4.32	4.32
10 mol% (L^O)Pd(phpy), phpy-H and NCS, 48 h at 120 °C	CH_3CN	9.23	5.66	4.32	4.32
10 mol% (L^O)Pd(phpy), bzq-H and NCS, 48 h at 120 °C	CH_3CN	8.97	5.94	4.52	4.52
10 mol% (L^O)Pd(phpy), *n*-BuOpy-H and NCS, 48 h at 120 °C	CH_3CN	8.87	6.49	4.81	4.81
10 mol% (L^O)Pd(phpy), Etpy-H and NBS, 48 h at 120 °C	CH_3CN	8.82	5.84	3.62	3.62
10 mol% (L^O)Pd(phpy), Etpy-H and $[Ph_2I]BF_4$, 48 h at 120 °C	CH_3CN	8.45	5.33	4.42	4.08
10 mol% (L^O)Pd(phpy), Etpy-H and $PhI(OAc)_2$, 12 h at 120 °C	CH_3CN	Decomposition			
5 mol% (L^O)Pd(phpy), *o*-tolylpy-H and $PhI(OAc)_2$, 48 h at 120 °C	CH_3CN	Decomposition			
5 mol% (L^O)Pd(phpy), *o*-tolylpy-H and $[Ph_2I]BF_4$, 24 h at 120 °C	CH_3CN	8.56	5.31	4.43	4.03

Table 10. Diagnostic ^1H NMR spectroscopic resonances.

X-ray Crystallography

X-ray data were recorded on a Brucker Smart Apex area detector diffractometer; Bruker AXS area detector diffractometer; Xcalibur, Eos diffractometer; SuperNova, Dual, Cu at zero, Atlas diffractometer; or Rigaku CCD area detector diffractometer. The structures were solved by heavy-atom or direct methods and were refined by least-squares methods on F^2 values, with anisotropic displacement parameters for non-hydrogen atoms, and with constrained riding hydrogen geometries; the default parameters were used. The largest residual electron density/densities in the final difference syntheses were close to heavy atoms.

	$[H_2L^{O,Ph}]I$	**$[H_2L^{O,iPr}]I$**	**$(L^{O,Me})Pd(phpy)$**	**$(L^{O,Ph})Pd(phpy)\cdot(CH_3)_2CO$**
Crystal data	iphzoi	po7005	po8011	p10042
Chemical formula	$C_{103}H_{23}IN_2O$	$C_{14}H_{27}N_2O\cdot I$	$C_{21}H_{25}N_3OPd$	$C_{31}H_{29}N_3OPd\cdot C_3H_6O$
M_r	434.30	366.28	441.84	624
Crystal system, space group	Monoclinic, $P2_1$	Monoclinic, *C*2/*c*	Monoclinic, $P2_1/c$	Monoclinic, $P2_1/c$
Temperature (K)	150	170	150	170
a, b, c (Å)	7.302 (3), 16.399 (7), 8.334 (4)	15.4824 (12), 23.3980 (16), 11.7983 (8)	10.3131 (2), 10.3288 (2), 18.8235 (3)	14.7547 (2), 17.5650 (2), 11.7721 (2)
β (°)	103.662 (7)	127.579 (4)	103.130 (1)	109.565 (2)
V ($Å^3$)	969.8 (7)	3387.2 (4)	1952.70 (6)	2874.78 (7)
Z	2	8	4	4
Radiation type	Mo *K*α	Mo *K*α	Mo *K*α	Mo *K*α
μ (mm^{-1})	1.66	1.89	0.96	0.68
Crystal size (mm)	0.42 × 0.29 × 0.17	0.25 × 0.15 × 0.12	0.31 × 0.23 × 0.22	0.42 × 0.10 × 0.09

Data collection				
Diffractometer	Bruker SMART APEX CCD diffractometer	Bruker *SMART APEX* CCD area detector diffractometer	Bruker SMART APEX CCD area detector diffractometer	Xcalibur, Eos diffractometer
Absorption correction	Multi-scan (SADABS; Bruker, 2001)	Multi-scan *SADABS*	Multi-scan SADABS	Multi-scan CrysAlisPro, Oxford Diffraction Ltd., Empirical absorption correction using spherical harmonics, implemented in SCALE3 ABSPACK scaling algorithm.
T_{min}, T_{max}	0.53, 0.75	0.609, 0.746	0.644, 0.746	0.763, 0.941
No. of measured, independent and observed [$I > 2\sigma(I)$] reflections	5673, 3603, 3495	30548, 4527, 3872	21320, 5935, 4982	33264, 6992, 5097
R_{int}	0.024	0.034	0.041	0.028
Refinement				
$R[F^2 > 2\sigma(F^2)]$, $wR(F^2)$, S	0.026, 0.062, 1.02	0.030, 0.075, 1.07	0.035, 0.079, 1.05	0.021, 0.048, 0.90
No. of reflections	3603	4527	5935	6992
No. of parameters	222	165	239	365
No. of restraints	2	0	0	0
H-atom treatment	Riding	Riding	Riding	Riding
$\Delta\rho_{max}$, $\Delta\rho_{min}$ (e Å^{-3})	0.74, -0.46	1.27, -0.44	0.92, -0.44	0.39, -0.39

Software	*SMART* (Siemens, 2001), *SAINT* (Siemens, 2000), *SIR92* (Giacovazzo, 1994), *SHELXL97* (Sheldrick, 1997), *ORTEP* (Farrugia, 1997), *enCIFer* (Allen *et al.*, 2004).	*SMART* (Siemens, 1993), *SAINT* (Siemens, 1995), *SIR92* (Giacovazzo, 1994), *SHELXL97* (Sheldrick, 1997), *ORTEP* (Farrugia, 1997), *enCIFer* (Allen *et al.*, 2004).	Bruker SMART-APEX, Bruker SAINT, SHELXS97 (Sheldrick, 1990), SHELXL97 (Sheldrick, 1997), ORTEP (Farrugia, 1997), enCIFer (Allen et al.l., 2004).	CrysAlisPro (Oxford Diffraction Ltd., 2010), SIR92 (Giacovazzo, 1994), SHELXL97 (Sheldrick, 2008), ORTEP (Farrugia, 1997), enCIFer (Allen et al., 2004).
	$(L^{O,Me})Pd(OMe\text{-}phpy)\cdot C_6H_{12}O_2\cdot 0.5(C_6H_{14})$	**$(L^{O,Me})Pd(bzq)$**	**$(L^{O,Me})Pd(bzq)Cl_2\cdot(CH_3)_2CO$**	**$(L^{OH,Me})Pd(bzq)Cl$**
Crystal data	p10005	smp196	smp232	smp230
Chemical formula	$C_{22}H_{27}N_3O_2Pd\cdot C_6H_{12}O_2\cdot 0.5(C_6H_{14})$	$C_{69}H_0N_9O_3Pd_3$	$C_{23}H_{25}Cl_2N_3OPd\cdot C_3H_6O$	$C_{23}H_{26}ClN_3OPd$
M_r	609.57	1321.98	594.86	502.32
Crystal system, space group	Monoclinic, $P2_1/c$	Orthorhombic, Pbca	Monoclinic, $P2_1/c$	Monoclinic, $P2_1/c$
Temperature (K)	170	85(2)	85	85
a, b, c (Å)	16.2071 (6), 13.9745 (6), 13.6992 (5)	24.703, 24.703, 24.703	13.5786 (7), 12.6706 (6), 15.1481 (8)	10.604 (6), 12.799 (7), 15.992 (9)
β (°)	93.226 (3)	-	97.18	99.688 (1)
V ($Å^3$)	3097.8 (2)	15074.7	2585.8 (2)	2140 (2)
Z	4	8	4	4
Radiation type	Mo *K*α	Mo *K*α	Mo *K*α	Mo *K*α
μ (mm^{-1})	0.64	0.75	0.95	1.01

Crystal size (mm)	0.36 × 0.14 × 0.07	0.31 × 0.28 × 0.17	0.31 × 0.16 × 0.14	0.08 × 0.05 × 0.04
Data collection				
Diffractometer	Xcalibur, Eos diffractometer	Bruker AXS area detector diffractometer	Brucker SMART APEX CCD area detector diffractometer	Brucker SMART APEX CCD area detector diffractometer
Absorption correction	Multi-scan CrysAlisPro, Oxford Diffraction Ltd., Empirical absorption correction using spherical harmonics, implemented in SCALE3 ABSPACK scaling algorithm.	Multi-scan SADABS	Multi-scan SADABS	Multi-scan SADABS
T_{min}, T_{max}	0.804, 0.957	0.785, 0.839	0.755, 0.823	0.828, 0.928
No. of measured, independent and observed [$I > 2\sigma(I)$] reflections	15656, 6842, 4585	370815, 18767, 17594	60537, 6431, 5766	55084, 4752, 3085
R_{int}	0.033	0.049	0.032	0.091
Refinement				
$R[F^2 > 2\sigma(F^2)]$, $wR(F^2)$, S	0.055, 0.170, 1.02	1.027, 0.873, 8.81	0.026, 0.069, 1.08	0.038, 0.080, 1.04
No. of reflections	6842	18767	6431	4752
No. of parameters	362	337	313	267
No. of restraints	36	0	0	0
H-atom treatment	Riding	Not modelled	Riding	Riding

$\Delta\rho_{max}$, $\Delta\rho_{min}$ (e Å^{-3})	1.55, -0.71	69.974	0.97, -0.39	0.51, -0.32
Software	Computer programs: CrysAlisPro (Oxford Diffraction Ltd., 2010), SIR92 (Giacovazzo, 1994), SHELXL97 (Sheldrick, 2008), ORTEP (Farrugia, 1997), enCIFer (Allen et al., 2004).	SMART (Siemens, 1993), SAINT (Siemens, 1995), SHELXS97 (Sheldrick, 2008), SHELXL97 (Sheldrick, 2008), ORTEP-3 for Windows (Farrugia, 1997), enCIFer (Allen et al., 2004).	Bruker SMART-APEX, Bruker SAINT, SHELXS97 (Sheldrick, 1990), SHELXL97 (Sheldrick, 1997), ORTEP (Farrugia, 1997), enCIFer (Allen et al.l., 2004).	Bruker SMART-APEX, Bruker SAINT, SHELXS97 (Sheldrick, 1990), SHELXL97 (Sheldrick, 1997), ORTEP (Farrugia, 1997), enCIFer (Allen et al., 2004).

	$[H_2L^{N,Ar}]I$	**$(L^{O,iPr})Pd(phpy)$**	**$(L^{O,Me})Pd(phpy^{Br})(succinimide)_2$**	**$[Ni(L^{O,Me})_2]_2 \cdot KI$**
Crystal data	smp334	p10012	smp157	po0005
Chemical formula	$C_{17}H_{26}N_3 \cdot I$	$C_{25}H_{33}N_3OPd$	$C_{29}H_{34}BrN_5O_5Pd$	$C_{40}H_{68}N_8Ni_2O_4 \cdot KI$
M_r	399.31	497.94	718.92	1008.44
Crystal system, space group	Triclinic, $P\bar{1}$	Triclinic, $P\bar{1}$	Triclinic, $P\bar{1}$	Monoclinic, C2/c
Temperature (K)	170	131	93	100
a, b, c (Å)	8.6783 (5), 10.3889 (5), 11.3567 (6)	11.6321 (7), 14.4851 (8), 14.8266 (5)	10.4187 (19), 10.9129 (19), 15.248 (3)	32.8416 (14), 15.8754 (5), 31.0791 (13)
α, β, γ (°)	112.897 (4), 93.601 (4), 100.551 (4)	74.174 (4), 77.238 (4), 89.976 (5)	68.53 (3), 71.83 (3), 68.64 (3)	128.441 (7) *(β only)*
V (Å^3)	917.06 (8)	2339.3 (2)	1470.3 (4)	12691.6 (9)

Z	2	4	2	8
Radiation type	Mo *K*α	Mo *K*α	Mo *K*α	Cu *K*α
μ (mm^{-1})	1.75	0.81	2.04	5.41
Crystal size (mm)	0.30 × 0.12 × 0.09	0.35 × 0.1 × 0.09	0.20 × 0.15 × 0.05	0.20 × 0.11 × 0.07
Data collection				
Diffractometer	Xcalibur, Eos diffractometer	Xcalibur, Eos diffractometer	CCD diffractometer	SuperNova, Dual, Cu at zero, Atlas diffractometer
Absorption correction	Multi-scan CrysAlisPro, Oxford Diffraction Ltd., Empirical absorption correction using spherical harmonics, implemented in SCALE3 ABSPACK scaling algorithm.	Multi-scan CrysAlisPro, Oxford Diffraction Ltd., Empirical absorption correction using spherical harmonics, implemented in SCALE3 ABSPACK scaling algorithm.	Multi-scan SADABS	Multi-scan CrysAlisPro, Oxford Diffraction Ltd., Empirical absorption correction using spherical harmonics, implemented in SCALE3 ABSPACK scaling algorithm.
T_{min}, T_{max}	0.623, 0.859	0.949, 1.000	0.668, 1.000	0.411, 0.703
No. of measured, independent and observed [$I > 2\sigma(I)$] reflections	7044, 3749, 3314	20118, 10306, 6604	9551, 5244, 3848	62445, 12516, 8894
R_{int}	0.024	0.025	0.129	0.067
Refinement				
$R[F^2 > 2\sigma(F^2)]$, $wR(F^2)$, S	0.024, 0.057, 0.98	0.026, 0.040, 0.75	0.115, 0.299, 1.13	0.040, 0.112, 0.96
No. of reflections	3749	10306	5244	12516
No. of parameters	196	553	376	522

No. of restraints	0	0	0	0
H-atom treatment	Riding	Riding	Riding	Riding
$\Delta\rho_{max}$, $\Delta\rho_{min}$ (e Å^{-3})	0.55, -0.38	0.71, -0.58	2.39, -1.47	2.821
Software	CrysAlisPro (Oxford Diffraction Ltd., 2010), *SIR92* (Giacovazzo, 1994), *SHELXL97* (Sheldrick, 2008), *ORTEP* (Farrugia, 1997), *enCIFer* (Allen *et al.*, 2004).	CrysAlisPro (Oxford Diffraction Ltd., 2010), SIR92 (Giacovazzo, 1994), SHELXL97 (Sheldrick, 2008), ORTEP (Farrugia, 1997), enCIFer (Allen et al., 2004).	CrystalClear (Rigaku Inc., 2007), SIR92 (Giacovazzo, 1994), SHELXL97 (Sheldrick, 1997), ORTEP (Farrugia, 1997), enCIFer (Allen et al., 2004).	CrysAlisPro (Oxford Diffraction Ltd., 2010), SUPERFLIP (Palatinus & Chapuis, 2007), SHELXL97 (Sheldrick, 2008), ORTEP (Farrugia, 1997), enCIFer (Allen et al., 2004).

Single crystals of ($L^{O,iPr}$)Pd(phpy)Cl were grown as blue blocks (0.2 x 0.2 x 0.2 mm) by diffusion of hexanes into a C_6D_6/CH_2Cl_2 solution. The data was collected on a Rigaku, Enraf-nonius CAD4 diffractometer but was not properly integrated preventing accurate solution of the structure. The crystals were of triclinic symmetry in the P-1 space group. The unit cell dimensions are a = 10.7705 (12), b = 11.4878 (9), c = 12.2121 (17) (Å) and α = 66.93 (3), β = 87.25 (6), γ = 72.83 (4) (°) with z = 2.

References

[1] A. B. Pangborn, M. A. Giardello, R. H. Grubbs, R. K. Rosen, and F. J. Timmers, *Organometallics*, 1996, **15**, 1518.

[2] G. K. Anderson and M. Lin, *Inorg. Synth.*, 1990, **28**, 60.

[3] I. Abrunhosa, L. Delain-Bioton, A.-C. Gaumont, M. Gulea, and S. Masson, *Tetrahedron*, 2004, **60**, 9263.

[4] T. Pugliese, N. Godbert, I. Aiello, M. Ghedini, and M. La Deda, *Inorg. Chem. Commun.*, 2006, **9**, 93.

[5] A. F. Littke, C. Dai, and G. C. Fu, *J. Am. Chem. Soc.*, 2000, **122**, 4020.

[6] A. Krief, W. Dumont, and M. Robert, *Chem. Comm.*, 2005, 2167.

[7] P. J. Stang, M. Boehshar, H. Wingert, and T. Kitamura, *J. Am. Chem. Soc.*, 1988, **110**.

[8] P. L. Arnold, M. Rodden, K. M. Davis, A. C. Scarisbrick, A. J. Blake, and C. Wilson, *Chem. Commun.*, 2004, 1612.

[9] P. L. Arnold, M. Rodden, and C. Wilson, *Chem. Commun.*, 2005, 1743.

[10] J. Adams, L. Hoffman, and B. M. Trost, *J. Org. Chem.*, 1970, **35**, 1600.

[11] J. Iskra, S. Stavber, and M. Zupan, *Synthesis*, 2004, 1869.

[12] R. C. Larock and L. W. Harrison, *J. Am. Chem. Soc.*, 1984, **106**, 4218.

[13] D. Kalyani, A. R. Dick, W. Q. Anani, and M. S. Sanford, *Org. Lett.*, 2006, **8**, 2523.